

UNIVERSITY OF SOUTHAMPTON

FACULTY OF ENGINEERING, SCIENCE & MATHEMATICS

School of Geography

**Late-Holocene Palaeoclimates: Cross-Validation of
Multiple Proxies from Lake and Bog Archives in
Northern England**

by

Alastair David Brown

Thesis for the degree of Doctor of Philosophy

September 2006

UNIVERSITY OF SOUTHAMPTON

ABSTRACT

FACULTY OF ENGINEERING, SCIENCE & MATHEMATICS
SCHOOL OF GEOGRAPHY

Doctor of Philosophy

LATE-HOLOCENE PALAEOCLIMATES: CROSS-VALIDATION OF MULTIPLE
PROXIES FROM LAKE AND BOG ARCHIVES IN NORTHERN ENGLAND

by Alastair David Brown

Peatland palaeoclimate studies typically involve two steps: 1) reconstruction of bog surface wetness (BSW) and 2) palaeoclimatic inference based on interpretation of the BSW record. The first step is well developed but the second remains equivocal because BSW results from the interplay between evapotranspirative efflux (driven primarily by temperature) and precipitative influx. Various studies have investigated the short-term (decadal) climate-BSW relationship but the nature of the long-term (centennial to millennial) connection remains unproven. This investigation is a test of the relationship using proxy data from northern England. BSW is reconstructed from Hulleter Moss in southern Cumbria and Malham Tarn Moss in North Yorkshire, using plant macrofossil, testate amoebae and peat humification analysis. The bog sites are paired with proximal lake sites, Bigland Tarn in southern Cumbria and Malham Tarn in North Yorkshire, and palaeotemperature estimates produced using chironomid analysis. Both bog sites displayed an impressive degree of internal consistency between proxy measures of BSW. A high degree of covariance was also found between the two sites and with the wider literature. Chironomid records were produced for both lake sites and modern temperatures were accurately inferred from core-top samples. A combination of ^{14}C , ^{210}Pb and spheroidal carbonaceous particles were used to date the cores, although the radiocarbon chronology of Malham Tarn was problematic. Nevertheless, comparison of the well constrained Bigland Tarn palaeotemperature estimates with an earlier study from Cumbria revealed a high degree of similarity, corroborating the idea that temperature is the primary signal recorded in the chironomid stratigraphy. Comparison between the BSW and chironomid-inferred temperature records therefore provides an empirical test of the closeness of the relationship between temperature and BSW. While similarities between the two records are evident there are also significant differences and the data do not support a dominant temperature control over BSW. However, significant reconstructive and chronological uncertainty hampers any assertion about the dominance of precipitation. The complexity of the climate-BSW response makes it unlikely that it will be possible to apply a universal rule which relates BSW to temperature or precipitation in a simple and consistent fashion.

CONTENTS

Abstract	i
Contents	ii-v
List of figures, tables and plates	vi-x
Figures	vi-viii
Tables	ix-x
Plates	x
Author's declaration	xi
Acknowledgements	xii-xiii
Table of Abbreviations	xiv
CHAPTER 1.0 INTRODUCTION	1-3
1.1 Project Rationale	1
1.2 Aims and Objectives	3
CHAPTER 2.0 BACKGROUND & CONTEXT	4-51
2.1 Introduction	4
2.2 Raised Bogs: An Overview	4
2.3 Bogs as Palaeoclimatic Archives	5
2.4 BSW Reconstruction (Step 1)	6
2.4.1 Plant Macrofossil Analysis	6
2.4.2 Testate Amoebae Analysis	9
2.4.3 Peat Humification (Colorimetric Technique)	10
2.4.4 Peatland Multiproxy Reconstructions	13
2.4.5 Intra-Site BSW Replicability	13
2.4.6 Inter-Site BSW Replicability	14
2.5 Climate BSW Relationship (Step 2)	21
2.5.1 Precipitation-Temperature Interrelations; BSW Consequences	23
2.5.2 Hydrological Sensitivity to Temperature & Precipitation	23
2.6 Palaeoecological Evidence of the Climate BSW Relationship	30

2.7	Lakes as Palaeoenvironmental Archives	33
2.8	Chironomidae (Non-Biting Midge) Analysis	34
	2.8.1 Introduction	34
	2.8.2 Chironomids as Palaeotemperature Indicators	35
	2.8.3 Chironomid Taxonomy	37
	2.8.4 Air or Water Temperature?	38
	2.8.5 Holocene Palaeotemperature Inference	38
	2.8.6 Holocene CI-T Records NW Atlantic	39
2.9	Holocene N Atlantic Climate Variability	40
	2.9.1 Introduction	40
	2.9.2 NW Atlantic Climate Records	41
	2.9.3 Ocean Circulation	43
	2.9.4 Atmospheric Circulation	46
	2.9.5 Precipitation-Temperature Interrelations	48
CHAPTER 3.0 METHODS		52-80
3.1	Site Selection	52
3.2	Peatland Methods	52
	3.2.1 Core Selection & Acquisition	53
	3.2.2 Plant Macrofossil Analysis	53
	3.2.3 Testate Amoebae Analysis	55
	3.2.4 Peat Humification 'Colorimetric Technique'	56
3.3	Palaeolimnological Methods	57
	3.3.1 Core Selection & Acquisition	57
	3.3.2 Loss on Ignition (LOI)	61
	3.3.3 Chironomid Analysis	63
3.4	Chronological Strategy	65
	3.4.1 Carbon-14 Measurement	65
	3.4.2 Spheroidal Carbonaceous Particle (SCP) Analysis	68
	3.4.3 Lead-210 Radiometric Dating	71
	3.4.4 Age-Depth Modelling	74
3.5	Quantitative Analysis	75

3.5.1	Detrended Correspondence Analysis (DCA)	75
3.5.2	Transfer Functions	77
CHAPTER 4.0	SITE DESCRIPTIONS	81-92
4.1	Hulleter Moss	82
4.2	Bigland Tarn	85
4.3	Malham Tarn Moss	87
4.4	Malham Tarn	91
CHAPTER 5.0	CHRONOLOGICAL RESULTS & INTERPRETATION	93-112
5.1	Introduction	93
5.2	Hulleter Moss	93
5.2.1	Carbon-14	93
5.2.2	SCP Analysis	93
5.2.3	Age-Depth Modelling	94
5.3	Bigland Tarn	97
5.3.1	Carbon-14	97
5.3.2	SCP Analysis	99
5.3.3	Lead-210	100
5.3.4	Age-Depth Modelling	101
5.4	Malham Tarn Moss	104
5.4.1	Carbon-14	104
5.4.2	SCP Analysis	104
5.4.3	Age-Depth Modelling	106
5.5	Malham Tarn	108
5.5.1	Carbon-14	108
5.5.2	SCP Analysis	109
5.5.3	Lead-210	110
5.5.4	Age-Depth Modelling	111
CHAPTER 6.0	PALAEOECOLOGICAL RESULTS & INTERPRETATION	113-168
6.1	Introduction	113

6.2	Hulleter Moss	113
	6.2.1 Plant Macrofossils	113
	6.2.2 Testate Amoebae	120
	6.2.3 Peat Humification	126
	6.2.4 Multi-Proxy Comparison	128
6.3	Bigland Tarn	132
	6.3.1 Loss on Ignition	132
	6.3.2 Chironomids	134
6.4	Malham Tarn Moss	141
	6.4.1 Plant Macrofossils	141
	6.4.2 Testate Amoebae	148
	6.4.3 Peat Humification	154
	6.4.4 BSW Multi-Proxy Comparison	156
6.5	Malham Tarn	160
	6.5.1 Loss on Ignition	160
	6.5.2 Chironomids	162
CHAPTER 7.0 DISCUSSION		169-194
7.1	Introduction	169
7.2	BSW Inter-site Comparison	169
7.3	CI-T Inter-site Comparison	180
7.4	BSW - CI-T Comparison	184
7.5	Methodological Appraisal & Recommendations for Further Work	191
CHAPTER 8.0 CONCLUSION		195-197
	Appendix 1 Malham Tarn SCP Profile (Rose, unpublished data)	198
	Reference List	199-221

LIST OF FIGURES, TABLES AND PLATES

<i>FIGURES</i>	Page number
Figure 2.1 BSW Wet-shift Frequency Diagram	19
Figure 2.2 Chironomid Life Cycle	34
Figure 2.3 Instrumental Temperature (CET) & Precipitation (EWP) Comparison	50
Figure 3.1 Mismatching Mackareth-Livingstone Core LOI Values	59
Figure 3.2 MLT Matching Livingstone-Livingstone Core LOI Values	59
Figure 3.3 BLT Matching Livingstone-Livingstone Core LOI Values	60
Figure 3.4 Transfer Function Schematic	78
Figure 4.1 Field Site Location Map	81
Figure 4.2 Hulleter Moss Site Map	83
Figure 4.3 Hulleter Moss Field Stratigraphy	85
Figure 4.4 Bigland Tarn Site Map	86
Figure 4.5 Malham Tarn Moss & Malham Tarn Site Map	88
Figure 4.6 Malham Tarn Moss Stratigraphy Cross-Section	90
Figure 4.7 Malham Tarn Moss Field Stratigraphy	90
Figure 4.8 Malham Tarn Bathymetric Map	92
Figure 5.1 HUL Calibrated Radiocarbon Age Relationship	94
Figure 5.2 HUL SCP Concentration Profile	95
Figure 5.3 HUL Age-Depth Model	96
Figure 5.4 BLT Calibrated Radiocarbon Age Relationship	98
Figure 5.5 BLT SCP Concentration Profile	99
Figure 5.6 BLT Lead-210 Activity Profile	100
Figure 5.7 BLT Lead-210 Activity Profile (Logarithmic Scale)	100

Figure 5.8	BLT Age-Depth Model	103
Figure 5.9	MTM Calibrated Radiocarbon Age Relationship	105
Figure 5.10	MTM SCP Concentration Profile	105
Figure 5.11	MTM Age-Depth Model	107
Figure 5.12	MLT Calibrated Radiocarbon Age Relationship	109
Figure 5.13	MLT SCP Concentration Profile	110
Figure 5.14	MLT Lead-210 Activity Profile	111
Figure 5.15	MLT Lead-210 Activity Profile (Logarithmic Scale)	111
Figure 6.1	HUL Plant Macrofossil Diagram	114
Figure 6.2	HUL Plant Macrofossil DCA Biplot	117
Figure 6.3	HUL Plant Macrofossil BSW Reconstruction	119
Figure 6.4	HUL Testate Amoebae Diagram	121
Figure 6.5	HUL Testate Amoebae DCA Biplot	123
Figure 6.6	HUL Testate Amoebae Water Table Reconstruction	125
Figure 6.7	HUL Peat Humification	127
Figure 6.8	HUL BSW Proxy Comparison	129
Figure 6.9	HUL BSW Combined Proxy Plot	130
Figure 6.10	BLT Loss on Ignition Graphs	133
Figure 6.11	BLT Chironomid Diagram	135
Figure 6.12	BLT Chironomid Palaeotemperature Reconstruction	139
Figure 6.13	BLT Chironomid DCA Biplot	140
Figure 6.14	MTM Plant Macrofossil Diagram	142
Figure 6.15	MTM Plant Macrofossil DCA Biplot	145
Figure 6.16	MTM Plant Macrofossil BSW Reconstruction	147
Figure 6.17	MTM Testate Amoebae Diagram	149
Figure 6.18	MTM Testate Amoebae DCA Biplot	151
Figure 6.19	MTM Testate Amoebae Water Table Reconstruction	153
Figure 6.20	MTM Peat Humification	155
Figure 6.21	MTM BSW Proxy Comparison	157
Figure 6.22	MTM BSW Combined Proxy Plot	158

Figure 6.23	MLT Loss on Ignition Graphs	161
Figure 6.24	MLT Chironomid Head Capsule Concentration	162
Figure 6.25	MLT Chironomid Diagram	164
Figure 6.26	MLT Chironomid DCA Biplot	165
Figure 6.27	MLT Chironomid Palaeotemperature Reconstruction	166
Figure 7.1	HUL-MTM BSW Comparison	170
Figure 7.2	HUL-MTM Radiocarbon Error Envelopes	176
Figure 7.3	HUL-MTM BSW Comparison (Tuned)	177
Figure 7.4	BLT-Talkin Tarn CI-T Comparison	182
Figure 7.5	CI-T BSW Comparison	187

1.1	Introduction to the Project
1.2	Project Objectives, Scope & Deliverables
1.3	Project Organisation & Roles
1.4	Project Management & Communication
1.5	Project Risk Management
1.6	Project Monitoring & Reporting
1.7	Project Closure
2.1	Background & Context
2.2	Project Objectives
2.3	Project Scope
2.4	Project Organisation
2.5	Project Management
2.6	Project Risk Management
2.7	Project Monitoring & Reporting
2.8	Project Closure
3.1	Introduction
3.2	Background
3.3	Objectives
3.4	Scope
3.5	Organisation
3.6	Management
3.7	Risk Management
3.8	Monitoring & Reporting
3.9	Closure

TABLES

Page number

Table 2.1	NW European BSW Wet-Shift Timings	16-17
Table 2.2	Wet Shift Comparison Table	21
2.3	Possible Climate-Bog Wetness Scenarios and Palaeoclimatic outcomes	22
Table 3.1	Lake Core Details	60
Table 3.2	Test Results of Ultrasonic Chironomid Preparation Procedure	64
Table 4.1	Hulleter Moss Site Details	82
Table 4.2	Bigland Tarn Site Details	85
Table 4.3	Malham Tarn Moss Site Details	87
Table 4.4	Malham Tarn Site Details	91
Table 5.1	HUL Radiocarbon Measurements & Calibration	94
Table 5.2	HUL Linear Interpolation Equations & Accumulation Rates	95
Table 5.3	BLT Radiocarbon Measurements & Calibration	98
Table 5.4	BLT Linear Interpolation Equations & Accumulation Rates	102
Table 5.5	MTM Radiocarbon Measurements & Calibration	104
Table 5.6	MTM Linear Interpolation Equations & Accumulation Rates	106
Table 5.7	MLT Radiocarbon Measurements & Calibration	108
Table 6.1	HUL Plant Macrofossil Zone Descriptions	115
Table 6.2	HUL Plant Macrofossil DCA Details	118
Table 6.3	HUL Testate Amoebae Zone Descriptions	122
Table 6.4	HUL Testate Amoebae DCA Details	123
Table 6.5	HUL Wet Shift Comparison Table	131
Table 6.6	HUL Dry Shift Comparison Table	132
Table 6.7	BLT Chironomid Zone Descriptions	136
Table 6.8	BLT Chironomid DCA Details	141

Table 6.9	MTM Plant Macrofossil Zone Descriptions	143
Table 6.10	MTM Plant Macrofossil DCA Details	146
Table 6.11	MTM Testate Amoebae Zone Descriptions	150
Table 6.12	MTM Testate Amoebae DCA Details	152
Table 6.13	MTM Wet Shift Comparison Table	159
Table 6.14	MTM Dry Shift Comparison Table	160
Table 6.15	MLT Chironomid Zone Descriptions	163
Table 6.16	MLT Chironomid DCA Details	167
Table 7.1	HUL-MTM Wet Shift Match Points	174
Table 7.2	Comparison of tuned records with select palaeohydrology records	179
Table 7.3	BLT-Talkin Tarn Cool phase comparison	184

PLATES

Plate 4.1	Hulleter Moss Aerial Photograph	84
Plate 4.2	Malham Tarn Moss Aerial Photograph	89

ACKNOWLEDGEMENTS

I would like to thank my supervisors Prof. Keith Barber and Dr Paul Hughes for all their help and support throughout. I would also like to thank Michael Grant, Kieron Doick, Susanna Way, Tim Daley and Paul Coombes for assistance with fieldwork. Dr Mary Edwards provided useful lake coring advice early in the project and Prof. Rick Battarbee (University College London) provided just the right advice at a difficult time, both of which were invaluable.

Access to the field sites was granted by Dee Doe of the Hay Bridge Nature Reserve and Adrian Pickles of the Malham Tarn Field Studies Centre and the Bigland Estate. None of this work could have been carried out without their kind permissions.

Radiocarbon dates were provided by the Natural Environment Research Council Radiocarbon Laboratory without which this project would have not been possible. Particular thanks go to Dr Charlotte Bryant and Dr Mark Garnet for advice and support when all did not go to plan. ²¹⁰Pb dating was undertaken at the Geosciences Advisory Unit at the National Oceanographic Centre, Southampton. Particular thanks go to Dr Ian Crowdace and Dr Frances Rowlands for advice and assistance. Neil Rose provided helpful advice on SCP identification and provided his SCP profile from Malham Tarn for comparison with my data, both of which are very much appreciated

Many thanks to Steve Brooks (Natural History Museum) and Dr Pete Langdon (Exeter University) who both provided valuable help with chironomid identification. Steve Brooks also applied the chironomid transfer function and Prof. Dan Charman (University of Plymouth) the testate amoebae transfer function to my datasets for which I am very grateful. Dr Pete Langdon also provided his Talkin Tarn chironomid data with which to compare my records which greatly helped with the site interpretation.

Particular thanks must also go to Dr Michael Grant (Kingston University) who was an especially long suffering fieldwork assistant and who also kindly undertook pollen analysis on Malham Tarn and Malham Tarn Moss in an attempt to save the unsaveable. Proof reading and constructive criticism of draft work was kindly undertaken by Keith Barber, Paul Hughes, Leanne Franklin-Smith, Antony Blundell (University of Liverpool) and my girlfriend Zoë Hazell. Zoë was particularly good at the constructive criticism!

On a more personal note I would like to thank my parents and my sister who managed to resist the temptation to repetitively ask when I was going to get a real job and who have been tremendously supportive throughout this and all of my endeavours. Special thanks must also go to Zoë who keeps me on the straight and narrow and without whom life would be so much less fun.

I would like to finish by thanking Dr Paddy O'Sullivan who is inadvertently responsible for my foray into the world of palaeoecology.

TABLE OF ABBREVIATIONS

APF	Atlantic Polar Front
BLT	Bigland Tarn (Site Code)
BSW	Bog Surface Wetness
CCA	Canonical Correspondence Analysis
CET	Central England Temperature Series
CI-T	Chironomid Inferred Temperature
DCA	Detrended Correspondence Analysis
EWP	England and Wales Precipitation Series
HUL	Hulleter Moss (Site Code)
JJA	June July August (summer season)
LIA	Little Ice Age
MLT	Malham Tarn (Site Code)
MOC	Meridional Ocean Circulation
MTM	Malham Tarn Moss (Site Code)
MWP	Medieval Warm Period
NADW	North Atlantic Deep Water
NAO	North Atlantic Oscillation
OD	Ordnance Datum
SCPs	Spheroidal Carbonaceous Particles
SST	Sea Surface Temperature
THC	Thermohaline Circulation

1.0 INTRODUCTION

1.1 PROJECT RATIONALE

The production of independently derived multiproxy data is an established method of reducing uncertainties in palaeoclimatic records. This can be accomplished by cross validation of datasets, providing a means of corroborating events recorded at similar times and helping to discriminate between site-specific and climatically forced changes. In addition, carefully selected proxy combinations may help to develop our understanding of a particular climate-proxy linkage leading to improved interpretative power and confidence.

Peatland records have proved to be an extremely successful means of reconstructing terrestrial climatic change (Barber *et al.*, 1994; Charman *et al.*, 1999; Mauquoy & Barber, 1999; Hughes *et al.*, 2000; Chiverrell, 2001; Barber *et al.*, 2003; Langdon *et al.*, 2003; Blundell & Barber, 2005). The majority of these studies involve two main steps: 1) reconstruction of bog surface wetness (BSW) from proxy data, and 2) palaeoclimatic inference based on the BSW record (Charman *et al.*, 2004). Much research to date has focussed upon improving the first reconstructive step and a number of techniques are now well-established (Blackford & Chambers, 1993; Barber *et al.*, 1994; Woodland *et al.*, 1998). However, the second step – relating BSW to climatic parameters – is less well developed, and constitutes the focus of this project. Complications arise because BSW is in effect a balance between inputs and outputs from the bog system; in its simplest terms, a balance based on the interaction of precipitation and temperature. BSW must therefore be considered a composite measure of climatic variables.

The water balance is a crucial variable in determining raised bog functioning in terms of ecology and carbon store potential (Charman, 2002) and this balance is chiefly controlled by climate. An improved understanding of the climate-BSW relationship is therefore of key importance not only in improving interpretation of bog palaeoclimatic archives but also in predicting the potential effects of future climate change scenarios on peatland development, biodiversity and carbon storage.

Work involving comparisons of Little Ice Age (LIA) records and the analysis of long documentary climate series has suggested the hypothesis that over decadal and centennial timescales, the temperature signal is more coherent and is dominant over the spatially and temporally incoherent precipitation signal (Barber *et al.*, 1999; Barber *et al.*, 2000). This view was supported by findings that instrumental temperature and precipitation series were both (at certain times) strongly negatively correlated with reconstructed water tables, implying that temperature increases overcame precipitation increases and caused water tables to fall even during periods of increased precipitation (Charman & Hendon, 2000).

However, this was not entirely supported by comparison of summer June-July-August (JJA) temperature and precipitation data with reconstructed water table data (Charman *et al.*, 2004), where the strongest correlation was between summer precipitation and reconstructed water tables. Nonetheless, when water tables were compared to instrumental data averaged over the preceding 20-40 years to investigate whether the hydrological response was dependent on the direction of persistent climatic change, rather than short-term fluctuations, a strong correspondence was also found with summer temperature.

The aforementioned studies hint that the nature of the relationship between climatic parameters and BSW may vary depending on the timescale in question. Investigations to date have focussed on historical times primarily due to the availability of meteorological data, but some measure of the longer-term (centennial, millennial) relationship is clearly desirable.

Non-biting midges (Insecta: Diptera: Chironomidae) are sensitive environmental indicators and a number of studies have revealed temperature to be the most important environmental variable in determining their modern distribution and abundance (Walker & Mathewes, 1989; Walker *et al.*, 1991b, 1992). The adoption of a transfer function approach to palaeotemperature reconstruction using fossil chironomid head capsules and modern tolerances has proved remarkably successful for Late-glacial sequences (e.g. Walker *et al.*, 1991a; Brooks & Birks, 2000, 2001) and shows promising results for the lower amplitude temperature variability of the

Holocene (Larocque & Hall, 2003; Langdon *et al.*, 2004). In addition to providing a means of simple cross-validation of palaeoclimatic records, a comparison between CI-T and BSW records from paired lake and bog sites will provide a rigorous empirical test of the strength of the relationship between temperature and BSW.

1.2 Aims & Objectives:

- The primary aim of this thesis is to investigate the nature of the climatic signal recorded in raised bogs and in particular, to test the hypothesis that temperature, rather than precipitation, is the main climatic signal recorded by changes in bog surface wetness over centennial to millennial timescales;

To facilitate the primary aim a key objective will be to test the ability of chironomid-inferred temperature reconstructions to reflect relatively low-magnitude temperature changes. The test will focus on detection of the Little Ice Age cooling and comparison of the near-surface record with instrumental data.

...the ... hydrological conductivity of the ...
...the ... conductivity of the ...
...the ... conductivity of the ...
...the ... conductivity of the ...
...the ... conductivity of the ...

...the ... conductivity of the ...
...the ... conductivity of the ...
...the ... conductivity of the ...
...the ... conductivity of the ...
...the ... conductivity of the ...

2.0 BACKGROUND & CONTEXT

2.1 INTRODUCTION

This chapter has been split thematically. The first section will deal with raised bogs as palaeoclimatic archives; the nature of palaeoclimatic reconstructions from peat will be described along with a brief discussion of the strengths and weaknesses of the proxy techniques most commonly employed. The climate-bog hydrology relationship will be a key area of discussion. Subsequent sub-chapters will summarise the relevant aspects of lakes as archives of palaeoenvironmental information and discuss the strengths and weaknesses of chironomid analysis. The theory and application of the statistical methods employed will also be discussed as well as the methods of comparing and synthesising palaeoclimatic records. Mechanisms of North Atlantic climate variability will also be summarised to place the project in its wider context.

2.2 RAISED BOGS: AN OVERVIEW

Raised bogs are peatlands which are characterised by a distinctly convex profile or peat dome, the surface topography of which is largely independent of the underlying mineral soil contours (Lindsay, 1995). The raised structure is formed as a result of the preservation and accumulation of the vegetation which once lived on the bog surface to produce thick organic deposits called peat. These deposits are not uniform and can be characterised in simple terms by the low hydraulic conductivity of the main bulk of the deposit (the catotelm) and the relatively high conductivity of the surface vegetation and immediately underlying, incompletely decayed peat (the acrotelm). The physical properties of these two zones and the rate of recharge are thought to account for the resultant dome structure. This concept originated from the groundwater mound hypothesis of Ingram (1982).

Peat accumulation is primarily dependent upon the maintenance of high near-surface water tables, which prevents the growth of aerobic microbes so that only the inefficient, anaerobic forms are active (Ivanov, 1981). High water tables are created and maintained by *Sphagnum* mosses and by the low hydraulic conductivity of the underlying catotelmic peat (Brown *et al.*, 1989; Rycroft *et al.*, 1975). Preservation is further aided by the ability of *Sphagnum* to extract nutrients such as potassium and

magnesium from the surrounding water, releasing hydrogen ions and thus acidifying the water (Clymo, 1984). As a result of the organic material accumulated, the surface of a raised bog is isolated from the regional water table and therefore directly dependent on atmospheric sources for moisture and nutrient inputs leading to their description as 'ombrotrophic' (meaning precipitation-fed) and 'oligotrophic' (meaning poorly-nourished). Barber (1981) demonstrated that microtopographic features previously thought to continually change and develop through autogenic cycles (Osvald, 1923) were often in fact more persistent, relatively long-lived features.

2.3 BOGS AS PALAEOCLIMATIC ARCHIVES

Due to the unique structure outlined above, raised bog hydrology is directly coupled with climatic conditions. Bog hydrology and in particular surface wetness is a dominant influence on community structure and composition and so a strong relationship exists between climate and bog surface ecology. By retracing this climate – bog hydrology – bog community relationship, palaeoclimatic inference can be made. The majority of peat-based palaeoclimatic studies therefore involve two main steps:

- 1) Reconstruction of BSW from proxy indicators, and;
- 2) Palaeoclimatic inference based on the BSW record.

A number of techniques for reconstructing BSW have been developed, the most widely used of which are; plant macrofossil analysis (Barber, 1981; Barber *et al.*, 1994; Barber *et al.*, 1998; Hughes *et al.*, 2000; Mauquoy & Barber, 1999b) colorimetric peat humification (Blackford & Chambers, 1991; Blackford & Chambers, 1995; Chambers *et al.*, 1997) and testate amoebae analysis (Charman *et al.*, 2000; Hendon *et al.*, 2001; Warner & Charman, 1994; Woodland *et al.*, 1998). In recent years there has also been an increasing trend towards combining two or more of these techniques to provide multiproxy records (Blundell & Barber, 2005; Charman *et al.*, 1999; Chiverrell, 2001; Langdon *et al.*, 2003; Mauquoy & Barber, 1999a). Some progress has also been made in establishing regional indexes of BSW change for northern England and Scotland (Charman *et al.*, 2006; Langdon & Barber, 2005).

The second stage of reconstruction, interpretation of BSW as a measure of past climates, is reliant upon a climate-bog hydrology response model. Palaeoclimatic interpretation is therefore critically dependent on the accuracy and comprehensiveness of this model. In its most basic terms a relatively direct relationship is assumed to exist between climate and bog hydrology because bogs are entirely dependent on meteoric sources of water for recharge. While there is strong evidence that water tables are directly influenced by climate the nature of the relationship is not well known. In particular, the relative roles of temperature and precipitation in governing water tables over the long term are unclear. The next few sub-chapters will discuss these two reconstructive steps in more detail, focussing particularly on the second step which has until now had less attention than the first and constitutes the main focus of this project.

2.4 BSW RECONSTRUCTION (STEP 1)

Three techniques are in regular use for reconstructing BSW (plant macrofossil, testate amoebae and peat humification analysis). Since these methods are now well established with all three being widely applied in a large number of investigations a detailed description and explanation of, for example, the hydrological tolerances of each plant or testate amoebae taxon found on ombrotrophic bogs is not necessary here. Instead, the discussion will be on a more functional level outlining the theoretical basis and highlighting the main assumptions, strengths, and limitations of the three techniques.

2.4.1 PLANT MACROFOSSIL ANALYSIS

Plant macrofossil analysis is perhaps the most obvious technique to utilise on raised bogs because the peat is composed almost entirely of plant remnants. Plant macrofossils are used as a proxy for palaeohydrology on the premise that the distribution of plants living on the bog surface is controlled primarily by BSW. Since the vast majority of deposition on raised bogs occurs *in situ*, the fossil assemblages can be assumed to be a direct consequence of the vegetation which once grew on the surface, with the additional complication of post-depositional processes. The accuracy of BSW reconstruction is therefore dependent on the sensitivity of plant

species to changes in BSW over and above other environmental variables (e.g. nutrient availability and competition) and the extent to which the fossil assemblage reflects the original living community.

The intimate link between ecology and hydrology of peatlands is well recognised and the term ecohydrology was coined by Göttlich (1977 [in] Charman, 2002) to describe their covariance. This relationship is strongest during the growing season when plants are active such that plant distribution is primarily a function of summer water tables. Numerous studies have demonstrated the strong relationship between depth to water table and bog vegetation (Andrus *et al.*, 1983; Malmer, 1986; Miserere *et al.*, 2003; Ratcliffe & Walker, 1958). The response of individual plants to the water table gradient is most likely a function of their ability to cope with waterlogging but is also influenced by competition between species (Charman, 2002). This competitive element goes some way to explaining the observed threshold response to changing hydrological conditions. Additionally certain species have very wide tolerances and once they have achieved dominance they are able to prevail through widely fluctuating conditions; *Sphagnum fuscum* exhibited this tendency in the study of Nordans Pond Bog in Newfoundland by Hughes *et al.* (2006). Plants therefore respond to changing water tables but they have a degree of complacency to low-magnitude and short-duration changes. As indicators of BSW plants can mask small-scale changes and lag behind larger-scale changes; both effects have been observed in multiproxy palaeoecological investigations (Blundell & Barber, 2005; Hughes *et al.*, 2006).

Fossil assemblages are always a depleted reflection of the original community and the extent of depletion is dependent on the conditions of deposition and the attributes of the species present. The preserving characteristics of raised bogs have already been noted (Section 2.2) but the speed at which material makes the transition into these conditions will depend upon the microtopographic position in respect to the water table and the more general level of the water table. This is discussed further in Section 2.4.3 in relation to peat humification. Various attributes of the species present can also have important consequences for preservation. Some plant groups are simply more susceptible to microbial decay than others, so for example, while

members of the lichen genus *Cladonia* are common components of bog communities, they break down readily and are rarely if ever preserved to a recognisable degree below ~ 30 cm in the peat profile. The sedge *Eriophorum vaginatum*, by contrast, is very resistant to decay and consequently is over-represented in the fossil peat record.

Different growth forms can also affect the ease and speed at which plant material is incorporated into the peat. Ericaceous species such as *Calluna vulgaris* and *Erica tetralix*, which have a shrub-like growth form, are relatively poorly represented in the peat profile, only preserving well if they fall into pools or waterlogged ground (Grosse-Brauckmann, 1986). Near-ground and below-ground plant components (predominantly roots) tend to preserve well since they are usually already in waterlogged conditions when they die. This tends to lead to an over representation of roots which are not always diagnostic to a high taxonomic level and are additionally problematic because they penetrate into 'earlier' stratigraphy and are incorporated into otherwise older peat.

Some errors and generalisations are inevitably made during identification and abundance estimation of the subfossil plant remains. Recounting of samples without referring to previous results reveals that it is possible to establish consistent results although systematic errors may well remain. Comparison of datasets produced by different workers, where the errors may be systematically different, is therefore likely to be most problematic in this regard.

While plant macrofossils exhibit some complexity in their relationship with water tables and there are some issues of selective preservation, large changes in water tables are generally reflected in the plant communities growing on the bog surface and the resultant peat composition. However plant macrofossils may at times display complacency to changes in BSW if the dominant species is able to tolerate wide hydrological conditions.

2.4.2 TESTATE AMOEBAE ANALYSIS

Testate amoebae in the superclass Rhizopoda are a group of protozoa which are well adapted to the wet conditions that prevail on ombrotrophic bogs (Warner & Charman, 1994). The bodies of these animals are contained in tests (shells), which are incorporated and preserved with the organic detritus as it becomes peat and are readily recoverable from fossil peat deposits (Warner & Charman, 1994).

Testate amoebae have been used as palaeoenvironmental indicators for over 100 years (Lindberg, 1899, [in] Tolonen, 1986). Renewed interest in their application was stimulated by advancements in the understanding of their modern ecology (Bobrov *et al.*, 1999; Charman & Warner, 1992, 1997; Woodland *et al.*, 1998) and statistical techniques to aid interpretation (Birks, 1995, 1998; ter Braak & Juggins, 1993).

Investigations into the modern ecology of testate amoebae have shown great variation in small-scale distribution patterns and work using multivariate statistical techniques (primarily Canonical Correspondence Analysis, CCA) revealed a close relationship between soil water conditions and species distribution (Warner & Charman, 1994; Woodland *et al.*, 1998). This relationship is strongest during the growing season when amoebae are most active. The principal reason for the link between testate amoebae and mire hydrology is that the water film on the host substrate is the living space for amoebae (Charman *et al.*, 2000). This primary link between testate amoebae abundance and diversity and bog hydrology allows a reconstruction of summer water table depth based on testate amoebae assemblages.

Testate amoebae systematics is not straightforward and this is largely because as with any organism which is uniparental, species definition is imprecise and depends necessarily upon morphological criteria (Bobrov *et al.*, 1999). This has led to various interpretations of testate amoebae taxonomy, with workers differing in opinion as to which species should be grouped under one taxon and which should be divided (Bobrov *et al.*, 1999) While these differences of opinion are legitimate, the description of ecological requirements for the reconstruction of past environments requires only the separation of taxa which have clearly different niches (Bobrov *et al.*, 1999). A

clear and reliable taxonomy is therefore required to ensure the replicability and comparability of results by different workers and this has been largely provided by Charman *et al.* (2000).

Testate amoebae appear to be particularly useful in providing quantitative data and this is largely because of the relatively large number of taxa which occur on raised bogs, typically around 15 taxa per sample (Woodland *et al.*, 1998) compared to somewhere between three and five plant taxa per sample (this study). Developments in testate amoebae identification, modern ecology and the use of transfer functions have allowed palaeo-water tables to be predicted to within ± 3.5 cm and palaeomoisture to within $\pm 4\%$ (Woodland *et al.*, 1998).

There are, however, some problems with selective preservation of tests. For example, the genus *Euglypha* is conspicuous by its almost complete absence from the fossil record. A second issue is the availability of good modern analogues. There are a few taxa, perhaps most notably *Diffflugia pulex* and *Hyalosphenia papilio* which have hydrological requirements that are ambiguous as a result of insufficient modern examples and apparently variable ecological requirements respectively (Blundell & Barber, 2005; Hughes *et al.*, 2006). Modern analogue issues are currently under investigation under the ACROTELM project (Charman *et al.*, in press).

2.4.3 PEAT HUMIFICATION 'COLORIMETRIC TECHNIQUE'

In addition to analysing specific subfossil remains, palaeoenvironmental information can be derived from analysing the peat matrix as a whole. The property most directly influenced by, and therefore related to, water tables is the degree of preservation or more specifically the rate and extent of decomposition. Decomposition is closely related to water tables because aerobic decomposition, which occurs in acrotelmic aerated peats (above the water table), is much more efficient than anaerobic decomposition, which occurs in the catotelmic peat below the water table where there is low oxygen availability. The length of time that floral and faunal remains spend above the water table therefore strongly influences the type and efficiency of microbial activity and subsequently the degree of decomposition that can occur. It

follows that when high water tables are maintained plant litter makes the transition from aerobic to anaerobic conditions more quickly and is subsequently better preserved. Whereas, when low water tables predominate, the opposite is true. Although bacterial activity occurs year round it is more rapid during the warmer months. This combined with the tendency for bogs to become fully saturated during the winter months (Section 2.5.2) means that the decomposition signature is primarily related to summer water tables.

Blackford & Chambers (1993) reviewed many of the possible methods of 'measuring' the degree of decomposition of the peat matrix favouring chemical extraction using 10% sodium hydroxide (NaOH) and went on to recommend a method for replicable NaOH extraction and colorimetric measurement of humic acids from peats. This procedure, commonly referred to as the 'colorimetric technique' is the most widely used method, having the advantage of being relatively quick, simple and applicable to both raised and blanket bogs (Chambers *et al.*, 1997).

The colorimetric method is based on the premise that 'humic acids' are produced during the decomposition of organic material and their proportion increases as peat decomposes. Solvents can be used to extract these 'humic acids' from peat and NaOH has been demonstrated to offer a satisfactory balance between efficient extraction and minimal structural alteration (Blackford & Chambers, 1993) although this is now in some dispute (Caseldine *et al.*, 2000). 'Humic acids' are dark brown in solution and the darkness of the NaOH extract is assumed to be related to the degree of humification. The concentration of humic acids can then be measured using a spectrophotometer in accordance with the Beer/Lambert Law which states that light absorbance by a solution is linearly related to the concentration of the solute (within a certain concentration range). However, this is complicated because 'humic acids' are in fact composed of a number of compounds, the relative ratio of which can influence the darkness of the resultant solution. Transmission readings are therefore not really concentration measurements but a kind of 'objective' measure of the relative degree of decomposition. Caseldine *et al.* (2000) used luminescence spectroscopy to investigate the presence/absence and relative importance of the differing absorbing, fluorescing compounds which, as a whole, produce the humification signal as defined

by the colorimetric technique. The study revealed that the NaOH extraction considerably altered the composition of organic acids but nevertheless concluded that the standard colorimetric technique “*May enable the separation of the relative difference in organic matter decomposition between samples especially if the amount of initial decay varies significantly*” (Caseldine *et al.*, 2000).

The colorimetric humification technique therefore remains useful but is perhaps overdue for development since a number of techniques exist which might improve understanding of the peat decay processes e.g. luminescence spectroscopy (Caseldine *et al.*, 2000) and Near-infrared reflectance spectroscopy (NIRS) (McTiernan *et al.*, 1998). The NaOH extraction procedure seems particularly in need of review but is beyond the scope of this investigation.

Additional to methodological issues a plant species effect is almost certainly present in the humification signal, resulting from changing plant community structure in response to changing hydrological conditions. Blackford & Chambers (1993) argue that the response of bog flora to climatic change should enhance rather than confuse the proxy BSW record obtained. However, this is not necessarily the case, for example *Eriophorum vaginatum* which is indicative of relatively dry conditions is very resistant to decay and may reduce the apparent degree of humification. Changes in botanical composition of the peat certainly have the potential to complicate interpretation, possibly delaying humification response and affecting the apparent magnitude of change through processes like differential decay and threshold community response.

Humification offers a relatively quick method of reconstructing BSW, which allows high-resolution contiguous sampling and is a useful addition to the other techniques. Caution should be taken however when interpreting humification records without augmentation by at least one other technique.

2.4.4 PEATLAND MULTIPROXY RECONSTRUCTIONS

Plant macrofossil, testate amoebae and humification derived palaeo-data are relatively independent from one another except through their common association with BSW. The production of multiproxy reconstructions utilising three or more proxies provides a means of cross-validating each proxy by comparison with the others. This increases the confidence with which significant changes can be identified and distinguished from ecological and methodological noise. In recent years, a number of multiproxy BSW records have been produced (Charman *et al.*, 1999; Chiverrell, 2001; Langdon *et al.*, 2003) but exactly how these differently derived indicators, which are not simply related, should be summarised remains an area for development. The added layer of complexity can make interpretation difficult and it was partly for this reason and partly the relative scarcity of multiproxy data which led Charman *et al.* (2006) to utilise only one proxy (testate amoebae) in the development of their regional BSW index. The most recent, and so far the most useful, method for combining these datasets was developed by Blundell & Barber (2005). The three datasets were normalised and plotted on the same graph, then through a subjective but standardised procedure an 'inferred line' was produced based on careful scrutiny of each reconstruction and the level of 'agreement' between the three curves. One of the main advantages of this approach is that it produces a single summary curve against which other datasets can be easily compared. It also enforces careful analysis of the various curves to identify potential complacency in the records.

Perhaps the primary limitation of combining records however is that the data are in a sense reduced to the lowest common denominator. For example quantitative testate amoebae data are combined with more qualitative data and the result is a semi-rather than fully-quantitative inference.

2.4.5 INTRA-SITE BSW REPLICABILITY

Demonstration of the replicability of the main shifts in BSW between profiles from a single site provides evidence that reconstructions from a single core are broadly representative of bog-wide changes, which might in turn be climatically driven.

An intra-site test of the variability in BSW changes between profiles was first undertaken by Barber *et al.* (1998) who found that multiple cores from a site could yield similar ('replicable') records. A careful sampling strategy was advocated since microtopography was found to affect climatic sensitivity. In general *Sphagnum* lawns were found to be more sensitive to climatic variation than drier hummock communities which hold 'complacent' records of climatic change (*sensu* Barber, 1994). Barber *et al.* (1998) went on to suggest a standard approach to site selection and sampling for optimising core sensitivity. It is noteworthy however that this method does not completely negate issues of varying microtopographic sensitivity, and differences between core stratigraphies are probably at least partly attributable to differing microtopography at the time of deposition. This was one of the issues identified by Charman *et al.* (1999) who produced a multi-proxy reconstruction of BSW on two closely spaced replicate cores and found that many of the changes were represented in both cores, but they also observed that one of the cores was much less variable prior to 1450 cal. BP than the other and explained this in terms of microtopographic differences which were no longer apparent at the surface. A second point made by Charman *et al.* (1999) was that the cores became more similar over time and this was explained in terms of mire development processes, with the implication that more recent records – or at least those from well developed fully ombrotrophic stratigraphy – are likely to hold the most complete and accurate climatic reconstructions. Hendon *et al.* (2001) also found an "impressive degree of similarity" in water table records derived from testate amoebae analysis within sites in spite of the fact that cores were deliberately selected to represent geographical extremes. Together with earlier work undertaken on open peat faces by among others, van Geel (1978) and Barber (1981), where it was possible to observe distinct stratigraphic layers that could be traced for several hundred metres (Barber *et al.*, 1998) there is a strong case supporting the idea that one or two cores can be broadly representative of bog-wide changes.

2.4.6 INTER-SITE BSW REPLICABILITY

A number of investigations into between-site variability of peat profiles have also been carried out, revealing similar changes in peat stratigraphy at a number of sites at local (Barber *et al.*, 1998; Hendon *et al.*, 2001; Mauquoy & Barber, 1999b, 2002) and

regional scales (Barber *et al.*, 2003; Barber *et al.*, 2000; Blackford & Chambers, 1991). Demonstration of inter-site replicability of changes in inferred BSW conditions is important because it provided a means of distinguishing between regional climatic and local site-specific variations. However Hendon *et al.* (2001) caution that the definition and identification of replicability must be based on an understanding and acceptance of the margins of error involved in both chronology and BSW reconstruction. This is particularly true when utilising data from multiple studies.

While comparisons between a few sites demonstrate that similar records can be retrieved from within a regional setting and have the advantage that consistent methods are employed, it is logical to expand the comparison to include records from a number of published studies. This has been attempted to some extent by a number of authors (e.g. Charman *et al.*, 1999; Hendon *et al.*, 2001; Mauquoy & Barber, 1999b). The first systematic and comprehensive, if rather tentative, comparison was made by Hughes *et al.* (2000) which was then added to by Barber *et al.* (2003). A more focussed comparison of northern England and the border regions was made by Barber & Charman (2003). These comparisons all used a tabular format as a means of compiling dates of wet-shifts from raised and blanket bog studies undertaken in Britain, Ireland and some in NW mainland Europe. Table 2.1 encompasses data from the aforementioned papers with some additional studies and is a comprehensive list of the BSW records of British, Irish and some NW mainland European sites to date. The format follows closely that of Hughes *et al.* (2000) but with the data deliberately limited to cover only the latter part of the Holocene. The Late Holocene was targeted since it is of primary relevance to this investigation and is the most intensively studied period. It therefore provides a larger dataset to test whether shifts to wetter conditions have been detected synchronously at different sites. Table 2.1 displays the estimated dates (cal. BP) of wet-shifts, defined as the onset of wetter mire conditions as interpreted by different authors subjectively, grouped into columns of around the same time. Most dates are derived by interpolation between radiocarbon dates and rounded to the nearest 50 years to avoid the suggestion of spurious precision. Nevertheless, the errors are likely to be larger than those of the dated events but are not shown as they are not easily quantifiable.

Table 2.1: British, Irish and Mainland NW European BSW Wet-shift Timings

SITES & REFERENCES		WET-SHIFT TIMINGS (cal. BP, rounded to the nearest 50 years)										
Draved Mose (Aaby, 1976)		c. 650 c. 450	c. 950		c. 1500	c. 1700		c. 2250	c. 2550	c. 3000	c. 3350	c. 4000 c. 4300 c. 4600
Engbertsdijksveen (van Geel, 1978)										c. 2850 c. 3020	c. 3750	c. 4350
Bourtangerveen (Dupont, 1986)							c. 1950				3300-3650	c. 4450
Faulshaw Moss, Heslington Moss, White Moss North, White Moss South, (Wimble, 1986)		c. 600	c. 800	c. 1050	c. 1350 c. 1500	c. 1700		c. 2250 c. 2250		c. 2900 c. 2900 c. 2900	c. 3400 c. 3400	c. 4300 c. 3800
NW Europe (Haslam, 1987)				c. 1150		c. 1850			c. 2550			c. 4200
20 bogs from N & C Norway (Nilssen & Vorren, 1991)	c. 400		c. 700 c. 850	c. 1150	c. 1400	c. 1700	c. 1950	c. 2250 c. 2450		c. 2800 c. 3100	c. 3350	c. 3800 c. 4300 c. 4700
Brecon Beacons Harolds Bog Migneint Letterfrack Wood Moss (Blackford & Chambers, 1991; 1995)	c. 300	c. 500 c. 550			1500-1210 1535-1160 1395-1220 1400-1260 1400-1210		c. 1900					
Bolton Fell Moss (Barber, 1981; Barber <i>et al.</i> , 1994)	c. 200	c. 500		c. 1000 c. 1170	c. 1300			c. 2200		c. 2900	c. 3600	c. 4350
Isosuo, Tremanskarr Kantosuo (Korhola, 1995)												c. 4300
Engbertsdijksveen (van Geel <i>et al.</i> , 1996)									2750- 2450			
Abbeyknockmoy (Hughes, 1997)											c. 3500	
Talla Moss (Chambers <i>et al.</i> , 1997)		c. 550		c. 1100		c. 1700	c. 1950	c. 2250	c. 2600		c. 3450	
Wester Ross - composite A Wester Ross - Composite B (Anderson, 1998)				c. 1000 c. 1000						c. 3000 c. 2800	c. 3900 c. 3500	
BB in Tragill Basin (Baker <i>et al.</i> , 1999)	c. 100 c. 400		c. 750		c. 1250		c. 1850					
Border Mires (Mauquoy & Barber, 1999a, b)	c. 200	c. 550	c. 850	c. 1050	c. 1400	c. 1750	c. 2000 c. 1950	c. 2150	c. 2550 c. 2700			
Coom Rigg Moss (Charman <i>et al.</i> , 1999)	c. 100	c. 450 c. 600	c. 850	c. 1000	c. 1350 c. 1550			c. 2150	c. 2700	c. 2900	c. 3500	

Table 2.1: British, Irish and Mainland NW European BSW Wet-shift Timings (Continued)

SITES & REFERENCES		WET-SHIFT TIMINGS (cal. BP, rounded to the nearest 50 years)											
Walton Moss (Hughes <i>et al.</i> , 2000)	c. 100 c. 350					c. 1450	c. 1750		2320-2040	3170-2860		c. 3500	4410-3900
Coom Rigg Moss & Butterburn Flow (Charman & Hendon, 2000)			c. 950						c. 2100	c. 2850		c. 3700	c. 4400
Kentra Moss (Ellis & Tallis, 2000)	c. 350	c. 600	c. 850	c. 1150	c. 1400				c.2150	c. 2550		c. 3250	
Fallahogy Bog (Barber <i>et al.</i> , 2000) Moine Mhor	c. 300 c. 300		c. 950	c. 1250		c. 1350		c. 2000					
May Moss (Chiverrell, 2001)	c. 250-150	550-330 c. 600-500		1280-970	1400-1300								
Coom Rigg Moss (Hendon <i>et al.</i> , 2001) Butterburn Flow The Wou	c. 400	c. 700	c. 800	c. 1100	c. 1500	c. 1650					c. 2800	c. 3450 c. 3850	
Traligil Basin (Charman <i>et al.</i> , 2001)	c. 400		c.750	c. 1250				c. 1850					
Walton Moss (Mauquoy <i>et al.</i> , 2002) Lille Vildmose	c. 350 c. 350	c. 500 c. 500	c. 750										
Bolton Fell moss Mongan Bog Abbeyknockmoy (Barber <i>et al.</i> , 2003)		c. 620 c. 700 c. 450 c. 600 c. 700		c. 1000	c. 1400				c. 2200 c. 2350	c. 2450 c. 2600	c. 2900 c. 3000	c. 3200 c. 3600 c. 3750	c. 4000 c. 4300 c. 4400 c. 4600
Temple Hill Moss (Langdon <i>et al.</i> , 2003)	250-150										2800-2450	c. 3400 c. 3850	c. 4500
Tore Hill Moss, Strathspey (Blundell & Barber, 2005)	c. 300		c. 850	c. 1250	c. 1400 c. 1525			c. 2000			c. 2500		

Age ranges = two sigma range, given when shifts are dated directly

Age ranges represent the 2σ range of calibrated radiocarbon dates and indicate that a shift has been dated directly.

Traditionally it is wet rather than dry-shifts that have been targeted because of concerns that bog growth may lead directly to drier conditions and a cessation of peat accumulation, thereby implying that dry phases are likely to be autogenically driven and may also represent hiatuses (Aaby, 1976; Tallis, 1983). These concepts of dominant autogenic bog processes have long since been overturned (Barber, 1981) and both wet and dry-shifts can be considered equally likely to be climatically driven. However, arguably through cultural or intellectual inertia, wet-shifts have maintained favour and the majority of studies to date have focused on wet-shifts. In addition centennial to millennial-scale climatic changes during the Holocene are believed to have been characterised primarily by climatic deteriorations (Magny *et al.*, 2003). On this basis, the comparison of wet-shifts should pick up much significant climatic variability and offers a good starting point with which to assess the coherence of the palaeoclimatic picture emerging from peatlands. However, focussing on wet-shifts excludes the possibility of contradictory records where, for example, one record infers a wet-shift and the other a dry-shift. Without the inclusion of dry-shifts, the null hypothesis would simply be that there is no significant similarity between the onset dates of wet-shifts between records.

Analysis of a regional dataset centred on Northern England (using data included in Table 2.1) by Barber & Charman (2003) revealed wet-shifts to have occurred around the following dates: 250, 600, 850, 1100, 1400, 1700, 2150, 2650, 2900, 3500 and 4400 cal. BP. In order to see if any structure exists in the BSW dataset and to try to sidestep problems of mutual reinforcement of shift dates Fig. 2.1 was produced; it summarises the data in Table 2.1 and was plotted to provide a more objective indication of whether wet-shift dates cluster around certain points in time and whether these points correspond with the published 'expected' dates listed above. Fig. 2.1 is a simple frequency plot, each bar represents the number of wet-shifts at a given point in time so that in simple terms the larger the bar the greater the number of records which detected a shift at that time. If BSW changes are driven by climate then shifts would be expected to concentrate around certain time periods.

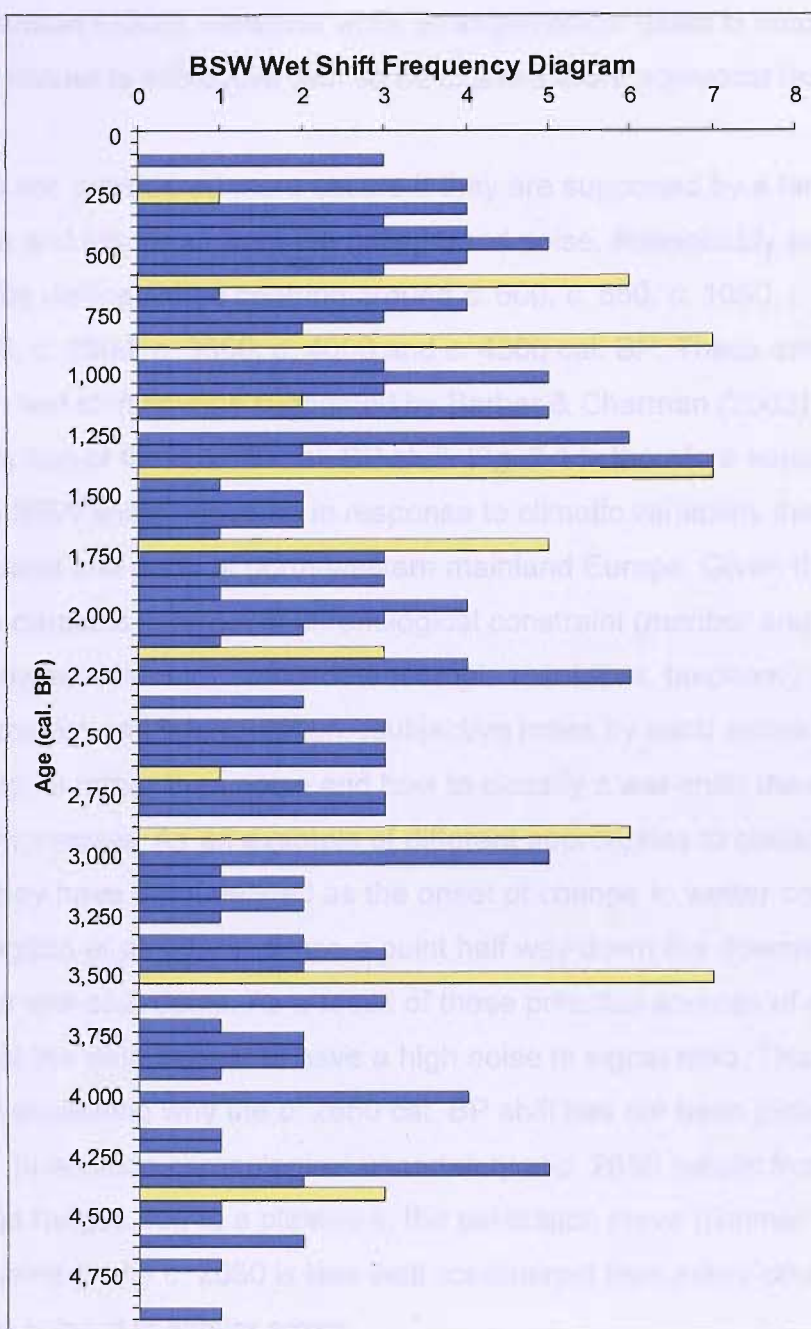


Fig. 2.1: Temporal frequency diagram of British, Irish and NW mainland European BSW shifts towards wetter conditions. Bar length is proportional to the number of shifts recorded at a given time. Yellow bars represent the time periods highlighted by Barber & Charman (2003) as key periods of increased wetness.

At first glance, probably the most noticeable aspect of Fig. 2.1 is that wet-shifts have been recorded at almost every 50 year interval throughout the last c. 5000 years in the 27 studies included. This is not immediately encouraging but on closer inspection there are a number of date clusters which can be compared to the timings noted by

Barber & Charman (2003). However while arrangement of dates is automatic what constitutes a cluster is subjective with some clusters more equivocal than others.

Date clusters are considered more secure if they are supported by a large number of investigations and stand out from the background noise. Reasonably secure wet shift clusters can be distinguished centring around *c.* 600, *c.* 850, *c.* 1050, *c.* 1350, *c.* 1700, *c.* 2250, *c.* 2900, *c.* 3500, *c.* 4000 and *c.* 4300 cal. BP. These dates correspond very well with wet shift timings suggested by Barber & Charman (2003) (Table. 2.2) with the exception of the *c.* 2650 cal. BP shift. Fig. 2.1 is therefore supportive of synchronous BSW shifts occurring in response to climatic variability throughout much of Britain, Ireland and parts of north-western mainland Europe. Given the variable quality of the datasets in terms of chronological constraint (number and type of radiocarbon measurements), proxy data (sample resolution, taxonomy and use of supportive proxies) and interpretation, (subjective ideas by each author on what constitutes signal rather than noise and how to classify a wet-shift) the similarity is particularly impressive. As an example of different approaches to classification of wet-shifts, here they have been defined as the onset of change to wetter conditions whereas Langdon *et al.* (2003) chose a point half way down the downward limb of the curve for their wet-shift dates. As a result of these potential sources of error it is not surprising that the data appear to have a high noise to signal ratio. This also goes some way to explaining why the *c.* 2650 cal. BP shift has not been picked out as a clear cluster. In addition chronological uncertainty at *c.* 2650 results from wide calibrated age ranges due to a plateau in the calibration curve (Reimer *et al.*, 2004), possibly explaining why *c.* 2650 is less well constrained than many other shifts which are otherwise subject to similar errors.

The most impressive clustering of shifts occurs around *c.* 1300 to 1400 cal. BP and is particularly persuasive since there are seven directly ¹⁴C dated shifts where errors can be quantified (see Table 2.1). While this is good support for the Dark Ages deterioration the relative strength of the shift may be a little misleading as it might partially reflect the concentration of study over this timescale.

Table 2.2: Wet-shifts

Barber & Charman	Clusters from Fig 2.1
c. 4400	c. 4300
---	c. 4000
c. 3500	c. 3500
c. 2900	c. 2900
c. 2650	---
c. 2150	c. 2250
c. 1700	c. 1700
c. 1400	c. 1350
c. 1100	c. 1050
c. 850	c. 850
c. 600	c. 600
c. 250	---

To conclude, Fig. 2.1 appears to reveal that shifts do cluster around key points in time, suggesting that there are shifts which are well represented at sites from a wide geographical range. This strongly supports the idea of climatic influence on bog hydrology. However errors already discussed blur the signal considerably, in fact given these potential uncertainties it is impressive that clusters are picked out at all. While existing data provides encouraging evidence of a climate-bog hydrology relationship it seems that if future palaeoclimatic evidence is to make any advancement in pinpointing the timing and extent of these shifts, then simple replication of the same type of investigations at new sites will meet with limited success. Instead, future research will need to use where possible a multiproxy BSW reconstruction to maximise the security of the reconstruction, focus dating on identified shifts using (the now widely available) AMS ¹⁴C dating of macrofossil components and wiggle-match dating and tephrachronology to provide as secure a chronology as possible. It would also be advantageous to collate raw data sets so that interpretation can be uniform; this offers a simple means of removing a whole layer of interpretative uncertainty.

2.5 CLIMATE-BSW RELATIONSHIP (STEP 2)

As has already been established, broadly speaking BSW is the result of the interplay between temperature and precipitation. However, the nature and extent of the hydrological response of a raised bog to climatic change will be dependent upon:

1. The nature of the relationship between the climatic variables themselves i.e. are temperature and precipitation covariant or are they relatively independent, and can this relationship change spatially and temporally?
2. The sensitivity of bog hydrology to changes in each of the climatic parameters. Some autogenic processes may lead to greater sensitivity to one variable than to the other.

The interplay between these two factors results in a number of possible climate-BSW response scenarios, summarised in Table 2.3 and evidence of the likely nature of these relationships is discussed below in Sections 2.5.1 & 2.5.2.

Table 2.3: Possible Climate-Bog wetness scenarios and palaeoclimatic outcomes

Temp. Precip. Relationship	Climate bog relationship	BSW Outcome
Temp & Precip are positively correlated	Bog wetness response is unbiased	(1) Variables partially cancel each other out and changes are therefore significantly dampened
	Bog respond primarily to temperature	(2) BSW will follow temperature changes closely (slightly dampened)
	Bog respond primarily to precipitation	(3) BSW will follow precipitation changes closely (slightly dampened)
Temp & Precip are negatively correlated	Bog wetness response is unbiased	(4) Variables reinforce each other and changes are therefore significantly enhanced
	Bog respond primarily to temperature	(5) BSW will follow temperature changes closely (slightly enhanced)
	Bog respond primarily to precipitation	(6) BSW will follow precipitation changes closely (slightly enhanced)
Temp & Precip are correlated but the nature of their relationship varies through time	Bog wetness response is unbiased	(7) BSW signal will sometimes dampen and sometimes magnify changes and this must be accepted when making climatic inference
	Bog respond primarily to temperature	(8) BSW will follow temperature changes closely (sometimes slightly enhanced sometimes slightly dampened)
	Bog respond primarily to precipitation	(9) BSW will follow precipitation changes closely (sometimes slightly enhanced sometimes slightly dampened)

2.5.1 *PRECIPITATION-TEMPERATURE INTERRELATIONS; BSW CONSEQUENCES*

There is a body of evidence that the relationship between temperature and precipitation can vary spatially and through time, and this is discussed in relation to North Atlantic climate drivers in Section 2.9.5. Had temperature and precipitation been correlated in a very consistent fashion, then changes in BSW would always be expected to be proportional to climate variability (albeit consistently dampened or exaggerated depending on the nature of the relationship). However, since temperature and precipitation can vary relatively independently from one another the relationship between the two variables is not always consistent. Consequently, climatic interpretation of BSW is equivocal because any given value of BSW can be produced by an almost infinite number of different temperature precipitation ratios, even within the constraints of 'realistic' climatic variability. An investigation into the sensitivity of bog water levels to changes in individual climatic parameters is therefore of value in order to ascertain whether changes are likely to follow one variable more closely than the other, and this requires an understanding of bog hydrology.

2.5.2 *HYDROLOGICAL SENSITIVITY TO TEMPERATURE & PRECIPITATION*

Peatland hydrology encompasses a large body of research. For detailed descriptions of the principles and reviews of the literature the reader is referred to Ivanov (1981), Ingram & Gore (1983), Eggelsmann *et al.* (1993), van der Schaaf (1999) and Charman (2002). Much of the extensive and valuable Russian literature which would otherwise be unavailable to non-Russian speakers is summarised in these reviews. This section is directed towards the fundamental hydrological relationships which underlie raised bog functioning and in particular those characteristics which determine water table sensitivity to temperature and precipitation changes over the medium and long-term.

Basic to bog hydrology is the water balance concept, which stipulates that it should be possible to account for all the water in a system (Ingram, 1983). In its simplest

form the water balance in a bog consists of influx (recharge), efflux (discharge) and storage and the changes in these components must balance (Eggelsmann *et al.*, 1993) so that:

$$\text{Influx} - \text{Efflux} - \text{Changes in storage} = 0$$

Before looking in more detail at the three components of the water balance equation, it will be useful to look at the basic hydrological properties of raised peat bogs. Firstly, in order to place the significance of hydrology in perspective it is interesting to consider that peatlands can consist of well over 95% water by weight. This should change the reader's perception of bogs, revealing them to be in effect giant bubbles (or mounds) of water held *in situ* by matrices of living and dead plant material (Charman, 2002), rather than perhaps the more commonly perceived compost heaps saturated with water. Viewing bogs in this way leads to the question of how these 'giant bubbles of water' maintain their convex structure. Ingram (1982) developed the concept of a groundwater mound to explain the domed structure of raised bogs:

Groundwater mound theory is based on the concept of a catotelm that loses water by lateral outflow and is compensated for by infiltration from the overlying acrotelm. The acrotelm and catotelm (*sensu* Ingram, 1978) refer to the thin unconsolidated surface layer – including the living plants and relatively fresh weakly humified material – and the underlying main peat mass – which is more humified and compacted – respectively. Because of the lateral outflow of the infiltrated water, the water level and subsequently the catotelm surface is highest at or near the centre of the bog (assuming a horizontal substrate). Van der Schaaf (1999 p. 27-34) reviewed the groundwater mound hypothesis finding that, "although the underlying assumptions are partially incorrect raised bogs undoubtedly are groundwater mounds and the shape of the water table in them is an essential element of the flow process which occurs within them". The components of the water balance equation are discussed in more detail below.

INFLUX (recharge)

The convex structure of raised bogs and the position of water tables above the surrounding groundwater make it hard to envisage telluric (groundwater) inputs as an influx component to raised bog water budgets, except in the specific circumstances where artesian flow has been recorded to cause upwelling of groundwater (Glaser *et al.*, 1997). There are few examples where total water budgets from undamaged sites have been measured, but work by Hemond (1980) is one example. Hemond measured the direction of flow of water from a bog in Massachusetts, USA, finding it to be consistently outwards and therefore supporting the atmospheric influx hypothesis. However this should not be regarded as a universally consistent relationship as Devito *et al.* (1997) demonstrated periodic flow reversals during low water levels in a Swedish raised bog. Nevertheless, it seems likely that in the majority of cases influx is received solely from the atmosphere. Significant influx to raised bogs can therefore be considered to be entirely through precipitation.

Precipitation comes in the form of rain, snow, hail, fog and dew. The most common form of precipitation for many bogs and certainly for those in the United Kingdom is rain. Whether rain falling directly onto a raised bog will be incorporated into the peat matrix will depend primarily on the depth of the water table at the time of precipitation. If there is spare capacity within the peat profile then rainfall will be incorporated almost immediately, resulting in an increase in water storage. However as water tables approach the surface (which represents full capacity), lateral outflow from the acrotelm will increase and eventually a point will be reached where increases in rainfall have little or no impact on storage. These conditions typically prevail each winter in Atlantic raised bogs, so that each summer season begins in a sense with the blank canvas of water tables at maximum capacity. However if these conditions were to prevail throughout the summer season BSW proxies would be insensitive to further increases in the precipitation to evaporation ratio. If water tables are very deep then it is conceivable that due to low transmissivity characteristic of degraded peat a proportion of rainfall could run off the surface before seeping into the peat matrix. Under these conditions recharge would not be proportional to rainfall but would occur, perhaps, at a slower rate.

Snow and hail, particularly when falling on a frozen surface, are subject to factors which may limit their ability to ultimately enter the bog system. Firstly, since bogs are usually large relatively flat landforms, much of the snow that falls directly onto the surface might blow off before it has melted. There is also the potential for melt water to run off the bog surface if the acrotelm is slower to thaw than the overlying snow. One or both of these factors might mean that bog water recharge from snowmelt is less than from the equivalent quantity of rainfall and further study of these processes would certainly aid interpretation.

The effects of fog and dew – sometimes known as ‘occult precipitation’ – are notoriously hard to quantify (Ingram, 1983) but should not be considered insignificant. The effects may be more to suppress efflux rather than to significantly increase influx. Since precipitation is the only significant influx, it will inevitably have a strong effect on water levels. However, the effects of influx are counteracted by efflux, and water storage is determined by the interaction of the two.

EFFLUX (discharge)

Efflux from a raised bog occurs predominantly through groundwater flow and evapotranspiration. Due to the very low hydraulic conductivity of catotelmic peat (Brown *et al.*, 1989; Rycroft *et al.*, 1975), groundwater discharge from raised bogs occurs effectively through acrotelm flow only, and this is only a significant component of efflux when water tables are very close to the surface (van der Schaaf & Schouten, 2002). As water table depth increases, acrotelm transmissivity falls sharply and groundwater discharge is reduced. Under normal conditions efflux is dominated by evapotranspiration, and this was illustrated by Hemond (1980), who found that of 1,448 mm of rainfall that fell on a raised bog in Massachusetts, USA, over a fifteen month period, only 246 mm (*c.* 17%) left the bog as runoff. This supports the hypothesis that raised bogs exchange moisture predominantly with the atmosphere and lose much of their moisture (>80%) through evapotranspiration.

The rate of evapotranspiration at any moment is dependent on three factors:

1. The energy available, determined primarily by the amount of solar radiation;

2. The ability of the atmosphere to take up the evaporated moisture, determined by atmospheric humidity and the aerodynamics of the system;
3. The water supply, determined by water levels and vegetative characteristics.

(Ingram, 1983)

The amount of energy available for evaporation is chiefly determined by the quantity of solar insolation. Insolation also drives temperature changes, although atmospheric circulation patterns complicate this relationship. Nevertheless, energy availability for evaporation would be expected to be strongly positively correlated with temperature. The ability of the atmosphere to take up evaporated moisture is dependent primarily on relative humidity because air which is close to saturation can take up less moisture than air which is far from saturation point. Relative humidity is also related to temperature since warmer air can hold more water vapour. Wind conditions can have an impact by carrying away vapour bearing air thus reducing relative humidity above evaporative surfaces. The first two factors which determine the rate of evapotranspiration, energy availability and atmospheric uptake, are closely related to temperature, the third factor, water supply is more closely related to antecedent water level which is in turn is related to past climatic conditions. Water availability is also influenced by the properties of the plants which occupy the bog surface. The effect of water availability may go some way to explaining why Valgma (1998a) found that the mean annual water table in a raised bog in Estonia depended strongly on the water level of the previous year. However this implies that water tables do not always reach saturation point during the winter months. This may simply be a difference in characteristics between the more continental setting of Estonia and the oceanic conditions which prevail in north-western Britain but the geographic difference points to the potential for temporal variability between these two modes of operation which might require quite different interpretation. In any case, water availability is the most likely area in which autogenic processes could moderate the allogenic influence of climatic conditions on evapotranspiration. These processes will be considered further in terms of physical processes related to raised bog structure and biological processes relating to the vegetative cover.

In purely physical terms moisture availability is strongly related to water table depth. This is because as water tables fall, the thickness of peat between the water and the zone of potential evaporation increases, providing an evaporative barrier. As a result, different evaporative flux rates might be expected from different microtopographic features because of their relative proximity to the water table such that open pools and lawn areas have the highest flux rates and hummocks the lowest. This relationship is confirmed by Valgma (1998b) who summarised some findings from the Russian literature (Kaljushnõi, 1974; Belotserkovskaja *et al.*, 1969; Romanov, 1961) which showed evapotranspiration rates from hollows to exceed that from hummocks by 20 - 30%. However, once water tables fall below the peat surface moisture availability is largely determined by the rate and extent of upward transport of water and consequently is strongly influenced by the features of the plants growing on the surface (Ingram, 1983).

The effects of upward water movement as a result of plant activity is superimposed upon the basic physical parameter of surface proximity to the water table complicating this basic relationship. Nicholas & Brown (1980) found that evapotranspiration can be higher from *Sphagnum* hollows than from open water basins and van der Molen & Wijnstra (1992) demonstrated that hummock evapotranspiration may exceed hollow evapotranspiration during extremely dry periods. This reversal in the relative rate of evapotranspiration from hummock and hollow microforms is likely to be related to the physiology of the plants which occupy them. So for example, Baden & Eggelsmann (1966 [in] Ingram, 1983) reported low evapotranspiration from *Sphagnum* during dry summer weather and hypothesised that this was due to the drying out of their capitula because *Sphagnum* have no mechanism for efficient upward transportation of water. A negative feedback effect may also be observed in *Sphagnum* communities during times of drought. When the Hyaline cells become empty of water the leaves take on a pale whitish appearance, increasing albedo and reflecting more incident radiation than when damp (Ingram, 1983).

By contrast, vascular bog plants including members of the Ericaceae and Cyperaceae families have the capacity to actively draw water upwards. Boggie *et al.* (1958) used a radioactive tracer technique to investigate the rooting depth of various bog plants,

finding that on a deep peat substrate *Calluna vulgaris* was surface rooting with absorption of the tracer occurring mainly in the 0 to 15 cm range. Sedges like *Eriophorum vaginatum* and *Trichophorum cespitosum* were found to be much deeper rooting with absorption occurring down to the maximum tracer placement depth of 60 cm. While both Ericaceae and Cyperaceae have the capacity to control evapotranspiration to some extent by stomatal closure they continue to draw water to the surface maintaining the necessary water supply element to evapotranspiration and thus allow water tables to continue to fall. During extended dry climatic periods vegetation might be expected to change towards a greater cover of deep rooted vascular plants which would facilitate further water loss through evapotranspiration.

In summary, bogs exchange the majority of their moisture with the atmosphere and influx in particular is from atmospheric input only (at least in the majority of cases). However the sensitivity of bog wetness to changes in influx is dependent on available storage capacity which is closely related to the water table depth, such that under extremely wet conditions BSW may become insensitive to further climatic deterioration. The type of precipitation may also influence the capacity of the bog to uptake the moisture which falls on the site. Efflux occurs predominantly through evapotranspiration with acrotelm outflow becoming more important under very high water table conditions. Evapotranspiration is strongly influenced by temperature but also by the water table depth and the characteristics of the bog plants. Some autogenic processes therefore impact upon evapotranspiration rates. This inevitably leads to some complacency in the record probably masking short duration events and lagging more persistent changes. However, longer duration changes in temperature would be expressed by changes in BSW in spite of these autogenic influences.

The study of modern bog hydrology has provided a wealth of information which aids understanding of bog functioning. It would be naive to expect there to be a simple linear relationship between either temperature or precipitation and BSW, and this would seem to be confirmed by bog hydrological monitoring. There are numerous autogenic mechanisms capable of influencing the degree to which water storage is affected by changes in influx and/or efflux making it probable that BSW sensitivity to temperature and precipitation varies spatially and therefore potentially temporally as

well. However bog hydrology instrumentation tends to be short, with even the longest records spanning only *c.* 50 years (Charman *et al.*, 2004) and the majority of studies covering just one or two years. Subsequently the records do not necessarily provide answers to questions about hydrological relationships which operate over long timescales, particularly how bogs respond to distinct, persistent changes in climatic regime and the associated changes in plant assemblage. Proxy data provide a window into these longer term processes.

2.6 PALAEOECOLOGICAL EVIDENCE OF THE CLIMATE-BSW RELATIONSHIP

A number of studies have investigated the climate-BSW relationship by taking a different approach to the cross-validation between sites method (Section 2.4.6). Early examples of these studies were able to support the idea that climate directly influenced BSW but were only able to touch on the nature of the relationship. For example, Barber *et al.* (1994) found that Lamb's (1977) documentary climate indices correspond well with BSW fluctuations reconstructed from Bolton Fell Moss, Cumbria. These findings were corroborated by Charman & Hendon (2000) who demonstrated a strong correspondence between instrumental climate data and reconstructed water table fluctuations at Coom Rigg Moss and Butterburn Flow, NE England. Subsequent studies focussed more specifically on the nature of the climate-BSW relationship.

Reconstructions from a lowland raised bog at Fallahogy, Northern Ireland and a montane blanket bog, Mhoine Mhore in the Cairngorms was undertaken by Barber *et al.* (2000). The bogs separated by >300 km in distance, almost 900 m in altitude and with markedly different vegetative cover, showed a sufficiently similar response over the 'Little Ice Age' (LIA) period for Barber *et al.* (2000) to hypothesised that the bogs were responding predominantly to temperature changes. This was argued on the basis that temperature is more spatially and temporally coherent than precipitation as portrayed by long instrumental datasets from England, Scotland and the Netherlands (Barber *et al.*, 1999). This is a persuasive line of argument for temperature as the dominant driving force but before this hypothesis can be confirmed a number of possible issues remain to be resolved. Firstly the correspondence between BSW

records from Ireland and Scotland (Barber *et al.*, 2000) are not yet well supported by subsequent studies. Corroboration of these datasets utilising other distant sites to produce a number of well-dated multiproxy reconstructions would improve confidence in this theory. In addition interpreting the potential signature of LIA climate on BSW is complicated since estimates of Northern Hemisphere mean annual temperature for the last millennium do not all show a clearly delimited LIA cooling (Crowley & Lowery, 2000; e.g. Mann *et al.*, 1999), but rather a gradual temperature decline from c. 950-450 BP. Furthermore there appear to be significant regional temperature variations (Nesje & Dahl, 2003) and glacial mass balance evidence also suggests that rapid glacier advance during the LIA might have been primarily driven by increased wintertime precipitation (Nesje & Dahl, 2003) which would have had little impact on British raised bogs. Comparison of BSW reconstructions with a summer temperature proxy could address this question and one of the secondary aims of this investigation is to assess the sensitivity of CI-T records to Holocene climate variability which might shed light on the LIA summer temperature BSW relationship. An existing late Holocene CI-T record from Cumbria (Langdon *et al.*, 2004) did not detect summer LIA cooling but this might be explicable in terms of the low sampling resolution used over this critical time period.

Based on correlation analysis of instrumental climatic records and reconstructed water tables at Männikjärve Bog, Estonia (50 year-long record) and Butterburn Flow, Northern England (200 year-long record) Charman *et al.* (2004) recommend that, contrary to the findings of Barber *et al.* (2000), BSW should be interpreted as primarily a function of summer precipitation. A relationship was also found with summer temperature, which was stronger (although still secondary to precipitation) in more continental settings and appeared to be more important when considering the possibility of system inertia operating over longer timescales. This appears to support the observation of Barber *et al.* (2000) who found that wet conditions once initiated continued through a period of reconstructed higher evaporation/longer growing season, indicating some degree of system inertia in the bog's response.

An additional interesting finding of Charman *et al.* (2004) was that measured and reconstructed water table data and climate data from Männikjärve bog reveal a

stronger correlation between summer temperature and reconstructed water tables than between summer temperature and measured water tables and multiple regression analysis showed temperature to have an impact on testate communities independent of water table changes. These statistical relationships appear ecologically plausible and it is reasonable to conclude that summer temperatures may play a more important part in dictating testate communities, and subsequently reconstructed water tables, than it does in controlling actual water tables. This apparently direct relationship is probably linked through soil moisture which may be more important than water table depth in determining testate amoebae communities. This may well be the case for other proxies as well and illustrates a problem encountered in all methods of proxy reconstruction whereby the multiple variability that occurs in a complex system is attributed predominantly and somewhat artificially, to just one underlying variable.

A study by Schoning *et al.* (2005) similar to that of Charman *et al.* (2004) compared BSW data with historical data from eastern central Sweden and found that reconstructed water tables were correlated with changes in mean annual temperature. The authors suggest that low rainfall in this region accounts for the peatland sensitivity to changing temperature and lack of response to precipitation was a function of low rainfall variability over the 125 year comparison period.

These sometimes opposing conclusions from the various investigations outlined above, reveal that this issue remains open and suggest that the nature of the relationship between climatic parameters and BSW may vary depending on the geographic location and timescale in question. Investigations to date have focussed primarily on historical times due to the availability of meteorological data but little information on the longer-term (centennial to millennial) relationship is currently available. This project is therefore designed to address the nature of the longer term relationship.

2.7 LAKES AS PALAEOENVIRONMENTAL ARCHIVES

Lakes represent a large and diverse group of ecosystems; they are excellent sensors of environmental change (Battarbee, 2000) and typically preserve a record of their ontogeny within the sediments which build up on the lake bed. These tend to accumulate sequentially, often providing a continuous high resolution, sub-decadal or even annual (O'Sullivan, 1983), archive of environmental change modulated through the lake system. Climatic changes influence lakes in many ways and the nature of the sediment 'rain' which ultimately forms the sediment archive is regulated by the lake response. In order to infer past conditions accurately it is therefore important to understand both the direct and indirect linkages between climate and the water column (Battarbee, 2000). The nature of this relationship varies depending on the size, shape and water residence time of the lake as well as the prevailing climatic conditions in which the lake is found and the type of catchment it lies within.

A range of proxy techniques for inferring past climatic conditions from lake sediments have been developed. Most of these fall loosely into three categories: (1) sedimentology, (2) isotope and elemental chemistry and (3) biology/ecology. While all of these categories produce useful data biological proxies are of most relevance to this investigation in terms of their methodology. All biological proxies work on the basis of identification of fossil or subfossil taxa from a sediment sample and inference of prevailing conditions at the time of deposition based on an understanding of the modern equivalents of those taxa and the ecosystem of which they were a part. The analysis is therefore similar to that already described for biological analysis of raised bog deposits (e.g. plant macrofossils and testate amoebae, Sections 2.4.1 & 2.4.2) but their interpretation differs due to the different nature of the lake ecosystem and the way in which climate affects that system. In particular biological response to temperature change is usually partially related to indirect mechanisms through water column stratification, nutrient cycling and oxygen availability. Of the many proxy biological techniques for reconstructing palaeotemperature chironomid analysis is regarded as one of the most promising (Battarbee, 2000).

2.8 CHIRONOMIDAE (NON-BITING MIDGE) ANALYSIS

2.8.1 INTRODUCTION

Chironomids are a diverse family of two-winged flies (Insecta: Diptera: Chironomidae) and are commonly referred to as non-biting midges to distinguish them from another midge family, the Ceratopogonidae. Like all Diptera, chironomids are holometabolous, undergoing complete metamorphosis where they progress through four stages to complete their life cycle (Fig. 2.2). Typically this involves the deposition of eggs into water, which then hatch into larvae. The larval form is usually the longest lived and is typically aquatic although a few terrestrial or semi-terrestrial forms do occur (Walker, 2001). During this period larvae undergo ecdysis (exoskeleton shedding) each time emerging as a larger form known as an instar. These are named according to the number of times they have undergone ecdysis such that newly hatched larvae are called first instars and the final stage before pupation fourth instars. The next stage of the life cycle is the pupae which is relatively short lived and can be thought of as a metamorphic (or transition) stage between larvae and eclosion (emergence of the morphologically distinct adults) (Porinchu & MacDonald, 2003). Once metamorphosis is complete and conditions are right, the pupae rise to the surface and the adults can emerge from the exuviae. Males typically form swarms prior to mating, which completes the life cycle.

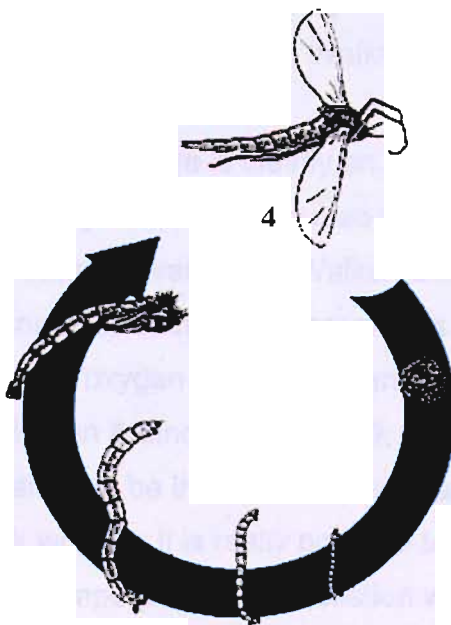


Fig. 2.2: Chironomid Life Cycle. 1 = egg mass, 2 = typically aquatic larval instars, 3 = pupae, 4 = winged adult

(Source: hi.is/HI/Stofn/Myvatn/mycycle.gif)

Chironomids are almost ubiquitous and are frequently the most abundant insects in freshwater environments (Armitage *et al.*, 1994). They constitute an important component of aquatic ecosystems playing a valuable role in nutrient cycling and as a food source for insectivorous fish and birds (Porinchu & MacDonald, 2003). Chironomids have long been recognised as sensitive environmental indicators (Gams, 1927; Thienemann, 1922) and have been found to be sensitive to eutrophication, acidification, pollution and physical disturbances (Lindegaard *et al.*, 1995) and more recently have been utilised for palaeoclimatic reconstruction (Brooks & Birks, 2000, 2001; Walker *et al.*, 1991b).

2.8.2 CHIRONOMIDS AS PALAEOTEMPERATURE INDICATORS

Temperature has a primary role in determining aquatic ecosystem productivity and functioning (Wiederholm *et al.*, 1984) and has direct and indirect effects on chironomids throughout their life cycle (Brooks, 2003), including rates of egg development (Pinder *et al.*, 1995), larval growth and feeding (MacKay, 1977; Oliver, 1971), pupation and emergence (Danks & Oliver, 1972) and adult flight and swarming behaviour (Kon, 1984). As a consequence, cold-water and warm-water lakes have their own characteristic chironomid assemblages (Brooks, 2003). Large bodied larvae including the Chironomini and Tanypodinae are typically warm-adapted while the smaller Orthoclaadiinae, Tanytarsini and Diamesinae are better adapted to cold conditions (Brooks, 2003; Walker, 2001).

While temperature is clearly an important variable in determining chironomid community structure, they also respond to changes in a wide variety of other environmental variables (Walker, 2001), and transfer functions have been developed for a number of different parameters including salinity (Heinrichs *et al.*, 2001), dissolved oxygen (Quinlan & Smol, 2002; Quinlan *et al.*, 1998) and nutrient status (Brodersen & Lindegaard, 1999; Brooks *et al.*, 2001). If chironomid abundance and diversity can be influenced by so many environmental variables then it is reasonable to ask whether it is really possible to attribute community variance to just one primary driver, temperature. This question was addressed by Walker *et al.* (1991b; 1992) who

used Canonical Correspondence Analysis (CCA) to explore the relationship between chironomid taxa and a variety of limnological variables in Labrador and Quebec. The investigations revealed that while within-lake variables like substrate type, pH and nutrient status are important controls on the local-scale chironomid distribution summer water temperature had an over-riding influence over a broad geographic scale.

The over-riding importance of temperature was initially disputed by Hann *et al.* (1992) but this did not discourage the development of a number of regional transfer function training sets, each of which support the observation that temperature is the best explanatory variable for broad-scale chironomid distribution, for example, in Switzerland (Lotter *et al.*, 1997), Canada (Walker *et al.*, 1997) north Finland (Olander *et al.*, 1999), western Norway (Brooks & Birks, 2000, 2001) and northern Sweden (Larocque *et al.*, 2001). An over-riding climatic influence means that while different chironomid assemblages can occur even in relatively proximal lakes because of within-lake variables like water chemistry and lake morphometry, climatic change still causes a distinct faunal response, albeit reflected by different taxa in each lake (Brooks, 2000).

Recent advances in statistical methods (Birks, 1995, 1998; ter Braak & Juggins, 1993) allow the production and application of calibration datasets (transfer functions) which can be applied to fossil data to produce a quantitative estimation of summer palaeotemperature, based on modern taxon tolerance and optima (Brooks & Birks, 2000, 2001; Larocque *et al.*, 2001; Lotter *et al.*, 1997; Olander *et al.*, 1999; Walker *et al.*, 1997). Investigations utilising these techniques have been highly effective for reconstructing Late-glacial temperature changes and these sequences display distinct faunal changes in response to the climatic variability of the Late-glacial (Bedford *et al.*, 2004; Brooks & Birks, 2000, 2001; Brooks *et al.*, 1997; Lotter *et al.*, 1999; Walker *et al.*, 1991a).

2.8.3 SUBFOSSIL CHIRONOMID TAXONOMY

Taxonomy is of key importance in palaeoecological investigations because misidentification can result in inaccurate palaeoenvironmental inference. Subfossil specimens can be problematic to identify because typically only the head capsules are preserved so many diagnostic features available to chironomid (neo)ecologists are unavailable to palaeoecologists. The key diagnostic features of the head capsule are the mentum, ventrumal plates, mandibles, premandibles, antennal pedestals and cephalic setae. It is rare for all of these features to be preserved, especially within older sediments and in any case not all are required for identification. Different features have more or less diagnostic power when applied to different groups which can be morphologically quite different. For example the premandibles and the presence and morphology of antennal pedestal spurs are important for *Tanytarsini* differentiation (Brooks, 2004, unpublished key) whereas the arrangement of cephalic setae are more useful for *Tanypodinae* (Rieradevall & Brooks, 2001).

Theoretically greater taxonomic resolution provides more precise and accurate information and subsequently improves palaeoenvironmental interpretation. However, largely because of preservation issues the level of taxonomic resolution is variable and inevitably involves grouping of taxa into species and/or genera groups. Consequently Walker (1991b) points out that there is a conceptual optimum between information loss as a result of species aggregation and the danger of misidentification when attempts are made to identify specimens to a level beyond the limits of the subfossils present.

Since there is not yet a single published guide for identifying subfossil chironomid head capsules, taxonomic consistency is also a potential problem. The main identification guides in use are Cranston (1982), Oliver & Roussel (1983), Wiederholm (1983), Hofmann (1971), Brooks, (2004, unpublished key) and Rieradevall & Brooks (2001). These provide a fairly complete resource but because subfossil chironomid analysis is a developing discipline keys are continually being refined. This is probably why some keys have remained unpublished, as they might otherwise quickly become out of date. The greatest need for consistency is within

individual calibration training sets and the fossil data they are applied to. Until the publication of a standard published taxonomy, (Brooks & Langdon, in prep.) this is best maintained by communication with key chironomid workers and during this project the author has benefited from the advice of Steve Brooks at the Natural History Museum who is jointly responsible for the Norwegian transfer function (Brooks & Birks, 2000, 2001) which was used to calibrate the data.

2.8.4 AIR OR WATER TEMPERATURE?

One of the more controversial aspects of chironomid inference models is the use of air rather than water temperature as an explanatory variable for chironomid assemblages. Livingstone & Lotter (1998) undertook an investigation into the similarity of summer air and lake surface temperatures of the Swiss Plateau, chiefly to tackle the problem of sparse water temperature data. They concluded that there is sufficient correlation between air and water temperature to recommend that standardised altitude-corrected air temperature series may be used as an alternative to surface water for calibrating chironomid inference models. This was taken to heart by many chironomid workers and most transfer functions now use air rather than water temperature in their inference models (Brooks & Birks, 2000, 2001; Larocque *et al.*, 2001; Lotter *et al.*, 1997; Olander *et al.*, 1999; Walker *et al.*, 1997). However water temperature probably has a greater influence on chironomid communities than air temperature and Brooks (2003) points out that problems with the reconstructions can therefore occur if the relationship between water and air temperature changes through time, for example, due to changes in the influence of snow-beds or glacier fed streams. Fortunately this is very unlikely to be a problem during late Holocene times at least in northern England and therefore should not compromise this investigation.

2.8.5 HOLOCENE PALAEOTEMPERATURE INFERENCES

While chironomid inference models perform well when applied to Late-glacial sequences the lower magnitude climatic fluctuations of the Holocene are more problematic. There are two main reasons for this: firstly, the likely magnitude of temperature changes is close to the limits of the prediction errors of existing models

(Brooks & Birks, 2001). Secondly, temperature changes, estimated to be 2-4 °C (Brooks & Birks, 2000; Langdon *et al.*, 2004), may not be of a magnitude sufficient to have an over-riding influence on chironomid distribution. Instead lake-water and sediment chemistry changes driven by catchment processes like vegetation succession and soil development might have an overriding influence (Brooks, 2006). Despite these reservations a number of chironomid inferred Holocene palaeotemperature reconstructions have been undertaken (e.g. Bigler *et al.*, 2003; Heiri *et al.*, 2003a; Langdon *et al.*, 2004; Larocque & Hall, 2003). While not all of these investigations yielded convincing palaeotemperature estimates (Bigler *et al.*, 2003) a number of studies have yielded encouraging results. For example, Heiri & Lotter (2003) concluded that although the chironomid-inferred climate signals were within the prediction error of the model the major inferred temperature changes correspond well with other northern and central European climate reconstructions. Larocque & Hall (2003) compared chironomid palaeotemperature estimates from short cores in northern Sweden with meteorological records and found chironomids to be “sensitive enough to record low-magnitude temperature changes such as those during the Holocene.” Chironomids therefore seem promising as Holocene palaeotemperature proxies but it is clear that great effort must be made to take account of the effect of non-climatic factors on the palaeotemperature estimates. Most authors therefore advocate a multiproxy approach utilising other proxies such as diatoms and pollen to cross-validate the chironomid palaeotemperature estimates (e.g. Brodersen & Anderson, 2002; Brooks & Birks, 2000; Langdon *et al.*, 2004; Larocque & Hall, 2003).

2.8.6 HOLOCENE CI-T RECORDS NW ATLANTIC

Interpretation of Holocene CI-T records is complex, primarily because catchment driven change can override temperature as the principal driver of chironomid assemblage dynamics. As a result CI-T records from the same region can display markedly different patterns of change (e.g. Velle *et al.*, 2005). Nevertheless, a number of chironomid palaeotemperature estimates have now been produced for Holocene sequences in and around the North Atlantic. Some points of general correspondence are emerging and many of these phases correspond with climate

change inferred from other proxy data. The following discussion draws on the excellent reviews of Brooks (2003) and Brooks (2006).

During the Early Holocene cool phases are recorded in Norway between 11150-11300 and 10800 -10500 cal. BP (Brooks & Birks, 2000) and a similar cooling between 11150-11300 is also detected in two lakes in Switzerland by Brooks (2000) and around 10500 to 10400 cal. BP by Heiri *et al.* (2003a). the widely reported 8.2 ka climatic deterioration can be found in CI-T records from Finland, Sweden and Switzerland by Korhola *et al.* (2002), Rosen *et al.* (2001) and Heiri *et al.* (2003b) respectively. The mid-Holocene seems generally warm and featureless in terms of climatic deterioration but a cool phase is detected in northern Finland between 5800-4200 by Korhola *et al.* (2002). Replacement of temperate taxa such as *Microtendipes*, *Chironomus* and *Dicrotendipes* with cool stenotherms, typically from the tribe Tanytarsini, occurs around 2600 throughout much of Europe including Scotland (Brooks, 1996), Northern England (Langdon *et al.*, 2004), Norway (Velle *et al.*, 2005), Sweden (Bigler *et al.*, 2002; Rosen *et al.*, 2001), and Switzerland (Heiri *et al.*, 2003b). Response to LIA cooling is currently not clearly recorded although in many cases this might be due to overprinting of the signal by anthropogenically driven change such as eutrophication (e.g. Brodin & Gransberg, 1993).

2.9 HOLOCENE NORTH ATLANTIC CLIMATE VARIATION

2.9.1 INTRODUCTION

This section is intended to provide a climatic context to the investigation by describing some of the current theory on the nature and extent of Holocene North Atlantic climate variability. Many drivers of Holocene climatic change have been proposed, including seasonality changes paced by harmonics of periodicities in the Earth's orbital elements (e.g. Broecker, 2000; Denton *et al.*, 2005; Hays *et al.*, 1976; Moros *et al.*, 2004), changes in solar luminescence (e.g. Bond *et al.*, 2001; Chambers *et al.*, 1999; Magny, 1993) ice-sheet dynamics (Teller *et al.*, 2002) and reorganisation of ocean circulation patterns (e.g. Bianchi & McCave, 1999; Bond *et al.*, 1997; Chapman & Shackleton, 2000; Hall *et al.*, 2004). However climatic responses to driving variables, whether they originate internally or externally to the climate system, are

modulated through complex processes within and between the atmosphere, ocean and cryosphere. Responses are non-linear and the physics involved in these changes is not yet clear (Broecker, 2000). Current understanding therefore falls short of a comprehensive theory for late Quaternary climatic variability. Palaeoclimatic investigations using proxy indicators are, however, building an increasingly thorough picture of the spatial and temporal patterns of change.

Irrespective of the ultimate climatic drivers, changes in atmospheric circulation patterns are directly responsible for the variations in climate as experienced at any given location on land. The atmosphere is closely coupled to the ocean and so an understanding of when and how atmospheric and oceanic circulation has varied over the Holocene is of fundamental importance to understanding natural climatic variation. These circulatory patterns strongly influence temperature and precipitation distribution over the North Atlantic and therefore constitute the operational level most relevant to this investigation.

2.9.2 NORTH ATLANTIC CLIMATE RECORDS

Oxygen isotope records from Greenland ice cores depict a remarkably stable Holocene relative to the climatic oscillations which characterised the Pleistocene with few climatic events or anomalies. Notable exceptions include the Preboreal Oscillation (c. 10 ka), 9.3 ka and 8.2 ka events (e.g. Dansgaard *et al.*, 1993; Johnsen *et al.*, 2001). While it is not in question that the Holocene is more stable than the Pleistocene numerous palaeoclimatic records now attest to a markedly more dynamic Holocene than conventionally believed. Instability appears to occur on a number of timescales, perhaps the most notable of which are cooling oscillations that punctuate the more gradual long term variability. Significant uncertainties remain as to the nature and extent of these oscillations but it is becoming clear that climatic changes are complex and while they are frequently widespread or even global in extent, the regional climatic outcomes are potentially asynchronous (Kreutz *et al.*, 1997; Nesje & Dahl, 2003) and regionally diverse.

Early Holocene climatic fluctuations such as the widely reported 8.2 ka event have until recently received the most attention owing to the magnitude and abruptness of change. However during the Early-Holocene ice sheets continued to exert a strong influence on ocean and atmospheric circulation and would still have played a major role in climatic change (Mayewski *et al.*, 2004). It does not necessarily follow therefore that climatic anomalies during this period are good analogues for the changes which occurred later in the Holocene (Rohling & Palike, 2005).

Nevertheless, there is mounting momentum behind the idea of a c. 1500 year climatic pacing which was pervasive though both glacial and interglacial conditions (Andrews & Giraudeau, 2003; Bond *et al.*, 1997; Campbell *et al.*, 1998; Rahmstorf, 2003; Viau *et al.*, 2002). This carries the implication that changes in the climate system are robust in the sense that the pattern of behaviour is similar through widely differing glacial and interglacial times, although the specific pacing may differ between the two phases by a few hundred years. Rahmstorf (2003) suggested that the regularity of this pacing is indicative of an external origin and numerous studies have linked this with solar variability (e.g. Bond *et al.*, 2001; Magny, 1993). An external stimulus must be modulated through the ocean-atmosphere system and this is thought to explain the observed variable outcome to a hypothesised consistent stimulus through changing system sensitivity. In other words the magnitude of response is dependant on the sensitivity of the system at any given time. It is noteworthy however that a c. 1500 year recurrence interval detected in different investigations does not necessarily mean that the timings of change correspond and the validity of this pervasive cyclicity is questioned by some authors (e.g. Schulz & Paul, 2002).

When comparing palaeoclimatic records a number of limitations exist; these are discussed in detail in Section 7.2 however it is worth reiterating here that compiling proxy records is not the simple procedure it might at first seem. Consequently there remains a large degree of uncertainty as to the extent to which records differ due to variable accuracy and sensitivity, as opposed to real climatic differences; inevitably this makes interpretation in terms of a unifying climatic theory difficult.

Notwithstanding these problems, a good deal of progress has been made in building

a picture of how Holocene climate has varied, particularly in the intensively studied North Atlantic Sector.

Typically between six and 15 shifts towards cooler climatic conditions are detected in North Atlantic palaeoclimatic records during the last c. 11 000 years and certain dates (BP) are beginning to emerge from the literature with increasing regularity. Some of the most commonly recorded climatic deteriorations occur at c. 10500, c. 8200, c. 6800, c. 4700, c. 4200, c. 3200, c. 2600 c. 2000, c. 1500, c. 1000, c. 500 cal. BP. Many of these climatic deteriorations appear in investigations using independently derived proxies and various different archives such as glacial advance in northern Iceland (Stotter *et al.*, 1999), cooler SSTs around southern Iceland (Malgorzata *et al.*, 2005), shifts to wetter conditions in raised bogs in Great Britain and Ireland (Barber & Charman, 2003; Charman *et al.*, 2006) and Newfoundland (Hughes *et al.*, 2006), and increased lake level in the European Alps (Magny & Begeot, 2004). In addition many of these climatic shifts occur beyond the North Atlantic realm and are detected globally (Mayewski *et al.*, 2004). The diverse archives in which Holocene climatic instability have been detected represent many different facets of the Earth system and testify to the far reaching effects that Holocene climatic instability has had upon the environment.

2.9.3 OCEAN CIRCULATION

Global ocean circulation is driven primarily by differences in water density which arise because of the differing temperature and salinity of waters around the Earth, often called the 'ocean conveyor' or 'thermohaline circulation' (THC). Although the specific trajectories of the components of the THC are dependant on many regional factors such as the position of the continents the general circulation acts to redistribute heat from the equator polewards (often termed meridional overturning circulation (MOC)). Surface waters can respond to internal or external changes over months to a few years but the deep ocean has considerable inertia and takes decades to centuries to respond (Maslin *et al.*, 2003).

In terms of volume, heat capacity and inertia, deep ocean currents are excellent contenders for driving or sustaining centennial to millennial climate fluctuations (Maslin *et al.*, 2003, p. 186). The deep water circulation and particularly the sinking cold, saline waters in the northernmost North Atlantic (North Atlantic Deep Water Formation NADW) perform a vital role in helping to drive ocean circulation. This causes the warm surface currents, the Gulf Stream and its extension, the North Atlantic Drift, to stretch further northward to replace sinking water (Davies *et al.*, 1997, p. 28). Changes in the NADW circulation may therefore have far reaching implications through its influence on the global pattern of meridional overturning (Broecker & Denton, 1989) which has been implicated as a trigger mechanism for climatic events of widespread significance (Weaver & Hughes, 1994).

Ocean-climate interactions are two way. There are, however, indications that sea surface temperature (SST) anomalies play an important role in forcing the circulation of the overlying atmosphere and in influencing the climate of Europe (Davies *et al.*, 1997, p.26). It is likely to be the precise pattern of SSTs which is important for climate, in particular the position/orientation of the zone of maximum SST gradient across the north Atlantic (Davies *et al.*, 1997, p.26-27; Kelly *et al.*, 1987). The implications for North Atlantic climate are that these THC oscillations result in changes in North Atlantic SST patterns which are known to have an important downstream influence on atmospheric state (Davies *et al.*, 1997, p. 29) and consequently climatic conditions experienced over the North Atlantic continents.

This contention that THC and in particular NADW intensity has varied over the course of the Holocene has been demonstrated by a number of authors (e.g. Bianchi & McCave, 1999; Bond *et al.*, 1997; Marchitto *et al.*, 1998). The hypothesised correspondence between deep ocean and surface water flow intensities has also been demonstrated by Hall *et al.* (2004), who produced a multiproxy record of both flow components from the same core. They found a persistent link between centennial to millennial scale fluctuations in the flow speed of Iceland-Scotland Overflow water and surface North Atlantic current intensity. Hall *et al.* (2004) also found a correspondence between THC intensity and pollen inferred Fennoscandian atmospheric temperature. Augmenting the findings of Chapman & Shackleton (2000)

that cold atmospheric conditions detected in the GISP2 ice core (more negative $\delta^{18}\text{O}$ values in the ice core) were generally found in association with intervals of reduced NADW circulation.

Holocene NADW flow is thought to be weakened by inputs of freshwater into the North Atlantic resulting from melting ice or increased precipitation (Maslin *et al.*, 2003, p. 204). Freshening of the surface waters reduces its density and consequently the rate at which the water sinks to form NADW. Maslin *et al.* (2003, p.204) list three mechanisms typically invoked to explain the reductions in the surface salinity of the Nordic Sea and subsequent reductions in NADW formation. These are:

- Internal Instability of Ice sheets, leading to periodic increases in the freshwater flux rate into the Nordic Sea and a freshening of surface waters;
- Ocean Oscillator and the Bipolar Climate Seesaw, an extension of the glacial/interglacial 'bipolar seesaw' concept (Broecker, 1998) into the Holocene. Based on the idea that differential deep water formation in the two hemispheres results in stronger meridional overturning of the oceans in one hemisphere with the knock on effect that more heat is transferred to that hemisphere (termed inter-hemispheric heat piracy). The warming hemisphere might eventually warm sufficiently to melt ice sheets leading to a freshening of high latitude waters and a reduction in deep water formation, effectively switching the heat piracy to the other hemisphere and reversing the seesaw. This scenario could be self sustaining;
- North Atlantic changes forced by Solar Variation, based on the idea that relatively weak forcing from apparently minor solar luminescence changes are amplified by the 'flickering switch' of the Nordic seas with their sensitivity to changes in surface salinity. The exact mechanism of change is still a matter of debate.

2.9.4 ATMOSPHERIC CIRCULATION

While ocean circulation is an excellent contender for either driving or modulating centennial to millennial scale climatic oscillations, it is only through interaction with the atmosphere that the climatic consequences are realised. The atmospheric circulation acts (like the ocean) to equalise pressure differences which arise due to differential heating between the equator and poles. As the air masses move they redistribute heat and moisture around the Earth. Changes in the pattern of circulation can therefore significantly alter regional climatic conditions. Dominant atmospheric circulation patterns vary through a number of processes and these operate over a range of timescales.

Much of the relatively short term (inter-annual to decadal) variability relates to movements of the quasi-stationary planetary waves in the westerlies jet and changes in the relative intensities of The Icelandic Low and the Azores High Pressure centres the relationship between which is known as the North Atlantic Oscillation (NAO) (Hurrell, 1995).

The decadal average position of the European planetary wave trough axis in the westerly jet has varied by as much as 20° longitude over the last 200 years (Davies *et al.*, 1997, p.19). Movements in the planetary wave pattern are probably caused by changes to the atmospheric heating pattern or internal (chaotic) processes (Hurrell *et al.*, 2003, p. 4). Cyclone development is influenced by the position of the trough and the path of cyclone propagation follows the westerly wave pattern of the upper flow (Davies *et al.*, 1997). The average nature of westerly jet stream flow and in particular the position of the European Trough could therefore translate into changes in the dominant latitudinal position of westerly flow. The extent to which these planetary wave patterns may vary over centennial to millennial timescales is not clear but if long term patterns do occur then they may well constitute part of the mechanism of change responsible for climatic variability detected during the Holocene. The hemispheric scale of the planetary wave flow also provides a mechanism for climatic teleconnections.

Surface pressure patterns also bring influence to bear on the pattern of atmospheric circulation. The most prominent and recurrent pattern of atmospheric variability in the middle and high latitudes is the NAO (Hurrell *et al.*, 2003, p. 1). The NAO refers to the distribution of atmospheric mass (expressed as pressure anomalies) between the Arctic and subtropical Atlantic. Changes in phase affect the mean wind speed and direction over the Atlantic and the neighbouring continents, and the number of storms, their intensity and paths of travel (Hurrell *et al.*, 2003, p. 1). The influence of the NAO on surface temperature and precipitation is greatest during the winter months, but coherent fluctuations occur throughout the year and decadal and longer term variability is not confined to winter (Hurrell *et al.*, 2003, p. 10). Nevertheless, winter season dominance is problematic to resolve since most proxy climatic indicators have a summer season bias. The NAO state can be summarised in terms of an index. During high positive index conditions enhanced westerly flow moves relatively warm maritime air over much of Europe. Stronger northerly winds over Greenland and north-eastern Canada carry cold air southwards decreasing land surface temperatures and SST over the northwest Atlantic (Hurrell *et al.*, 2003, p. 17). Meanwhile, the axis of maximum moisture transport shifts to a more southwest-to-northeast orientation across the Atlantic and extends much farther north and eastwards into northern Europe and Scandinavia. This is accompanied by a reduction in moisture transport to southern Europe and the Mediterranean (Hurrell, 1995).

While the NAO has a coherent impact on North Atlantic temperature and precipitation patterns there is little evidence from historical NAO indices that the NAO varies on any preferential time-scale (Hurrell *et al.*, 2003, p. 14) and this supports the idea that variation arises predominantly through internal stochastic processes. As such, variations are chaotic and should display little long term trending that could drive centennial to millennial scale climatic variations. This supports the findings of Charman & Hendon (2000) that changes in the intensity of the westerlies in their existing location (related to the NAO) seem unlikely to account for Holocene changes detected by, for example, northern British bog water tables (e.g. Charman *et al.*, 2006; Hughes *et al.*, 2000) Greenland (GISP2) Ice core accumulation rates (e.g. Kapsner *et al.*, 1995) or European lake levels (e.g. Magny, 2004).

Climatic oscillations in the North Atlantic might instead be related to long term latitudinal shifts in pressure centres (Charman & Hendon, 2000; Hughes *et al.*, 2006; Magny *et al.*, 2003) possibly related to movement of the Atlantic Polar Front (APF) in a similar but smaller scale movement to that postulated by Ruddiman & McIntyre (1981) to explain the last glacial-interglacial transition. Charman and Hendon (2000) postulated that a southward shift of the APF might manifest itself as a southward movement of the Icelandic low which would strengthen westerlies, increase summer precipitation and decrease temperatures in Britain and presumably much of mid latitude Europe. This idea is in accordance with the findings of Eiriksson *et al.* (2000) who attributed the MWP and LIA climatic 'events' to south-northwards movements of cyclone tracks. The lake level data of Magny *et al.* (2003) demonstrated variable hydrological response to North Atlantic cooling such that in response to the widely reported 8.2 ka BP climatic deterioration, European mid latitudes (50° - 43°) underwent wetter conditions whereas northern and southern Europe were marked by drier climate. A similar relationship was observed during other Holocene climate deteriorations. This pattern was explained in similar terms through southward displacement of the Atlantic westerly jet and more intense cyclonic activity over the European mid latitudes (Magny, 2004).

Longitudinal variations in North Atlantic climatic response identified by Hughes *et al.* (2006) were also explained in terms of latitudinal movements in the APF but with asymmetric movement where APF moves through a larger latitudinal range in the eastern Atlantic than in the west (*sensu*. Ruddiman & McIntyre, 1981).

2.9.5 PRECIPITATION-TEMPERATURE INTERRELATIONS

The nature of the precipitation-temperature relationship has consequences for the connection between climate and BSW and as a result the way BSW records should be interpreted (see Section 2.5.1). Both temperature and precipitation are controlled chiefly by prevailing atmospheric circulation patterns and are subsequently linked. It might therefore seem intuitive to assume that they are directly related so that for example as temperature rises precipitation falls and *visa versa*. However, the

relationship is not this simple and both parameters do not necessarily move in unison, evidence of their degree of co-variance is discussed below.

Madden and Williams (1978) analysed instrumental temperature and precipitation records of the first half of the 20th century from Europe and North America and found significant correlation. However, the correlation, while often negative, was also sometimes positive and the changing nature of this relationship has obvious implications for precipitation / evaporation ratios. While Madden and Williams (1978) found that the relationships were, “prevalent at all timescales” the relative shortness of their record prevented them from making assertions about the long term (centennial-millennial) relationships. It seems reasonable to assume that the nature of the relationship may vary over time as well as space. This hypothesis can be tentatively supported by comparing data from the Central England Temperature (CET) series (Manley, 1974; Parker *et al.*, 1992; Wigley *et al.*) and the England and Wales Precipitation (EWP) series (Barber *et al.*, 1999; Jones & Conway, 1997). Since BSW is thought to predominantly reflect summer conditions the comparison is based on summer (JJA) data. Fig. 2.3 displays decadal averaged JJA temperature and precipitation data, normalised to the AD 1770-1986 average for ease of comparison. Although the datasets are predominantly negatively correlated (0.185, p-value = 0.006) the data clearly do not show a simple and consistent correlation between the two variables. For example from AD 1825-1836 the correlation is 0.624 (p-value = 0.013), whereas from AD 1926-1955 the correlation is -0.863 (p-value = 0.000). This indicates that temperature and precipitation can vary independently. While these datasets are most representative of central and southern England the variable relationship is supported by Barber *et al.* (1997) who analysed numerous long instrumental datasets from the UK and found temperature to be spatially and temporally coherent and precipitation much more variable in space and time which requires a degree of independence between the two variables.

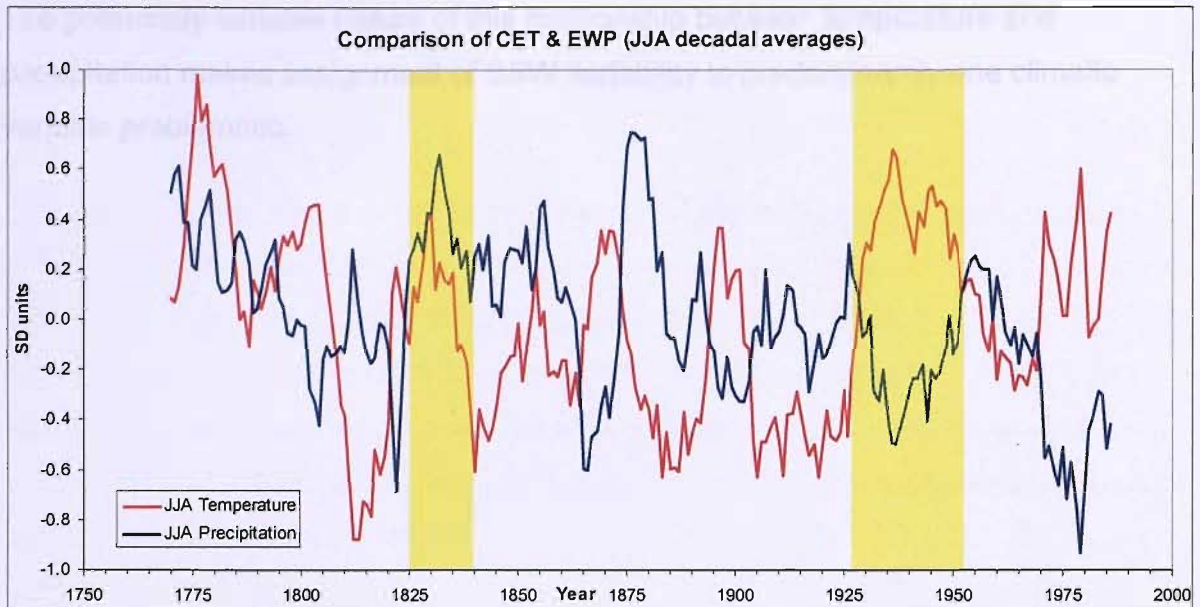


Fig. 2.3: Central England Temperature (CET) and England and Wales Precipitation (EWP) comparison based on decadal averaged JJA data. Yellow shading = examples of periods where the relationship between the two variable is quite different.

Evidence from these recent instrumental climate series provides interesting data but may not provide good analogues to longer scale centennial to millennial relationships between temperature and precipitation because, for example, the degree of variability experienced in recent time is probably significantly lower than that which has occurred previously during the Holocene. Furthermore, relatively short-term change is driven primarily by changes in atmospheric circulation and resulting air mass characteristics. However in the longer term sustained changes in for example temperature may result in changes in characteristics such as SST which might accentuate or attenuate circulation driven changes (Magny *et al.*, 2003).

Evidence that the temperature / precipitation relationship may vary over longer timescales is provided by who found that the mid latitudes between ca 50° and 43° underwent wetter conditions in response to the 8.2 ka cooling compared to northern and southern Europe which experienced a drier climate. They also suggested that a similar 'tripartite division of Europe' can be observed during other Holocene cooling phases and that during phases of weaker climate cooling the middle zone characterised by wetter climatic conditions could have been more extensive.

The potentially variable nature of this relationship between temperature and precipitation makes assignment of BSW variability to predominantly one climatic variable problematic.

... ..

... ..

... ..

... ..

3.0 METHODS

3.1 SITE SELECTION

Site selection was made primarily on the basis of palaeoecological considerations in order to maximise the likelihood of recovering meaningful palaeoclimatic records. In addition to these site specific factors the close proximity of a suitable lake or bog site for comparison was necessary in order to fulfil the project aims and inevitably some compromise was reached between these two requirements. Two pairs of sites were chosen; the first in Southern Cumbria and the second in North Yorkshire. Detailed site descriptions are given in Chapter 4.

3.2 PEATLAND METHODS

The main palaeoecological criteria for bog site selection were

- To confirm ombrotrophy in order to maximise the chance that climatic rather than groundwater related changes were recorded in the stratigraphy. This was assessed by observing the position of the bog within the wider landscape, the vegetation on the bog surface and the peat stratigraphy (through a field stratigraphy, see below);
- To avoid as far as possible human impact such as peat cutting and drainage which would disturb the peat stratigraphy. This was achieved by examining aerial photographs for possible topographic irregularities and through field examination, taking into account factors such as vegetation and microtopographic features. The master coring locations were established following detailed stratigraphical work;
- Proximity of a lake site for comparison: Selection of proximal sites minimises the chances that differences between records reflect a genuine climatic disparity and consequently records are more readily cross-validated. the maximum distance between paired sites was c. 5.5 km.

3.2.1 CORE SELECTION & ACQUISITION

The procedure for core selection and acquisition followed the protocol of Barber *et al.*, (1998). Five to seven cores were taken a transect through the central, relatively undisturbed, part of each bog using a Russian pattern corer (1 m x 4 cm). The cores were analysed using the Tröels-Smith (1955) sediment description criteria and the von Post (1924) 10 point humification scale. A field stratigraphy was then drawn up and the location that displayed the most stratigraphic changes and the wettest stratigraphy overall was chosen for the master coring site. Field stratigraphies were later redrawn using the Tröels-Smith Plotting Program (TSPP) of Duller (1995).

Master cores (HUL & MTM) were taken using a 30 cm x 9 cm Russian pattern corer. Following the procedure of Barber *et al.*, (1994) cores were extracted alternately from two adjacent boreholes leaving 5 cm overlaps between sections to ensure that the full stratigraphic sequence was recovered. The surface (top 30 cm) was taken with a monolith tin. Cores were transferred into plastic guttering, marked for depth and orientation and wrapped in sealable, carbon-stable bags. Cores were stored in a refrigerator at 4°C.

3.2.2 PLANT MACROFOSSIL ANALYSIS

INTRODUCTION

Plant macrofossil analysis involves the identification and abundance estimation of subfossil plant material preserved in the peat archive. On raised bogs plant abundance and distribution is chiefly determined by surface moisture. The strengths and limitations of the technique are discussed in the Literature Review (Section 2.4.1)

LABORATORY PROCEDURE

Subsamples were taken at 4 cm intervals throughout both cores. Sharp stainless steel scissors were used to extract each 4 cm³ (1 cm vertical extent) subsample of peat which was then washed through a 125 µm sieve. A large volumetric container was used to ensure that a consistent 5 litres of water was used to wash each sample (Hughes *et al.*, 2000) in order to minimise any bias in the amount of UOM that passed

through the sieve. Samples were analysed wet in a plastic trough, at 10 x magnification under a dissecting binocular microscope, employing the Quadrat and Leaf Count (QLC) method described by Barber *et al.*, (1994). The percentage cover of each plant macrofossil component was estimated using a 10 x 10 grid graticule mounted in the microscope eyepiece. Fifteen replicate estimates were undertaken for each level to provide a representative estimate of the relative abundance of macrofossil components. Small discrete components like fruits, seeds and fungal bodies were assessed on a five point abundance scale where 1 = rare, 2 = occasional, 3 = frequent, 4 = common and 5 = abundant (Barber, 1981; Hughes *et al.*, 2000).

Sphagnum abundance was estimating by mounting leaves on a microscope slide and identifying under a compound microscope at x200 magnification. A minimum of 100 leaves were counted except when very little *Sphagnum* was found, when lower counts were more practical.

Plant macrofossils were identified using type material held in the Palaeoecology Laboratory at the University of Southampton (PLUS) and according to Grosse-Brauckmann (1986). Where identification required analysis of diagnostic cell structure, material was mounted on a slide and viewed on a high power compound microscope at x200 or x400 magnification. *Sphagnum* nomenclature followed Daniels and Eddy (1990) and vascular plants followed Stace (1991). After analysis sample residue was stored in 30 ml plastic Steralin tubes with a little 10% Ethanol as a preservative.

Latent structure in the data was explored by Detrended Correspondence Analysis (DCA) using the computer program CANOCO 4.52 (ter Braak & Smilauer, 2003).

3.2.3 TESTATE AMOEBAE ANALYSIS

INTRODUCTION

Testate amoebae (Rhizopoda) are unicellular organisms which form shells (or tests) that are preserved in the peat. Their distribution on the bog surface is closely linked to moisture conditions and consequently they make excellent palaeomoisture indicators. The strengths and limitations of the technique are discussed in the Literature Review (Section 2.4.2). Laboratory procedure followed standard methods (Charman *et al.*, 2000; Hendon & Charman, 1997).

LABORATORY PROCEDURE

1. 2 cm³ sub-samples were placed into a 250 ml beaker and two *Lycopodium clavatum* tablets were added as marker spores; these were dissolved in a little 10 % HCL to release the spores;
2. 100 ml of distilled water was added and the solution boiled on a hot plate for ~ 10 minutes with occasionally stirring to help to disaggregate the peat;
3. Each sample was then washed (with distilled water) through a 300 µm sieve to remove the coarse detritus, and the fines removed using a 15 µm mesh. The material between 15 and 300 µm was retained;
4. The retained fraction was washed into a 10 ml glass vial and centrifuged at 1000 rpm for 5 minutes and the supernatant water was decanted off;
5. A small drop of concentrate was mounted on a slide and covered with a large (50ml) coverslip and sealed using nail varnish.

Slides were counted under a light microscope at x200 magnification, x400 was also used for identification of more difficult taxa. At least 100 testate amoebae were counted along with all of the *Lycopodium* spores encountered. Taxonomy followed Charman *et al.*, (2000) and was consistent with the modern analogue transfer function of Woodland *et al.*, (1998). Remaining residues were preserved in their 10 ml glass vials with a little 10% ethanol.

Reconstructed mean annual depth to water table was calculated using the transfer function developed by Woodland *et al*, (1998) and applied using Weighted Averaging (WA) calibration using the program C2 (Juggins, 2003). Sample specific root mean squared errors of prediction (RMSEP) was estimated using 1000 bootstrap cycles, generating 95% confidence intervals on the mean water table reconstruction.

3.2.4 PEAT HUMIFICATION 'COLORIMETRIC TECHNIQUE'

INTRODUCTION

Humification analysis provides a measure of how fresh or degraded the peat matrix is. As organic material decays a group of compounds collectively termed humic acids are formed and this is where the term humification originates. Degraded peats are termed highly humified and fresh peat lightly humified. The strengths and limitations of the technique are discussed in the Literature Review (Section 2.4.3). Laboratory procedure followed the standard 'colorimetric technique' of Blackford & Chambers (1993).

LABORATORY PROCEDURE

1. 4 cm³ subsamples of peat (1cm vertical extent) were taken and dried under a heat lamp. Once dried the samples were ground with a mortar and pestle and 200 mg accurately weighed on four decimal place scales;
2. Samples were then placed in a 250 ml beaker and 100 ml of fresh 8% NaOH was added. This was placed on a hot plate, brought to the boil and then allowed to simmer for one hour at low temperature to minimise evaporation;
3. The solution was allowed to cool and decanted into a 200 ml volumetric flask, this was then topped up with distilled water so that all samples contained 200 ml of solution. Each flask was then shaken to thoroughly mix the sample;
4. Samples were then filtered through Fisherbrand Qualitative 100 filter paper to remove particulate matter and 50 ml of this filtrate was transferred into a 100 ml volumetric flask using a volumetric syringe. The flasks were then topped up with distilled water to the 100 ml mark and mixed well;

5. 4 hours after the initial mixing (stage 2) percentage transmission through each sample was measured at wavelength 540 nm on a WPA S106 digital spectrophotometer. Three readings were taken for each sample and averaged to give the final value. The spectrophotometer was calibrated between each reading by reference to a blank sample which was distilled water.

3.3 PALAEO LIMNOLOGICAL METHODS

The palaeoecological suitability of lake sites was judged according to the criteria below. Site selection was partially based on a qualitative estimation of the optimal mixture of attributes.

- Complete absence or presence of only minor inflowing stream: in order to reduce the chance that changes were in response to alterations in catchment dynamics rather than climatic change e.g. deforestation, hydrological modification etc;
- Relatively undisturbed location: minimal modern human interference increases the chance of recording climatic changes up to the present without overprinting by for example eutrophication; this is perhaps rather unrealistic in Britain, with the exception of some high mountain tarns, but some sites are clearly less modified than others;
- Availability of suitable datable material was considered: in practice however this is difficult to predict and therefore plan for;
- The proximity to a bog site was also considered and this was a major factor in the selection of Malham Tarn (being directly adjacent to Malham Tarn Moss).

3.3.1 CORE SELECTION & ACQUISITION

Suitable coring locations were identified by reference to bathymetric maps when available and this information was checked in the field using a Navman Fish400 echo depth sounder. Inflowing streams were avoided when present and care was taken to core away from overhanging cliffs or steeply inclined sections of lake bed to minimise the chances of sediment disturbance by slope instability. The depth to which wave

base reaches varies according to the size and exposure of the lake. It is obviously desirable to core in a location which has experienced minimal stratigraphic disturbance of the sediments so where possible greater water depth was favoured but this was counteracted by the practicality of coring over the side of a boat without any sort of mechanical aid. At Bigland Tarn an intermediate depth of c. 5 m was chosen (total depth 10 m). Malham Tarn is considerably shallower. The deepest parts (4.5 m) of the lake were small foci (Fig 4.8) and might therefore not represent the most uniform sedimentation. A relatively deep (c. 3 m) section of uniform bed was therefore chosen for coring. Cores from a similar depth have yielded apparently intact stratigraphy (Nunez *et al.*, 2002). All cores were taken over the side of an inflatable Zodiac dinghy.

Initially surface cores were taken with a 100 x 6.5 cm mini Mackereth corer (labelled with the site code and the suffix *_Mac*, e.g. BLT_*Mac*) and the deeper sediments taken with a modified 180 x 5 cm Livingstone corer (labelled with the site code and the suffix *_LivB*, e.g. BLT_*LivB*). A minimum overlap of 20 cm was attempted but the actual coring depth of the Mackereth was difficult to control or predict. Consequently a good overlap was apparently achieved at Bigland Tarn but not at Malham Tarn. Subsequent correlation of the core sections using LOI values revealed a serious mismatch in the data from both Bigland and Malham Tarns (Fig. 3.1). The reason for this mismatch between Mackereth and Livingstone cores has not been fully resolved although there is some possibility that the Mackereth coring occurred at an oblique rather than the desired vertical angle. However at Malham, due to the shallow coring depth the corer could be seen to be upright while in action. Following the advice of Prof. Rick Battarbee this issue was sidestepped by resampling the surface sediments with a 180 x 7 cm modified Livingstone corer (labelled with the site code and the suffix *_LivT*, e.g. BLT_*LivT*) this time with a minimum 50 cm overlap. The two core sections were correlated using LOI values and the overlapping curves resembled each other closely (Fig. 3.2 and 3.3a). In order to improve the fit between the two curves from Bigland Tarn the depth of the lower core was increased by 12 cm compared to field measurement to bring it into line with the surface core where the

sediment-water interface was preserved allowing confidence in sediment depth measurements (Fig. 3.3B) Core information is summarised in Table 3.1 below.

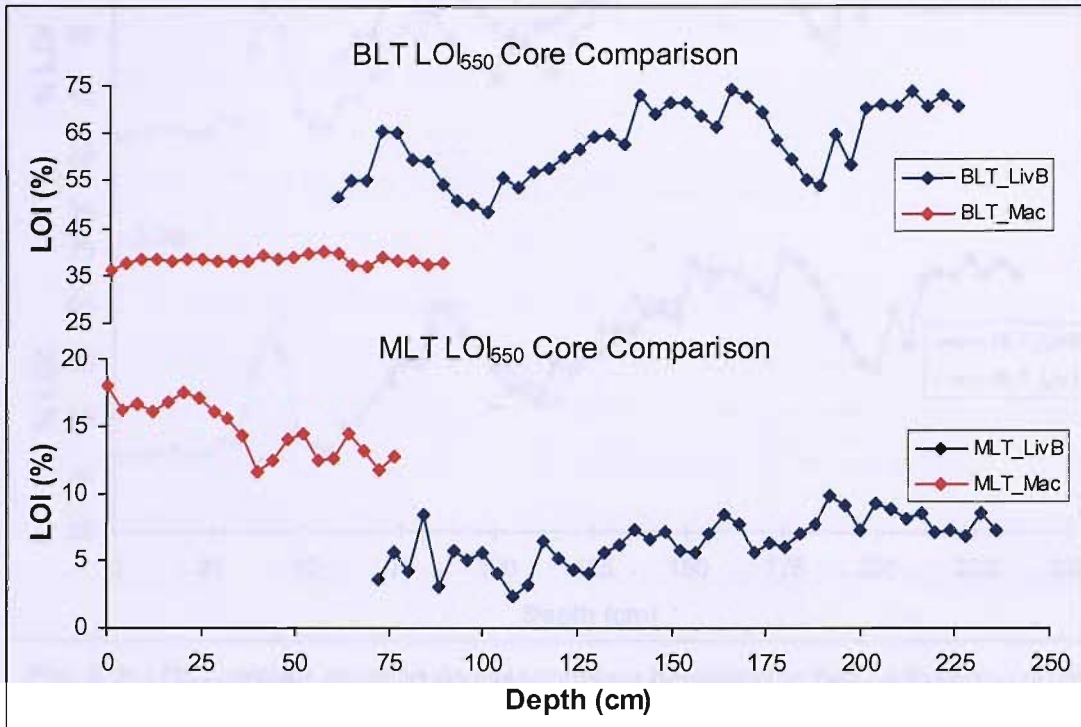


Fig. 3.1: Mismatch between LOI_{550} values of Mackareth and Livingstone cores from Bigland Tarn and Malham Tarn.

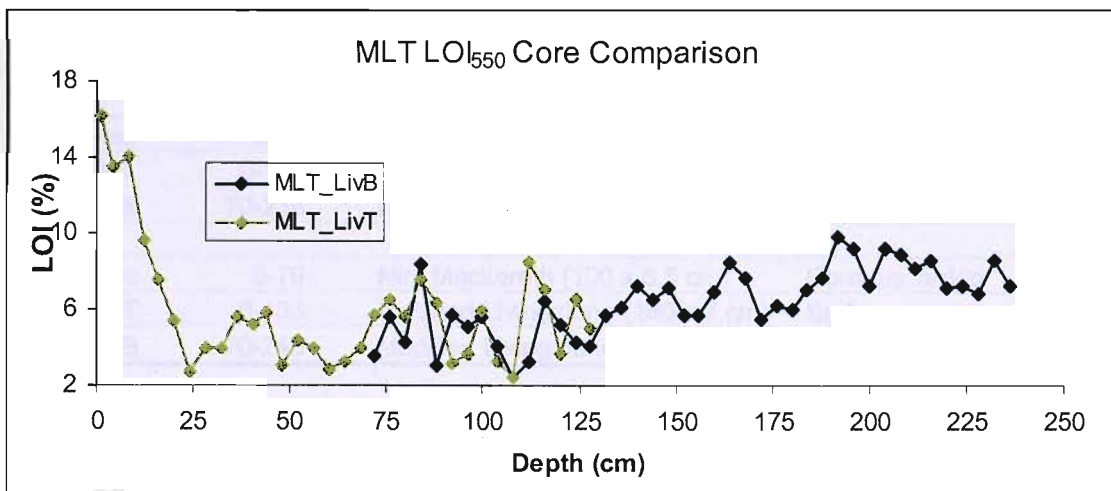


Fig. 3.2: LOI_{550} values showing good correspondence between the two Livingstone cores from Malham Tarn.

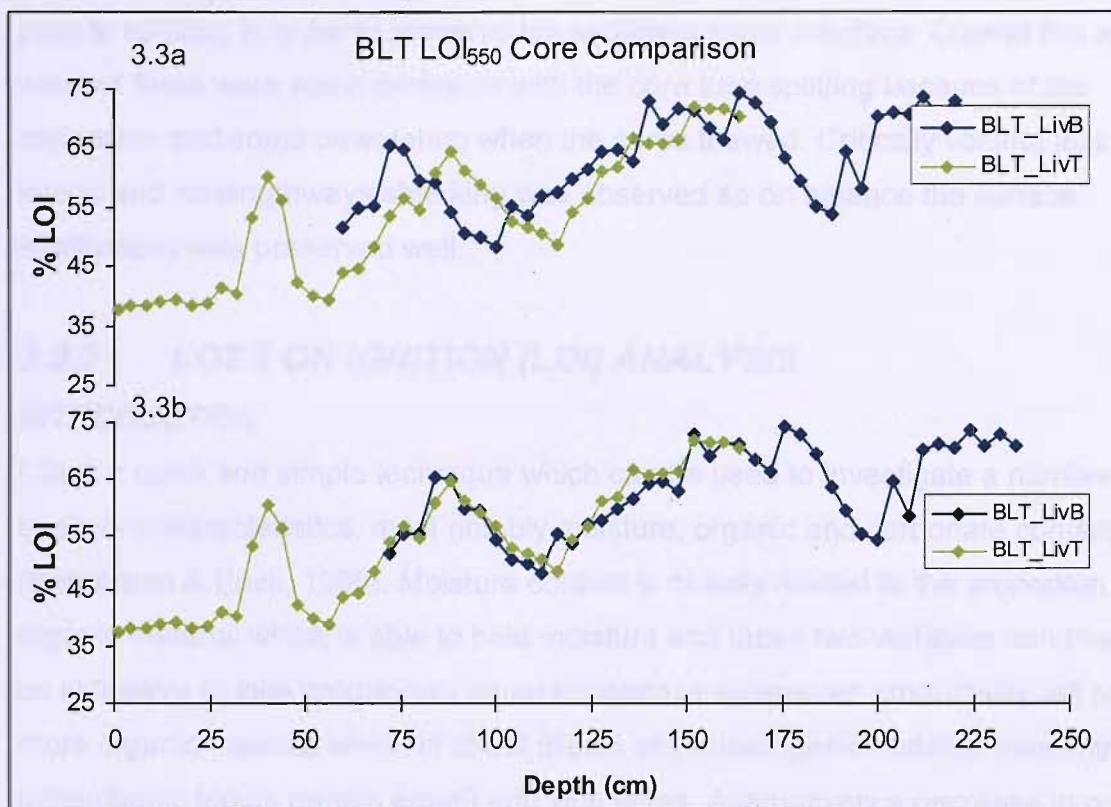


Fig. 3.3: LOI₅₅₀ values showing correspondence between the two Livingstone cores from Bigland Tarn. Fig. 3.3a = depth mismatch due to field measurement error. Fig. 3.3b = very close correspondence following depth correction of the lower core to match the upper core which preserved the sediment water interface.

Table 3.1: Lake Core Details

Core Codes	Sediment Depth (cm)	Corer Used	Details
BLT_Mac	0-91	Mini Mackereth (100 x 6.5 cm)	Core discarded
BLT_LivT	0-165	Modified Livingstone (180 x 7 cm)	Surface
BLT_LivB	70-238	Modified Livingstone (180 x 5 cm)	Depth adjusted (+12cm)
MLT_Mac	0-79	Mini Mackereth (100 x 6.5 cm)	Core discarded
MLT_LivT	0-133	Modified Livingstone (180 x 7 cm)	Surface
MLT_LivB	70-240	Modified Livingstone (180 x 5 cm)	

Mackereth cores were extruded using a hydraulic piston extruder and subsampled as 1 cm contiguous slices. Each subsample was placed in a re-sealable plastic bag and refrigerated at 4 °C. All Livingstone cores were split lengthways and half of each core was frozen and the other half refrigerated. The topmost Livingstone cores were frozen

prior to splitting in order to preserve the sediment water interface. Overall this worked well but there were some problems with the core tube splitting because of the expansion and some dewatering when the cores thawed. Critically volume loss was lateral and no lengthways shrinking was observed so on balance the surface stratigraphy was preserved well.

3.3.2 LOSS ON IGNITION (LOI) ANALYSIS

INTRODUCTION

LOI is a quick and simple technique which can be used to investigate a number of sediment characteristics, most notably moisture, organic and carbonate content (Bengtsson & Enell, 1986). Moisture content is closely related to the proportion of organic material which is able to hold moisture and these two variables can therefore be indicative of lake productivity as an increase in ecosystem productivity will produce more organic material which in effect dilutes any minerogenic material (assuming minerogenic inputs remain equal) and vice versa. Alternatively a decrease in organic material may indicate an increase in minerogenic input resulting from inwash from the catchment. Identifying a significant carbonate component to the sediments is valuable in assessing any potential 'hard water effect' which might influence radiocarbon dates and changes in the ratio of carbonate may also indicate changes in lake productivity. Changes in productivity or the rate of sediment inwash can exert a strong influence on sediment accumulation rates so LOI values provide an important aid to chronological interpretation and age-depth model selection.

The proportion of these sediment components is estimated by heating at sequentially higher temperatures such that moisture is estimated by heating the sample to c. 100 °C, a temperature which is high enough to evaporate the moisture but enough to oxidise the organic material. Organic content is estimated by oxidising to ash and carbon dioxide (CO₂) at 500-550 °C and carbonate (CaCO₃) by evolving CO₂ from the CaCO₃ at 900-1000 °C. The weight loss during each stage is measured by weighing the samples before and after heating and is closely correlated to the moisture content and organic and carbonate matter in the sediment respectively (Heiri *et al.*, 2001). In

addition to providing a quick and effective measure of sediment characteristics LOI is a useful tool for aligning and correlating core sections. However, the accuracy of estimates can vary depending on the method used (e.g. Sutherland, 1998). A standardised procedure was proposed by Heiri *et al.*, (2001) to improve inter-study comparability of results and this procedure was followed and is described below.

LABORATORY PROCEDURE

1. 1 cm³ subsamples were taken at 4 cm resolution placed in pre-weighed ceramic crucibles and weighed on precision scales;
2. Crucibles were covered and samples were dried in an oven at 105 °C overnight and then reweighed;
3. Next samples were ignited in a muffle furnace at 550 °C for 4 hours to combust the organic matter, allowed to cool and reweighed;
4. Finally the samples were put back into the furnace and heated to 950 °C for 2 hours to remove carbonate;
5. The proportion of organic and carbonate content were then calculated as a percentage of dry weight and water content as a percentage of the wet weight according to the formulas below.

Moisture Content

$$DW_{105} = (WW - DW_{105} / WW) \times 100 \quad \text{(Equation 3.1)}$$

Organic Content

$$LOI_{550} = ((DW_{105} - DW_{550}) / DW_{105}) \times 100 \quad \text{(Equation 3.2)}$$

Carbonate Content

$$LOI_{950} = (((DW_{550} - DW_{950}) \times 1.36) / DW_{105}) \times 100 \quad \text{(Equation 3.3)}$$

Where:

LOI₅₅₀ = LOI at 550 °C as a percentage

DW₁₀₅ = dry weight of the sample before combustion

DW₅₅₀ = dry weight of the sample after combustion at 550 °C

LOI₉₅₀ = dry weight of the sample after combustion at 950 °C

The weight loss by LOI₉₅₀ was multiplied by 1.36 to calculate the weight of carbonate in the original sample (Bengtsson & Enell, 1986).

3.3.3 CHIRONOMID ANALYSIS

INTRODUCTION

Chironomids or non-biting midges are a group of flies (Diptera) which are highly sensitive to environmental conditions and to summer temperature in particular. The larval head capsules are readily preserved in lake sediments and they are consequently excellent palaeotemperature indicators. The strengths and limitations of the technique are discussed in the Literature Review (Section 2.8).

LABORATORY PROCEDURE

Slightly different preparatory procedures were required for the different sediment characteristics of the two sites, the differences are detailed below. A protocol for carbonate sediments advocated by Lang *et al.*, (2003) was trialled on the carbonate sediments from Malham Tarn but although this greatly increased the amount of carbonate which passed through the sieves it also considerably reduced the head capsule yield (Table 3.2) and was consequently not used.

1. Organic rich sediments were deflocculated in 10% KOH at 75°C for 10-15 minutes. The solution was not allowed to boil as this can cause head capsules to disintegrate. Carbonates were deflocculated in warm water (45°C);
2. Samples were then gently washed through 180 and 90 µm sieves and the two size fractions kept separate to aid sorting;

3. Sieve residue was washed into a Steralin tube and pipetted into a grooved Perspex (Bogorov) sorter (Gannon, 1971) with a 5 mm by 5 mm groove.
4. All head capsules were picked from each fraction using fine forceps at x30 magnification under a binocular dissecting microscope;
5. Head capsules were mounted directly onto microscope slides using the water based mountant Hydromatrix. Three capsules were placed under each 6 mm coverslip and ten coverslips arranged on each slide.

A minimum of 50 head capsules were counted per level (Heiri & Lotter, 2001; Larocque, 2001) and more material prepared when this number was not found. Only in rare cases were less than fifty head capsules counted. Material was then identified under a compound microscope at x100, x200 and x400 magnification according to Cranston (1982), Oliver & Roussel (1983), Wiederholm (1983), Hoffman (1971), Rieradevall & Brooks (2001) and Brooks (2004, unpublished key).

Table 3.2: Ultrasonic Chironomid Test Preparations after Lang et al. (2003)

Depth (cm)	No. of Head Capsules	Preparation Details
75	13	Conventional treatment (see below)
75	2	Ultrasonic (35kHz) 180 µm fraction 2 min / 90 µm fraction 3 min
75	7	Ultrasonic (35kHz) 180 µm fraction 10 sec / 90 µm fraction 15 sec
75	10	Ultrasonic (35kHz) 180 µm fraction 5 sec / 90 µm fraction 5 sec
75	16	Conventional treatment (see below)
30	22	Conventional treatment (see below)
30	6	Ultrasonic (35kHz) 180 µm fraction 5 sec / 90 µm fraction 5 sec
30	8	Ultrasonic (35kHz) 180 µm fraction 2 sec / 90 µm fraction 3 sec
30	24	Conventional treatment (see below)

Samples were homogenised and then 2 cc subsamples prepared and picked for head capsules

Reconstructed mean July air temperatures were calculated using the Norwegian transfer function Brooks & Birks (2000; 2001) and applied using weighted averaging partial least squares (WA-PLS) calibration using the program WA-PLS (Juggins & Ter Braak, 1995). Sample specific root mean squared errors of prediction (RMSEP) were estimated by leave one out (jack-knifing) cross-validation, generating 95% confidence intervals on the mean July air temperature reconstruction.

3.4 CHRONOLOGICAL STRATEGY

The establishment of a secure chronology is critical to palaeoclimatic investigation and errors in its derivation impose limits on interpretation of the data, particularly in correlating proxy records from different sites. Smart & Frances (1991) list three criteria of prime importance in the selection of a dating method:

- Applicability – is there something datable in a particular deposit?
- Time range – does the time range of the method match the probable age of the deposit?
- Precision/accuracy – is the method capable of resolving the age difference of the events of interest?

For this investigation AMS ^{14}C assay satisfied the three criteria as fully as current techniques allow (with the exception of Malham Tarn). Near surface dating was provided in all cores by SCP analysis and this was augmented in the lake cores by ^{210}Pb measurements. Where possible the main shifts in proxy inferred conditions were dated directly as recommended by Telford *et al.*, (2004). Age-depth models were also constructed for each core to facilitate age estimation of those shifts not dated directly and to provide a context for understanding stratigraphic integrity and sediment accumulation rates.

3.4.1 CARBON-14 MEASUREMENT

INTRODUCTION

All radiocarbon determinations were funded through the Natural Environment Research Council Radiocarbon Steering Committee (NERC RSC) and subsequently processed at the Radiocarbon Laboratory, East Kilbride (NERC RCL). Raw radiocarbon dates were calibrated using the computer program Calib 5.0.1 (Stuiver *et al.*, 2005) and the INTCAL 04 calibration dataset (Reimer *et al.*, 2004).

PEAT SUBSAMPLING

Peat samples were sieved through 125 µm mesh with distilled water, residue was then washed into a glass petri dish and analysed under a binocular dissecting microscope. Between 100 and 300 mg (wet weight) of material which could be positively identified as being above-ground plant macrofossil components such as *Sphagnum*, Monocotyledon and Ericaceous leaves and stems were then picked and stored in 10 ml glass vials with a little distilled water. One sample from Malham Tarn Moss (SUERC-7047) had insufficient material to pick and consequently 1 cm³ of bulk peat was used.

LAKE SEDIMENT SUBSAMPLING

Where possible terrestrial macrofossils were picked for dating however they were only available from Bigland Tarn. Identifiable terrestrial macrofossil samples were picked from a glass petri dish containing distilled water under a binocular dissecting microscope. Material was washed in distilled water before being stored in 10 ml glass vials with a little distilled water. Where insufficient terrestrial macrofossil material was available 1 cm³ samples of bulk sediment were used.

Malham Tarn - core MLT proved awkward to date from the outset, which was not unexpected since Malham is a carbonate lake. Initial efforts focussed on searching for terrestrial macrofossils, which generally provide reliable age estimates, but these were not forthcoming; there was potential to identify this material during chironomid picking as well as through separate sieved fractions and none came to light.

Furthermore when this material is occasionally found it is not guaranteed to yield accurate dates (e.g. Haweswater, Bedford, pers. comm., 2006) and so an alternative was required. Dating of pollen concentrates seemed like a promising alternative and a number of techniques were trialled using sieving, centrifugation, density separation and various combinations of these (e.g. Brown *et al.*, 1989; Mensing & Southon, 1999; Regnell, 1992; Regnell & Everitt, 1996; Vandergoes & Prior, 2003).

Unfortunately none of these yielded satisfactory results as it proved impossible to remove sufficient detrital material from the pollen residue. A colleague, Dr Michael

Grant, kindly produced an outline (8 cm resolution) pollen diagram for both Malham Tarn and Malham Tarn Moss in the hope that changes might be matched and these used to correlate the lake profile with the adjacent well dated peat profile but there was insufficient stratigraphic change to allow correlation between profiles. Charcoal had been initially discounted due to the low concentration but experimentation revealed that sufficient material could be isolated if several contiguous samples of sediment were processed (typically 4-5 cm vertical extent). Carbonate was dissolved with HCl and the residue sieved through a 90 µm sieve and analysed under a binocular dissecting microscope. Charcoal and identifiable terrestrial plant fragments were picked using fine forceps and stored in 10 ml glass vials with a little distilled water.

LABORATORY PROCEDURE

All samples were sent to the NERC RCL, East Kilbride for pre-treatment and measurement. Pre-treatments varied according to the material submitted for analysis. Samples composed of above ground material (bog) or terrestrial macrofossil material (lake) were digested in 2M HCL at 80 °C for eight hours and washed free from mineral acid with distilled water before being dried and homogenised.

Bulk sediment samples were digested in 1M HCl at 80 °C for eight hours, washed free from mineral acid with distilled water and then digested in 0.5M KOH at 80 °C for two hours. The digestion was repeated using distilled water until no further humics were extracted. Residue was then rinsed free of alkali, digested in 1M HCl at 80 °C for two hours then rinsed free of acid before being dried and homogenised.

The small predominantly charcoal samples from Malham Tarn were soaked overnight in 0.5M HCL at room temperature. Samples were filtered and rinsed free of mineral acid with deionised water then dried and homogenised

In all cases following pre-treatment total carbon in a known weight of sample was converted to CO₂ by heating with CuO in a sealed quartz tube. The gas was then

converted to graphite by Fe/Zn reduction and mounted on a pellet for measurement by atomic mass spectrometry (AMS) on the SUERC AMS facility on a 5MV National Electrostatic Corporation AMS system.

3.4.2 SPHEROIDAL CARBONACEOUS PARTICLE (SCP) ANALYSIS

INTRODUCTION

When burned at industrial temperatures of up to 1750 °C fossil fuels burn efficiently leaving only porous spheroids of mainly elemental carbon and fused inorganic spheres formed from mineral inclusions present within the fuel (Rose *et al.*, 1995). These spheroidal carbonaceous particles (SCP) and inorganic ash spheres (IAS) are collectively known as spherical fly ash particles (Rose *et al.*, 1995). SCPs are most commonly counted because they are chemically robust, readily identifiable and have no natural source.

SCPs are released into the atmosphere along with the plume of flue gases and can be transported long distances through the atmosphere to be deposited in remote areas (Yang *et al.*, 2001). As peat accumulates, deposited SCPs are preserved with contemporary peats. Experiments carried out by Punning & Alliksaar (1997) on the trapping of fly ash particles on *Sphagnum* mosses showed there to be 'essentially no movement of particles in the moss sequence.' It is therefore reasonable to assume that the SCP profile in an undisturbed and steadily accumulating peat core faithfully records historical atmospheric SCP deposition (Yang *et al.*, 2001). The sedimentary record of SCPs can therefore be used as a dating tool for post industrial times by correlating features in the particle concentration profiles with the known fuel combustion history of the region

LABORATORY PROCEDURE

SCP analysis was used as a tool to date the near surface sediments of all four sites. Procedure followed Rose (1994) for the lake sites and Yang *et al.*, (2001) for the peatland sites. Age estimates are made by comparison of SCP concentration profiles

with those of Rose *et al.*, (1995) and Rose, (2005, unpublished data). Typically three phases of change in SCP concentration can be used to date near surface sediments. These are (1) the start of the SCP record, (2) the rapid increase in concentration and (3) the subsurface peak in concentration (Rose *et al.*, 1995). A number of factors complicate interpretation of SCP profiles including local industrial history, changes in accumulation rate and changes in the bulk density of the sediments, a factor particularly relevant to peat cores which tend to undergo a significant change in bulk density over the acrotelm/catotelm transition (Yang *et al.*, 2001):

SCP extraction procedure for peats following Yang *et al.*, (2001).

1. Subsamples were dried overnight under a heat lamp and 200 mg accurately weighed into 50 ml beakers.
2. 6 ml of concentrated nitric acid (HNO₃) was then added to each beaker and the whole batch heated to 100 °C on a hotplate until the solution reduced to ~1 ml (during heating the beaker was rocked every 6 -8 minutes to ensure that material did not stick to the beaker walls);
3. The beakers were then removed from the hotplate, 10 ml of distilled water added to each and the suspension transferred into 12 ml polypropylene tubes. These were centrifuged at 1,500 rpm for 5 minutes and the supernatant liquid decanted;
4. The beaker walls were then rinsed and the washings transferred into the same tubes. This procedure was repeated until the beakers were clean and the tubes were then centrifuged again and the supernate decanted;
5. Tubes were then washed as necessary until the supernate became relatively clear (usually twice is plenty);
6. Labelled 10 ml glass vials were weighed and the polypropylene tubes decanted into them. The vials were then centrifuged and as much of the supernate as possible pipetted off before the vials and residues were weighed
7. A little of each residue was then pipetted onto a cover slip and left to evaporate and the vial reweighed. Once dry the coverslip was mounted on a labelled slide using the water based mountant Hydromatrix.

The SCP extraction procedure for lakes following Rose (1994).

1. 0.1-0.2g of dried sediment was accurately weighed in a labelled 12 ml polypropylene tube. 1.5 ml of concentrated nitric acid (HNO_3) was then added to each tube which were covered and left in a fume cupboard overnight;
2. Another 1.5 ml of concentrated nitric acid was then added and the tubes before heating in a water bath at 80 °C for 2 hours. Tubes were then removed from the water bath and topped-up with distilled water before being centrifuged at 1500 rpm for 5 minutes;
3. The supernatant nitric acid was pipetted off. 3 ml of hydrofluoric acid (HF) was then added to each tube before returning them to the water-bath for a further two hours at 80 °C;
4. Samples were removed from the water bath, topped-up with distilled water and left, overnight in the fume cupboard;
5. Tubes were centrifuged at 1500 rpm for 5 minutes and the supernatant liquid pipetted off. 3 ml 6M HCl was then added to each tube before heating in a water-bath at 80°C for a further 2 hours;
6. Tubes were removed from the water bath topped-up the distilled water and centrifuge at 1500 rpm for 5 minutes. The HCl was pipetted off;
7. Samples were washed with distilled water and centrifuged at 1500 rpm for 5 minutes. Supernatant liquid was pipetted off;
8. Step seven was repeated;
9. A small 10 ml glass vial was labelled and weighed and the residue transferred before re-weighing;
10. A little of each residue was then pipetted onto a cover slip and left to evaporate and the vial reweighed. Once dry the coverslip was mounted on a labelled slide using the water based mountant Hydromatrix.

SCPs were counted using a light microscope at x400 magnification. All the SCPs on the cover-slip were counted and care was taken to ensure the full area of the dried

sample droplet was covered. Concentration is expressed as numbers of particles per gram dry mass of sediment (or gDM^{-1}).

3.4.3 LEAD-210 RADIOMETRIC DATING

INTRODUCTION

^{210}Pb measurement can be used as a tool for dating recent (near surface) sediments and was used for both of the lakes investigated. Standard methods were applied. The theory of ^{210}Pb dating is outlined below, and draws heavily on the work of Appleby (2001, p. 171-203).

^{210}Pb ($t_{1/2} = 22.26$ y) occurs naturally as one of the radionuclides in the ^{238}U decay series. A fraction of the ^{222}Rn atoms produced by the decay of ^{226}Ra in soils escape into the atmosphere where they decay through a series of short lived radionuclides to ^{210}Pb (Appleby, 2001) this is removed from the atmosphere by both wet and dry deposition. Much of the material which is deposited into lakes either directly or via its catchment is incorporated into the sediments. The total ^{210}Pb activity in sediments has two components, supported ^{210}Pb derived from *in situ* decay of the parent radionuclide ^{226}Ra , and unsupported ^{210}Pb derived from the atmospheric flux. Unsupported ^{210}Pb in sediments decays in accordance with the radioactive decay law (Equation 3.4) and in most cases equilibrium between total ^{210}Pb and supporting ^{226}Ra is achieved after a maximum of 6-7 ^{210}Pb half lives (130-150 years), (Appleby, 2001). Within this time frame the decay of unsupported ^{210}Pb can usually be used to date the sediments provided that reliable estimates can be made of the initial ^{210}Pb activity in each sediment layer at its time of formation (Appleby, 2001).

$$C_{\text{Pb}} = C_{\text{Pb}}(0)e^{-\lambda t} + C_{\text{Ra}}(1-e^{-\lambda t}) \quad \text{(Equation 3.4)}$$

Where:

λ = ^{210}Pb radioactive decay constant
 $C_{\text{Pb}}(0)$ = Initial ^{210}Pb activity at the time of deposition

Measurements of ^{210}Pb deposition show that, although fluxes can vary significantly over short timescales, it tends to be relatively uniform over longer periods of a year or more (Appleby, 2001). Constant flux rate is therefore usually a safe assumption when trying to establish the ^{210}Pb activity of sediments at the time of deposition. A second significant variable is the rate of sediment accumulation which in effect governs the dilution ratio of ^{210}Pb within the sediment and consequently the activity per unit of sediment.

In lakes with steady catchment erosion and water column productivity sediment accumulation rates remain fairly consistent and it is reasonable to assume that the dilution ratio is constant. Under conditions of constant flux and constant sedimentation each layer of sediment will have the same initial unsupported ^{210}Pb activity and it is easy to calculate sediment age based on the ^{210}Pb activity. This scenario is known as the simple model or the constant flux, constant sedimentation (CF:CS) model (Appleby & Oldfield, 1992). In order to establish a relatively constant sedimentation rate ^{210}Pb activity can be plotted against depth. Since radioactive decay occurs exponentially the data should be well described by an exponential curve with highest activity at the surface falling to supported levels at depth. If the data do not fit this model then sedimentation rates have probably fluctuated and an alternative model is required in order to date the sediments using ^{210}Pb . If however the data are a reasonable fit unsupported ^{210}Pb activity can be plotted on a logarithmic scale against sediment depth in which case the relationship appears linear. Mean sedimentation rate can then be determined from the slope of the profile using a least-squares fit according to the equation (3.5 below)

$$C(m) = C(0)e^{-\lambda m/r} \tag{Equation 3.5}$$

Where:

- m = depth below the sediment water interface
 - λ = ^{210}Pb radioactive decay constant
 - r = Sedimentation rate
 - $C(0)$ = unsupported ^{210}Pb activity at the surface of the core
-

LABORATORY PROCEDURE

Analysis was undertaken at the National Oceanography Centre, Southampton (NOC,S) and followed the protocol of the Geosciences Advisory Unit ^{210}Pb dating: proxy method using alpha spectrometric determination of ^{210}Po following acid leaching and autodeposition onto Ag discs. The procedure describes the determination of ^{210}Po in sediment samples, following aqua regia digestion and autodeposition of Po onto silver discs. The discs are then counted via alpha spectrometry. Detection limits are nominally 0.1 Bq/kg.

1. 1-3 g of dry powdered sediment was accurately weighed into a 250 ml beaker and the scales Tared;
2. 0.5 ml of tracer was added by pipette, and the weight of tracer added immediately recorded (since the tracer is diluted in HNO_3 , fizzing will be observed when tracer is added to sediment, hence the need for immediate measurement);
3. 30 ml aqua regia was then added slowly and the beakers left for 3 to 5 hours;
4. A further 30 ml aqua regia was then added, the beakers were covered with watch glasses and refluxed on a hotplate at $70\text{ }^\circ\text{C}$ for 4 hours;
5. Once cool the residue was centrifuged and washed 3 times with distilled water (after this stage, the sediment residue may be disposed of);
6. The resulting supernatant was collected in 250 ml beakers and carefully evaporated to dryness at $80\text{ }^\circ\text{C}$. Care was taken to avoid loss of solution due to bumping;
7. Residue was dissolved once more in a small volume of 6M HCl and again evaporated to dryness (this ensures conversion of extract into chloride form). Step seven was repeated;
8. Residue was dissolved once more in 8 ml 6M HCl and transferred to 100 ml beakers. The 250 ml beaker was washed several times with distilled water and the washings added to the 100 ml beaker. The volume of liquid in the cell was made

- up to 60 ml (using distilled water, at which point the molarity of the acid is approximately 0.8M);
9. Approximately 1.5 g Ascorbic Acid (reducing agent) was added and stirred until the solution changed to a pale yellow colour;
 10. A PTFE disc holder with a freshly burnished silver disc was added (the silver disc had PVC tape on one side, to ensure plating of one side of the disc only);
 11. Samples were left to plate for 36 hours or more, on a warm hotplate or furnace top out of any draught;
 12. At the end of the plating the discs were removed, washed with distilled water followed by acetone and the sample number marked on the back before being left covered by a plastic beaker for a minimum of 24 hours before counting by alpha spectrometry;

3.4.4 AGE-DEPTH MODELLING

While it may be desirable to bracket important shifts with radiocarbon dates it is not always feasible due, for example, to a lack of datable material or simply because of time or financial constraints. An age-depth model provides a means of estimating the age of samples which fall between radiocarbon dates and also a context for understanding sediment accumulation rates. Age-depth models are therefore useful aids to analysis but must be used with caution since much interpretation rests upon them.

Commonly used models include linear interpolation, polynomial line fitting, linear regression and smooth cubic splines (Bennett, 1994). A test of the most commonly applied methods by Telford *et al.*, (2004) using simulated data on a varved chronology found that no model performed consistently well with few dates. The smooth cubic spline models performed best when there were many dates relative to sediment changes but overall it was felt that this required considerably more dates than are employed in the majority of studies (Telford *et al.*, 2004). Linear interpolation forces the model to pass through the dates and as a result cannot deviate too far from reality, the negative consequence of this is that the error term inherent in radiocarbon

dating is incorporated into the model (Telford *et al.*, 2004). Nevertheless linear interpolation was felt to offer a good balance between robustness and simplicity.

The main limitations of the linear interpolation model are

- That only two dates are taken into account at a time and consequently no allowance is made for the relationship to the other dates.
- Changes in accumulation rate are forced to occur at the dated horizons producing linear accumulation punctuated by rapid, sometimes quite significant changes over the dated horizons. Needless to say the sediments may well have not accumulated in this way, with changes occurring more gradually or having occurred elsewhere in the core.

It is quite reasonable to assume that at least some of the changes in accumulation of the peat cores occur on the dated horizon since dates were targeted on stratigraphic changes as represented by the plant macrofossil data. However dates were targeted on wet rather than dry shifts so not all of the stratigraphic changes were dated and some changes will inevitably be smoothed or exaggerated to some extent.

The assumption that changes in accumulation rate change occur at the dated horizons is more problematic for the lake cores since they did not exhibit visible stratigraphic changes so it was not possible to target likely changes in accumulation rate. In practice however there are few major changes in accumulation rate forced by the linear interpolation model (Section 5.3.4) so linear interpolation offers a reasonable fit to these lake data also.

3.5 QUANTITATIVE ANALYSIS

3.5.1 DETRENDED CORRESPONDENCE ANALYSIS (DCA)

DCA is a method of multivariate statistical analysis known as ordination, the purpose of which is to set in order the data, in this case the arrangement of fossil assemblages in relation to each other in terms of their similarity of species composition. DCA is

widely employed by ecologists and is a useful means of exploring ecological data. Comprehensive texts on the topic are provided by Kent & Coker (1992), Kovach (1995) and ter Braak (1995).

DCA can also be termed gradient analysis since it is designed to relate variation in species composition with variation in environmental factors, which can usually be represented by environmental gradients (Kent & Coker, 1992). However the analysis is indirect in the sense that it reveals structure within the biological data. This structure is attributed to a number of independent axes which are then related to environmental gradients on an interpretative level based on an understanding of the ecological requirements of the species/taxa present.

Computationally DCA is related to the method of weighted averaging of Whittaker (1967) so that quadrat scores are derived from species scores and weightings and species scores are derived from sample scores and weightings. These are carried out iteratively and stabilise out to give a set of scores for species and samples which are used to construct species and sample ordinations respectively (Kent & Coker, 1992). DCA adjusts for some of the problems encountered with CA (correspondence analysis) most notably the arch and axis compression effects (Hill & Gauch, 1980).

DCA output is typically displayed as ordination graphs which usually display two axes on which each point represents a sample or species. The distances between points on the graph (ordination space) are a measure of their degree of similarity/dissimilarity so that points which plot close together represent samples which are similar compositionally (sample plot) or species which often co-occur (species plot).

One problem with DCA is in dealing with a crossed gradient, i.e., where a few of the samples are quite different to the others due to an unusual event or driver. This structure is picked out by the DCA but dominates the ordination relegating all other drivers to axes of lower importance despite the fact that they might have been important drivers for the majority of the samples. This is a common problem where

anthropogenic influence has significantly altered community structure in recent time. This problem can be remedied by omitting the unusual data. However this can only be justified if the cause can be identified and its overall relevance assessed.

3.6 *TRANSFER FUNCTIONS*

This section provides an overview of the theory which underlies the use and application of transfer functions as a means of quantitative palaeoecological reconstruction. For a more in-depth overview the reader is referred to Birks (1995), a work which this section draws heavily upon.

Early palaeoenvironmental studies which utilised biological proxies involved largely qualitative interpretation of fossil assemblages. Such interpretation was revolutionised in by Imbrie & Kipp, (1971) who presented for the first time quantitative procedures for the reconstruction of past environmental variables from fossil assemblages involving transfer (or calibration) functions (Birks, 1995). Quantitative palaeoenvironmental reconstruction aims to express the value of an environmental variable (e.g. temperature or soil moisture) as a function of biological data (e.g. testate amoebae or chironomid assemblages). This function is termed the transfer function or biotic index and its configuration is called calibration (Birks, 1995). Calibration is the opposite of regression where the aim is to model the response of a biological taxon as a function of one or more environmental variables. Calibration and regression differ because the causal and statistical relationships between taxa and their environment are not symmetrical (ter Braak, 1987).

The basic idea of quantitative environmental reconstruction is shown in Fig. 3.4 Where there is one or more environmental variable X_0 that requires reconstructing from fossil biological data Y_0 consisting of m taxa in t samples. To estimate values of X_0 it is necessary to model the response of the same m taxa today in relation to the environmental variable(s) of interest. This involves the use of a modern 'training set' of m taxa at n sites (Y) studied as assemblages preserved in surface sediments with an associated set of modern environmental variables (X) for the same n sites. The

modern relationships between Y and X are modelled statistically and the resulting function used to transform the fossil data Y_0 into quantitative estimates of the past environmental variable(s) X_0 .

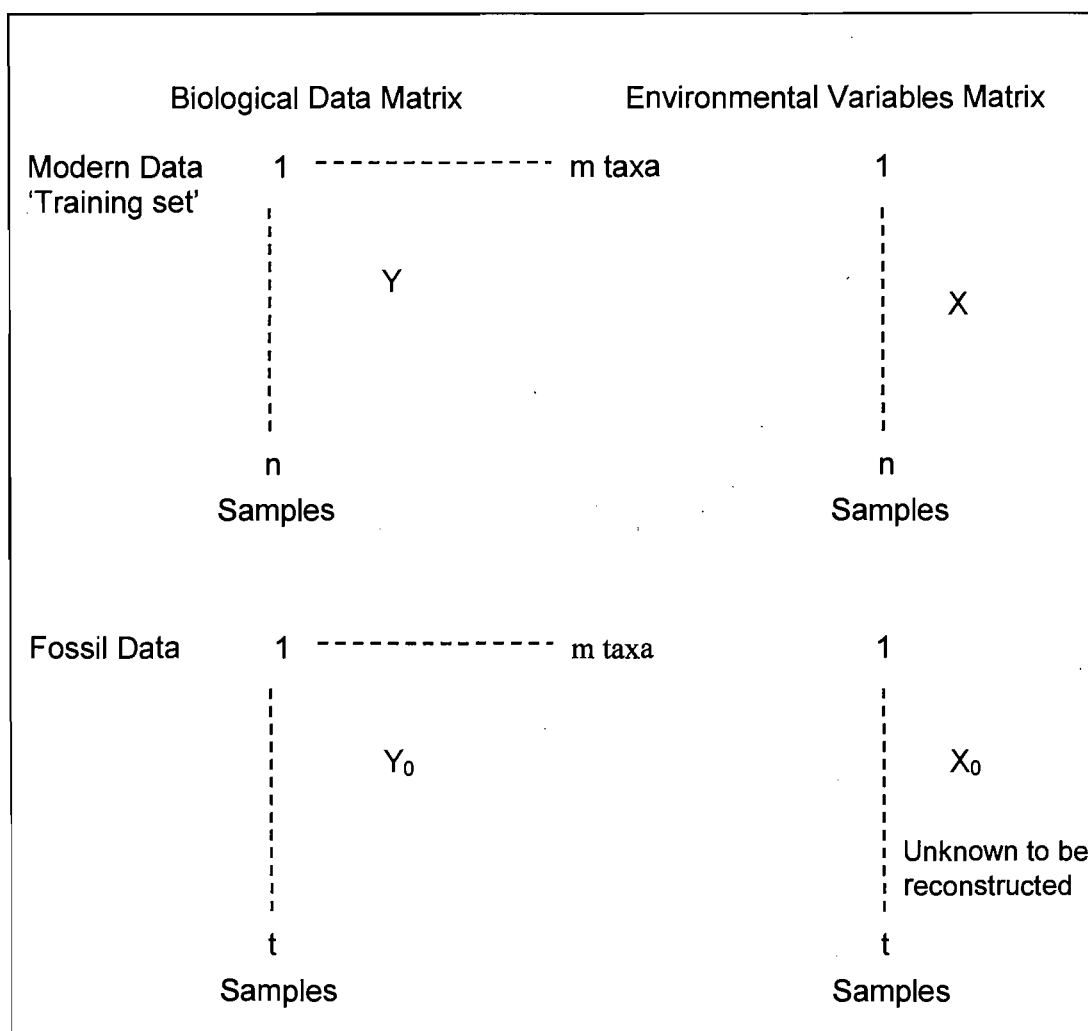


Fig. 3.4: Principles of quantitative palaeoenvironmental reconstruction. X_0 the unknown environmental variable to be reconstructed from fossil assemblages Y_0 , and the role of a modern training set consisting of modern biological and environmental data, X and Y respectively. Source: Birks (1995).

Five major assumptions are made in quantitative palaeoenvironmental reconstructions. Real ecological systems never conform perfectly to these assumptions; nevertheless the closeness of fit is an important factor in assessing the reconstruction.

1. Taxa in the modern training set (Y) are systematically related to the environment (X) in which they live;
2. The environmental variable(s) to be reconstructed (x) is, or is linearly related to, an ecologically important determinant in the system of interest;
3. The taxa in the training set (Y) are the same biological entities as in the fossil data (Y_0) and their ecological response \hat{U} to the environmental variable(s) of interest have not changed significantly over the time span represented by the fossil assemblage;
4. Mathematical methods in regression and calibration adequately model the biological responses to the environmental variable(s) of interest and yield calibration functions with sufficient predictive power to allow useful, accurate, and unbiased reconstruction of X;
5. Other environmental variables to the ones of interest have negligible influence, or their joint distribution with the environmental variable in the fossil set is the same as in the training set.

(Birks, 1995)

The fundamental difference between the various numerical methods in use relate to the assumed taxon-environment response model. Some methods assume a linear response model and for each of these there are corresponding techniques that assume a unimodal response (Birks, 1998). Within the linear and unimodal based methods, different procedures for estimating the parameters of the model can be used, for example maximum likelihood, least squares, weighted averaging, partial least squares (Birks, 1995) and more recently bayesian statistics (Korhola *et al.*, 2002). Unimodal based techniques are largely accepted as being more ecologically plausible since modern taxa-environment relationships are generally observed to be non-linear and the abundance of taxa can often be explained by a unimodal relationship with a given environmental variable. These unimodal methods are often well solved by a simple and computationally fast algorithm involving weighted averaging (WA) estimation (Birks, 1998) and quantitative reconstructions are usually

based on some variation of this method. The most commonly employed WA variant is the weighted averaging partial least squares (WA-PLS) procedure of ter Braak & Juggins (1993). WA-PLS incorporates further components that utilize residual structure within the data to improve the species optima in the final weighted average predictor (ter Braak & Juggins, 1993). This procedure forms the basis of most current transfer functions (e.g. Brooks & Birks, 2000 ; 2001; Larocque *et al.*, 2001; Olander *et al.*, 1999).

4.0 SITE DESCRIPTIONS

The northwest of England has an abundance of lakes and raised bogs and provided a promising area from which to select paired lake and bog sites for palaeoecological study. Particular effort was made to minimise the distance between each lake and bog pair so that differences in the records would be unlikely to reflect climatic differences between the two locations. Two field site-pairs were selected and their locations are shown on the map below (Fig. 4.1). The first pair consists of Hulleter Moss and Bigland Tarn in southern Cumbria and the second pair Malham Tarn Moss and Malham Tarn in the North Yorkshire Dales.

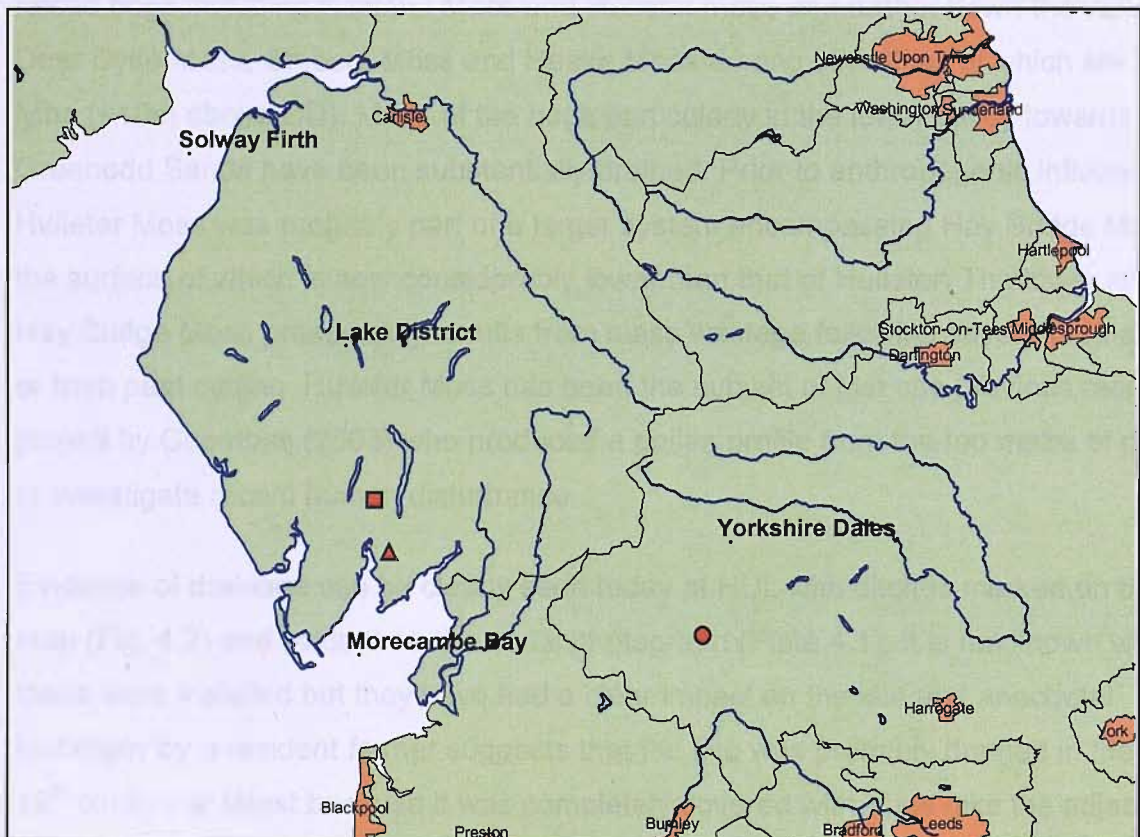


Figure 4.1: Field Site Location Map. Square = Hulleter Moss, Triangle = Bigland Tarn and circle = Malham Tarn and adjacent Malham Tarn moss

4.1 Hulleter Moss

Table 4.1 Hulleter Moss Site Details

Site code	HUL
NGR	333390, 488030
Altitude	c. 10 m OD
Area	9.4 ha

Hulleter Moss lies within the Hay Bridge Nature Reserve, which can be found in the Rusland Valley in southern Cumbria. The reserve is approximately four kilometres north of Haverthwaite; it is privately owned by the John Strutt Conservation Foundation (JSCF) and is co-managed by the JSCF and the Hay Bridge Nature Reserve Society (a registered charity). The Rusland Valley contains a number of raised bogs including Rusland Moss and Hulleter moss and further down the valley Deer Dyke Moss, Stribers Moss and Reake Moss among others, all of which are low lying (<10m above OD). Many of the bogs particularly in the lower valley towards Greenodd Sands have been substantially drained. Prior to anthropogenic influence Hulleter Moss was probably part of a larger system encompassing Hay Bridge Moss, the surface of which is now considerably lower than that of Hulleter. The lower level of Hay Bridge Moss presumably results from mass wastage following severe drainage or from peat cutting. Hulleter Moss has been the subject of just one previous research project by Coombes (2003) who produced a pollen profile from the top metre of peat to investigate recent human disturbance.

Evidence of drainage can be clearly seen today at HUL with ditches marked on the map (Fig. 4.2) and evident on the aerial photograph (Plate 4.1). It is not known when these were installed but they have had a clear impact on the site and anecdotal testimony by a resident farmer suggests that the site was probably drained in the late 19th century at latest because it was completely covered with trees (like the adjacent Rusland Moss today) until the early 1950s when a fire destroyed most of the trees. There is also some evidence of additional disturbance to the eastern edge of the bog most likely due to spoil tipping from ditch installation and subsequent clearance (Plate 4.1). In spite of the drainage, water levels were still very high at the time of coring and *Sphagnum* communities were common.

Surface vegetation consists of: *Molinia caerulea*, *Rhynchospora alba*, *Eriophorum vaginatum*, *Eriophorum angustifolium*, *Calluna vulgaris*, *Erica tetralix*, *Trichophorum cespitosum*, *Myrica gale*, *Andromeda polifolia*, *Betula*, *Pinus sylvestris*, *Sphagnum papillosum*, *Sphagnum tenellum*, *Sphagnum capillifolium* var. *rubellum*, *Sphagnum subnitens*, *Cladonia* and algal mud. Some of these species, particularly *Myrica gale* and *Sphagnum subnitens*, are atypical raised bog plants and are indicative that the site has undergone some alteration, probably relating to the drainage and possibly nutrient enrichment from surrounding farmland.

Prior to choosing a sampling location a field stratigraphy was produced which involved seven four-metre cores taken at 20 m intervals along the transect marked on Fig. 4.2 and Plate 4.1. The cores were numbered one to seven running east to west and the stratigraphy is drawn up in Fig. 4.3. The master core was taken from a location close to field core three (marked by a blue circle on the map (Fig. 4.2) and aerial photograph (Plate 4.1)).

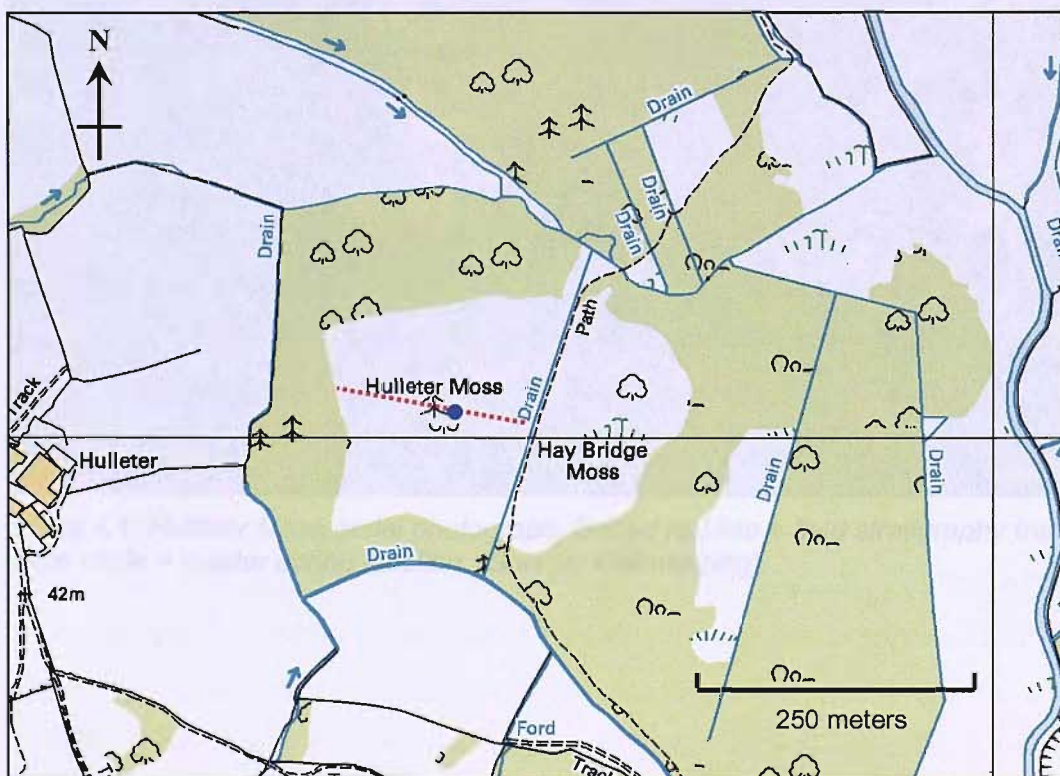


Figure 4.2: Hulleter Moss Site Map. Dotted red line = field stratigraphy transect. Blue circle = master coring location. (Source: Ordnance survey via EDINA)

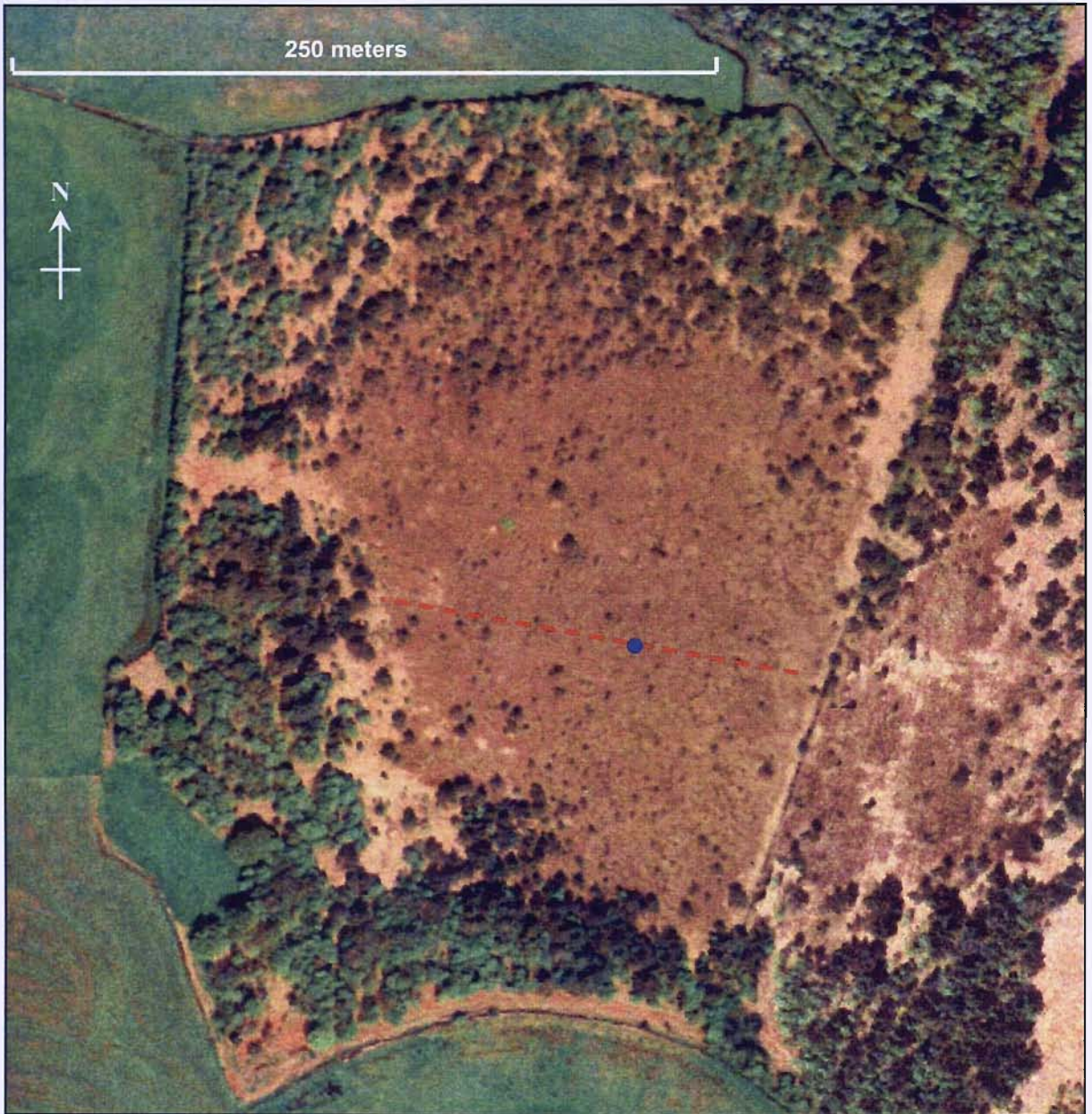


Plate 4.1: Hulleter Moss aerial photograph. Dotted red line = field stratigraphy transect. Blue circle = master coring location. (Source: Getmapping).

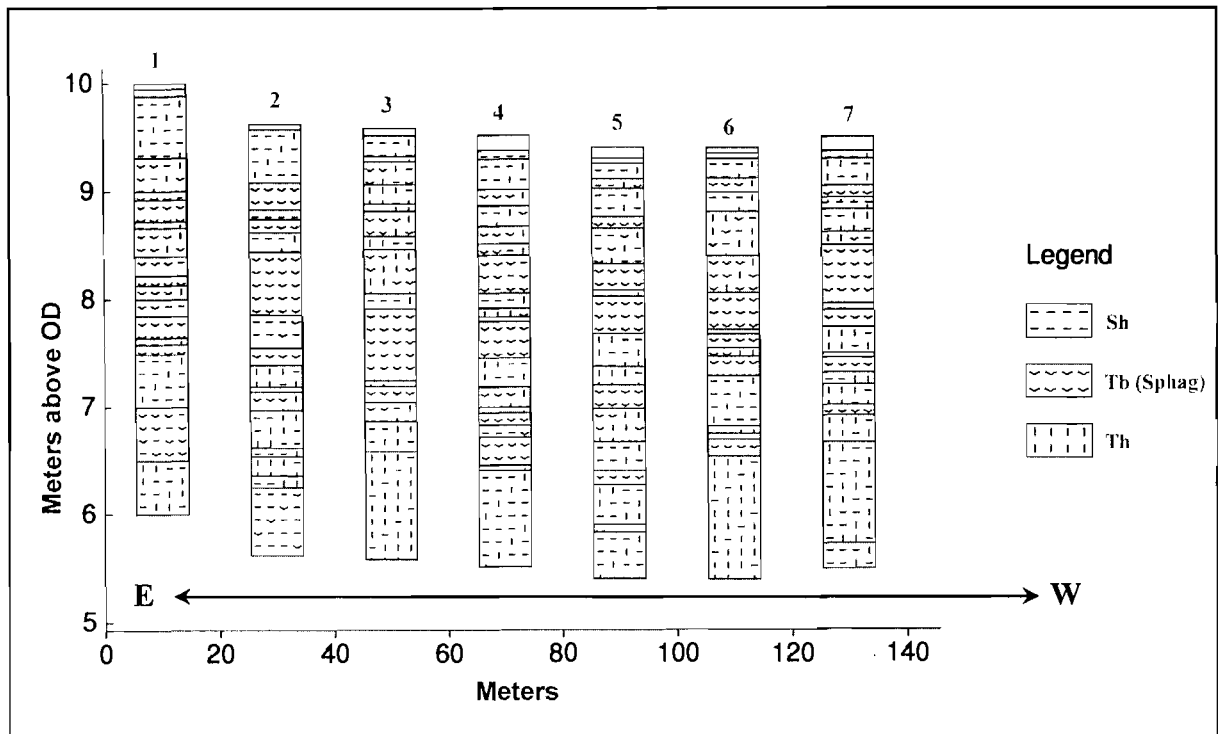


Figure 4.3: Hulleter Moss Field Stratigraphy. The cores follow a transect running east to west across the site (Fig. 4.2).

4.2 Bigland Tarn

Table 4.2: Bigland Tarn Site Details

Site code	BLT
NGR	335554, 482900
Altitude	160 m OD
Area	6 ha
Maximum depth	10 m
Core Lithology	Uniform black organic gyttja

Bigland Tarn is a small kettle-hole lake which lies within the privately owned Bigland Estate a few miles south of Newby Bridge in southern Cumbria. The tarn has a small catchment with no inflowing stream but there is a small outflow to the west (Fig. 4.4). The geology in the area is dominated by clay with flints and morainic drift. Bigland Tarn has not been the subject of any previous investigation of which the author is aware and the bathymetry has not been mapped. Field analysis with an echo depth sounder revealed the lake bed to be a classic basin shape, which sloped gently from

shallow margins towards a central depth of 10 m. An intermediate water depth of five metres was chosen for sampling and the location is marked on the map (Fig. 4.4).

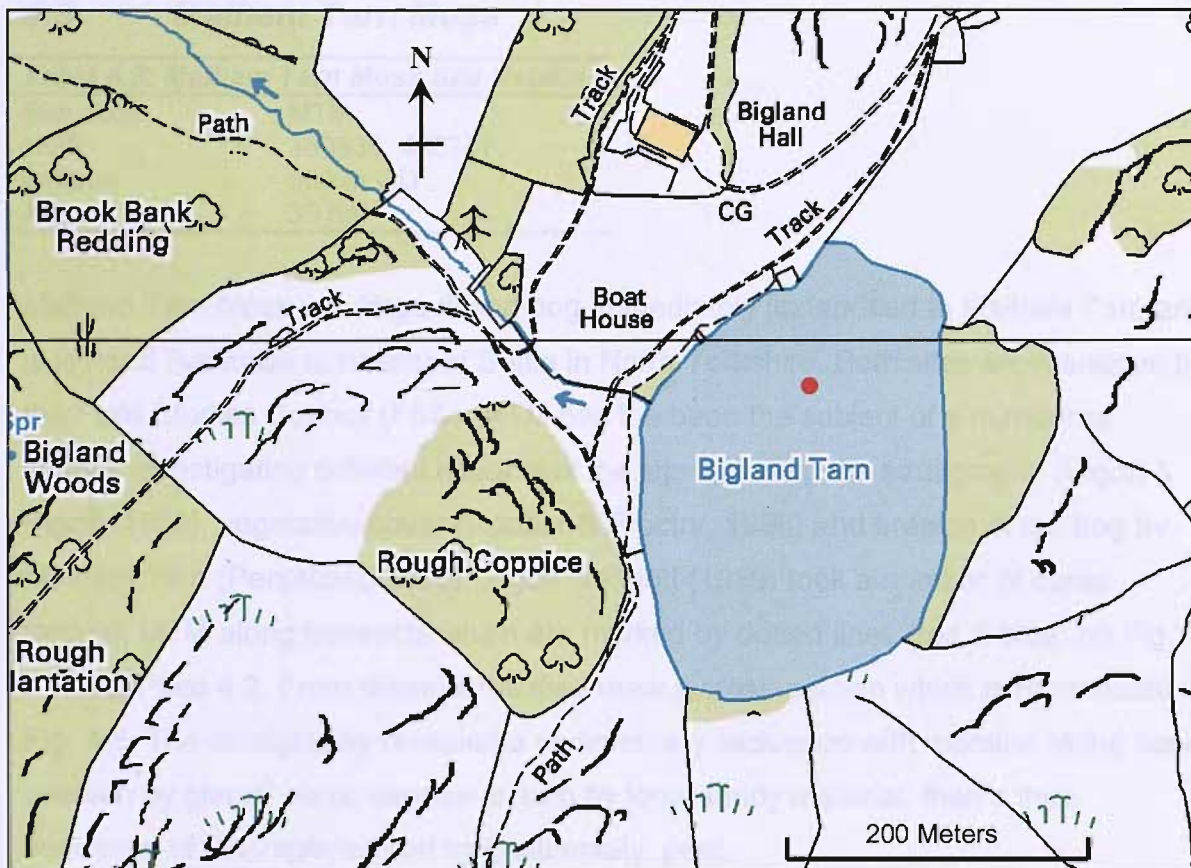


Figure 4.4: Bigland Tarn Site Map. Red circle = master coring location (Source: Ordnance survey via EDINA Digimap)

The Bigland Estate can be traced to have been owned by the Bigland family in some form since AD 1161 (Anon, 1895). A search of the Kendal Records office revealed little direct information about the Tarn, for example, whether it had been stocked with fish or dredged, but some indirect information could be gleaned. The information was primarily related to the small structure on the west of the tarn which today looks like a boat house and is marked on the map as such (Fig. 4.4). However, it is clear from the literature that this was in fact originally an ice house (David, 1981). The water level must have subsequently been increased in order that the ice house is now

flooded. The earliest ice house in Cumbria was recorded in AD 1732 so the raising of the Tarn must have post dated this (David, 1981).

4.3 Malham Tarn Moss

Table 4.3: Malham Tarn Moss Site Details

Site code	MTM
NGR	389339, 466747
Altitude	380 m OD
Area	39 ha

Malham Tarn Moss is a large raised bog immediately juxtaposed to Malham Tarn and is located five miles northeast of Settle in North Yorkshire. Both sites are managed by the Field Studies Council (FSC). MTM has been the subject of a number of studies investigating different aspects of the site including the stratigraphy (Pigott & Pigott, 1959), vegetative cover (Cooper & Proctor, 1998) and erosion of the bog by Malham Tarn (Pentecost, 2000). Pigott & Pigott (1959) took a number of cores through MTM along transects which are marked by dotted lines (red & blue) on Fig. 4.5 and Plate 4.2. From these cores they drew a cross-section which is reproduced in Fig. 4.6. The stratigraphy revealed a sedimentary sequence with moraine at the base overlain by glacial clays, overlain in turn by local sandy material, then a thick sequence of Charaphyte marl and, ultimately, peat.

Prior to sampling a field stratigraphy was produced. This involved five four-metre cores taken at 20 m intervals along part of one of the transect lines of Pigott & Pigott, (1959) marked on the map and aerial photograph by a blue dotted line. This stratigraphy focussed in more detail on the peat stratigraphy than that of Pigott & Pigott (1959). The cores were numbered one to seven running north to south and the stratigraphy is drawn up in Fig. 4.7. The master core was taken from close to core two and the location is marked by a blue circle on the map and aerial photograph (Fig. 4.4 & Plate 4.2).

At the time of coring surface vegetation was dominated by *Molinia caerulea*, *Eriophorum vaginatum*, *Calluna vulgaris*, *Erica tetralix*, *Trichophorum cespitosum*,

Pinus sylvestris, *Sphagnum papillosum*, *Sphagnum tenellum*, *Sphagnum capillifolium* var. *rubellum*, *Sphagnum subnitens*, *Cladonia* and algal mud.

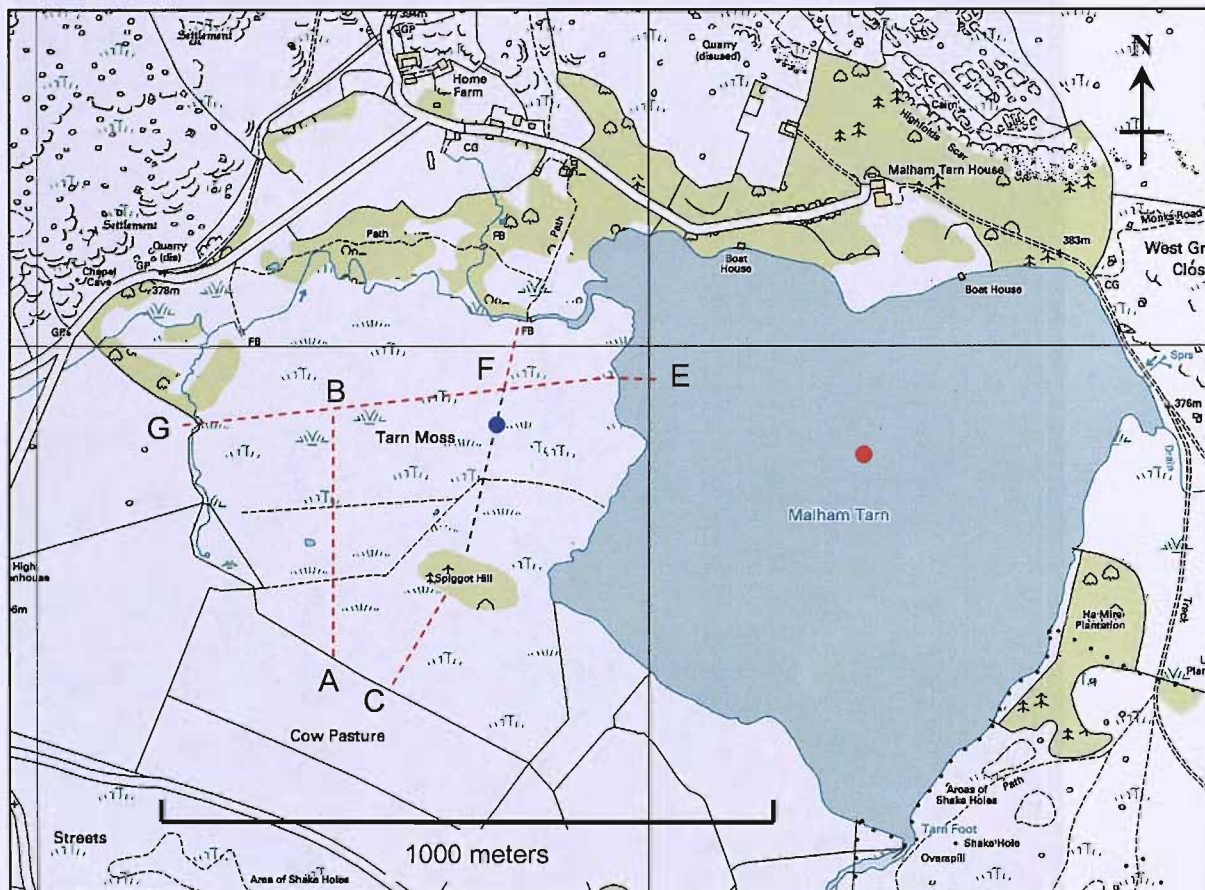


Figure 4.5: MTM and MLT Site Map. Dotted lines and letter codes show the transects of Pigott & Pigott (1959). Blue dotted line shows the part of the transect used for the field stratigraphy (Fig.4.7). Blue circle marks the coring location on MTM. Red circle marks the coring location from MLT. (Source: Ordnance survey via EDINA Digimap)



Plate 4.2: Aerial Photograph of MTM. Dotted lines show the transects of Pigott & Pigott (1959). Blue dotted line shows part of transect used for the field stratigraphy (Fig.4.7). Blue circle marks the coring location on MTM. (Source: Getmapping).

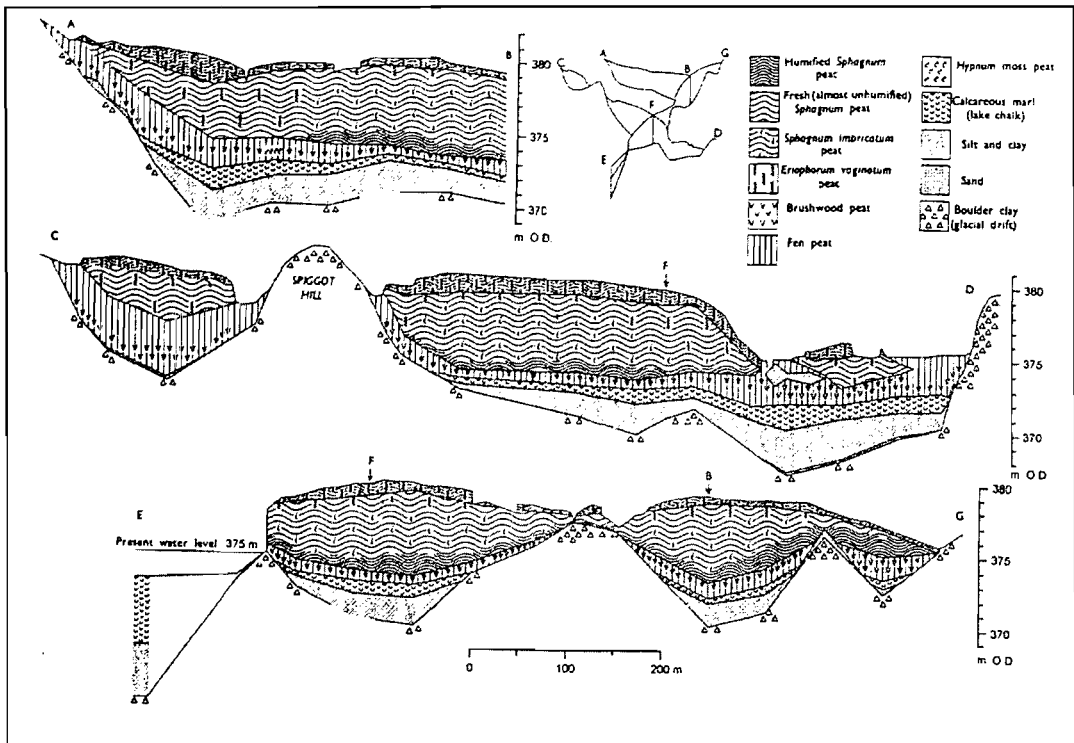


Figure 4.6: Cross section of MTM reproduced from Pigott & Pigott (1959)

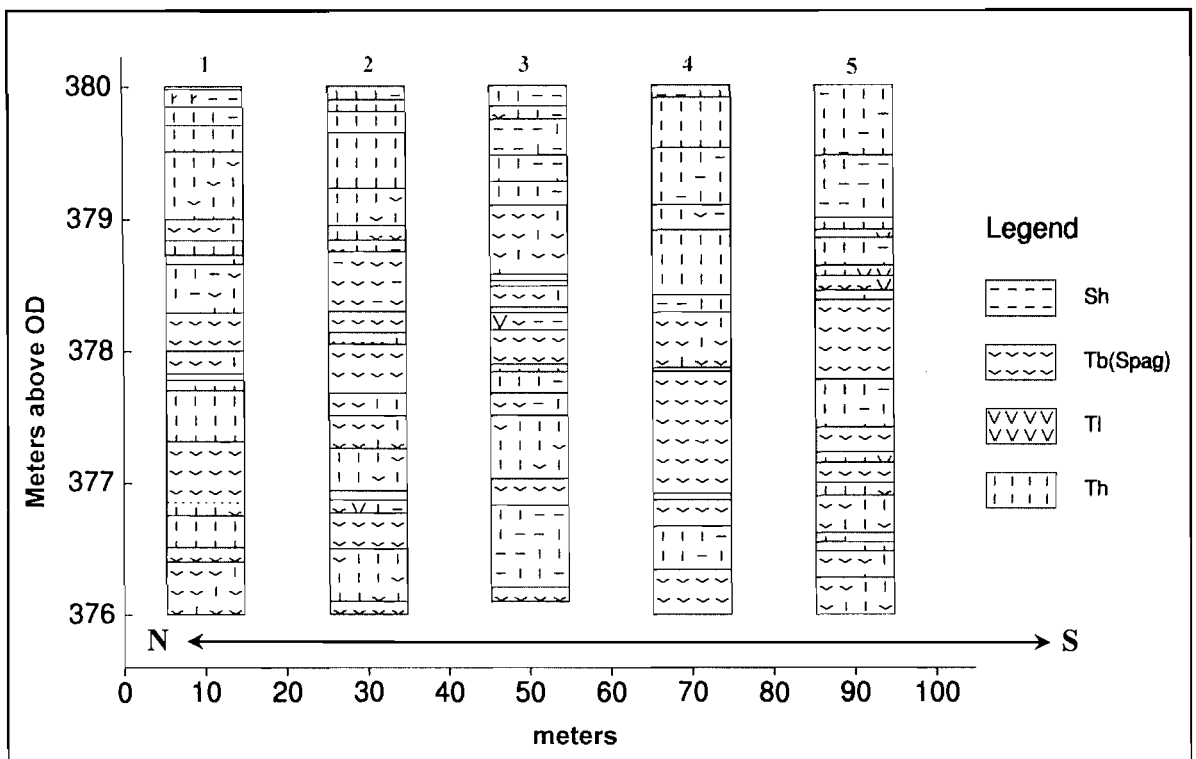


Figure 4.7: Malham Tam Moss Field Stratigraphy. The cores follow a transect running north to south across the site (Fig. 4.2).

4.4 Malham Tarn

Table 4.4: Malham Tarn Site Details

Site code	MLT
NGR	388611, 466843
Altitude	376.6 m
Surface Area	61.9 ha
Maximum depth	4.4 m
Catchment area	6 km
Core Lithology	0-24 cm Organic gyttja 24-240 carbonate with occasional bands of aquatic moss

Malham Tarn is the highest calcareous lake in Britain. The tarn lies largely over Silurian slates covered with glacial drift and autochthonous marl deposits.

Surrounding the Tarn is limestone predominately Carboniferous in age (Holmes, 1965). The main inflow to the tarn takes the form of a small stream which enters at the north-western corner (Fig. 4.5) but there are also a number of small springs which issue from close to the limestone/shale boundary on the eastern shore. An outflowing stream leaves the tarn from its southern end (Fig. 4.5). Malham is a shallow lake with only a few areas greater than 3.5 m in depth (see bathymetric map, Fig. 4.8). A relatively flat, uniform section of lake bed was chosen as the coring location in a water depth of 3 m (Fig. 4.5 & 4.7). In 1791 the embankment and sluice gate at the outflow were added in order to raise the tarn level this has resulted in erosion of Tarn Moss and an apparent increase in the organic content of the tarn sediments (Pentecost, 2000).

Malham Tarn has been the subject of numerous investigations the most relevant being the stratigraphical investigation of Pigott & Pigott (1959) and stable isotope analysis of Nunez *et al.* (2002).

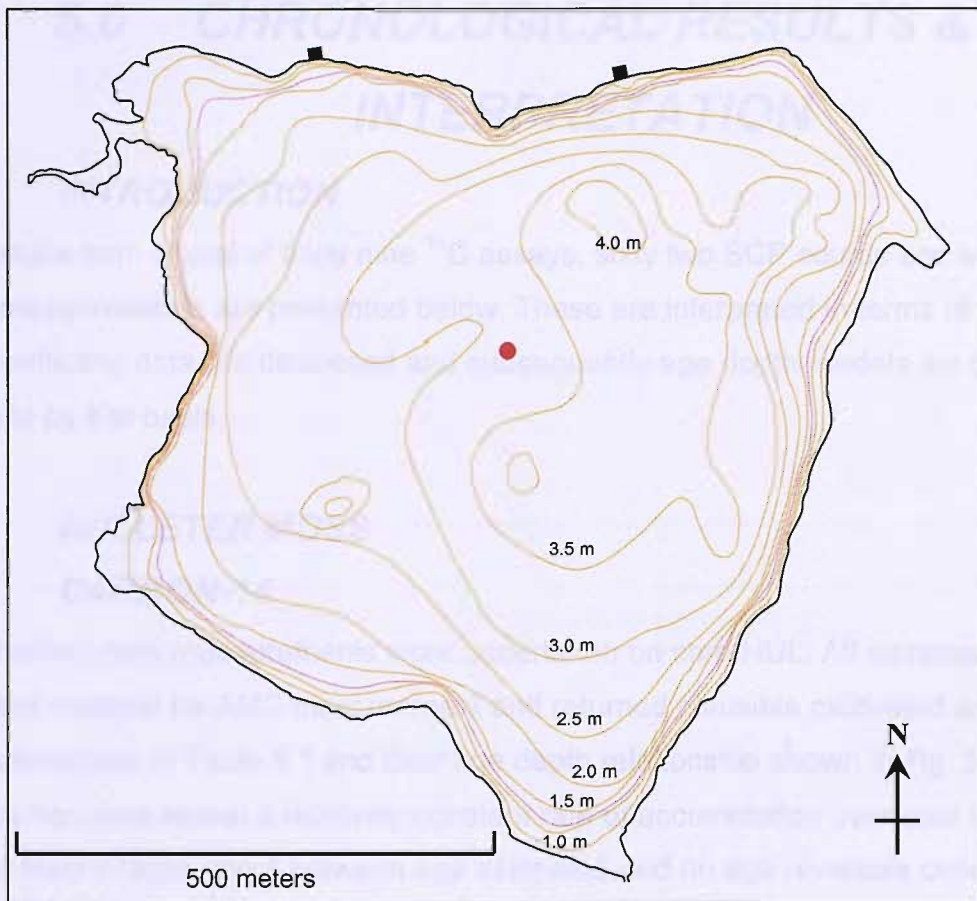


Figure 4.8: MLT Bathymetry provided by Pietro Coletta redrawn after Round (1953). Red dotted line designates the 1791 shore line as calculated by Pentecost (2000) prior to the raising of the water level. Red circle indicates the coring location

5.0 CHRONOLOGICAL RESULTS & INTERPRETATION

5.1 INTRODUCTION

The results from a total of thirty nine ^{14}C assays, sixty two SCP counts and twenty ^{210}Pb measurements are presented below. These are interpreted in terms of sample age, conflicting data are discussed and subsequently age depth models are produced on a site by site basis

5.2 HULLETER MOSS

5.2.1 CARBON-14

Eight radiocarbon measurements were undertaken on core HUL. All samples yielded sufficient material for AMS measurement and returned plausible calibrated ages; data are summarised in Table 5.1 and their age depth relationship shown in Fig. 5.1. The radiocarbon data reveal a relatively constant rate of accumulation over core HUL with a good level of agreement between age estimates and no age reversals over the ~3,600 years represented. The most recent radiocarbon date taken from a depth of 52 cm yielded an age of 1281-1339 cal. BP which is in line with the other radiocarbon dates but is perhaps older than might be expected from a pristine site at this depth. There is therefore some indication that the near surface record may have suffered from some disturbance and this will be explored further below.

5.2.2 SCP ANALYSIS

SCP counts were undertaken at 2 cm resolution over the top 38 cm of core HUL. The concentration curve (Fig. 5.2) displays a double peak similar to that of Burnmoor Tarn, the most proximal site analysed by Rose *et al.*, (1995). Based on comparison with the dated profile from Burnmoor Tarn the rapid increase which starts at 12cm corresponds to the 1950s (taken as AD1955 \pm 5 [-5 BP]) and the subsurface peak at 4 cm corresponds to AD 1978 \pm 2 (-28 BP).

Table 5.1: Hulleter Moss Radiocarbon Measurements & Calibration

Publication Code	Depth (cm)	¹⁴ C Age	Calibrated Age (BP) 2σ Range	*WA	Sample Contents
SUERC-7043	52 ± 0.5	1388 ± 25	1281 - 1339	1310	Sphagnum leaves & stems & E. vaginatum nodes
SUERC-4241	64 ± 0.5	1596 ± 20	1415 - 1531	1473	Sphagnum leaves & stems
SUERC-4242	120 ± 0.5	2181 ± 46	2060 - 2331	2196	Sphagnum leaves & stems
SUERC-4244	160 ± 0.5	2458 ± 26	2362 - 2703	2487	Sphagnum leaves & stems
SUERC-7045	196 ± 0.5	2611 ± 26	2720 - 2767	2744	Sphagnum leaves & stems, Calluna flowers & E. vaginatum leaves/stems
SUERC-4247	240 ± 0.5	2914 ± 26	2963 - 3160	3062	Sphagnum leaves & stems,
SUERC-7050	280 ± 0.5	3259 ± 27	3405 - 3561	3500	Sphagnum, Calluna leaves & flowers and beetle elytra
SUERC-7046	303 ± 0.5	3381 ± 23	3571 - 3689	3630	E. tetralix leaves, stems & flowers & E. vaginatum leaves/stems

Calibrated using Calib 5.0.1 (Stuiver *et al.*, 2005) and the INTCAL 04 dataset (Reimer *et al.*, 2004). * WA = weighted average

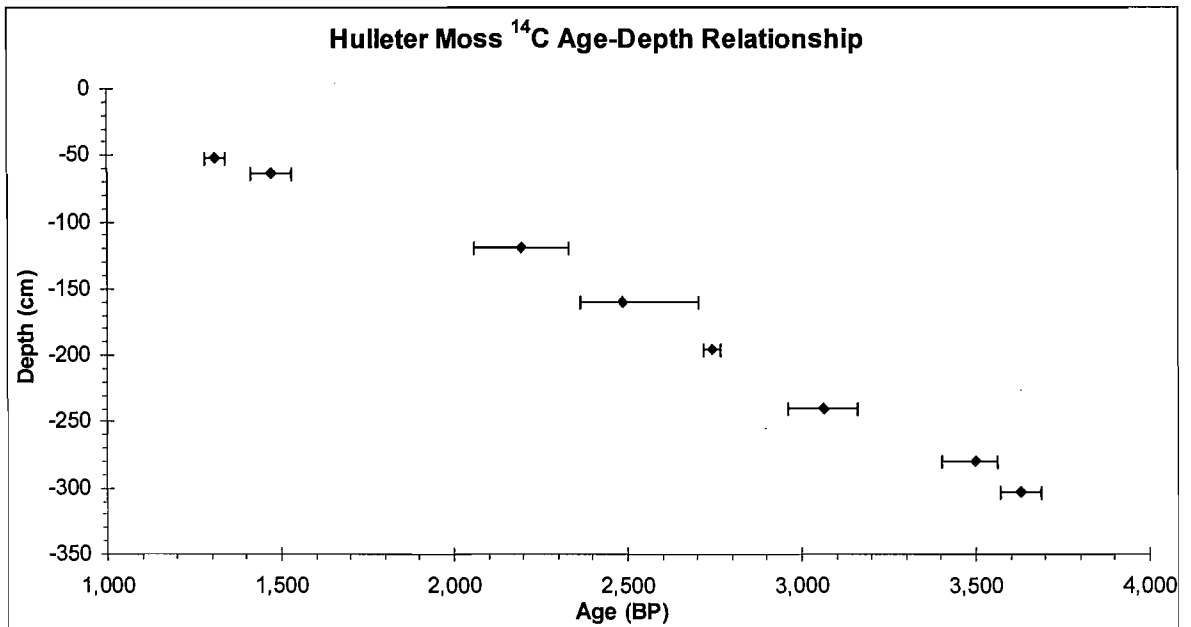


Figure 5.1: Hulleter Moss radiocarbon age depth relationship. Diamonds represent the weighted average (WA) of the age probability distribution and error bars represent the 2σ range

5.2.3 AGE-DEPTH MODELLING

An age-depth model for core HUL was constructed (Fig. 5.3) using the radiocarbon dates (WA of the 2σ age ranges), the rapid rise in SCP concentration and the surface at the time of coring. A simple linear interpolation method was applied, which is summarised in Table 5.2. This model assumes that changes in accumulation occur at

the dated levels, which is a reasonable assumption since dates were deliberately placed on stratigraphic boundaries. The resultant age-depth model predicts an average rate of accumulation for the whole core of 0.8 mm y⁻¹ which is quite typical for British raised bogs e.g.

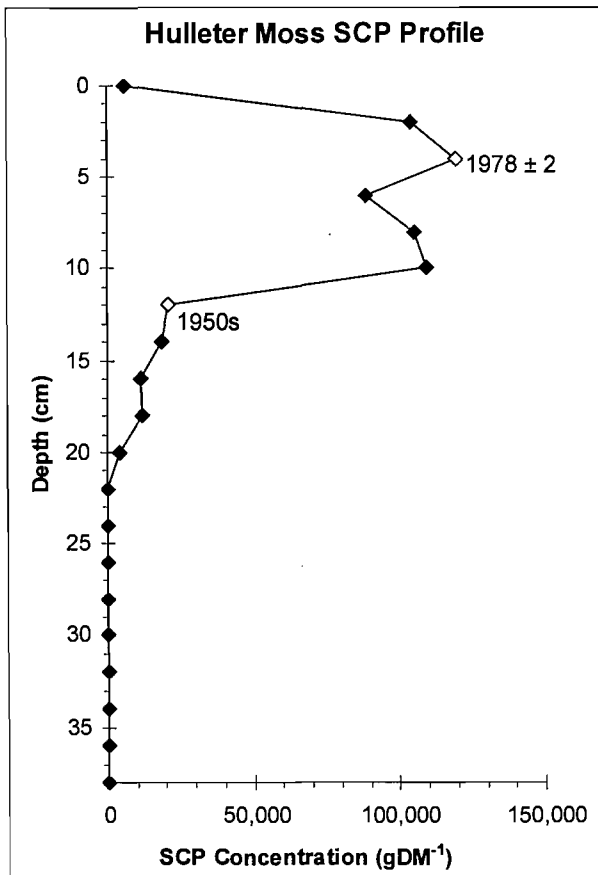


Figure 5.2: Hulleter Moss SCP concentration profile. Diamonds represent particle concentrations per gram dry mass (gDM⁻¹). Unshaded diamonds and associated numbers represent age estimates

Depth Range (cm)	Age Range cal. BP	Equation	Accumulation	
			y mm ⁻¹	mm y ⁻¹
0-11	153 to -9	AGE = 4 x DEPTH - 53	0.4	2.5
12-51	-5 to 1277	AGE = 32.875 x DEPTH - 399.5	3.3	0.3
52-63	1310 to 1459	AGE = 13.583 x DEPTH + 603.67	1.4	0.7
64-119	1473 to 2183	AGE = 12.911 x DEPTH + 646.71	1.3	0.8
120-159	2194 to 2480	AGE = 7.275 x DEPTH + 1323	0.7	1.4
160-195	2477 to 2727	AGE = 7.1389 x DEPTH + 1344.8	0.7	1.4
196-239	2744 to 3055	AGE = 7.2273 x DEPTH + 1327.5	0.7	1.4
140-279	1967 to 3489	AGE = 10.95 x DEPTH + 434	1.1	0.9
280-304	3500 to 3636	AGE = 5.6522 x DEPTH + 1917.4	0.6	1.7
Mean			1.1	0.8

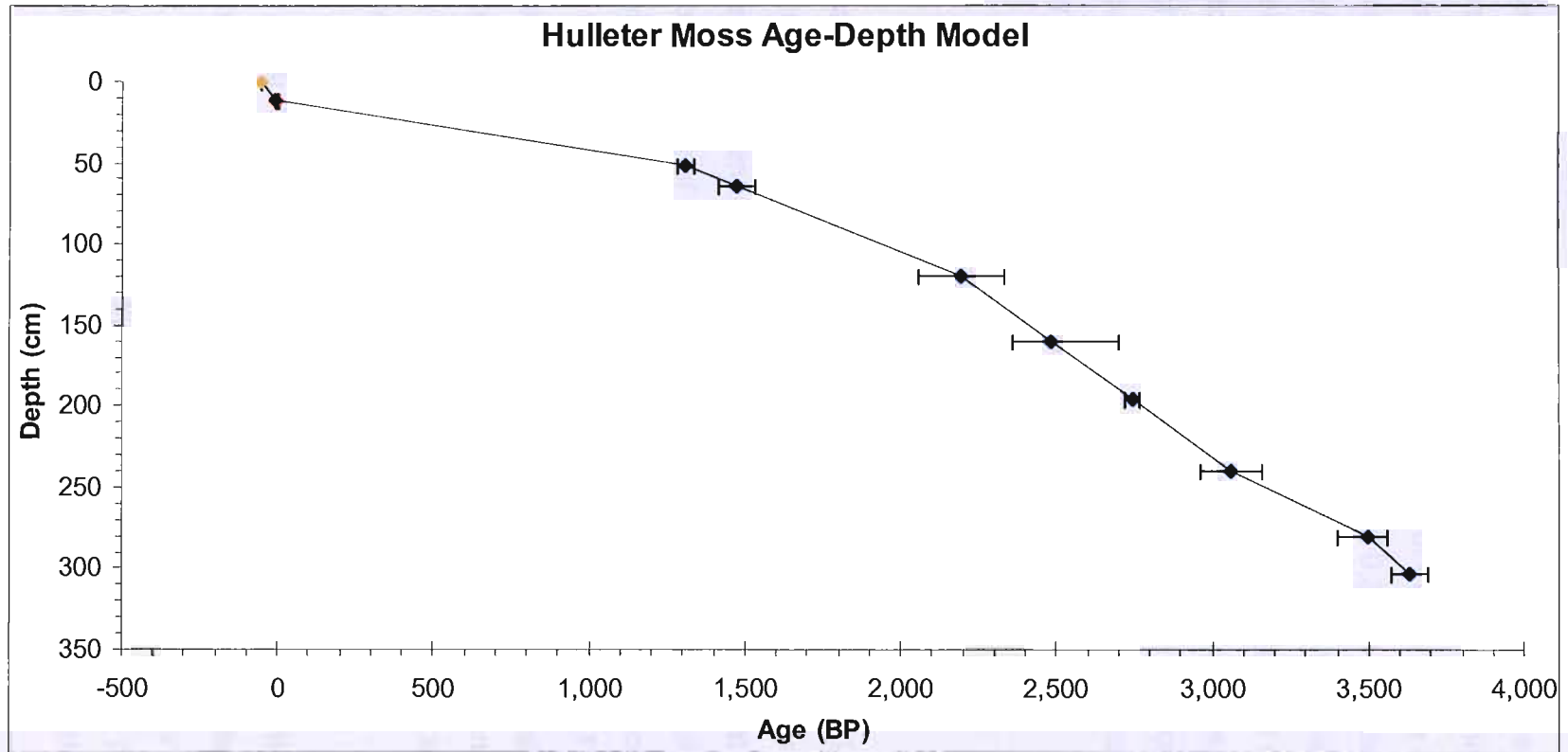


Figure 5.3: Hulleter Moss Age Depth Model based on linear interpolation between points. Blue diamonds = WA of radiocarbon date range and errors bars = the 2σ calibrated age range. The yellow diamond = the surface at the time of coring (2003) and the red diamond = SCP inferred age estimate

The fastest rate of accumulation (2.6 mm y^{-1}) occurs in the near surface peats (0-11cm) and this is to be expected because the peat is still relatively uncompacted. Accumulation rates fluctuate over the remainder of the core from a maximum of 1.7 mm y^{-1} between 280 and 304 cm to a minimum of 0.3 mm y^{-1} between 12 and 51 cm. The latter is considered to be anomalously low compared to the rest of the core and is most likely to result from human disturbance, either through peat cutting or drainage leading to reduced growth rates and possibly mass wastage. The age depth relationship between 12 and 51 cm (-5 to 1277 cal. BP) is therefore poorly constrained compared to the rest of the core and the timing of changes over this section must therefore be regarded as approximate.

5.3 BIGLAND TARN

5.3.1 CARBON-14

Twelve radiocarbon measurements were undertaken on core BLT. All samples yielded sufficient material for AMS measurement and returned plausible calibrated ages. Data are summarised in Table 5.3 and their age depth relationship shown in Fig. 5.4 below. Four of the dates were based on terrestrial macrofossil material and the remaining on bulk sediment and there is good correspondence between dates from the two types of material. Two age reversals are apparent (Fig. 5.4); both of these are on bulk sediments and could represent localised mixing by, for example, bioturbation. The remaining ten age estimates show close agreement and reveal a relatively consistent rate of accumulation over much of the core, which represents ~4,700 years.

Towards the surface there is a notable increase in the accumulation rate indicated by the top three dates (excluding the reversals). The uppermost date taken from a depth of 32 cm yielded an age estimate of 934 -1,055 cal. BP. This is rather older than would be expected so close to the surface, particularly when the preceding dates indicate that the rate of accumulation was increasing. Once again this indicates

possible disturbance of the near surface sediments and this will be discussed further in the sections below.

Table 5.3: Bigland Tarn Radiocarbon Measurements & Calibration

Publication Code	Depth (cm)	¹⁴ C Age	Calibrated Age (BP) 2σ Range	*WA	Sample Contents
SUERC-7051	28 ± 0.5	1204 ± 24	1060 - 1227	1120	Bulk sediment (LOI ~ 40%)
SUERC-7052	32 ± 0.5	1082 ± 24	934 - 1055	989	Bulk sediment (LOI ~ 40%)
SUERC-7053	36 ± 0.5	1130 ± 22	965 - 1079	1022	Bulk sediment (LOI ~ 50%)
SUERC-7054	43 ± 0.5	1129 ± 24	963 - 1121	1023	Wood
SUERC-7031	68 ± 0.5	1229 ± 25	1071 - 1259	1129	Bracken leaf fragments
SUERC-4713	76 ± 0.5	1582 ± 35	1394 - 1541	1468	Bulk sediment (LOI ~55%)
SUERC-7056	96 ± 0.5	2305 ± 26	2185 - 2355	2331	Bulk sediment (LOI ~ 60%)
SUERC-4714	118 ± 0.5	2013 ± 43	1876 - 2109	1971	Tree leaf fragments
SUERC-7057	140 ± 0.5	2454 ± 26	2361 - 2702	2454	Bulk sediment LOI ~ 70%)
SUERC-7060	164 ± 0.5	2732 ± 26	2767 - 2872	2820	Bulk sediment LOI ~ 70%)
SUERC-7061	204 ± 0.5	3534 ± 37	3698 - 3906	3802	Bulk sediment LOI ~ 65%)
SUERC-4716	232 ± 0.5	4137 ± 30	4539 - 4822	4696	Tree leaf fragments

Calibrated using Calib 5.0.1 (Stuiver *et al.*, 2005) and the INTCAL 04 dataset (Reimer *et al.*, 2004). * WA = weighted average.

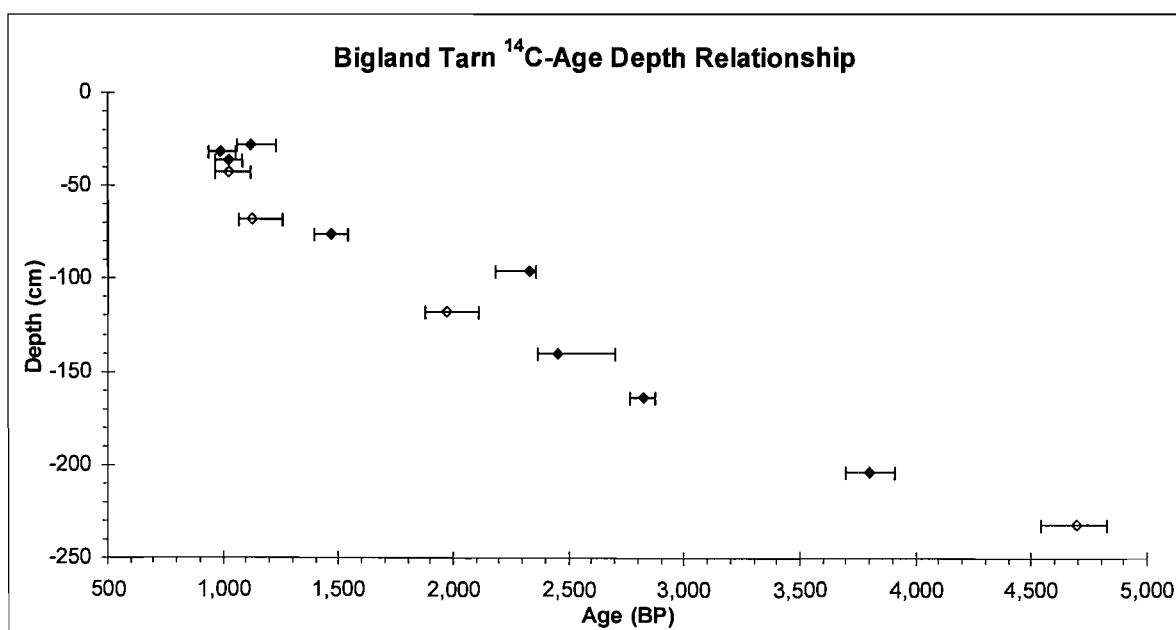


Figure 5.4: Bigland Tarn radiocarbon age depth relationship. Diamonds represent the weighted average (WA) of the age probability distribution; solid diamonds are based on bulk sediment and hollow diamonds on terrestrial macrofossils. Error bars represent the 2σ range.

5.3.2 SCP ANALYSIS

SCP counts were undertaken at 4 cm resolution over the top 40 cm of core BLT. The concentration curve (Fig. 5.5) displays an atypical profile compared to those of Rose *et al.*, (1995). SCPs do not appear until very close to the surface (5 cm) and the concentration just below the sediment water interface (1 cm) is at least one order of magnitude lower than expected.

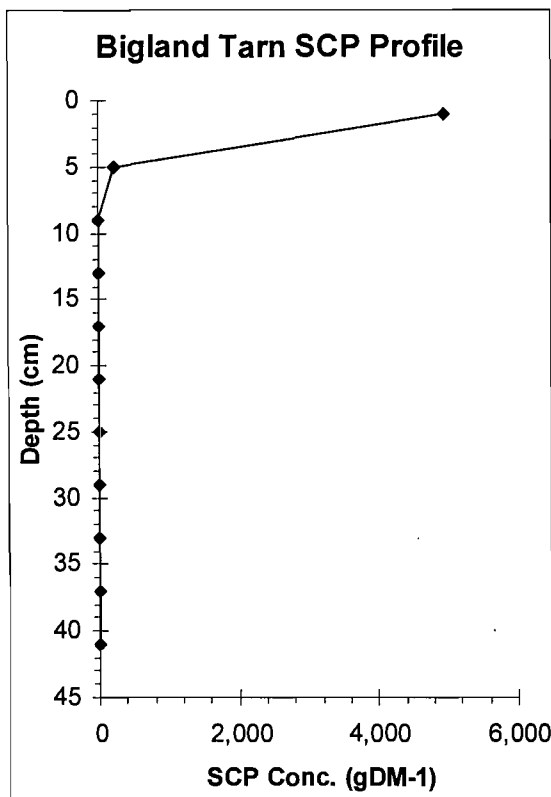


Figure 5.5: Bigland Tarn SCP concentration profile. Diamonds represent particle concentrations per gram dry mass (gDM⁻¹)

The SCP profile does not provide distinct phases which can be used to infer a specific date but does offer some qualitative information on near surface sedimentation. It is hard to explain this profile in terms of mixing because it would then be expected to find SCPs deeper within the profile. Similarly, a reduction in the rate of sediment accumulation would result in very high surface concentrations of SCPs, but this is not the case. The SCP profile would therefore seem to imply that some sediment is missing from the surface of Bigland Tarn. The most likely explanation for this would be relatively recent dredging or perhaps anchor disturbance. If the site has had

surficial material removed then the near surface sediments will be older than expected for an undisturbed site and this is a reasonable explanation for the SCP profile.

5.3.3 LEAD-210

Ten contiguous ^{210}Pb analyses were undertaken from 1-11 cm at the top of core BLT. The simplest model for interpreting lead data is a constant flux, constant sedimentation rate (CF:CS) model. Under these conditions the unsupported ^{210}Pb component decays and activity falls away from the surface with depth following an exponential decay curve. Core BLT broadly follows this pattern although the fit is not perfect (Fig. 5.6, $r^2 = 0.7568$).

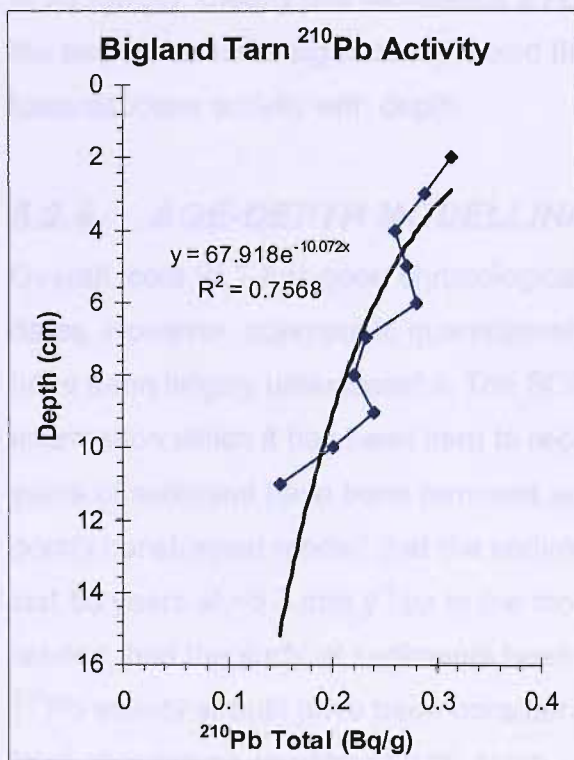


Figure 5.6: Bigland Tarn ^{210}Pb activity profile. The blue diamonds represent activity determinations and the bold black line is an exponential best fit curve.

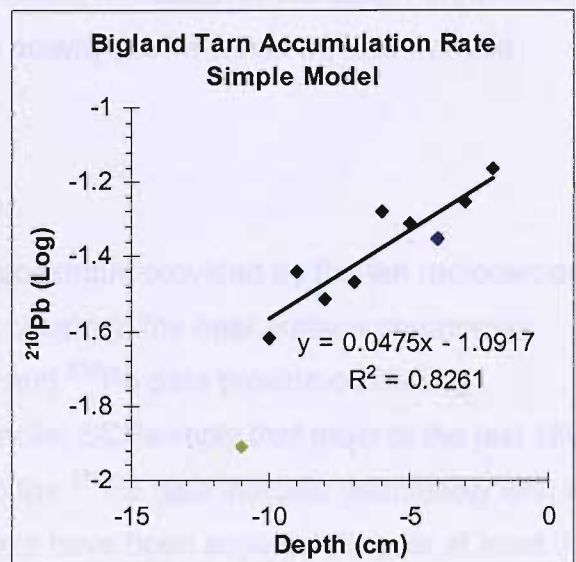


Figure 5.7: Bigland Tarn ^{210}Pb activity profile plotted on a logarithmic scale. The blue diamonds represent activity determinations and the bold black line is a linear best fit curve, the green diamond is a measurement which was judged to be an outlier and was omitted from the accumulation rate calculation

This is probably due to some variability in the sedimentation rate and the fact that measurements did not continue sufficiently far down core to reach supported levels. Unfortunately insufficient time was available for further ^{210}Pb analysis. Nevertheless the data fits the exponential decay curve reasonably well. Since the decay curve is exponential, plotting the activity on a log scale against depth produces a linear relationship which can be summarised by a best fit line (Fig. 5.7, $r^2=0.8261$).

The gradient of this line can be used to calculate the average accumulation rate of the sediment; in this case $\sim 6.5 \text{ mm y}^{-1}$ is predicted. The ^{210}Pb activity profile provides no indication that a significant amount of sediment is missing. However extrapolation of this accumulation rate predicts an age at 32 cm (the level of the topmost ^{14}C date) of 1 BP (54 years old) whereas the radiocarbon analysis returned a date of 989 BP (WA of 2σ range). Clearly this represents a significant mismatch in the data. Furthermore if the sediments were significantly mixed the activity profile would be less trended towards lower activity with depth.

5.3.4 AGE-DEPTH MODELLING

Overall, core BLT has good chronological constraint provided by the ten radiocarbon dates. However, attempts to quantitatively constrain the near surface chronology have been largely unsuccessful. The SCP and ^{210}Pb data provide conflicting information which it has been hard to reconcile. SCPs imply that most of the last 150 years of sediment have been removed and the ^{210}Pb data indicate (admittedly with a poorly constrained model) that the sediments have been accumulating for at least the last 50 years at $\sim 6.5 \text{ mm y}^{-1}$ up to the modern day. Even if the CF:CS model is refuted, had the surficial sediments been removed as suggested by the SCPs, the ^{210}Pb activity should have been considerably lower and remained at the supported level showing no clear trend with depth, which is not the case. Simple extrapolation from the uppermost radiocarbon date to the surface returns an accumulation rate of 0.3 mm y^{-1} which is very similar to the accumulation rate of other well constrained (by ^{14}C dates) parts of the core, but this scenario is not particularly supported by either the SCP or the ^{210}Pb data. It has therefore not been possible to accurately constrain

near surface (< 28 cm) sediments except to say that they are younger than ~ 989 cal. BP (WA of 2σ range).

As a result of conflicting data for the near surface sediments, an age depth model was constructed (Fig. 5.8 & Table 5.4) using linear interpolation between the radiocarbon and surface data. The SCP and ²¹⁰Pb data were used as qualitative aids to interpretation only.

Table 5.4: BLT Linear Interpolation Equations & Accumulation Rates

Depth Range (cm)	Age Range cal. BP	Equation	Accumulation	
			y mm ⁻¹	mm y ⁻¹
0-31	-53 to 956	AGE = 32.563 x DEPTH - 53	3.3	0.3
32-42	998 to 1025	AGE = 2.7581 x DEPTH + 909.28	0.3	3.3
43-67	1023 to 1124	AGE = 4.22 x DEPTH + 841.54	0.4	2.5
68-75	1128 to 1426	AGE = 42.438 x DEPTH - 1757.3	4.2	0.2
76-117	1464 to 1958	AGE = 11.964 x DEPTH + 558.71	1.2	0.8
118-139	1971 to 2432	AGE = 21.955 x DEPTH - 620.14	2.2	0.5
140-163	2454 to 2805	AGE = 15.271 x DEPTH + 315.58	1.5	0.7
164-203	2820 to 3777	AGE = 24.55 x DEPTH - 1206.2	2.5	0.4
204-232	3802 to 4696	AGE = 31.911 x DEPTH - 2707.8	3.2	0.3
Mean			2.1	1.0

Having discussed at length the problems with near surface dating, it is worth reiterating that the core chronology is generally well constrained and only the top 28 cm of the core should be subject to scepticism. Based on the age depth model the mean accumulation rate of the whole core is 1 mm y⁻¹. The lowest accumulation rate is 0.3 mm y⁻¹ and the majority of the core accumulates at a rate of less than 1 mm y⁻¹. However, two phases of much higher accumulation occur between 43 and 67 cm (2.5 mm y⁻¹) and 32 and 42 cm (3.3 mm y⁻¹), 2.2 and 3.3 times higher than the average respectively. The chronology for this part of the core is very secure having four radiocarbon dates, two of which are on terrestrial macrofossil material. Rapid accumulation over this part of the record is therefore thought to be genuine.

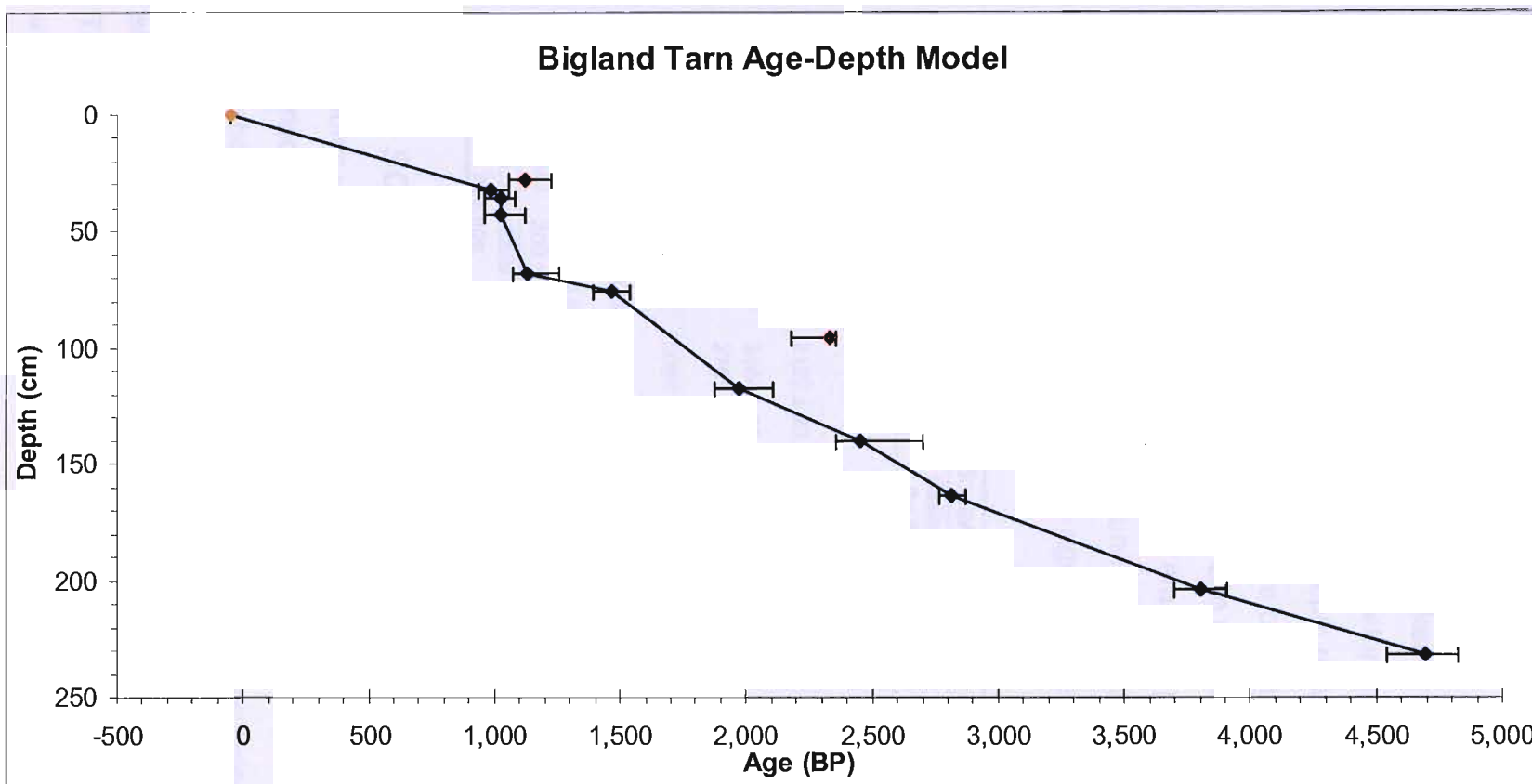


Figure 5.8: Bigland Tarn Age depth model Blue diamonds = WA of radiocarbon dates and errors = the 2 σ calibrated age range. Red diamonds = rejected radiocarbon dates. Yellow diamond = the surface at the time of coring (2003).

5.4 MALHAM TARN MOSS

5.4.1 CARBON-14

Nine radiocarbon measurements were undertaken on core MTM. All samples yielded sufficient material for AMS measurement and returned plausible calibrated ages. Data are summarised in Table 5.5 and their age depth relationship shown in Fig. 5.9 below. The graph displays a relatively consistent rate of accumulation with a good level of agreement between age estimates and no age reversals over the ~4,300 years which the core represents. MTM conforms to the emerging pattern that recent sediments are older than might be expected in an undisturbed site, with the uppermost date taken from a depth of 32 cm yielding an age estimate of 793-914 cal. BP.

Table 5.5: Malham Tarn Moss Radiocarbon Measurements & Calibration

Pub. Code	Depth (cm)	¹⁴ C Age	Calibrated Age (BP) 2σ Range	*WA	Sample Contents
SUERC-7032	32 ± 0.5	930 ± 19	793 - 914	854	Charred Ericaceae remains
SUERC-7047	56 ± 0.5	1400 ± 25	1286 - 1344	1315	Bulk peat (mostly UOM, some monocot. remains)
SUERC-7034	100 ± 0.5	2192 ± 23	2141 - 2311	2226	Sphagnum with some E. vaginatum nodes and spindles
SUERC-7035	132 ± 0.5	2464 ± 26	2364 - 2706	2525	Sphagnum leaves & stems
SUERC-7036	152 ± 0.5	2765 ± 22	2786 - 2925	2842	E. vaginatum leaves/stems & sphagnum leaves & stems
SUERC-7037	184 ± 0.5	3080 ± 27	3219 - 3367	3304	Sphagnum leaves & stems & E. tetralix stem wood
SUERC-7040	212 ± 0.5	3308 ± 27	3463 - 3615	3529	Sphagnum leaves & stems & some Calluna stems & flowers
SUERC-7041	264 ± 0.5	3648 ± 28	3887 - 4083	3949	Sphagnum leaves & stems
SUERC-7042	300 ± 0.5	3858 ± 23	4159 - 4409	4318	Sphagnum leaves & stems

Calibrated using Calib 5.0.1 (Stuiver *et al.*, 2005) and the INTCAL 04 dataset (Reimer *et al.*, 2004). * WA = weighted average

5.4.2 SCP ANALYSIS

SCP counts were undertaken at 2 cm resolution over the top 38 cm of core MTM. Comparison of the concentration curve (Fig. 5.10) with that of Rose (2005, unpublished data), from Malham Tarn (Appendix. 1) provides two datable phases. The rapid increase in concentration at 14 cm corresponds to ~1940 (10 BP) and the subsurface peak in concentration at 8 cm corresponds to a date of ~1976 (-26 BP). The rapid increase in core MTM is of a similar shape to that of Rose, (2005, unpublished data) but the subsurface peak displays only one peak (compared to

Rose's two peaks) and is represented by only one data point. It may therefore not be a reliable age indicator.

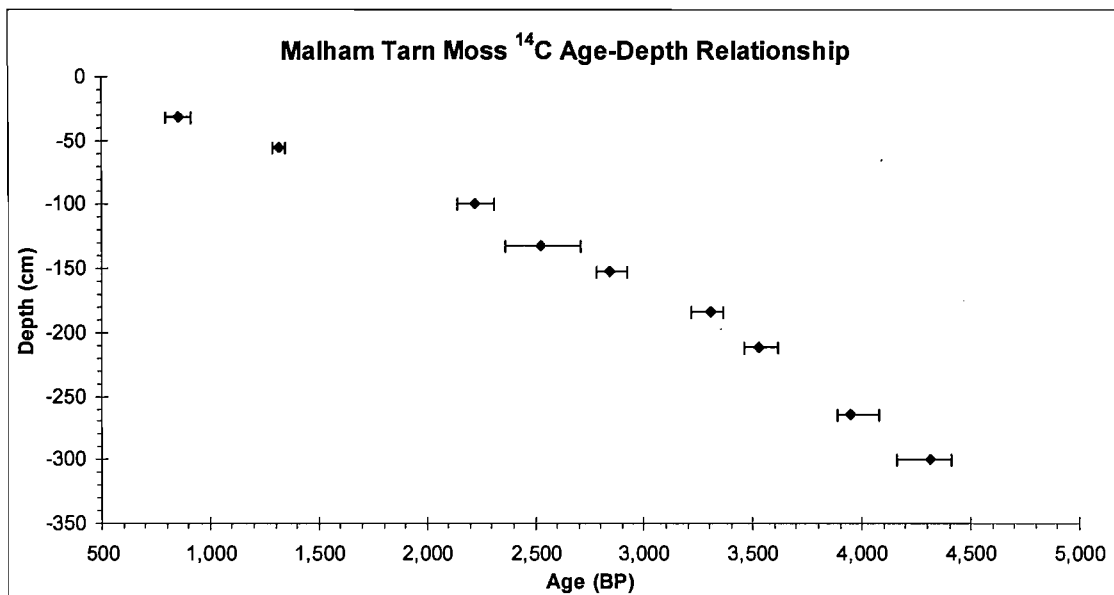


Figure 5.9: Malham Tarn Moss radiocarbon age depth relationship. Diamonds represent the weighted average (WA) of the age probability distribution and error bars represent the 2σ range

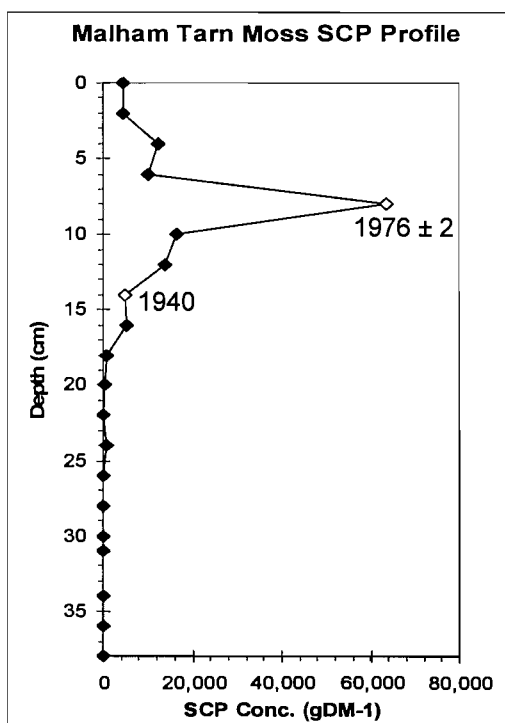


Figure 5.10: Malham Tarn Moss SCP concentration profile. Diamonds = particle concentrations per gram dry mass (gDM⁻¹). Unshaded diamonds and associated numbers = age estimates.

5.4.3 AGE-DEPTH MODELLING

An age-depth model for core MTM was constructed (Fig. 5.11 & Table 5.6) using linear interpolation between the radiocarbon dates (WA of the 2σ age ranges), the rapid rise in SCP concentration and the surface at the time of coring. The resultant age-depth model predicts an average accumulation rate of 1 mm y^{-1} . The fastest rate of accumulation (2.5 mm y^{-1}) occurs in the near surface peats (0-11 cm).

Accumulation rates fluctuate over the remainder of the core from a maximum of 1.1 mm y^{-1} (100-131 cm) to a minimum of 0.2 mm y^{-1} (14-31 cm). An accumulation rate of 0.2 mm y^{-1} is thought to be anomalously low compared to the rest of the core and probably results from peat cutting or drainage. Overall core MTM is well constrained by the dates obtained but the age-depth relationship between 14-31 cm (5 to 806 cal. BP) is poorly constrained and the timing of changes over this section must therefore be regarded with some suspicion.

Table 5.6: MTM Linear Interpolation Equations & Accumulation Rates

Depth Range (cm)	Age Range cal. BP	Equation	Accumulation	
			y mm^{-1}	mm y^{-1}
0-13	-54 to 1	AGE = 4.2143 x DEPTH - 54	0.4	2.5
14-31	5 to 806	AGE = 47.139 x DEPTH - 654.94	4.7	0.2
32-55	856 to 1296	AGE = 19.229 x DEPTH + 238.17	1.9	0.5
56-99	1315 to 2205	AGE = 20.705 x DEPTH + 155.55	2.1	0.5
100-131	2226 to 2516	AGE = 9.3438 x DEPTH + 1291.6	0.9	1.1
132-151	2525 to 2802	AGE = 15.825 x DEPTH + 436.1	1.6	0.6
152-183	2842 to 3289	AGE = 14.438 x DEPTH + 647	1.4	0.7
184-211	3303 to 3520	AGE = 8.0357 x DEPTH + 1824.9	0.8	1.3
212-263	3529 to 3941	AGE = 8.0865 x DEPTH + 1814.2	0.8	1.3
264-304	3949 to 4359	AGE = 10.25 X DEPTH + 1243	1.0	1.0
Mean			1.6	1.0

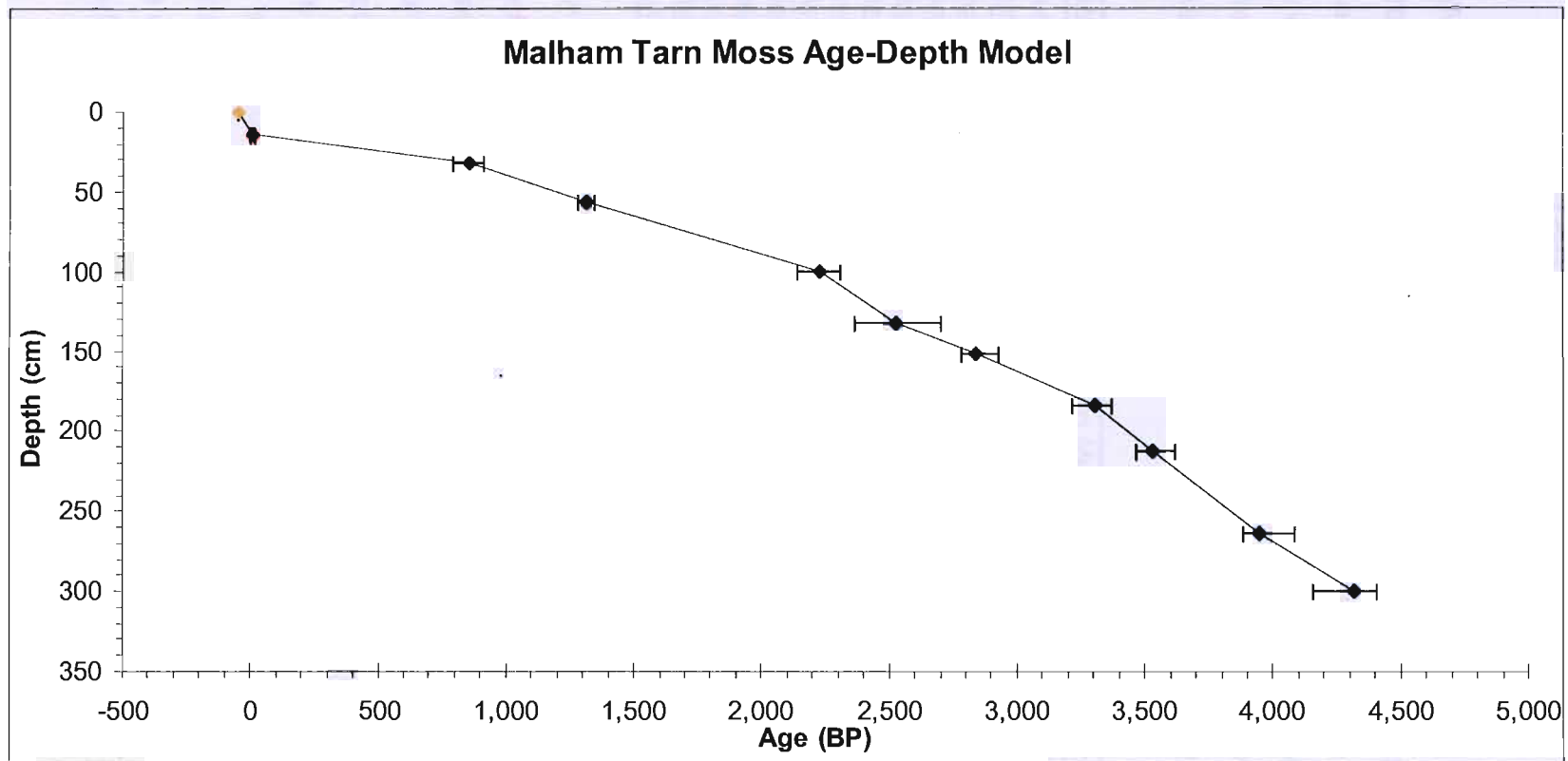


Figure 5.11: Malham Tarn Moss age-depth model. Blue diamonds = WA of radiocarbon dates and the errors are the 2σ calibrated age range. The yellow diamond = the surface at the time of coring (2004) and the red diamonds = the SCP inferred age estimate.

5.5 MALHAM TARN

5.5.1 RADIOCARBON MEASUREMENT

Great effort was required to identify and isolate sufficient material suitable for radiocarbon measurement from core MLT (see Section 3.4.1). Samples were mostly composed of charcoal fragments with the addition of above ground Ericaceous remains which were known to be of terrestrial origin. Sufficient material for measurement was collected but unfortunately the resultant data did not demonstrate an increasing age with depth relationship (Table 5.7 and Fig. 5.12).

Table 5.7: Malham Tarn Radiocarbon Measurements & Calibration

Pub. Code	Depth (cm)	¹⁴ C Age	Calibrated Age (BP) 2σ Range	*WA	Sample Contents
SUERC-7879	44.5 ± 2	3494 ± 26	3695 -3837	3766	Charcoal & C. vulgaris
SUERC-7880	73.5 ± 2	3426 ± 24	3592 -3821	3669	Charcoal & C. vulgaris
SUERC-7881	88.5 ± 2	3566 ± 28	3728 -3966	3876	Charcoal & C. vulgaris
SUERC-7884	120.5 ± 2	3219 ± 31	3368 -3553	3426	Charcoal & C. vulgaris
SUERC-7886	140 ± 2.5	3706 ± 29	3934 -4148	4037	Charcoal & C. vulgaris
SUERC-7887	150 ± 2.5	3253 ± 108	3218 -3818	3481	Charcoal & C. vulgaris
SUERC-7889	168 ± 2.5	3102 ± 97	3005 -3556	3275	Charcoal & C. vulgaris
SUERC-7890	187.5 ± 2	3501 ± 26	3696 -3842	3769	Charcoal & C. vulgaris
SUERC-7894	206.5 ± 2	3337 ± 24	3480 -3637	3593	Charcoal & C. vulgaris
SUERC-7895	233 ± 2.5	3581 ± 115	3578 -4229	3870	Charcoal & C. vulgaris

Calibrated using Calib 5.0.1 (Stuiver *et al.*, 2005) and the INTCAL 04 dataset (Reimer *et al.*, 2004).
*WA = weighted average

Clearly it is not possible to use the radiocarbon measurements to infer sediment age; nevertheless it is desirable to try to explain the occurrence of these peculiar age estimates. The most obvious explanation might be that the sediments have undergone mixing but this hypothesis is not supported by the LOI and chironomid data (Sections 6.5.1 & 6.5.2). A less stringent sample pre-treatment was used to minimise sample loss from already small samples (Section 3.4.1) but it seems unlikely to have contributed significantly to the results, because if the problem was related to contamination due either to the 'hard water effect' or old carbon inwash, then the data would be expected to have some age trend which was offset by the older carbon. Instead all the samples appear to be of similar age.

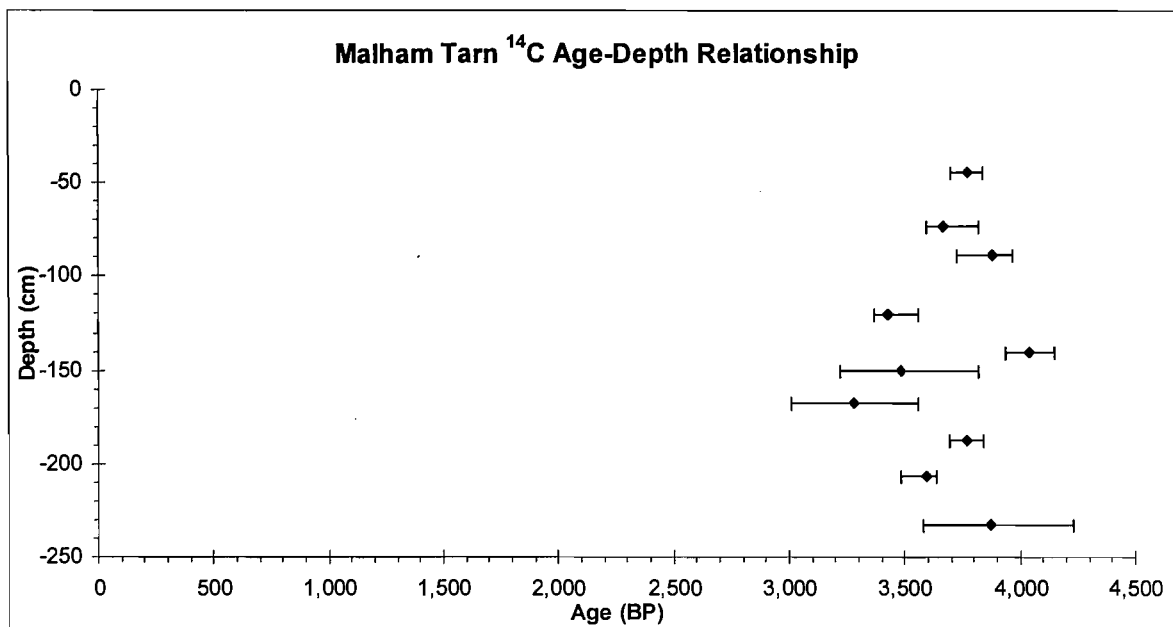


Figure 5.12: Malham Tarn radiocarbon age-depth relationship. Diamonds = the weighted average (WA) of the age probability distribution and error bars represent the 2σ range.

One possible explanation could be that the charcoal within the sediments is predominantly sourced from an erosional horizon within the catchment which has deposited material into the lake over the entire period represented by the core. If this theory is correct then picking individual charcoal fragments was in fact selecting reworked material containing ‘old carbon’ rather than material deposited directly into the lake. This would explain the similarity of the age determinations. The most likely source of this reworked charcoal is the adjacent bog (Malham Tarn Moss) or its marginal fen through which the inflowing stream cuts.

5.5.2 SCP ANALYSIS

SCP counts were undertaken at 4 cm resolution over the top 40 cm of core MLT. The profile (Fig. 5.13) exhibits a typical shape suggesting that the sediments, at least over the top 40 cm, have not undergone significant mixing. Comparison with the dated profile from Malham Tarn (Appendix 1) produced by Rose (2005, unpublished data) provides two initial age estimates. The rapid rise in concentration at 21 cm corresponds to ~ 1940 (10 BP) and the subsurface peak at 5 cm corresponds to c. 1976 (-26 BP). However, the profile of Rose (2005, unpublished data) is much more

highly resolved than the MLT profile (1 cm as opposed to 4 cm resolution). Consequently, much of the detail of Rose's profile is not detected here. It is therefore possible that the increase in SCP concentration at 25 cm actually equates to c. AD 1905 (55 BP).

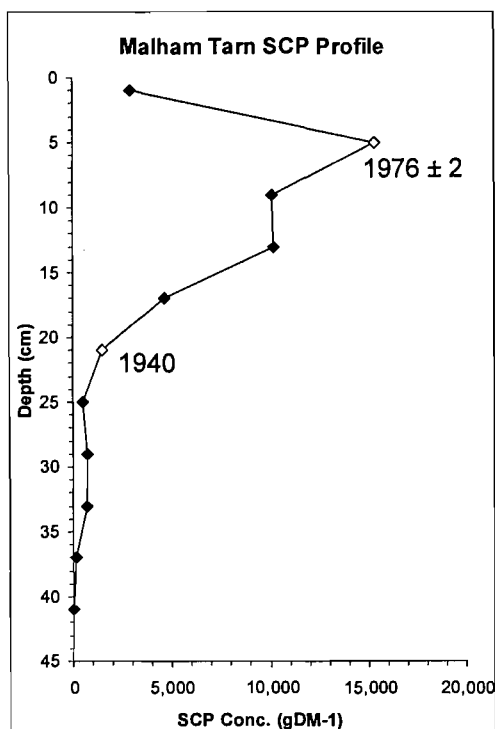


Figure 5.13: MLT SCP Profile.
*Diamonds = particle concentrations per gram dry mass (gDM⁻¹).
 Unshaded diamonds and associated numbers = age estimates*

5.5.3 LEAD-210

²¹⁰Pb analysis was undertaken at 2 cm resolution on the top 20 cm of core MLT; the resultant ²¹⁰Pb activity profile is shown in Fig. 5.14. The data fit an exponential curve well and by 18 or 20 cm down core ²¹⁰Pb activity is thought to be at, or close to, supported levels. Two samples show a notable departure from the exponential curve which indicates that sediment accumulation rates changed over that part of the profile. Nevertheless, the overall fit is good ($r^2 = 0.8584$) and it is appropriate to use the CF:CS model to predict age. Plotting the activity on a log scale against depth produces a linear relationship which can be summarised by a best fit line (Fig. 5.15, $r^2 = 0.9376$) the gradient of which can be used to calculate the average accumulation rate of the sediment; in this case it is 1.8 mm y⁻¹.

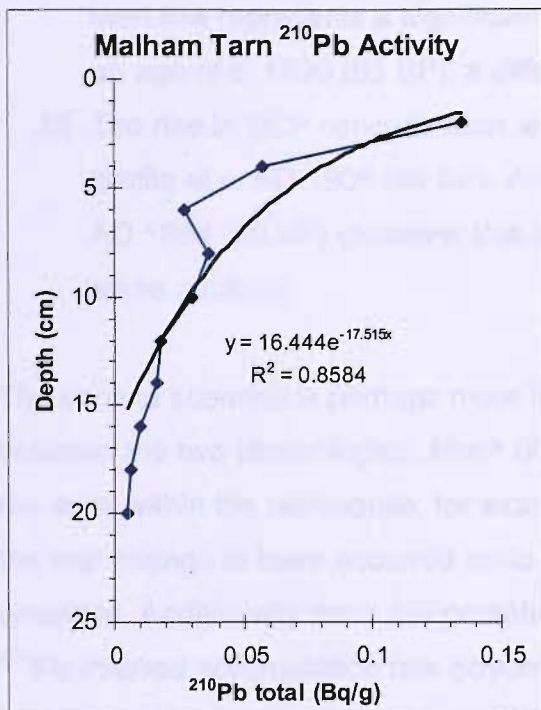


Figure 5.14: Malham Tarn ^{210}Pb activity profile. The blue diamonds represent the activity determinations and the bold black line is an exponential best fit curve

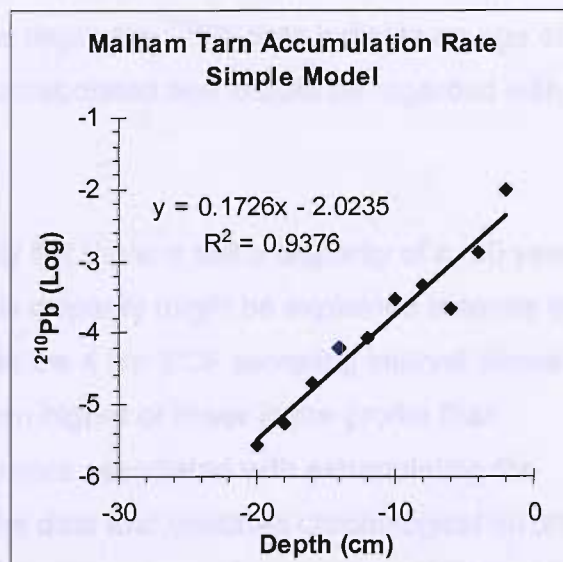


Figure 5.15: Malham Tarn ^{210}Pb activity profile plotted on a logarithmic scale. The blue diamonds represent activity determinations and the bold black line is a linear best fit curve.

5.5.4 AGE-DEPTH MODEL

Due to the problems encountered with radiocarbon dating Malham Tarn it is only possible to construct an age-depth model for the topmost sediments where SCP and ^{210}Pb data are available. The age inferred by the subsurface peak in SCPs is corroborated by the mean accumulation rate of 1.8 mm y^{-1} indicated by the ^{210}Pb data, with both techniques predicting a date of AD1976 (-26 BP) for sediment at 5 cm. The rise in SCP concentration has more than one possible chronological interpretation:

- a) If the 21 cm rapid increase in concentration corresponds to c. AD 1940 (10 BP) then this represents a significant departure from the ^{210}Pb data which indicates an age of c. 1890 (63 BP), a difference of c. 50 years, or;
- b) The rise in SCP concentration at 25 cm represents the increase seen in Rose's profile at c. AD 1905 (45 BP). At this depth the ^{210}Pb data indicate an age of AD 1864 (86 BP) (however this is extrapolated and should be regarded with some caution).

The second scenario is perhaps more likely but there is still a disparity of c. 30 years between the two chronologies. Much of this disparity might be explained in terms of the error within the techniques, for example the 4 cm SCP sampling interval allows for the real change to have occurred up to 3 cm higher or lower in the profile than recorded. Additionally there are potential errors associated with extrapolating the ^{210}Pb inferred accumulation rate beyond the data and unstated chronological errors inherent in Rose's analysis.

The SCP and ^{210}Pb analysis indicates that the surface sediments of Malham Tarn are intact by displaying a characteristic SCP concentration profile and exponential decline in ^{210}Pb activity. There is some disparity between the two indicators with depth but the indication is that the sediments at 25 cm are somewhere between 55 and 85 years old. Had this near surface chronology been critical to the project both estimates could have been improved - the SCPs by increasing the sampling resolution and the ^{210}Pb by measuring the supported ^{210}Pb activity. However due to the problems with radiocarbon dating and subsequent lack of chronological constraint down core this was not seen to be worthwhile in terms of time investment.

6.0 PALAEOECOLOGICAL RESULTS & INTERPRETATION

6.1 INTRODUCTION

Plant macrofossil, testate amoebae and humification data are presented from Hulleter Moss (HUL) and Malham Tarn Moss (MTM). Loss on ignition and chironomid data are presented from Bigland Tarn (BLT) and Malham Tarn (MLT). Some basic palaeoecological interpretation of the data is considered but substantial palaeoclimatic inference is explored in the Discussion (Chapter 7).

6.2 HULLETER MOSS

6.2.1 PLANT MACROFOSSILS

The plant macrofossil composition of core HUL is presented in Fig. 6.1. The diagram has been divided into zones with each zone boundary representing a significant change in assemblage composition. These divisions were determined by eye. Nine major zones were identified and their main compositional features are summarised in Table 6.1.

The vegetative cover of Hulleter Moss appears to have alternated between relatively wet-dwelling *Sphagnum* dominated communities (zones HUL-a, c, e, g and i) and relatively dry-tolerant Cyperaceae-dominated communities (zones HUL-b, d and f). Ericaceae are also important at times and are found in association with and occasionally dominate over both *Sphagnum* and Cyperaceae suggesting that they represent intermediate conditions (e.g. within zones HUL-a, b and c). The boundaries between different community types are generally sharp indicating that community structure may exhibit a rapid threshold-type response to water table variability. In contrast, Zone h is characterised by a high proportion of UOM. The *Sphagnum* communities are particularly rich in *S. imbricatum*. *S. s. Acutifolia* is also important with *S. papillosum* and *S. s. Cuspidata* occurring generally at much lower abundances.

Hulleter Moss (core HUL) Plant Macrofossil Diagram

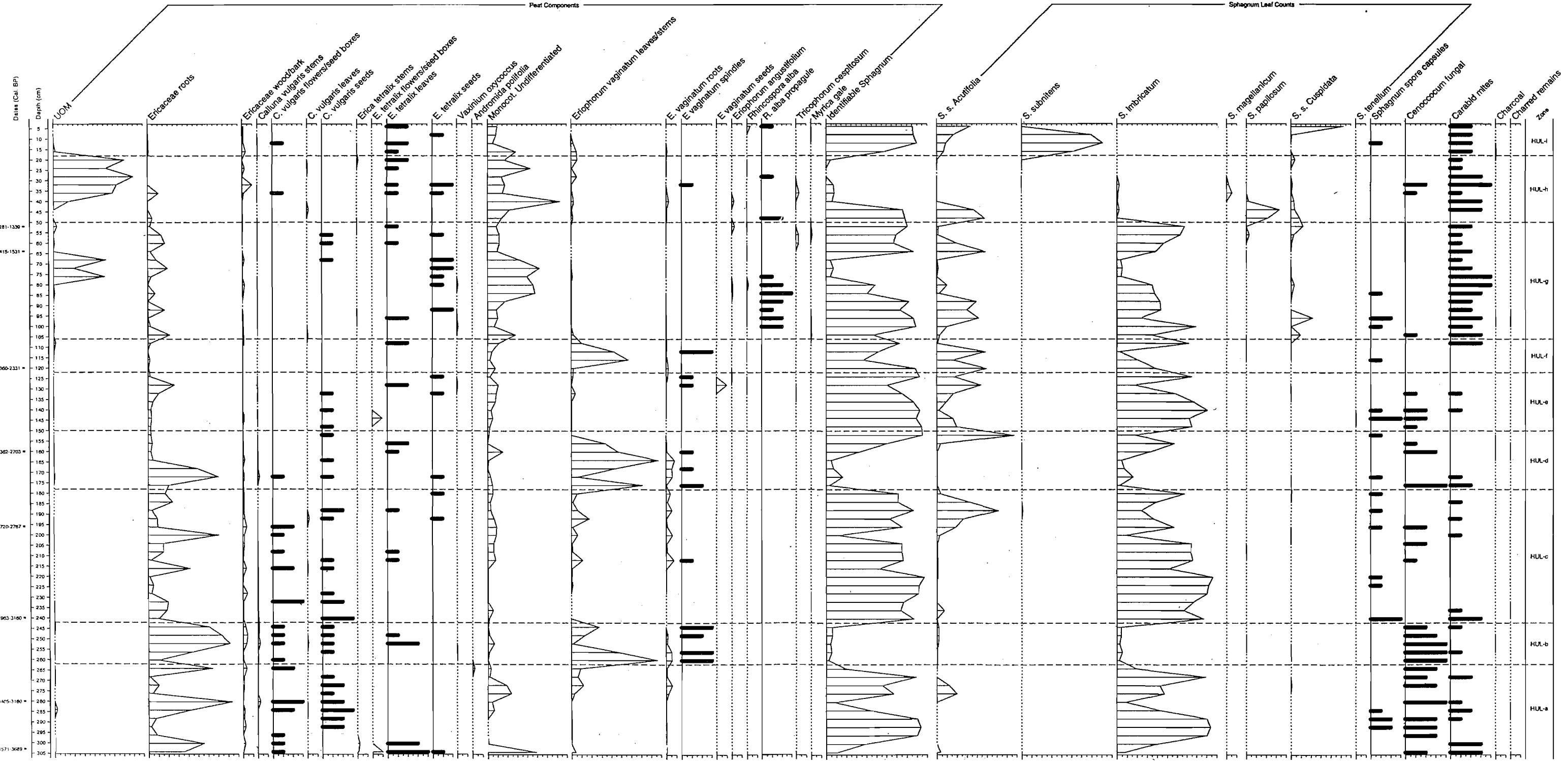


Table 6.1: Plant macrofossil zone descriptions for core HUL

Depth (cm)	Zone	Description	Age (cal. BP)
0-18	HUL-i	This topmost zone is mostly dominated by <i>S. subnitens</i> . <i>S. s. Acutifolia</i> is also important and <i>S. s. Cuspidata</i> dominates the topmost sample	-53 to c. 190
18-50	HUL-h	UOM dominates much of this zone. <i>S. papillosum</i> and <i>S. s. Acutifolia</i> are also quite abundant for a brief spell at the base. Undifferentiated monocotyledon remains are present throughout and rise to dominance in a few samples. Carabid mites are rare to common throughout.	c. 190 to c. 1240
50-106	HUL-g	<i>S. imbricatum</i> and <i>S. s. Acutifolia</i> co-dominate for much of this zone although undifferentiated monocotyledon remains and UOM become abundant during the middle phase. <i>S. s. Cuspidata</i> also reaches relatively high abundance towards the bottom of the zone. <i>R. alba</i> propagules are occasionally found in the lower half of the zone and Carabid mites are rare to common throughout	c. 1240 to c. 2020
106-122	HUL-f	<i>E. vaginatum</i> leaves/stems and <i>S. s. Acutifolia</i> are both abundant. <i>S. imbricatum</i> is abundant at the top and bottom of the zone but absent from the middle. <i>E. vaginatum</i> spindles are frequent	c. 2020 to c. 2210
122-150	HUL-e	Dominated by <i>S. imbricatum</i> also with high abundance of <i>S. s. Acutifolia</i> at the top and bottom of the zone. Undifferentiated monocotyledon remains and Ericaceous roots are found throughout at low abundance. Cenococum fungal spores are also found occasionally in the lower half of the zone	c. 2210 to c. 2410
150-178	HUL-d	Dominated by <i>E. vaginatum</i> leaves/stems with Ericaceae having greater abundance towards the bottom. <i>S. imbricatum</i> is present throughout at relatively low abundance and becomes more important towards the top. Cenococum fungal spores are also common at the bottom of the zone	c. 2410 to c. 2620
178-242	HUL-c	Dominated by <i>S. imbricatum</i> also with high abundance of <i>S. s. Acutifolia</i> towards the top. Ericaceae shows brief periods of abundance. Calluna flowers/seed boxes and seeds occur occasionally	c. 2620 to c. 3080
242-262	HUL-b	Dominated by Ericaceous remains <i>E. vaginatum</i> is abundant near the bottom of the zone. <i>S. imbricatum</i> is scarce throughout and <i>C. vulgaris</i> seeds and <i>E. vaginatum</i> spindles are found frequently. Cenococum fungal spores are common	c. 3080 to c. 3300
262-304	HUL-a	Dominated predominantly by <i>S. imbricatum</i> although Ericaceous remains are abundant for a brief period around the middle of the zone. A Small amount of <i>S. s. Acutifolia</i> is present. <i>C. vulgaris</i> seeds are occasional and Cenococum fungal spores are frequent	c. 3300 to c. 3640

Age estimates are based on interpolated data and rounded to the nearest 10 years. Negative numbers are years post 1950

The lower boundary of zone HUL-h is marked by a sharp fall in *S. imbricatum* followed by its complete disappearance in the middle of the zone (32cm c. / 650 cal.

BP). This zone also contains the first appearance of *S. magellanicum*, and the highest abundance of *S. papillosum* within the core. This pattern and timing of floral change is common near the surface of British and Irish raised bogs but the driving mechanism is still unclear (Mauquoy & Barber, 1999). The topmost zone (HUL-i) is dominated by *S. subnitens* which is very rare elsewhere in the core. *S. subnitens* generally thrives in more nutrient rich environments and its presence may well indicate some nutrient enrichment in recent time, possibly resulting from increased fertilization of the surrounding farmland, or from large fires in the early 1950s (see Section 4.1).

Cyperaceae-dominated communities are particularly rich in *E. vaginatum*, while *E. angustifolium*, *T. cespitosum* and *R. alba* occur in very low proportions. *R. alba* thrives in wetter conditions than the other *Cyperaceae* mentioned. Its propagules are occasional-to-frequent in the bottom half of zone HUL-g, and are found in association with high *Sphagnum* abundance. Ericaceae remains are dominated by roots and it is therefore not possible to attribute these to a particular species, however, samples that are rich in Ericaceous roots tend also to have diagnostic *E. tetralix* or *C. vulgaris* remains such as leaves, stems or seeds. These diagnostic remains indicate that both *E. tetralix* and *C. vulgaris* have grown throughout much of the time period represented by the core and coexisted for much of this time. However, over the first three zones (HUL-a, b & c) *C. vulgaris* remains are more common and over the remainder of the core *E. tetralix* remains are prevalent.

UOM is rare throughout most of the core but makes a significant contribution to zone HUL-g and is particularly dominant in zone HUL-h. UOM abundance is associated with undifferentiated monocotyledon roots and very low *Sphagnum* abundance, indicating that UOM develops under very dry conditions.

Myrica gale is generally not found on ombrotrophic bogs, thriving only in more nutrient-rich environments, however it was common on the bog surface at the time of coring and small quantities were found at a number of levels within the core, the deepest of which occurred at a depth of 232 cm (c. 3000 cal. BP). This early

occurrence is unlikely to be anthropogenically driven; Hulleter Moss is very low lying and spring tides bring brackish water close to the bog. Whilst there is no evidence that this has inundated the bog, or indeed influenced the perched water table, it is possible that this proximity of brackish water could have led to some minor nutrient enrichment which would account for the presence of *Myrica gale* within the peat stratigraphy. Greater surface abundance might however require an anthropogenic explanation, for example, aerosols from farm sprays and/or fires during the 1950s.

The plant macrofossil data were explored using detrended correspondence analysis (DCA) in order to investigate latent structure within the data. Rare taxa were omitted from the analysis and surface samples which contained taxa that only occurred in the anthropogenically disturbed near surface were also omitted to prevent problems caused by a crossed gradient (Section 3.5.1). The DCA biplot of Axes One and Two is displayed in Fig. 6.2.

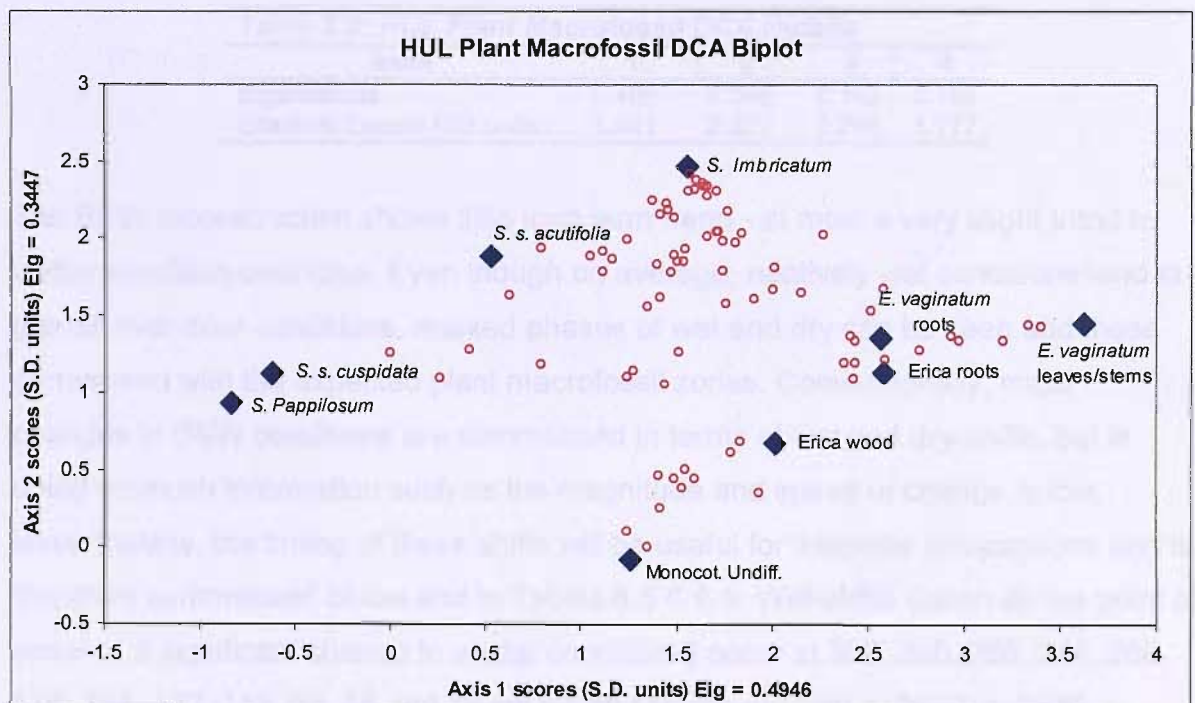


Figure 6.2: Biplot of DCA Axis One and Two scores for plant macrofossil data from core HUL. Diamonds = taxa scores based on their distribution within the samples and circles = sample scores based on their floral composition.

The First Axis seems to represent a water availability gradient with taxa that typically occupy pool edges and low lawn microenvironments such as *S. s. Cuspidata* and *S. papillosum* present at one end of the axis (low scores) and plants tolerant of deeper water tables such as the Ericaceae and *E. vaginatum* present at the other end of the axis (high scores). This analysis confirms the nature of the relationship inferred from the macrofossil diagram. Axis One has an Eigenvalue of 0.495 (Table 6.2), indicating that about 50% of the variability in taxon abundance can be attributed to water table variability, and it spans 3.4 standard deviations. The relatively long gradient implies that the water table has fluctuated quite widely over the time period represented by the core. Since Axis One can be shown to represent a water table gradient, the sample scores have been plotted against depth to provide a semi-quantitative proxy measure of BSW based on plant macrofossil remains. This, together with the plant macrofossil zones, is shown in Fig. 6.3.

Axes	1	2	3	4
Eigenvalues	0.495	0.345	0.142	0.105
Gradient Length (SD units)	3.401	2.421	2.298	1.727

The BSW reconstruction shows little long term trend - at most a very slight trend to wetter condition over time. Even though on average, relatively wet conditions tend to prevail over drier conditions, marked phases of wet and dry can be seen and these correspond with the expected plant macrofossil zones. Conventionally, major changes in BSW conditions are summarised in terms of wet and dry-shifts, but in doing so much information such as the magnitude and speed of change is lost. Nevertheless, the timing of these shifts will be useful for inter-site comparisons and is therefore summarised below and in Tables 6.5 & 6.6. Wet-shifts (taken as the point of onset of a significant change to wetter conditions) occur at 300, 280, 260, 244, 200, 176, 164, 132, 116, 68, 56 and 16 cm which correspond with *c.* 3610, *c.* 3500, *c.* 3280, *c.* 3110, *c.* 2770, *c.* 2600, *c.* 2520, *c.*

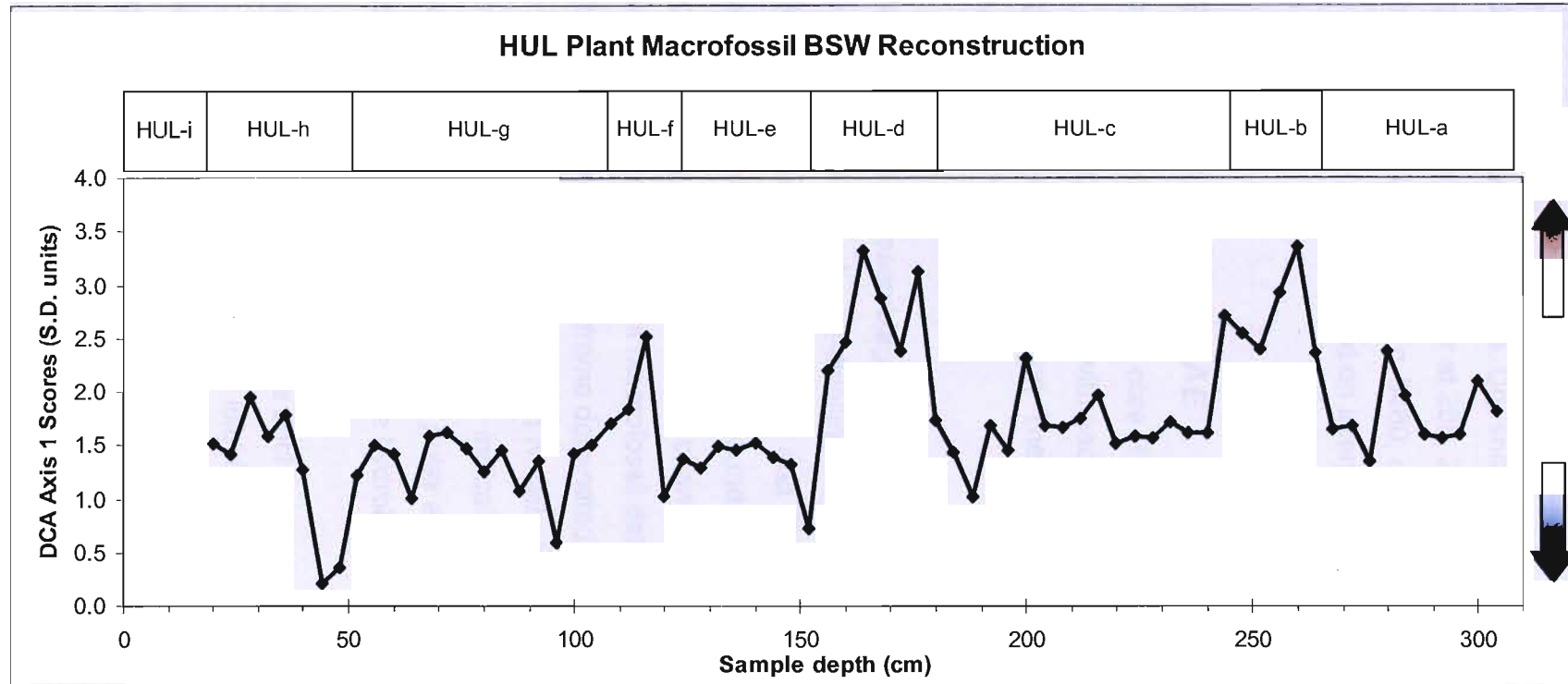


Figure 6.3: Plant Macrofossil BSW reconstruction for HUL. Blue curve is a relative measure of BSW. Peaks and troughs indicate the direction of change, but their amplitude is not necessarily proportional to the environmental change represented. The brown arrow = drier and the blue arrow wetter conditions. Bars above the curve = the plant macrofossil zones derived from the plant macrofossil component diagram and the codes are those used on the diagram and referred to in the text

2280, c. 2140, c. 1530, c. 1360 and c. 130 cal. BP, based on interpolated dates rounded to the nearest 10 years. Dry-shifts taken as the point of onset of a significant change to drier conditions occur at 288, 276, 252, 188, 172, 152, 120, 64 and 44 cm which correspond with c. 3550, c. 3460, c. 3190, c. 2690, c. 2570, c. 2430, c. 2200, c. 1470 and c. 1050 cal. BP, based on interpolated dates rounded to the nearest 10 years.

6.2.2 TESTATE AMOEBAE

Testate amoebae composition of core HUL is presented in Fig. 6.4. The diagram has been divided into zones by eye, with each zone boundary representing a significant change in assemblage composition. These zones are summarised in Table 6.3 below.

The testate amoebae assemblage appears to have switched between phases dominated by the relatively wet-dwelling *Amphitrema* taxa particularly *A. flavum* and *A. wrightianum* (Zones HUL-Tb, Td, Te and Tf) and the dry-tolerant *H. subflava* (Zones HUL-Ta and Tc). Many of the boundaries between zones exhibit sharp changes indicating rapid threshold like changes to water table forcing. However, this is less marked than in the plant macrofossil data, possibly as a result of the greater variety of taxa present. *Amphitrema* dominated communities tend to also be relatively rich in *C. aculeata* type, *H. papilio* and *N. flabellulum*, whilst *H. Subflava* dominated communities tend to also be rich in *B. indica* and *T. arcula*. *Amphitrema muscorum*, *A. seminulum*, *C. arcelloides* type, *D. pulex* and *N. militaris* are all common throughout, apparently exhibiting wide hydrological tolerances.

The topmost zone (HUL-Tg) is quite uncharacteristic when compared to the others. Here, taxa such as *A. discoides*, *D. leidy*, *E. rotunda*, *E. strigosa*, *E. tuberculata* and *N. flabellulum* reach high abundances, but are absent or of low abundance throughout the remainder of the core. *Euglypha* taxa are known to preserve poorly, which explains their absence from all but the near surface samples, however this does not explain the increases in the other taxa.

Hulleter Moss (Core HUL) Testate Amoebae Diagram

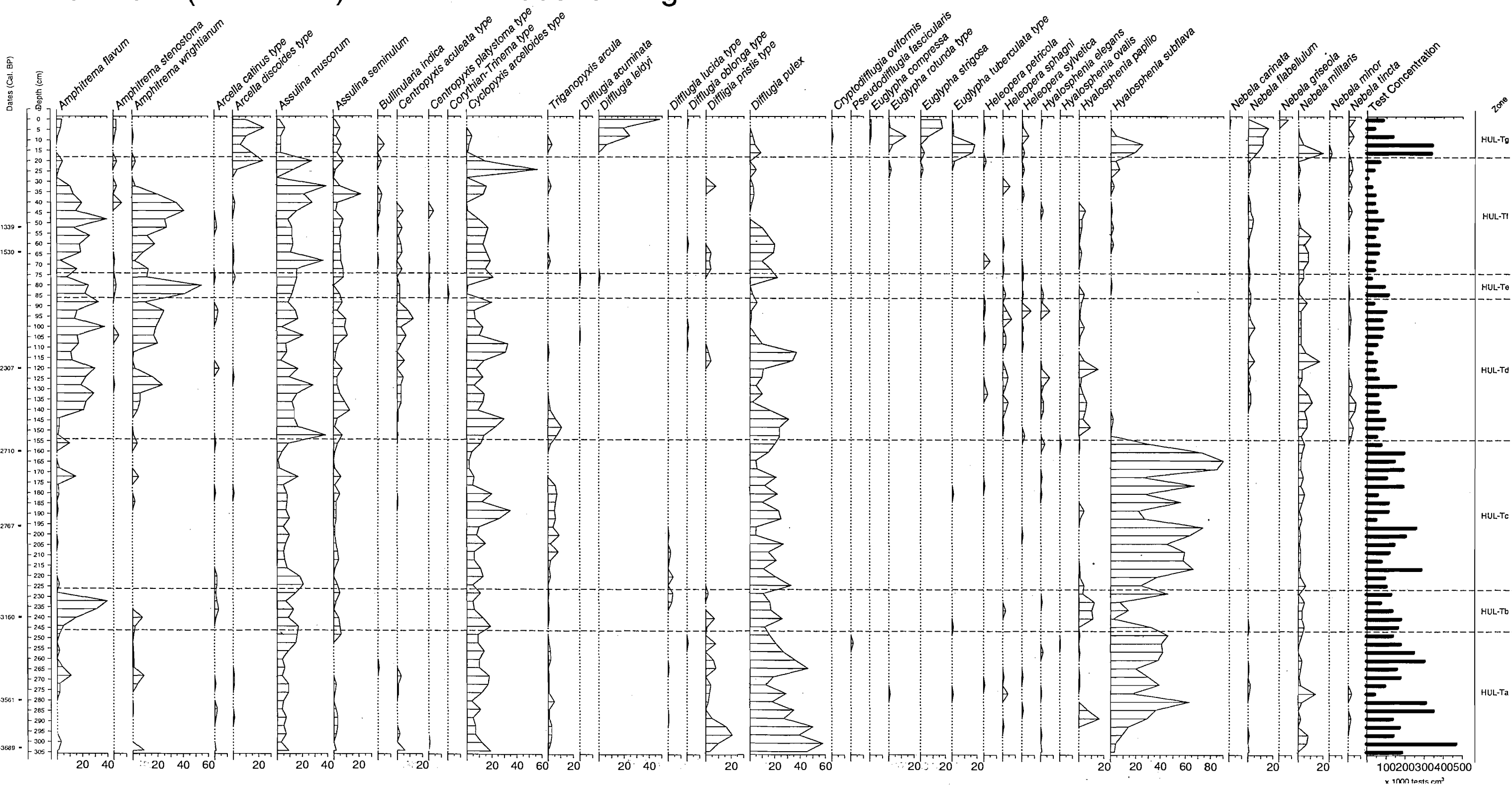


Table 6.3: Testate amoebae zone descriptions for core HUL

Depth (cm)	Zone	Description	Age (cal. BP)
0-18	HUL-Tg	<i>D. leidyi</i> dominates this topmost zone but declines rapidly towards the bottom. The <i>Euglypha</i> taxa <i>E. rotunda</i> , <i>E. strigosa</i> , and <i>E. tuberculata</i> are all relatively abundant in this zone. <i>N. flabellalum</i> and <i>A. discooides</i> are also relatively abundant. <i>H. subflava</i> increases in abundance towards the bottom	-53 to c. 190
18-74	HUL-Tf	<i>A. flavum</i> and <i>A. wrightianum</i> dominate much of the zone but decline at the top. <i>A. muscorum</i> , <i>C. arcelloides</i> and <i>D. pulex</i> are also abundant at times. <i>A. discooides</i> increases in abundance at the top of this zone	c. 190 to c. 1600
74-86	HUL-Te	<i>A. wrightianum</i> dominates. <i>A. flavum</i> and <i>A. muscorum</i> are also relatively abundant. <i>C. arcelloides</i> displays a notable fall in abundance	c. 1600 to c. 1760
86-154	HUL-Td	<i>A. flavum</i> and <i>A. wrightianum</i> dominate much of the zone. <i>C. arcelloides</i> and <i>D. pulex</i> rise to dominance for a brief spell in the middle (this could be considered a separate zone). <i>H. subflava</i> is notably absent or in very low abundance throughout	c. 1760 to c. 2440
154-226	HUL-Tc	The boundary between this zone and HUL-Td above displays the largest single faunal change in the core. <i>H. subflava</i> dominates, <i>C. arcelloides</i> and <i>D. pulex</i> are also common and <i>A. flavum</i> and <i>A. wrightianum</i> are absent to rare throughout. <i>T. arcula</i> is also relatively common throughout much of the zone	c. 2440 to c. 2960
226-246	HUL-Tb	<i>A. flavum</i> dominates. <i>H. papilio</i> is also relatively abundant. <i>D. pulex</i> and <i>C. arcelloides</i> are also common throughout. <i>H. subflava</i> displays a notable fall in abundance	c. 2960 to c. 3130
246-304	HUL-Ta	Dominated by <i>D. pulex</i> which remains important throughout but is partially displaced by <i>H. subflava</i> in the middle and upper parts of the zone. <i>D. pristis</i> is also at its highest abundance. <i>A. flavum</i> and <i>A. wrightianum</i> are absent to rare throughout	c. 3130 to c. 3640

Age estimates are based on interpolated data and rounded to the nearest 10 years. Negative numbers are years post 1950

The most likely explanation is that recent assemblages have been affected by some anthropogenic disturbance such as an increase in nutrient influx which also appears to have affected the plant macrofossils.

The testate amoebae data were explored using DCA in order to investigate latent structure within the data. Rare taxa were omitted from the analysis and surface samples which contain taxa that only occur at the anthropogenically disturbed near surface were also omitted to prevent problems caused by a crossed gradient. The

DCA biplot of Axes One and Two is displayed in Fig. 6.5. Axis One appears to represent a water availability gradient, with hygrophilous taxa such as *A. wrightianum*, *C. aculeata* and *A. flavum* occurring at one end of the axis (lower scores) and taxa which thrive in drier conditions such as *H. subflava* and *T. arcuata* occurring at the other end (high scores). Axis one has an Eigenvalue of 0.507 (Table 6.4) and spans approximately 3.8 standard deviations, indicating that just over 50% of the variability in taxon abundance can be attributed to water table and that water tables have fluctuated quite widely over the time period represented by the core. This analysis supports the interpretation made from the raw testate amoebae diagram.

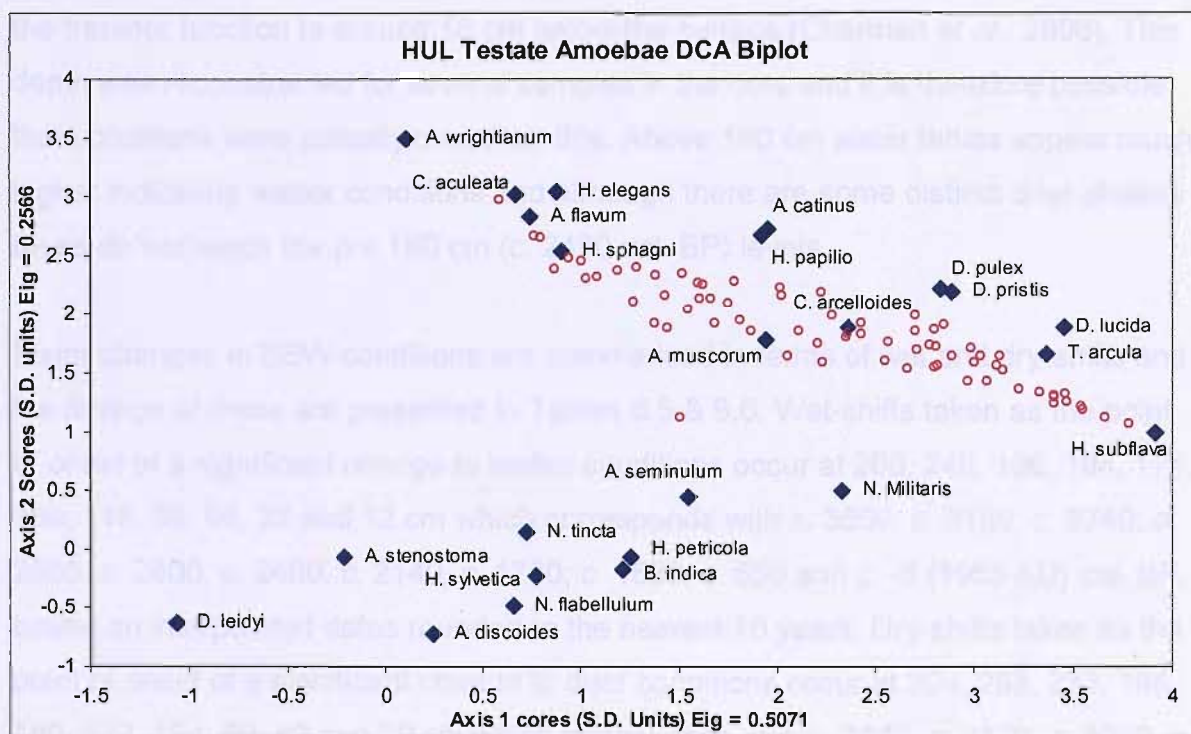


Figure 6.5: Biplot of DCA axis One and Two scores for testate amoebae data from core HUL. Diamonds = taxa scores based on their distribution within the samples and circles = sample scores based on their faunal composition

Table 6.4: HUL Testate Amoebae DCA Details				
Axes	1	2	3	4
Eigenvalues	0.507	0.257	0.091	0.076
Gradient Length (SD units)	3.781	2.983	1.612	1.918

Quantitative estimates of palaeo-water tables were calculated through the application of a transfer function (Woodland *et al.*, 1998) and the results are displayed in Fig. 6.6 along with the testate amoebae zones. Encouragingly, the transfer function based water table reconstruction shows close agreement with the DCA Axis One sample scores (Fig. 6.6). There is no clear long term trend in the water table reconstruction, only a slight movement towards higher water tables over time. However, this is primarily because of a step change in reconstructed water table depth which occurs at c. 160 cm (c. 2490 cal. BP). Below 160 cm water tables were on average low, indicating primarily dry conditions, but with some notable departures, these are summarised below. It is noteworthy that maximum water table depth is constrained by the transfer function to around 16 cm below the surface (Charman *et al.*, 2006). This depth was reconstructed for several samples in the core and it is therefore possible that conditions were actually drier than this. Above 160 cm water tables appear much higher indicating wetter conditions and although there are some distinct drier phases these do not reach the pre 160 cm (c. 2490 cal. BP) levels.

Major changes in BSW conditions are summarised in terms of wet and dry-shifts and the timings of these are presented in Tables 6.5 & 6.6. Wet-shifts taken as the point of onset of a significant change to wetter conditions occur at 280, 248, 196, 184, 176, 160, 116, 88, 68, 32 and 12 cm which corresponds with c. 3500, c. 3150, c. 2740, c. 2660, c. 2600, c. 2490, c. 2140, c. 1780, c. 1530, c. 650 and c. -5 (1955 AD) cal. BP, based on interpolated dates rounded to the nearest 10 years. Dry-shifts taken as the point of onset of a significant change to drier conditions occur at 304, 268, 232, 188, 180, 172, 124, 80, 40 and 20 cm which corresponds with c. 3640, c. 3370, c. 3000, c. 2690, c. 2630, c. 2570, c. 2230, c. 1680, c. 920 and c. 258 cal. BP, based on interpolated dates rounded to the nearest 10 years.

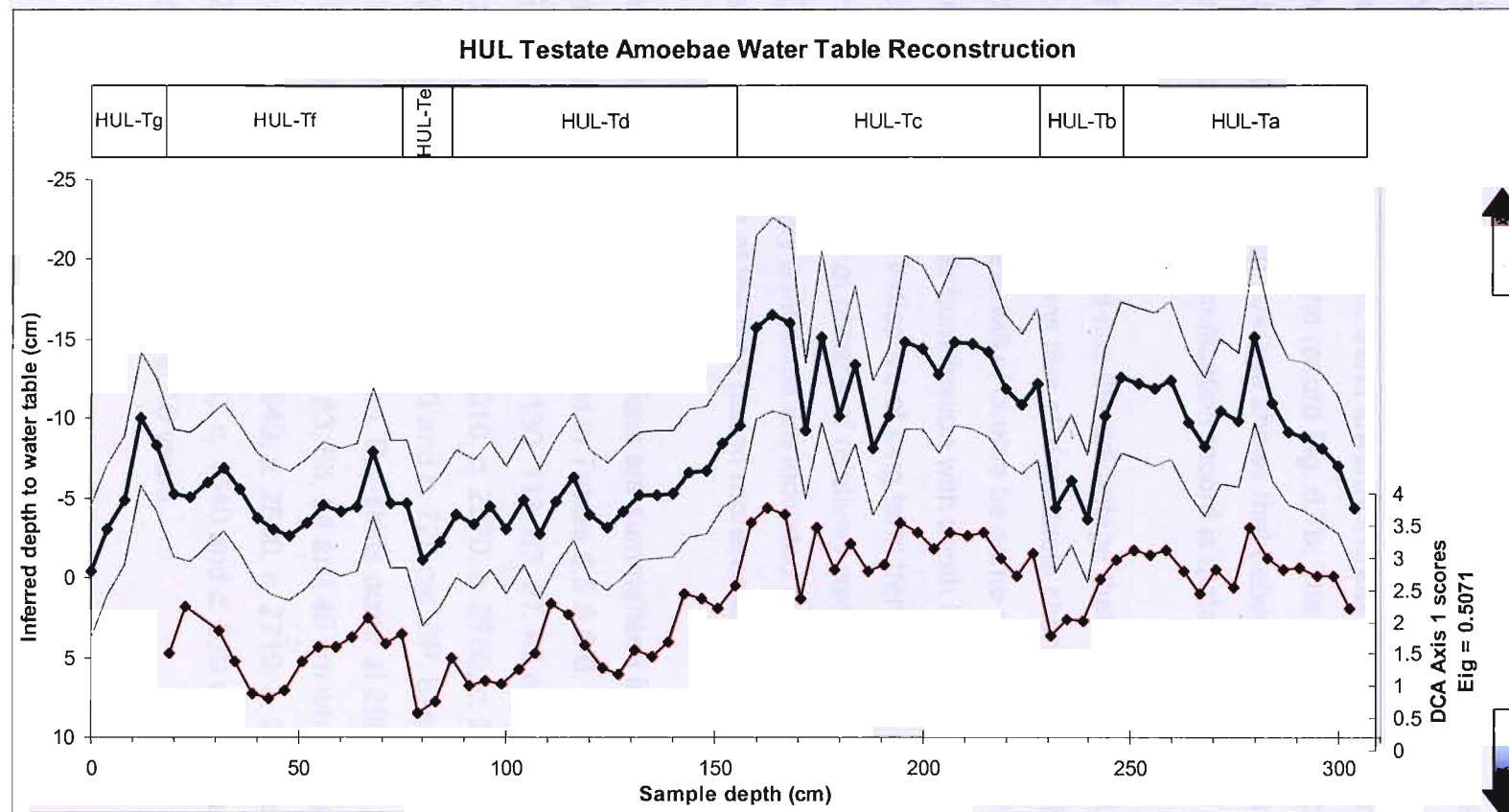


Figure 6.6: Blue curve = quantitative water table depth reconstruction. Brown arrow = drier and the blue arrow = wetter conditions. Feint curves = sample specific root mean squared errors of prediction (RMSEP). Red curve = First Axis DCA sample scores. The bars above the graph are testate amoebae zones derived from the testate amoebae diagram and the codes are those used on the diagram and referred to in the text.

6.2.3 PEAT HUMIFICATION

Raw percentage light transmission values as a measure of peat humification are plotted in Fig. 6.7a. A linear regression model was fitted through the data to take account of the autogenic trend towards increased humification with depth. This model was used to 'detrend' the record Fig. 6.7b. The degree of smoothing produced by the three sample moving average shows that between-sample variability is high and this is indicative that the humification record is quite 'noisy'.

The humification record has the advantage that it was possible to sample contiguously. This means that all detectable changes should be represented to some degree, although there will of course be some smoothing of the record. The long term trend towards greater humification with depth is related to autogenic decay processes and is therefore not indicative of long term trends in the hydrological conditions. However, a number of phases of relatively wet and dry conditions are recorded. Overall wet and dry conditions are indicated to have prevailed for an approximately similar proportion of the time period represented by the core.

Major changes in BSW conditions are summarised in terms of wet and dry-shifts and the timing of these is presented in Tables 6.5 & 6.6. Wet-shifts occur at 300, 273, 249, 233, 213, 197, 167, 149, 130, 113, 67, 57, 47 and 34 cm which corresponds with *c.* 3610, *c.* 3420, *c.* 3160, *c.* 3010, *c.* 2870, *c.* 2750, *c.* 2540, *c.* 2410, *c.* 2270, *c.* 2110, *c.* 1510, *c.* 1380, *c.* 1150 and *c.* 720 cal. BP, based on interpolated dates rounded to the nearest 10 years. Dry-shifts occur at 295, 286, 261, 243, 223, 203, 191, 181, 156, 135, 123, 103, 83, 63, 54 and 40 cm which corresponds with *c.* 3590, *c.* 3530, *c.* 3290, *c.* 3100, *c.* 2940, *c.* 2800, *c.* 2710, *c.* 2640, *c.* 2460, *c.* 2310, *c.* 2220, *c.* 1980, *c.* 1720, *c.* 1460, *c.* 1340 and *c.* 920 cal. BP, based on interpolated dates rounded to the nearest 10 years.

HUL Humification BSW Reconstruction

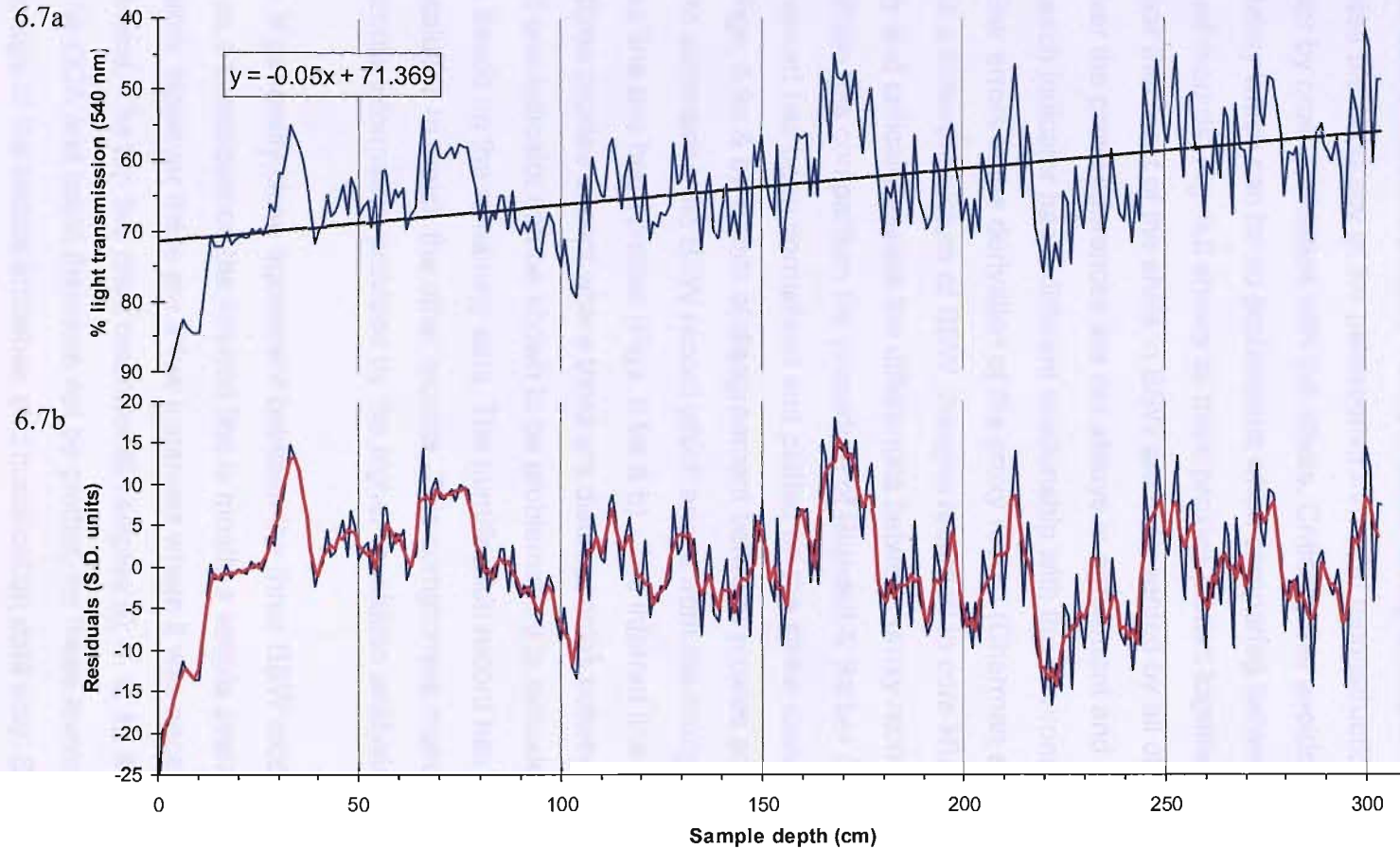


Figure 6.7: Peat Humification record for core HUL. Graph A shows the raw light transmission data. The linear trend line illustrates the general trend towards greater humification with depth. This was used to produce the 'detrended' record (graph B). Bold red line = a three point moving average

6.2.4 MULTI-PROXY COMPARISONS

Comparison of different proxies from the same core provides an excellent opportunity to assess the accuracy of the palaeoenvironmental reconstruction from each proxy indicator by cross validation with the others. Critically this avoids the chronological uncertainty which can be so problematic when comparing between non-annually resolved records. Fig. 6.8 shows all three proxies plotted together for comparison and it is clear that most of the shifts in BSW are represented by all of the proxies. However the proxy inferences are not always in agreement and this is to be expected since each indicator has a different relationship with the environment and is subject to particular errors in the derivation of the proxy record (Charman *et al.*, 2006). In order to build a coherent picture of BSW changes recorded in core HUL it is necessary to identify and critically assess the differences between proxy reconstructions. In order to facilitate this comparison the procedure of Blundell & Barber (2005) was adopted. Each record has been normalised and plotted on the same axes, against depth and age (Figs. 6.9a & b). Points of disagreement between proxies are discussed below. In order to summarise the BSW record which arises from the multiproxy comparison an inferred line has been plotted (Figs. 6.9a & b). The inferred line is simply an average of all three proxies except where there are discrepancies between proxies. In this case if one indicator can be shown to be problematic it is excluded and the inferred line is based on the remaining data. The humification record has been reduced to 4 cm resolution to match the other records. This compromise makes comparison fairer but ignores information provided by the higher resolution analysis.

There is generally close agreement between the three BSW reconstructions from HUL; as a consequence the inferred line is mostly a simple average of all three indicators. However there are a few instances where it was necessary to make some adjustment. The top five plant macrofossil samples (0, 4, 8, 12 & 16 cm) were omitted from the DCA and could therefore not be plotted, for these levels the inferred line is an average of the testate amoebae and humification data only. Samples from 164 cm and 260 cm are dry according to the testate amoebae and plant macrofossils but

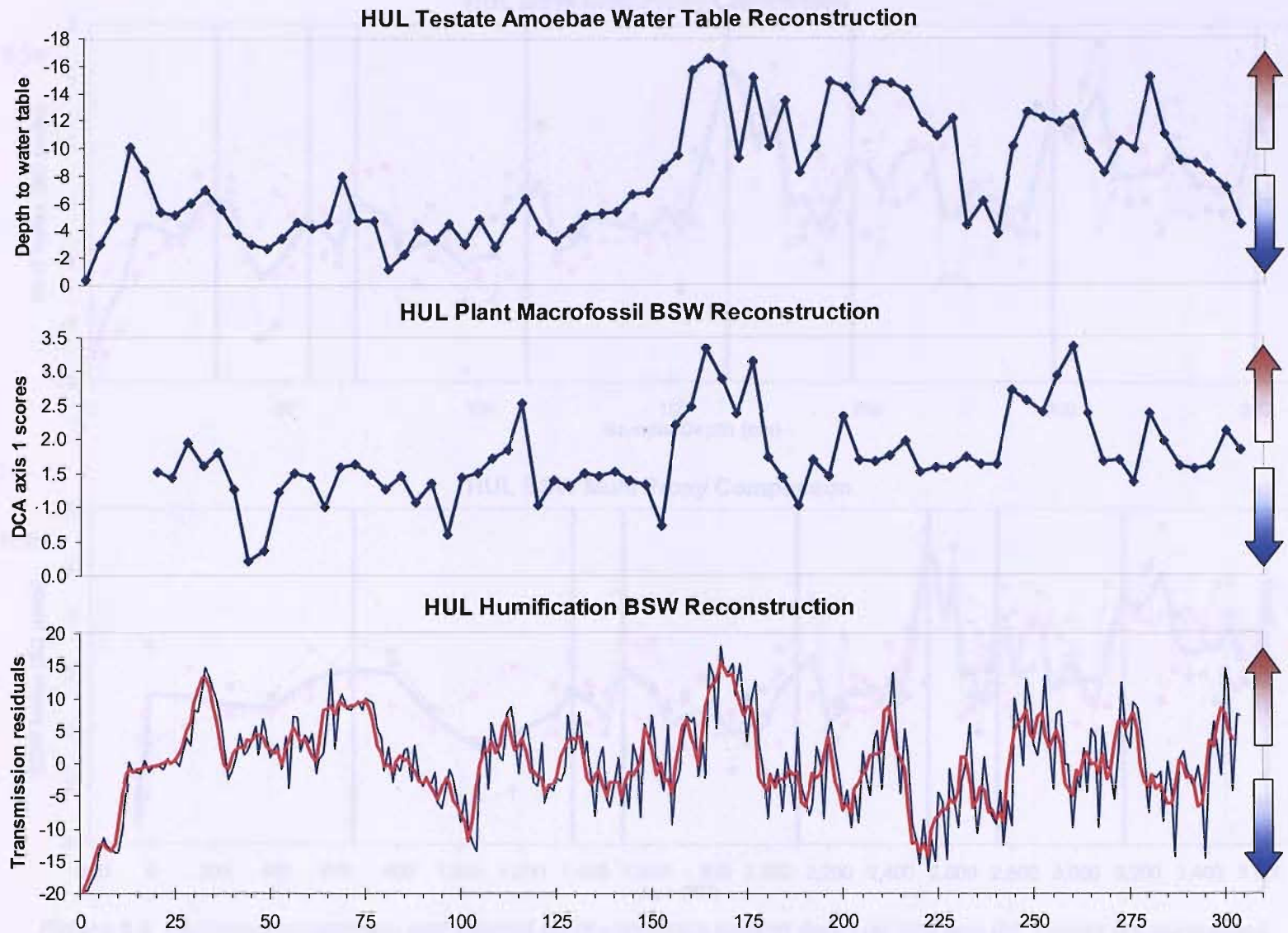


Figure 6.8: Hulleter Moss BSW multiproxy comparison against depth (cm). From the top downwards testate amoebae water table reconstruction, plant macrofossil BSW index and degree of peat humification (red curve = 3 point moving average)

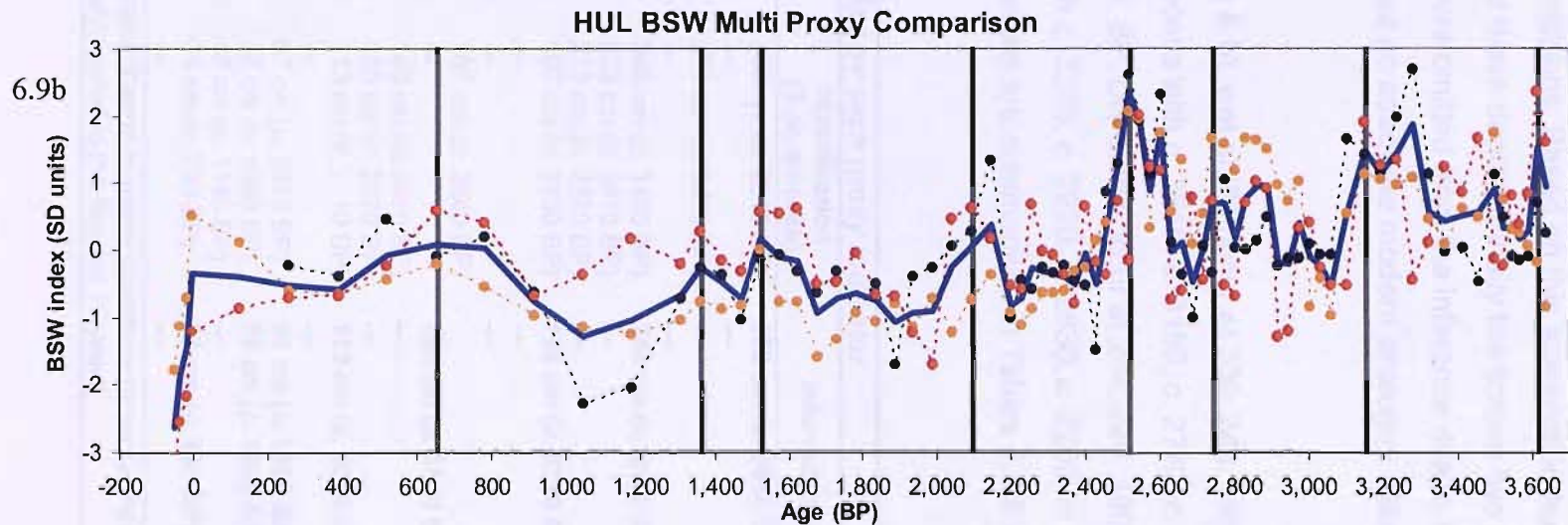
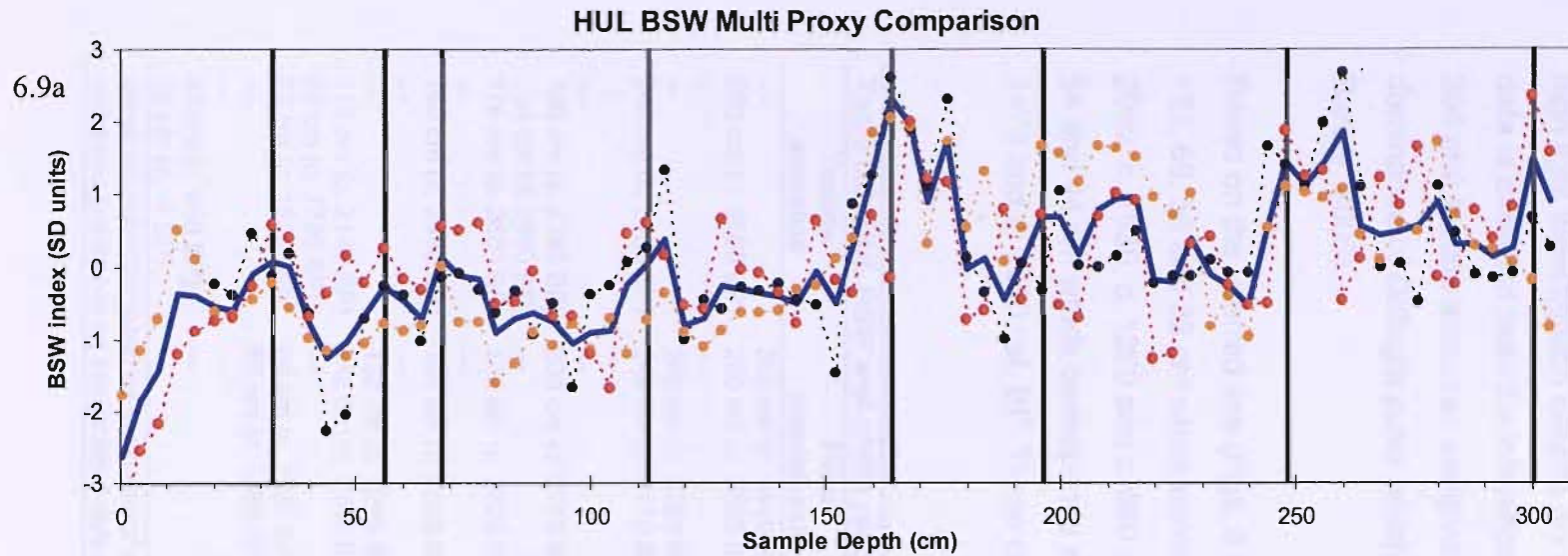


Figure 6.9: Multiproxy comparison and inferred BSW conditions against depth (a) and age (b). Values are normalised for ease of comparison. Black = plant macrofossils, yellow = testate amoebae and red = humification. Bold blue = Inferred BSW conditions based on interpretation of all the data.

much wetter by the humification analysis. *Eriophorum vaginatum* is abundant in both of these levels and is known to be resistant to decay, which could explain relatively high light transmission despite dry conditions. Based on this assumption humification data is excluded from the inference at these depths. Finally the bottom two (300 and 304 cm) testate amoebae samples were omitted from the inference due to the dominance of *Diffflugia pulex* which has no adequate modern analogue (Blundell & Barber, 2005).

Based on the inferred line (Figs. 6.9a & b) wet-shifts occur at 300, 248, 196, 164, 122, 68, 56 and 32 cm which corresponds with c. 3610, c. 3150, c. 2740, c. 2520, c. 2090, c. 1530, c. 1360 and c. 650 cal. BP. Dry-shifts occur at 264, 220, 180, 120, 80, 64 and 44 cm which corresponds with c. 3370, c. 2920, c. 2630, c. 2200, c. 1680, c. 1470 and c. 1050 cal. BP. These changes are summarised in Tables 6.5 & 6.6.

Table 6.5: HUL BSW wet-shifts recorded by each proxy indicator

Testate amoebae	Plant macrofossils	Humification (3 pt. smooth)	Inferred Line
---	300 cm (c. 3610 BP)	300 cm (c. 3610 BP)	300 cm (c. 3610 BP)
280 cm (c. 3500 BP)	280 cm (c. 3500 BP)	---	---
---	---	273 cm (c. 3420 BP)	---
---	260 cm (c. 3280 BP)	---	---
248 cm (c. 3150 BP)	244 cm (c. 3110 BP)	249 cm (c. 3160 BP)	248 cm (c. 3150 BP)
---	---	233 cm (c. 3010 BP)	---
---	---	213 cm (c. 2870 BP)	---
196 cm (c. 2740 BP)	200 cm (c. 2770 BP)	197 cm (c. 2750 BP)	196 cm (c. 2740 BP)
184 cm (c. 2660 BP)	---	---	---
176 cm (c. 2600 BP)	176 cm (c. 2600 BP)	---	---
---	---	167 cm (c. 2540 BP)	---
160 cm (c. 2490 BP)	164 cm (c. 2520 BP)	---	164 cm (c. 2520 BP)
---	---	149 cm (c. 2410 BP)	---
---	132 cm (c. 2280 BP)	130 cm (c. 2270 BP)	---
116 cm (c. 2140 BP)	116 cm (c. 2140 BP)	113 cm (c. 2110 BP)	112 cm (c. 2090 BP)
88 cm (c. 1780 BP)	---	---	---
68 cm (c. 1530 BP)	68 cm (c. 1530 BP)	67 cm (c. 1510 BP)	68 cm (c. 1530 BP)
---	56 cm (c. 1360 BP)	57 cm (c. 1380 BP)	56 cm (c. 1360 BP)
---	---	47 cm (c. 1150 BP)	---
32 cm (c. 650 BP)	---	34 cm (c. 720 BP)	32 cm (c. 650 BP)
12 cm (c. -5 BP)	---	---	---

Onset of wet-shifts taken as the onset of a major change to wetter conditions by proxy. Age estimates are based on interpolated data and rounded to the nearest 10 years.

Table 6.6: HUL BSW Dry-shifts recorded by each proxy indicator

Testate amoebae	Plant macrofossils	Humification (3 pt. smooth)	Inferred Line
304 cm (c. 3640 BP)	---	---	---
---	---	295 cm (c. 3590 BP)	---
---	288 cm (c. 3550 BP)	286 cm (c. 3530 BP)	---
---	276 cm (c. 3460 BP)	---	---
268 cm (c. 3370 BP)	---	---	---
---	---	261 cm (c. 3290 BP)	264 cm (c. 3370 BP)
---	252 cm (c. 3190 BP)	---	---
---	---	243 cm (c. 3100 BP)	---
232 cm (c. 3000 BP)	---	---	---
---	---	223 cm (c. 2940 BP)	220 cm (c. 2920 BP)
---	---	203 cm (c. 2800 BP)	---
188 cm (c. 2690 BP)	188 cm (c. 2690 BP)	191 cm (c. 2710 BP)	---
180 cm (c. 2630 BP)	---	181 cm (c. 2640 BP)	180 cm (c. 2630 BP)
172 cm (c. 2570 BP)	172 cm (c. 2570 BP)	---	---
---	152 cm (c. 2430 BP)	156 cm (c. 2460 BP)	---
---	---	135 cm (c. 2310 BP)	---
124 cm (c. 2230 BP)	120 cm (c. 2200 BP)	123 cm (c. 2220 BP)	120 cm (c. 2200 BP)
---	---	103 cm (c. 1980 BP)	---
80 cm (c. 1680 BP)	---	83 cm (c. 1720 BP)	80 cm (c. 1680 BP)
---	64 cm (c. 1470 BP)	63 cm (c. 1460 BP)	64 cm (c. 1470 BP)
---	---	54 cm (c. 1340 BP)	---
40 cm (c. 920 BP)	44 cm (c. 1050 BP)	40 cm (c. 920 BP)	44 cm (c. 1050 BP)
20 cm (c. 258 BP)	---	---	---

Onset of dry-shifts taken as the onset of a major change to drier conditions by proxy. Age estimates are based on interpolated data and rounded to the nearest 10 years.

6.3 BIGLAND TARN

6.3.1 LOSS ON IGNITION

LOI was undertaken at 4 cm resolution throughout the lake cores and used to correlate core sections (Section 3.3.2). Moisture, organic and carbonate content of the sediments were estimated and results are displayed in Fig. 6.10. Percentage moisture and LOI₅₅₀ are highly correlated since the ability of the sediments to hold water is in part controlled by the amount of organic material present. The moisture content from the top core was generally lower than the bottom and this is almost certainly an artefact of the freezing process which the top core was subjected to in order to preserve the sediment water interface. Organic matter estimated by LOI₅₅₀ accounts for between 38 and 74 % of sediment dry weight. There is a general increase in organic matter down core although there are some notable departures from this trend.

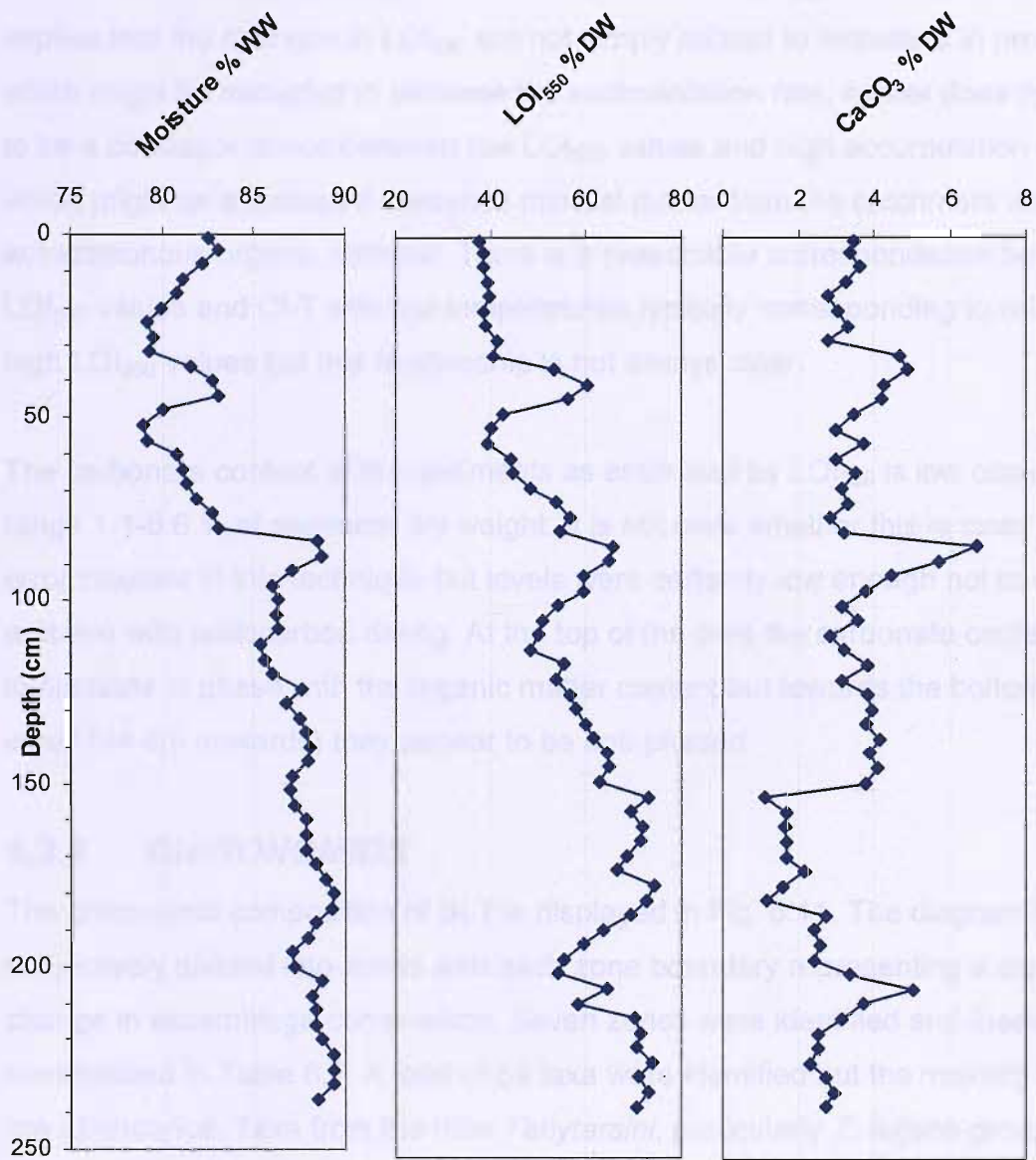


Figure 6.10: Moisture and Loss on Ignition (LOI) data for Bigland Tarn. From the left curves represent moisture content as a percentage of wet weight (WW), organic content as a proportion of dry weight (DW) and carbonate content as a proportion of dry weight

There appears to be little relationship between the accumulation rates predicted by the age-depth model and the organic content of the sediment, although the most rapid accumulation rate in the core (3.3 mm y^{-1}) which is predicted from 32-44 cm does correspond with high LOI_{550} values of c. 60 %. However further down core

(204-232 cm) an accumulation rate of only 0.3 mm y^{-1} is predicted and LOI_{550} values are c. 75 %. The lack of a clear relationship between LOI_{550} and accumulation rate implies that the changes in LOI_{550} are not simply related to increases in productivity which might be expected to increase the sedimentation rate, neither does there seem to be a correspondence between low LOI_{550} values and high accumulation rates which might be expected if inwashed mineral matter from the catchment were diluting autochthonous organic material. There is a reasonable correspondence between LOI_{550} values and CI-T with low temperatures typically corresponding to relatively high LOI_{550} values but this relationship is not always clear.

The carbonate content of the sediments as estimated by LOI_{950} is low occurring in the range 1.1-6.6 % of sediment dry weight. It is not clear whether this is close to the error inherent in this technique but levels were certainly low enough not to cause a problem with radiocarbon dating. At the top of the core the carbonate content appears to fluctuate in phase with the organic matter content but towards the bottom of the core (144 cm onwards) they appear to be anti-phased.

6.3.2 CHIRONOMIDS

The chironomid composition of BLT is displayed in Fig. 6.11. The diagram has been subjectively divided into zones with each zone boundary representing a significant change in assemblage composition. Seven zones were identified and these are summarised in Table 6.7. A total of 59 taxa were identified but the majority occur in low abundance. Taxa from the tribe *Tanytarsini*, particularly *T. lugens*-group but also *T. no spur* and *T. undiff.* dominate much of the core and changes in community structure chiefly involve changes in the relative abundance of taxa from the tribe *Chironomini*, particularly *C. anthracinus*-group, *Glyptotendipes* and *Microtendipes*. The tribes *Tanypodinae* and *Orthoclaadiinae* are also represented but these tend to make only a small contribution to the assemblage, with the exception perhaps of *Procladius* which is relatively common throughout most of the core.

Bigland Tarn (core BLT) Chironomid Diagram

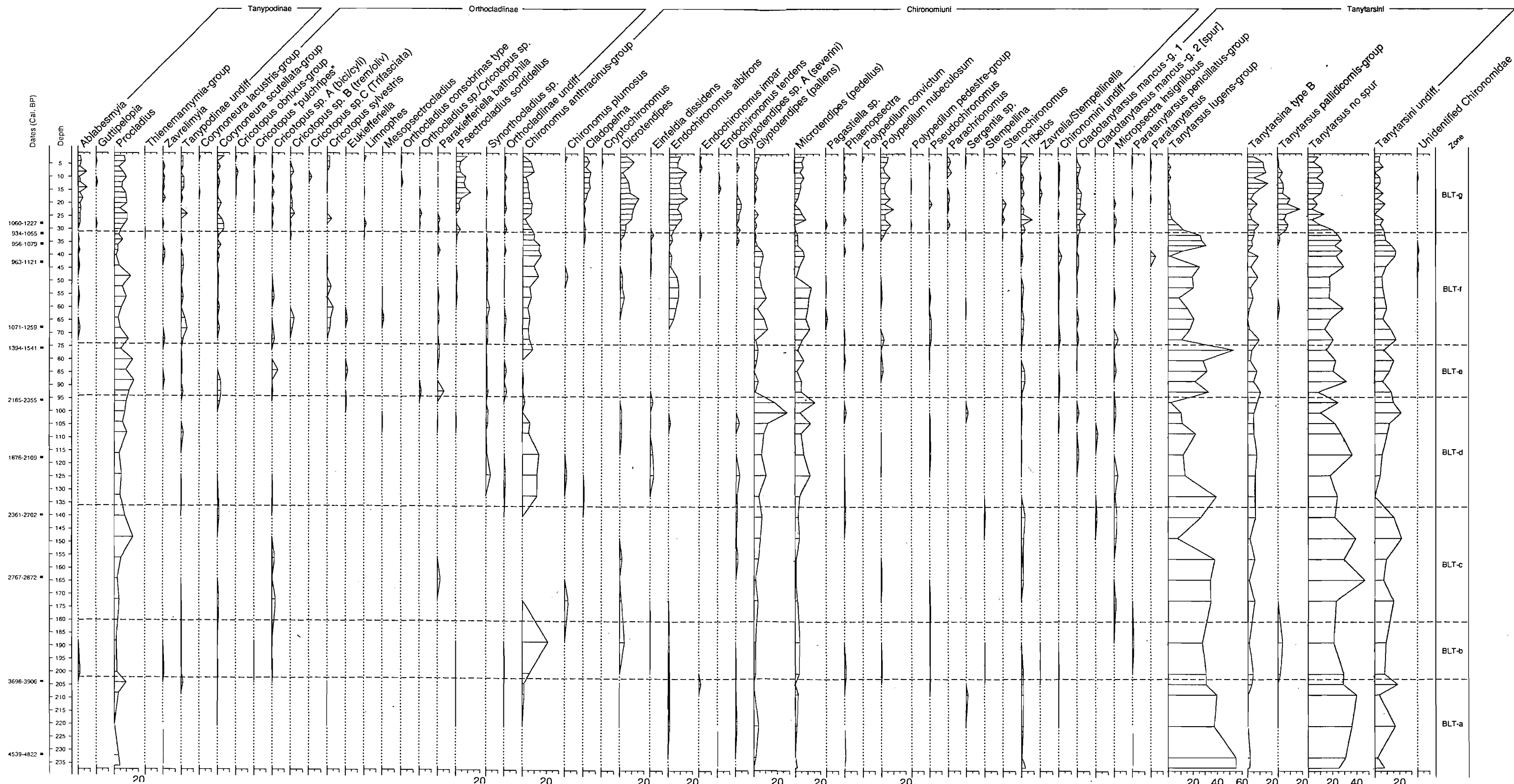


Table 6.7: Chironomid zone descriptions for core BLT

Depth (cm)	Zone	Description	Age (cal. BP)
2-31	BLT-g	This topmost zone is characterised by the very low abundance of <i>T. lugens</i> -group, which is replaced by a number of taxa which either appear or reach abundance for the first time in the core, these include; <i>P. sordidellus</i> , <i>Cladopelma</i> , <i>Dicrotendipes</i> , <i>E. albifrons</i> , <i>P. nubeculosum</i> and <i>T. pallidicornis</i> -group.	c. -20 to c. 960
31-74	BLT-f	This zone has a relatively low proportion of <i>T. lugens</i> -group, <i>T. no spur</i> and <i>T. undiff.</i> <i>C. anthracinus</i> -group while <i>Glyptotendipes (pallens)</i> , <i>Microtendipes</i> and <i>E. albifrons</i> are all relatively abundant.	c. 960 to c. 1490
74-94	BLT-e	<i>T. lugens</i> -group dominates this zone <i>T. type B</i> , <i>T. no spur</i> , <i>T. undiff.</i> and <i>Procladius</i> are also abundant. Chironomini taxa are notably low in occurrence.	c. 1490 to c. 1680
94-136	BLT-d	This zone is characterised by a fall in the abundance of <i>T. lugens</i> -group, although <i>T. no spur</i> abundance is high. Chironomini taxa including <i>C. anthracinus</i> -group, <i>Glyptotendipes (pallens)</i> and <i>Microtendipes</i> are relatively abundant.	c. 1680 to c. 2370
136-180	BLT-c	This zone is characterised by high <i>T. lugens</i> -group and <i>T. no spur</i> abundance and a notably low occurrence of Chironomini taxa. <i>C. anthracinus</i> -group in particular is completely absent.	c. 2370 to c. 3210
180-202	BLT-b	This zone is characterised by an increase in Chironomini particularly <i>C. anthracinus</i> -group and <i>Dicrotendipes</i> . <i>T. lugens</i> -group declines but only slightly and <i>T. pallidicornis</i> -group appear at low abundance.	c. 3210 to c. 3750
202-236	BLT-a	<i>T. lugens</i> -group, <i>T. no spur</i> and <i>t. undiff.</i> dominate particularly towards the bottom of the zone.	c. 3750 to c. 4820

Age estimates are based on interpolated data and rounded to the nearest 10 years. Negative numbers are years post 1950

The lack of clear differentiation between *Tanytarsini* remains is a common problem with sites rich in these taxa (e.g. Bigler *et al.*, 2002; Langdon *et al.*, 2004) as well as in the modern training set data (Brooks & Birks, 2000), this situation has been somewhat improved by the addition of the *T. no spur* taxon (Brooks, 2004, unpublished key) which separates out some of the individuals that would previously have been classified simply as *T. undiff.*, The *T. no spur* taxon must be either *T. lugens*-group or *T. type B*-group. Nevertheless, *T. undiff.* still accounts for up to 20% of the assemblage and *T. no spur* up to 40% of the assemblage at this site. This low taxonomic resolution must be taken into account when interpreting the assemblage

The abundance of *Chironomini* is typically lower than the *Tanytarsini* even during phases of peak abundance, nevertheless these changes are quite significant so that in some samples *Chironomini* are very scarce to absent (zones, BLT-a, c and e) whereas in others they are common (zones BLT-b, d and f). This pattern would seem to indicate temperature fluctuations with phases of *Chironomini* abundance representing warmer conditions and scarcity representing cooler conditions.

The topmost zone, BLT-g (0-31 cm) displays a different pattern to that described above with *Tanytarsini* and particularly *T. lugens*-group falling to the lowest abundance in the core and a whole variety of other taxa (including, *Psectrocladius sordidellus*, *Cladopelma*, *Dicrotendipes*, *Endochironomus albifrons*, *Polypedilum nubeculosum* and *Tanytarsus pallidicornis*-group) increasing, many of which have been very rare or absent elsewhere in the core. This change in species composition is likely to be a response to relatively recent anthropogenic disturbance.

Dicrotendipes, *E. albifrons*, *P. nubeculosum* and *P. sordidellus* are identified in the literature as acidophiles (Brodin, 1986; Pinder & Morley, 1995; Brooks, 2005, unpublished notes) indicating potential acidification although this is unlikely to be the driver since pH testing at the time of coring revealed the lake waters to be pH 8. *P. nubeculosum* is known to thrive in eutrophic conditions (Brodin, 1982;1986; Brooks, 2005, unpublished notes) but is the only strong eutrophic indicator and is not the most abundant taxa making this unlikely to be the main explanatory variable. *P. sordidellus*, *Dicrotendipes* and *E. albifrons* have all been found to have an association with aquatic macrophytes (Brodersen *et al.*, 2001) indicating that the surface zone might represent a response to a change in macrophyte abundance or community structure, which may in turn be related to eutrophication or an increase in the water level. Whatever the explanation for this topmost zone it is unlikely to be directly related to climate variability and the reconstruction above 31 cm is therefore probably unreliable in palaeotemperature terms. This is unfortunate since high resolution analysis was carried out over the top of the core in an attempt to correlate the reconstruction with instrumental records; unfortunately the anthropogenic influence and the chronological uncertainty of the near surface sediments make this impossible.

Quantitative estimates of mean July palaeotemperature were calculated through the application of the Norwegian training set (Brooks & Birks, 2000) and the results are displayed in Fig. 6.12 along with the zones derived from Fig. 6.11. CI-T for the top sample (2 cm) is 14.4 °C, a very close match with the 1979-2000 average mean July temperature of 15 °C recorded at Newton Rigg (METOffice, 2005b) (approx. 30 miles NNE) and well within the errors of prediction. The accuracy of this reconstruction despite probable anthropogenic influence on the chironomid community at this level supports the applicability of the Norwegian training set to this data.

The CI-T reconstruction for BLT shows a slight warming trend throughout the core although this is accentuated by the relatively warm near surface values which are probably at least partly driven by non-climatic factors. The curve displays some marked temperature trends in particular very cool conditions are indicated at 236 cm where mean July temperature estimates fall as low as 9.2 °C, between 92 and 76 cm temperatures are generally low fluctuating between 10.5 and 11.9 °C. Less pronounced cool conditions occur at 204 cm (11.2 °C), 164 cm (10.9 °C) and 36 cm (11.4 °C). Particularly warm temperatures are inferred at 104 cm (14.2 °C), 56 cm (14.3 °C) and above 30 cm (15.5 -13.5 °C).

The total range of variability is 6.2 °C if the top 30 cm are included and 5 °C if they are excluded. This is a wide range of variability, over twice the range of Langdon *et al.*, (2004). In particular the temperatures at the low end of the spectrum seem very low for mean July temperature at this latitude during the late Holocene. This may be partially explained by the findings of Heiri *et al.*, (2003) where relative to the mid-lake samples, cooler temperatures were inferred at intermediate depths and partially because the training set is skewed towards the cooler conditions typically found in Norway. Nevertheless there is no reason to suspect that the temperature trend is inaccurate, even if some of the absolute values are not precise.

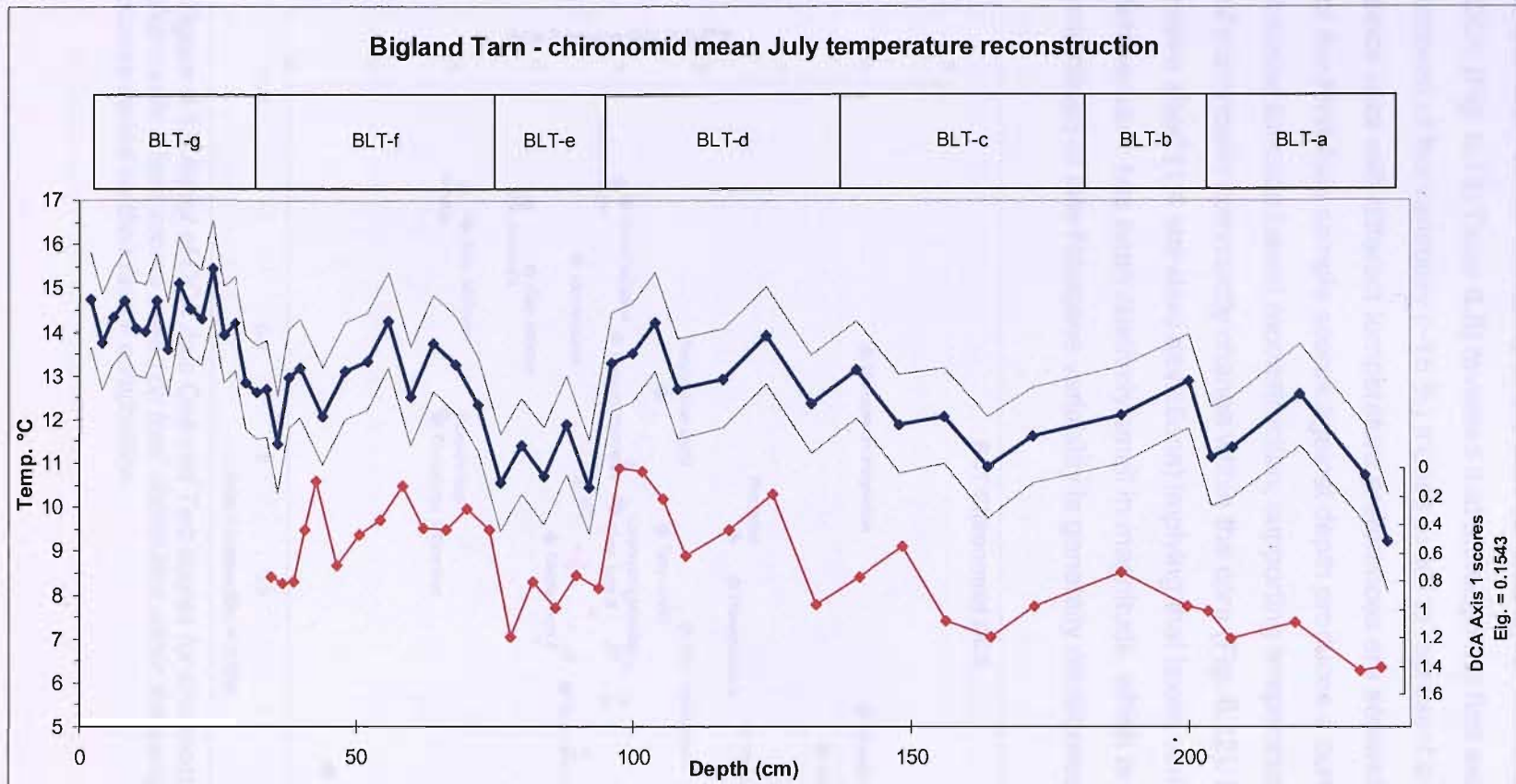


Figure 6.12: Chironomid inferred palaeotemperature reconstruction for core BLT. Blue curve = quantitative palaeotemperature reconstruction. Faint curves = sample specific root mean squared errors of prediction (RMSEP). Red curve = First Axis DCA sample scores. The bars above the graph are chironomid zones derived from the chironomid diagram and the codes are those used on the diagram and referred to in the text.

Exploration of the variability in the data (excluding rare taxa and the top 30 cm) using DCA (Fig. 6.13, Table 6.8) revealed that although the first axis explained only a small amount of the variability (~15 %) it does seem to represent a temperature gradient since taxa with different temperature preferences are separated along the axis. A plot of the First Axis sample scores against depth produces a curve very similar to the transfer function based reconstruction, supporting temperature as the primary driver of chironomid community change within the core (Fig. 6.12). However, the gradient is rather short (1.4 standard deviations) implying that taxon variation in response to temperature has been relatively small in magnitude, which is to be expected as the magnitude of late Holocene variability is generally considered to be quite low.

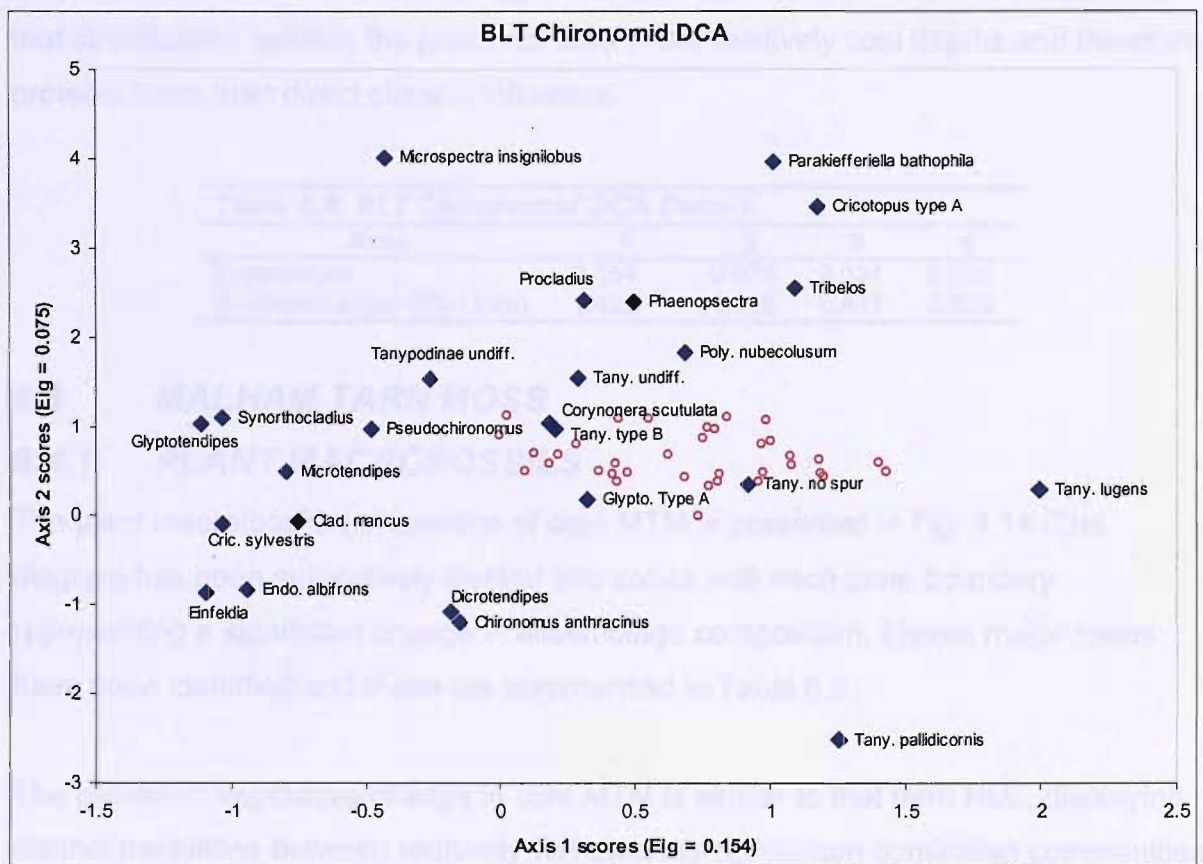


Figure 6.13: Biplot of DCA Axis One and Two scores for chironomid data from core BLT. Diamonds = taxa scores based on their distribution within the samples. Circles = sample scores based on their faunal composition.

Some of the reconstructed temperature variability may also be explicable in terms of the relative contribution to the assemblage from profundal and littoral taxa, for example an increase in the ratio of profundal taxa might appear to indicate cooler conditions and vice versa. The most likely mechanism for this change in ratio would be thermal stratification which directly influences oxygen levels in the profundal zone and consequently can change the proportion of the assemblage made up of profundal taxa. Stratification is typically related to temperature and summer wind conditions and is consequently still related to climate variability but may lead to a more complex relationship e.g. a threshold change in assemblage resulting from a relatively small change in temperature. An alternative explanation for temperature underestimates due to thermal stratification was suggested by Seppa *et al.*, (2002) who postulated that stratification isolates the profundal taxa in the relatively cool depths and therefore protects them from direct climatic influence.

Table 6.8: BLT Chironomid DCA Details

Axes	1	2	3	4
Eigenvalues	0.154	0.075	0.037	0.023
Gradient Length (SD Units)	1.429	1.118	0.841	0.823

6.4 MALHAM TARN MOSS

6.4.1 PLANT MACROFOSSILS

The plant macrofossils composition of core MTM is presented in Fig. 6.14. The diagram has been subjectively divided into zones with each zone boundary representing a significant change in assemblage composition. Eleven major zones have been identified and these are summarised in Table 6.9.

The pattern of vegetative change in core MTM is similar to that from HUL, displaying distinct transitions between relatively wet dwelling *Sphagnum* dominated communities (zones MTM-a, c, e, g, l and k), intermediate-dry Ericaceae (zone MTM-b) and dry tolerant Cyperaceae dominated communities (zones MTM-d, f, h and i). The boundaries between communities types are also quite sharp indicating that community structure may exhibit a threshold type response to water table variability.

Malham Tarn Moss (core: MTM) Plant Macrofossil Diagram

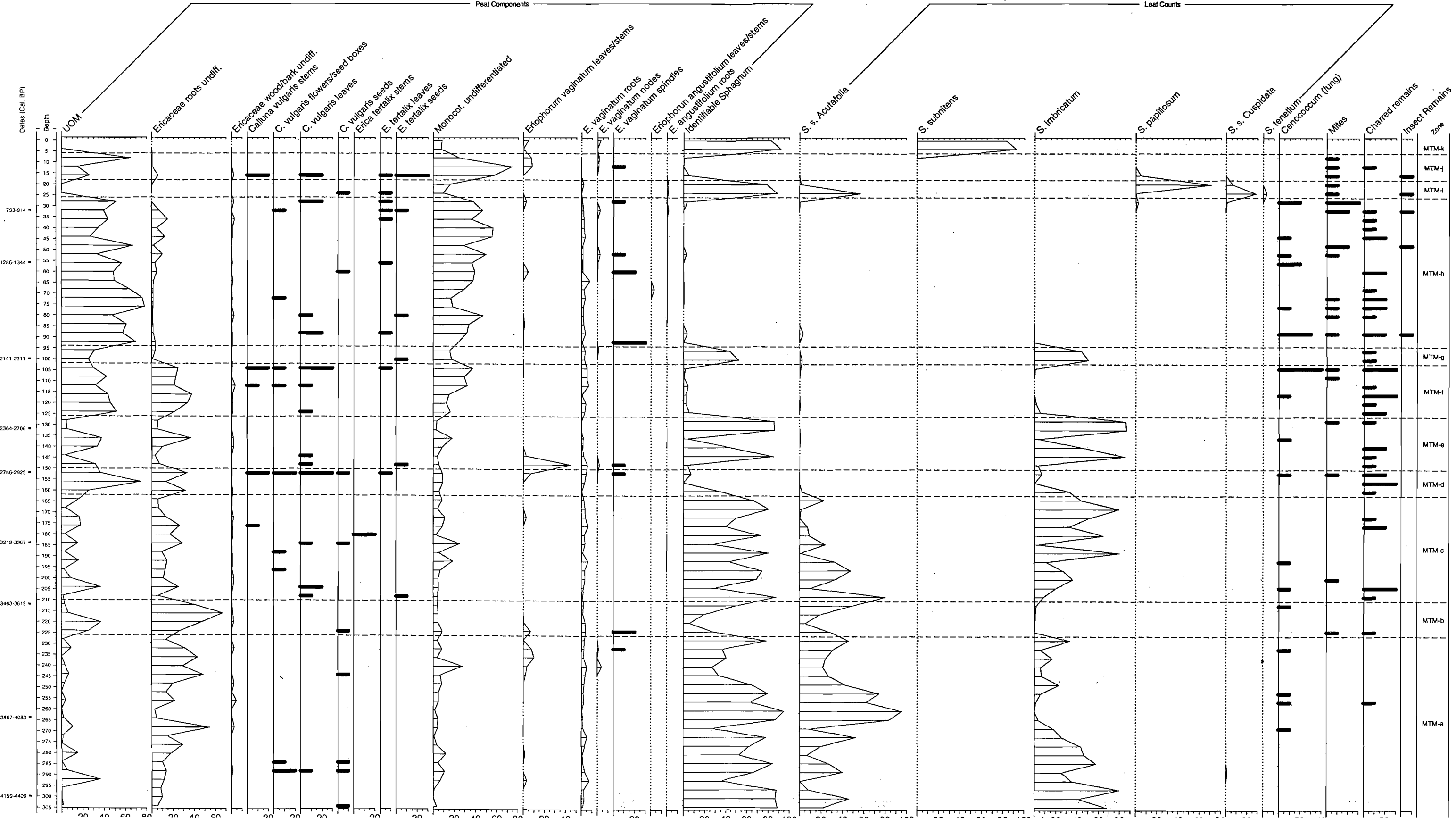


Table 6.9: Plant macrofossil zone descriptions for core MTM

Depth (cm)	Zone	Description	Age (cal. BP)
0-6	MTM-k	<i>S. subnitens</i> dominates this topmost zone. <i>E. vaginatum</i> leaves/stems and undifferentiated monocotyledon roots are also present	-53 to c. -29
6-18	MTM-j	Undifferentiated monocotyledon roots are dominant. UOM occurrence is also high, particularly at the top of the zone. Carabid mites are rare but present throughout	c. -29 to c. 192
18-26	MTM-i	<i>S. papillosum</i> is dominant, <i>S. s. Acutifolia</i> and <i>S. s. Cuspidata</i> are also abundant. UOM and undifferentiated monocotyledon roots are of notably low occurrence. Carabid mites are rare but present throughout	c. 192 to c. 460
26-94	MTM-h	UOM dominates. Undifferentiated monocotyledon roots are also abundant. <i>Sphagnum</i> is almost completely absent from the zone. Charred remains are found occasionally throughout most of the zone	c. 460 to c. 1860
94-102	MTM-g	<i>S. imbricatum</i> is dominant, UOM and undifferentiated monocotyledon roots also occur at medium abundance	c. 1860 to c. 1960
102-126	MTM-f	UOM dominates. Ericaceous roots and undifferentiated monocotyledon roots are also abundant. <i>Sphagnum</i> is almost completely absent. Charred remains are occasional throughout	c. 1960 to c. 2240
126-150	MTM-e	<i>S. imbricatum</i> dominates overall, although there is a brief spell in the middle of the zone where UOM rises to dominance. Ericaceous roots and <i>E. vaginatum</i> leaves/stems are also briefly abundant.	c. 2240 to c. 2410
150-162	MTM-d	UOM dominates this zone. Ericaceous roots are also abundant. <i>Sphagnum</i> abundance is notably low	c. 2410 to c. 2500
162-210	MTM-c	<i>S. imbricatum</i> dominates much of this zone. <i>S. s. Acutifolia</i> is also abundant. UOM, Ericaceous and undifferentiated monocotyledon roots occur at medium abundance throughout	c. 2500 to c. 2850
210-226	MTM-b	Ericaceous roots dominate this zone. UOM is also abundant in the lower half of the zone. <i>S. s. Acutifolia</i> occurs in medium to high abundance at the top and bottom of the zone but is low throughout the middle.	c. 2850 to c. 2960
226-304	MTM-a	<i>S. imbricatum</i> dominates at the base and is replaced by <i>S. s. acutifolia</i> as the dominant taxon towards the top of the zone. Ericaceous roots are also abundant throughout much of the zone. UOM is relatively low throughout.	c. 2960 to c. 3640

Age estimates are based on interpolated data and rounded to the nearest 10 years. Negative numbers are years post 1950

UOM occurs throughout much of the stratigraphy of MTM (particularly zones MTM-d, f, g, h and j) indicating that prevailing conditions have been drier than at Hulleter Moss.

Sphagnum communities are particularly rich in *S. imbricatum* and *S. s. Acutifolia* with *S. papillosum* and *S. s. Cuspidata* occurring generally at much lower abundance. *S. magellanicum* is absent from MTM. The lower boundary of zone MTM-h is marked by the disappearance of *S. imbricatum*. The zone is almost completely devoid of *Sphagnum*. When conditions favour *Sphagnum* growth again at the base of zone MTM-i *S. imbricatum* does not return, instead *S. papillosum* dominates briefly. This pattern is slightly atypical with *S. imbricatum* disappearing at 88cm (c. 1980 cal. BP), c. 1300 years earlier than usual (Mauquoy & Barber, 1999), probably because of the dry conditions which prevailed at the time. The first appearance of *S. papillosum* at 28 cm (c. 670 cal. BP) does however coincide with the expected timing of *S. imbricatum* decline and associated *S. papillosum* and *S. magellanicum* proliferation.

The topmost zone (MTM-k) is dominated by *S. subnitens*, which is absent from the rest of the core. *S. subnitens* generally thrives in more nutrient-rich environments and its presence may indicate recent nutrient enrichment of the bog surface, perhaps as a result of decomposition of the peat facilitated by peat cutting and subsequent reduction in water-table level.

The majority of Cyperaceae and Ericaceae remains are only distinguishable to group level however diagnostic leaves, stems and seeds reveal that both *E. tetralix* and *C. vulgaris* have grown on the bog, coexisting for much of the time but with *Calluna* tending to be more abundant. Some diagnostic epidermal material from *E. vaginatum* is evident but is not abundant. *E. vaginatum* spindles are also common and are not only found at the same levels as the diagnostic root and epidermal material suggesting that much of the undifferentiated monocotyledon material may be *E. vaginatum*.

DCA was used in order to investigate latent structure within the plant macrofossil data. Rare taxa and surface samples were omitted. The DCA biplot of Axis One and Two is displayed in Fig. 6.15. Axis One can be shown to represent a water availability gradient with taxa that typically occupy lawn microenvironments such as *S.*

s. Cuspidata and *S. imbricatum* at one end of the axis (high scores) and indicators of drier conditions such as UOM and undifferentiated monocotyledon remains at the other end (low scores), confirming the nature of the relationship inferred from the macrofossil diagram.

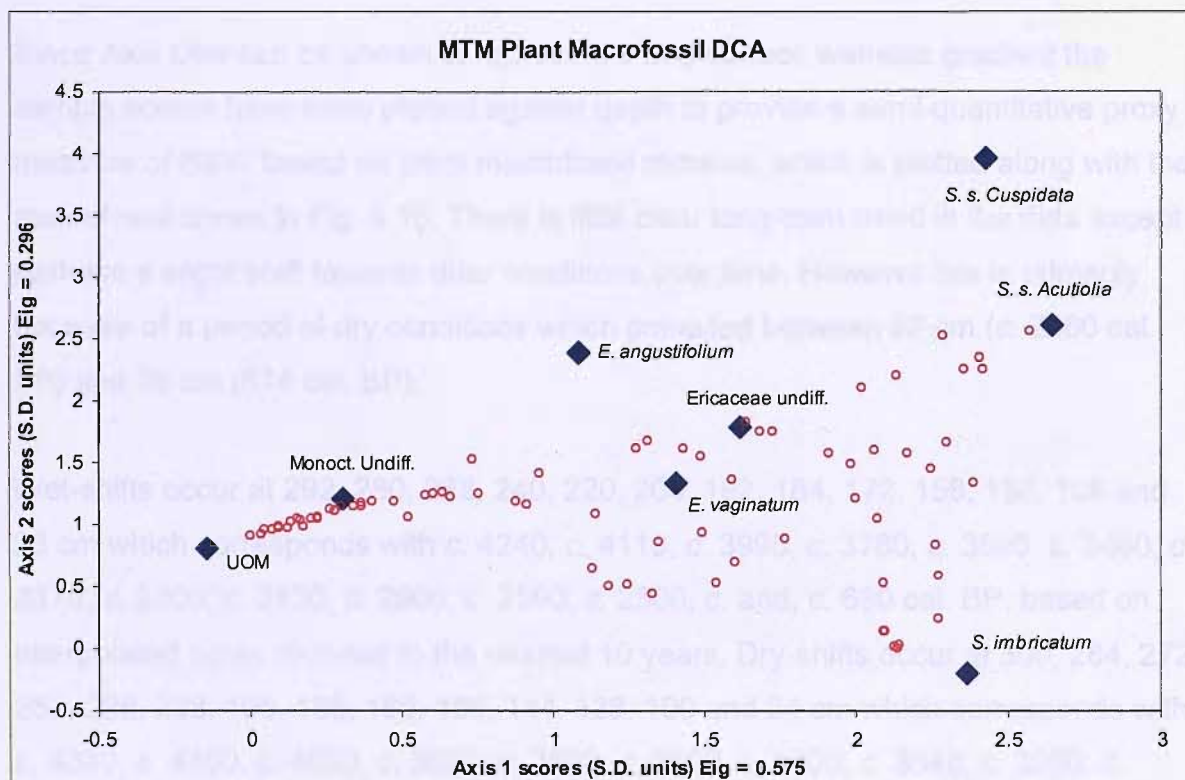


Figure 6.15: Biplot of DCA Axis One and Two scores for plant macrofossil data from core MTM. Diamonds = taxa scores based on their distribution within the samples. Circles = sample scores based on their floral composition

Axis One has an Eigenvalue of 0.575 and spans approximately 2.6 standard deviations (Table 6.10) indicating that just under 60% of the variability in taxon abundance can be attributed to water tables and that the amplitude of BSW change has remained relatively low over the time period represented by the core. Furthermore the plant remains present indicate that fluctuation has been biased towards the drier end of the spectrum with conditions switching between intermediate lawn type conditions and dry hummock like conditions.

Table 6.10: MTM Plant Macrofossil DCA Details

Axes	1	2	3	4
Eigenvalues	0.575	0.295	0.080	0.050
Gradient Length (SD Units)	2.572	2.561	1.824	1.568

Since Axis One can be shown to represent a bog surface wetness gradient the sample scores have been plotted against depth to provide a semi-quantitative proxy measure of BSW based on plant macrofossil remains, which is plotted along with the macrofossil zones in Fig. 6.16. There is little clear long-term trend in the data except perhaps a slight shift towards drier conditions over time. However this is primarily because of a period of dry conditions which prevailed between 92 cm (c. 2060 cal. BP) and 28 cm (674 cal. BP).

Wet-shifts occur at 292, 280, 268, 240, 220, 204, 192, 184, 172, 156, 136, 108 and 28 cm which corresponds with c. 4240, c. 4110, c. 3990, c. 3760, c. 3590, c. 3460, c. 3370, c. 3300, c. 3130, c. 2900, c. 2590, c. 2300, c. and, c. 680 cal. BP, based on interpolated dates rounded to the nearest 10 years. Dry-shifts occur at 300, 284, 272, 252, 228, 208, 196, 188, 180, 168, 144, 128, 100 and 24 cm which corresponds with c. 4320, c. 4150, c. 4030, c. 3850, c. 3660, c. 3500, c. 3400, c. 3340, c. 3250, c. 3070, c. 2720, c. 2490, c. 2230 and c.490 cal. BP, based on interpolated dates rounded to the nearest 10 years (Tables 6.13 & 6.14).

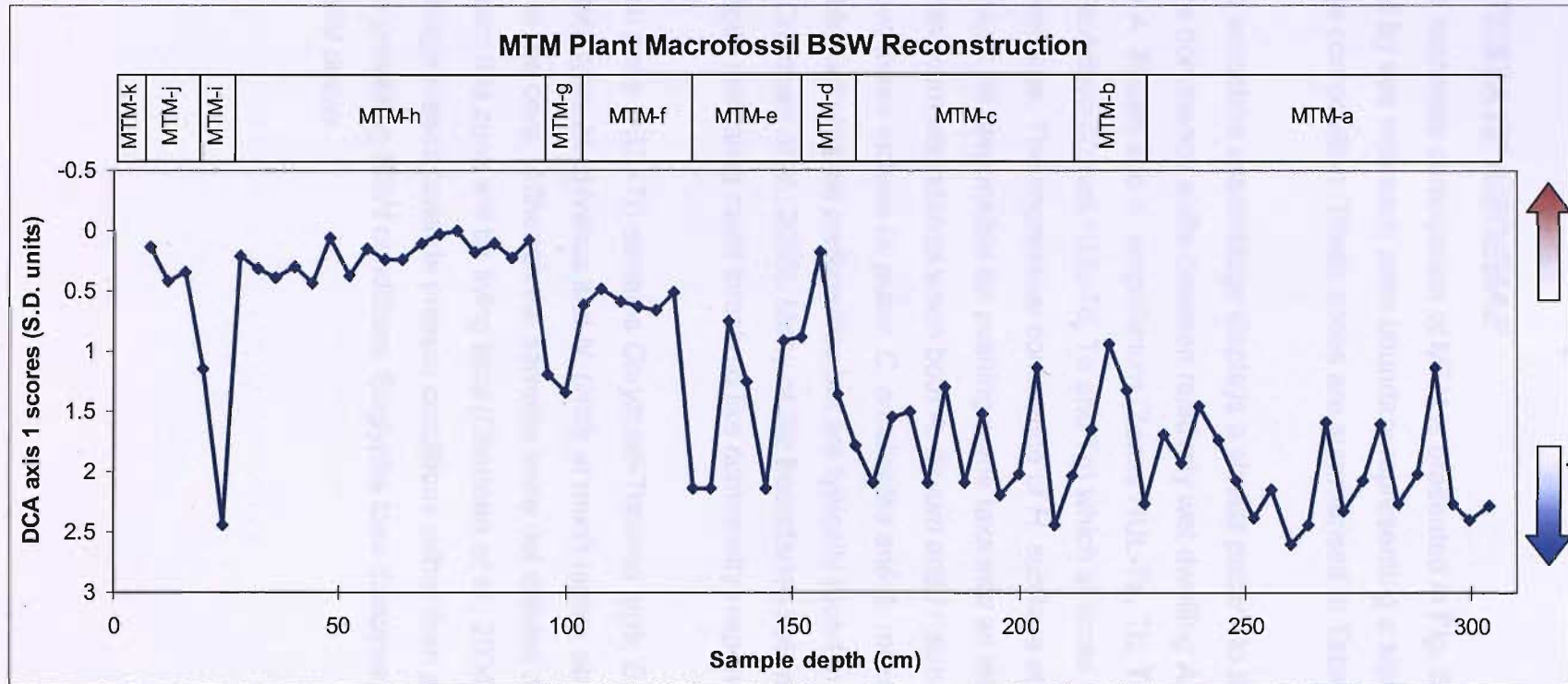


Figure 6.16: Plant Macrofossil BSW Reconstruction for Core MTM. Blue curve = BSW where peaks and troughs indicate the direction of change, but their amplitude is not necessarily proportional to the environmental change represented. Brown arrow indicates drier and the blue arrow wetter conditions. Bars above the curve = plant macrofossil zones derived from the plant macrofossil diagram and the codes are those used on the diagram (Fig. 6.14) and referred to in the text

6.4.2 TESTATE AMOEBAE

The testate amoebae composition of MTM is presented in Fig. 6.17; the diagram has been zoned by eye with each zone boundary representing a significant change in assemblage composition. These zones are summarised in Table 6.11 below.

The testate amoebae assemblage displays a similar pattern to that from Hulleter Moss where dominance shifts between relatively wet dwelling *Amphitrema* taxa particularly *A. flavum* and *A. wrightianum* (Zones HUL-Ta, Tb, Te and Tf) and the dry tolerant *H. subflava* (Zones HUL-Td, Te and Tg) which at times accounted for >80 % of the assemblage. The impressive dominance of *H. subflava* at the dry end of the spectrum might be responsible for pushing some taxa into an intermediate position reaching maximum abundance when both *A. flavum* and *H. subflava* abundance is relatively low; these include *D. pulex*, *C. arcelloides* and *A. muscorum*, all of which have variable hydrological preferences but are typically found in the drier half of the spectrum (Charman *et al.*, 2000). Many of the boundaries between zones display sharp changes indicating rapid threshold like community response.

The topmost zone (HUL-Ti) contains *Corythian-Trinema* type, *E. strigosa*, *E. rotunda*, *E. tuberculata* type, *H. sylvatica* and *N. tincta* at much higher abundances than elsewhere in the core. Although the samples were not stained many of the taxa identified from this zone will be living taxa (Charman *et al.*, 2004) and consequently the assemblage biased towards present conditions rather than accurately reflecting longer term prevailing BSW conditions. Euglypha taxa disappear from the record due to preferential decay.

Malham Tarn Moss (core MTM) Testate Amoebae Diagram

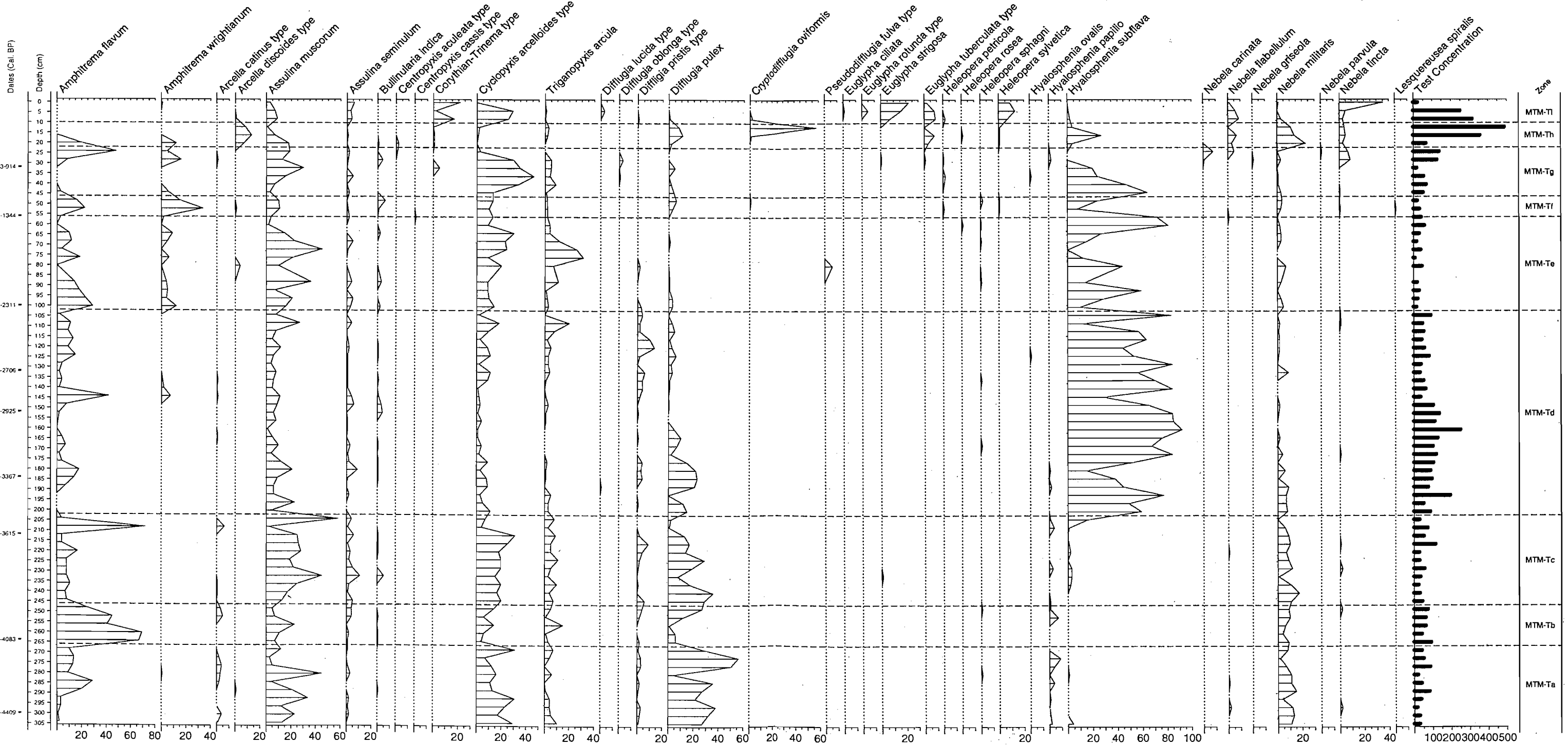


Table 6.11: Testate amoebae zone descriptions for core MTM

Depth (cm)	Zone	Description	Age (cal. BP)
0-10	MTM-Ti	This topmost zone is dominated by <i>C. arcelloides</i> . <i>Euglypha strigosa</i> , <i>E. tuberculata</i> <i>H. sylvatica</i> and <i>Corythian-Trinema</i> are also relatively abundant. <i>N. tincta</i> dominates the surface sample.	-53 to c. -10
10-22	MTM-Th	There is no clearly dominant taxon for this zone. <i>C. oviformis</i> is abundant in one sample at the top of the zone and <i>A. flavum</i> increases rapidly in abundance towards the bottom. The middle is characterised by <i>H. subflava</i> and <i>N. militaris</i> and <i>A. discoides</i> .	c. -10 to c. 320
22-46	MTM-Tg	Much of this zone is dominated by <i>C. arcelloides</i> but <i>H. subflava</i> is also abundant and increases in importance towards the bottom. <i>A. muscorum</i> and <i>T. arcula</i> are also important.	c. 320 to c. 1110
46-56	MTM-Tf	<i>A. wrightianum</i> and <i>A. flavum</i> dominate this zone. <i>H. subflava</i> is notably low in abundance. <i>A. muscorum</i> and <i>C. arcelloides</i> occur throughout.	c. 1110 to c. 1360
56-102	MTM-Te	This zone is quite varied. Dominance switches predominantly between <i>H. subflava</i> and <i>A. muscorum</i> . <i>C. arcelloides</i> is abundant throughout and <i>T. arcula</i> reaches it highest abundance in the middle of the zone. <i>A. flavum</i> and <i>A. wrightianum</i> occur in low to moderate abundance throughout.	c. 1360 to c. 1960
102-202	MTM-Td	<i>H. subflava</i> dominates the majority of the zone. <i>D. pulex</i> and <i>A. flavum</i> are abundant at times. <i>A. muscorum</i> and <i>C. arcelloides</i> are of moderate abundance throughout. <i>A. wrightianum</i> is notably absent or low.	c. 1960 to c. 2790
202-246	MTM-Tc	This zone is has no clearly dominant taxon. <i>A. Muscorum</i> , <i>C. arcelloides</i> and <i>D. pulex</i> are all abundant. <i>A. flavum</i> and <i>N. militaris</i> are of low to medium abundance throughout and the former rise to a brief dominance near the top of the zone. <i>A. wrightianum</i> and <i>H. subflava</i> are notably absent or low in abundance.	c. 2790 to c. 3130
246-266	MTM-Tb	<i>A. Flavum</i> dominates. <i>D. pulex</i> becomes important towards the top of the zone. <i>A. muscorum</i> , <i>C. arcelloides</i> and <i>N. militaris</i> occur throughout. <i>A. Wrightianum</i> and <i>H. subflava</i> are absent.	c. 3130 to c. 3350
266-304	MTM-Ta	<i>D. pulex</i> dominates. <i>C. arcelloides</i> , <i>A. muscorum</i> and <i>A. flavum</i> are also abundant although the latter declines towards the bottom of the zone. <i>N. militaris</i> and <i>T. arcula</i> are of low to medium abundance throughout	c. 3350 to c. 3640

Age estimates are based on interpolated data and rounded to the nearest 10 years. Negative numbers are years post 1950

The testate amoebae data were explored using DCA in order to investigate latent structure, rare taxa and surface samples were omitted from the analysis. The DCA biplot of Axis One and Two is displayed in Fig. 6.18. Axis One can be shown to

represents a water availability gradient with hygrophilous taxa such as *A. flavum* occurring at one end of the axis (high values) and taxa which thrive in drier conditions such as *H. subflava* occurring at the other end (low values). Rather surprisingly *D. pulex* and *N. militaris* plot on the wet end of the gradient, with *D. pulex* in particular plotting at a very similar point along the first axis to *A. flavum*; these taxa would usually be expected to be drier indicators although there are currently no good analogues for *D. pulex* (Charman *et al.*, 2000). Furthermore *A. wrightianum*, which is usually hygrophilous, plots as an intermediate taxon. These apparent hydrological affinities are probably partially an artefact of the short gradient (2.3 standard deviations) and the fact that taxon variation occurs predominantly over the dry half of the hydrological gradient. As a result medium to wet taxa cannot be separated by the DCA analysis because variability is small compared to that which occurs between medium and dry taxa.

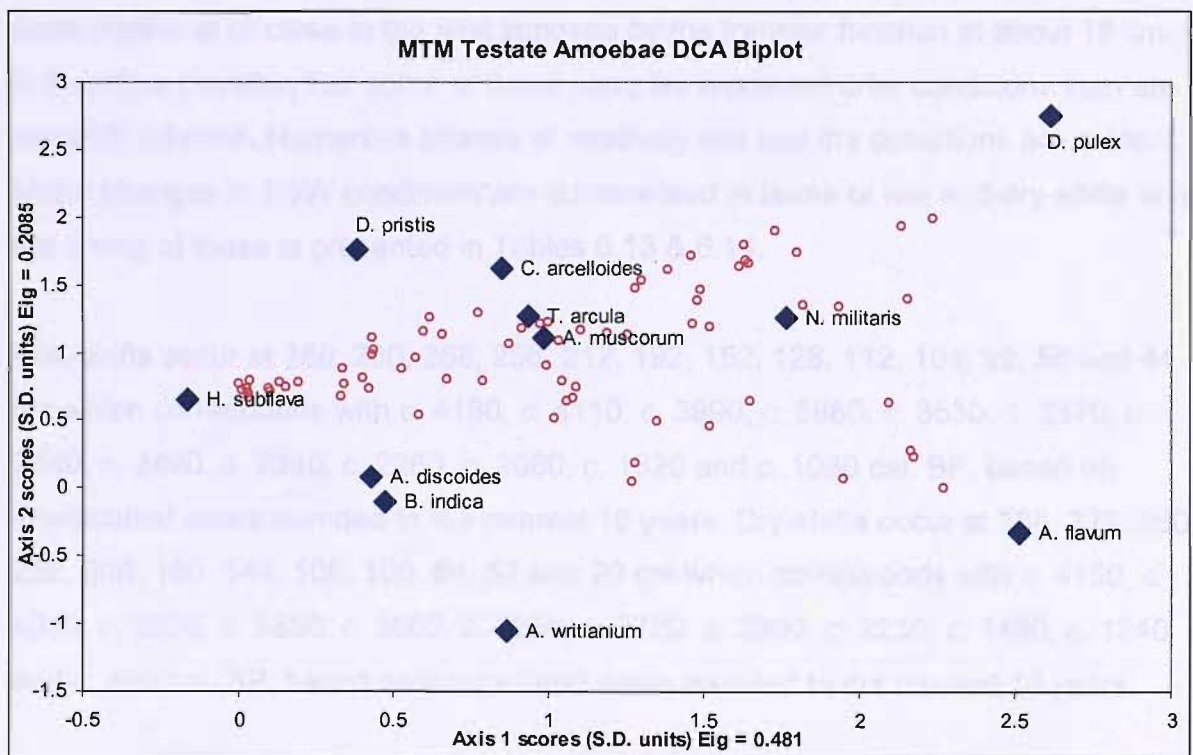


Figure 6.18: Biplot of DCA Axis One and Two scores for testate amoebae data from core MTM. Diamonds = taxa scores based on their distribution within the samples. Circles = sample scores based on their testate amoebae composition.

Axis One has an Eigenvalue of 0.507 (Table 6.12) indicating that just over 50% of the variability in taxon abundance can be attributed to water tables. This analysis augments the interpretation made from the raw testate amoebae diagram.

Axes	1	2	3	4
Eigenvalues	0.481	0.208	0.103	0.069
Gradient Length (SD Units)	2.273	1.990	1.879	1.522

Quantitative estimates of palaeo-water tables were calculated through the application of the Woodland *et al.*, (1998) transfer function and results are displayed in Fig. 6.19 along with the zones derived from Fig. 6.17. Encouragingly the quantitative palaeo-water table estimates show close agreement with the DCA Axis One sample scores (Fig. 6.19). There is little long term trend although the early part of the core (before 208cm / 3500 cal. BP) is generally wetter. Several samples have reconstructed water table depths at or close to the limit imposed by the transfer function at about 16 cm; it is therefore possible that some of these samples represent drier conditions than are currently inferred. Numerous phases of relatively wet and dry conditions are evident. Major changes in BSW conditions are summarised in terms of wet and dry-shifts and the timing of these is presented in Tables 6.13 & 6.14.

Wet-shifts occur at 286, 280, 268, 256, 212, 192, 152, 128, 112, 104, 92, 56 and 44 cm which corresponds with *c.* 4180, *c.* 4110, *c.* 3990, *c.* 3880, *c.* 3530, *c.* 3370, *c.* 2840, *c.* 2490, *c.* 2340, *c.* 2260, *c.* 2060, *c.* 1320 and *c.* 1080 cal. BP, based on interpolated dates rounded to the nearest 10 years. Dry-shifts occur at 284, 272, 260, 252, 208, 180, 144, 108, 100, 64, 52 and 20 cm which corresponds with *c.* 4150, *c.* 4030, *c.* 3920, *c.* 3850, *c.* 3500, *c.* 3250, *c.* 2720, *c.* 2300, *c.* 2230, *c.* 1480, *c.* 1240 and *c.* 490 cal. BP, based on interpolated dates rounded to the nearest 10 years.

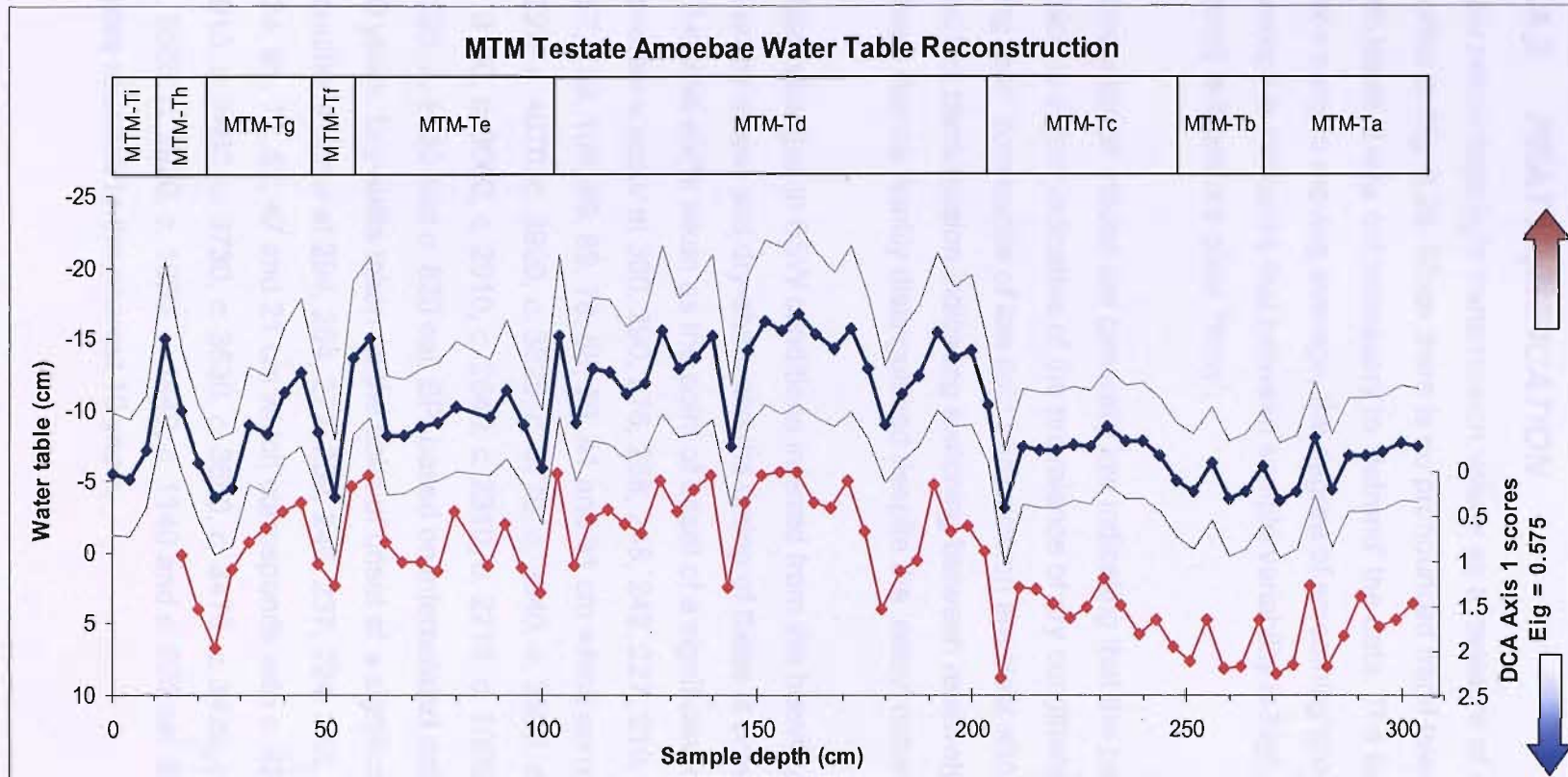


Figure 6.19: Testate amoebae water table reconstruction for core MTM. Blue curve = quantitative water table reconstruction. Brown arrow indicates drier and the blue arrow wetter conditions. Faint curves = sample specific root mean squared errors of prediction (RMSEP). Red curve = First Axis DCA sample scores. Bars above the graph are testate amoebae zones derived from the testate amoebae diagram and the codes are those used on the diagram and referred to in the text.

6.4.3 PEAT HUMIFICATION

Raw percentage light transmission values as a measure of peat humification are plotted in Fig. 6.20. Since there is no pronounced trend towards greater humification with depth it was not necessary to 'detrend' the data. The bold red line represents a three sample moving average, the degree of smoothing produced by the moving average is indicative that between sample variability is high and the humification record is therefore quite 'noisy'.

Transmission values are generally low indicating that the peat is quite highly humified which is in turn indicative of the prevalence of dry conditions. Superimposed on this long term dominance of low light transmission are clear shorter term phases of high and low transmission indicating switching between relatively wet and dry conditions. These can be readily distinguished despite the 'noisy' nature of the record.

Major changes in BSW conditions inferred from the humification data are summarised in terms of wet and dry-shifts and the timing of these is presented in Tables 6.13 & 6.14. Wet-shifts taken as the point of onset of a significant change to wetter conditions occur at 300, 290, 276, 268, 248, 242, 227, 219, 210, 201, 186, 172, 167, 157, 139, 109, 99, 89, 78, 68, 56, 41 and 31 cm which corresponds with *c.* 4320, *c.* 4220, *c.* 4070, *c.* 3990, *c.* 3820, *c.* 3770, *c.* 3640, *c.* 3590, *c.* 3510, *c.* 3440, *c.* 3320, *c.* 3130, *c.* 3060, *c.* 2910, *c.* 2640, *c.* 2310, *c.* 2210, *c.* 2000, *c.* 1770, *c.* 1560, *c.* 1320, *c.* 1030 and *c.* 820 cal. BP, based on interpolated dates rounded to the nearest 10 years. Dry-shifts taken as the point of onset of a significant change to drier conditions occur at 294, 284, 272, 259, 245, 237, 224, 215, 205, 198, 175, 164, 145, 134, 85, 72, 62, 47 and 21 cm which corresponds with *c.* 4260, *c.* 4150, *c.* 4030, *c.* 3910, *c.* 3800, *c.* 3730, *c.* 3630, *c.* 3550, *c.* 3470, *c.* 3420, *c.* 3170, *c.* 3020, *c.* 2730, *c.* 2560, *c.* 1920, *c.* 1650, *c.* 1440, *c.* 1140 and *c.* 920 cal. BP, based on interpolated dates rounded to the nearest 10 years.

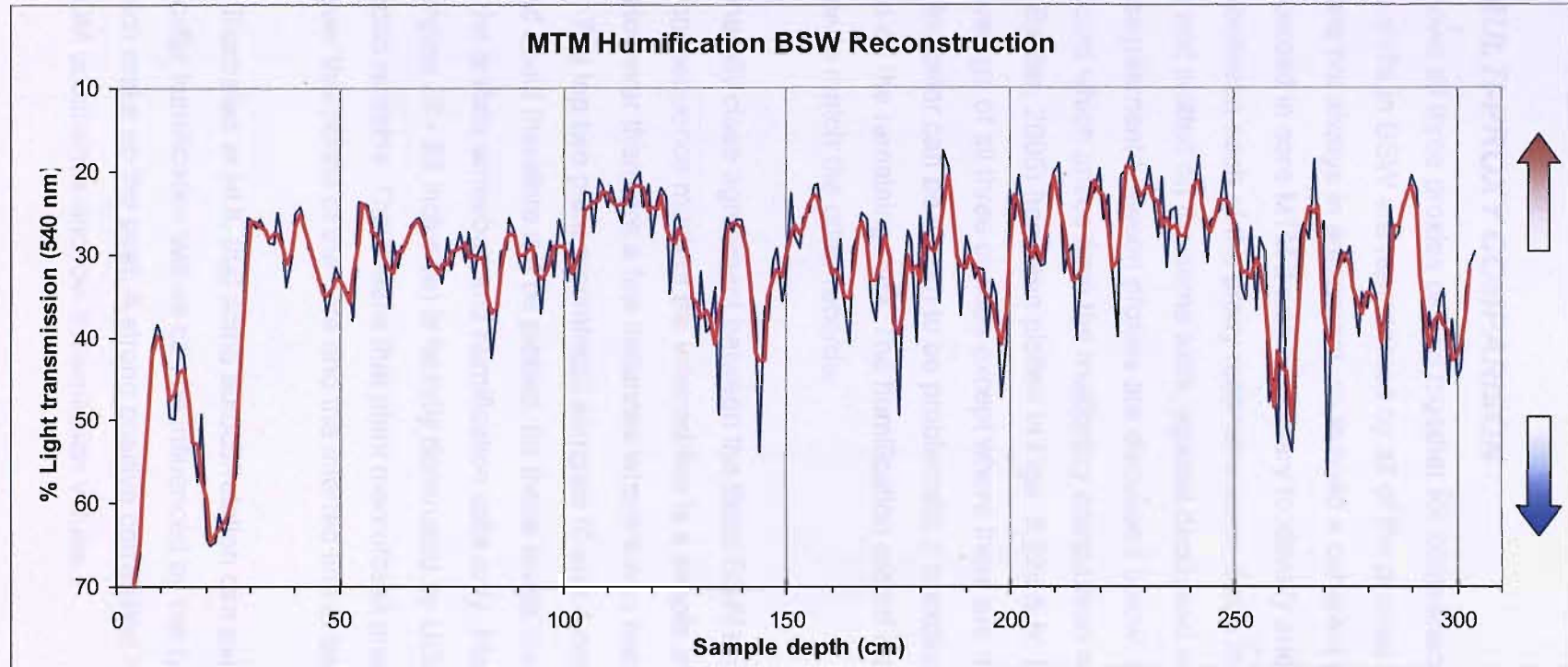


Figure 6.20: Peat humification record for core MTM. There is no pronounced trend towards greater humification with depth so it has not been necessary to 'detrrend' the data. Blue curve = raw data. Red curve = three point moving average

6.4.4 MULTI-PROXY COMPARISON

Fig. 6.21 shows all three proxies plotted together for comparison and it is clear that many of the shifts in BSW are represented by all of the proxies. However the proxy inferences are not always in agreement, so to build a coherent picture of BSW changes recorded in core MTM it was necessary to identify and critically assess the differences between each of the proxy reconstructions. Each record has been normalising and plotted on the same axes, against depth and age (Fig. 6.22a & b). Points of disagreement between proxies are discussed below. In order to summarise the BSW record which arises from the multiproxy comparison an inferred line (Blundell & Barber, 2005) has been plotted in Figs. 6.22a & b. The inferred line is simply an average of all three proxies except where there are discrepancies. In this case if one indicator can be shown to be problematic it is excluded and the inferred line is based on the remaining data. The humification record has been reduced to 4 cm resolution to match the other records.

There is generally close agreement between the three BSW reconstructions from MTM; as a consequence much of the inferred line is a simple average of all three indicators. However there are a few instances where it was necessary to make some adjustment. The top two plant macrofossil samples (0 and 4 cm) were omitted from the DCA and could therefore not be plotted, for these levels the inferred line is an average of the testate amoebae and humification data only. Plant macrofossil zone MTM-h (samples 28 - 92 inclusive) is heavily dominated by UOM and undifferentiated monocotyledon remains. This means that plant macrofossil analysis is an insensitive technique over this period of the core and the inferred line is based on the other data.

It has been illustrated at HUL that some autocorrelation can exist between proxies and in particular humification values can be influenced by the type of vegetative remains which make up the peat. A strong positive correlation might be expected between UOM occurrence and low transmission values.

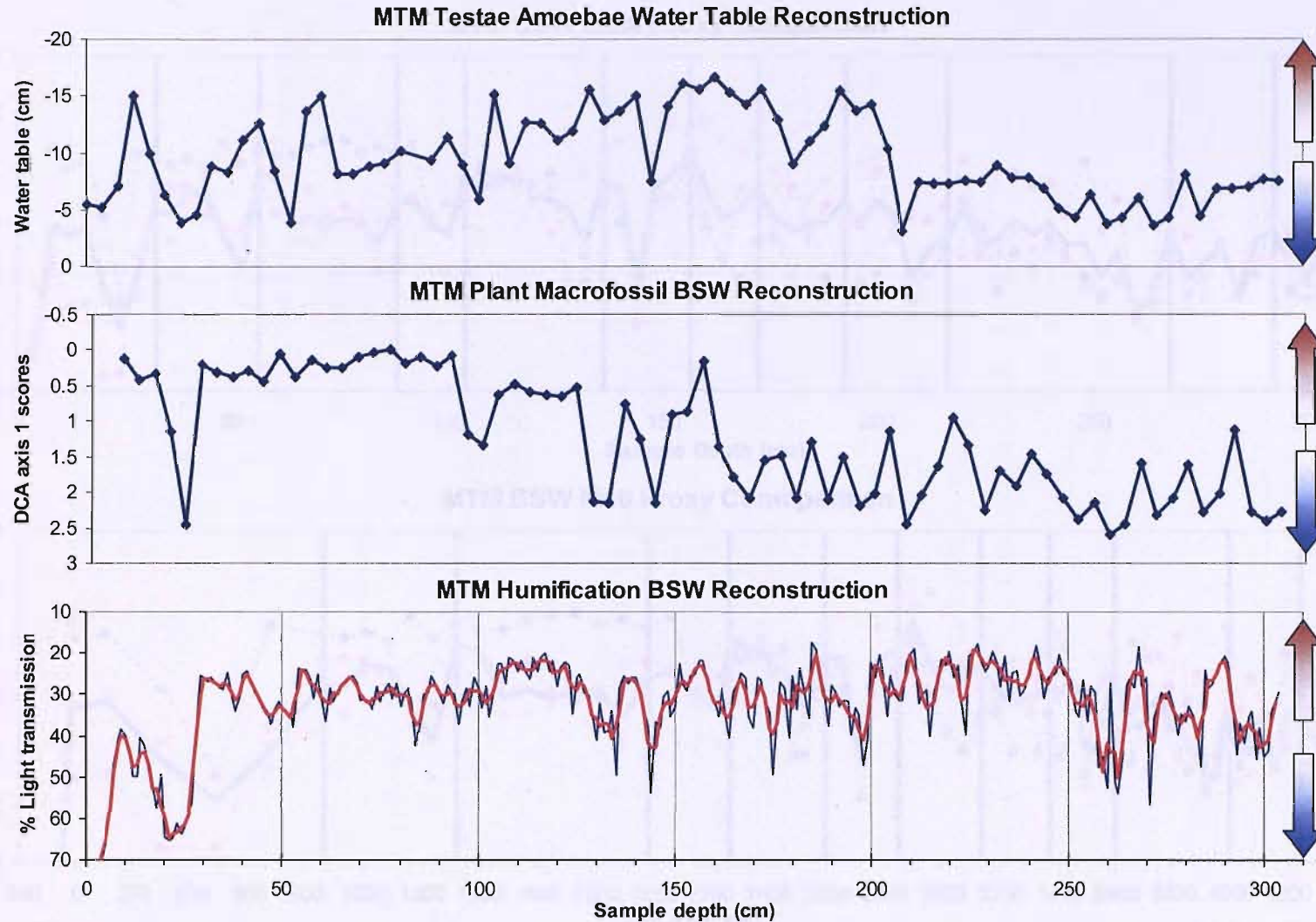
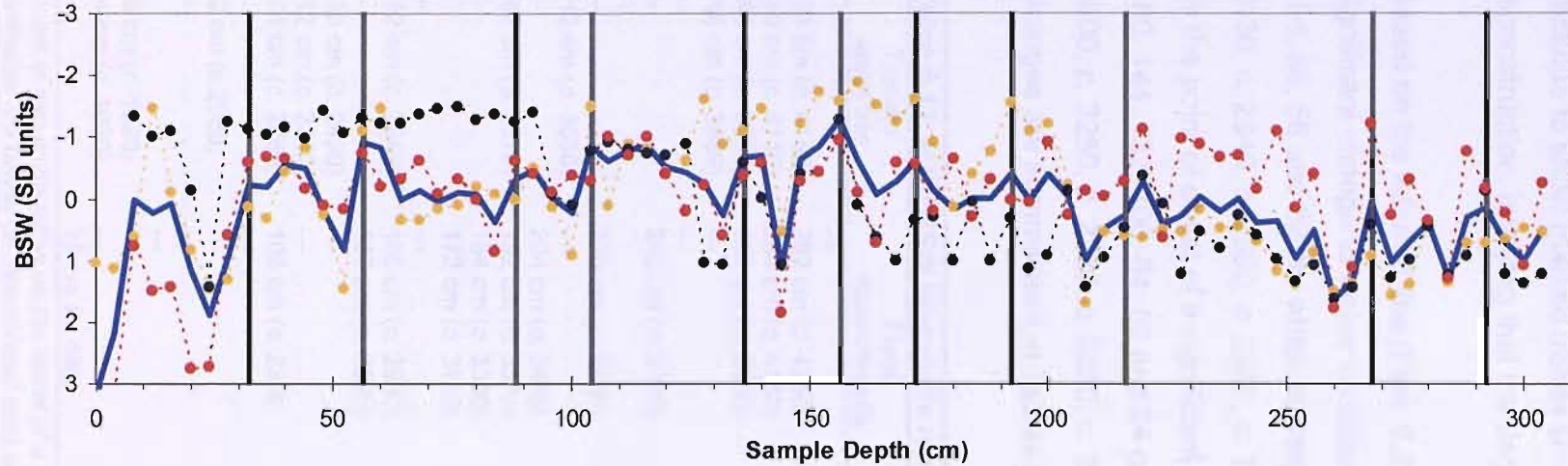


Figure 6.21: Malham Tarn Moss BSW multiproxy comparison against depth (cm). From the top downwards testate amoebae water table reconstruction, plant macrofossil BSW index and degree of peat humification (red curve = 3 point moving average)

6.22a

MTM BSW Multi Proxy Comparison



6.22b

MTM BSW Multi Proxy Comparison

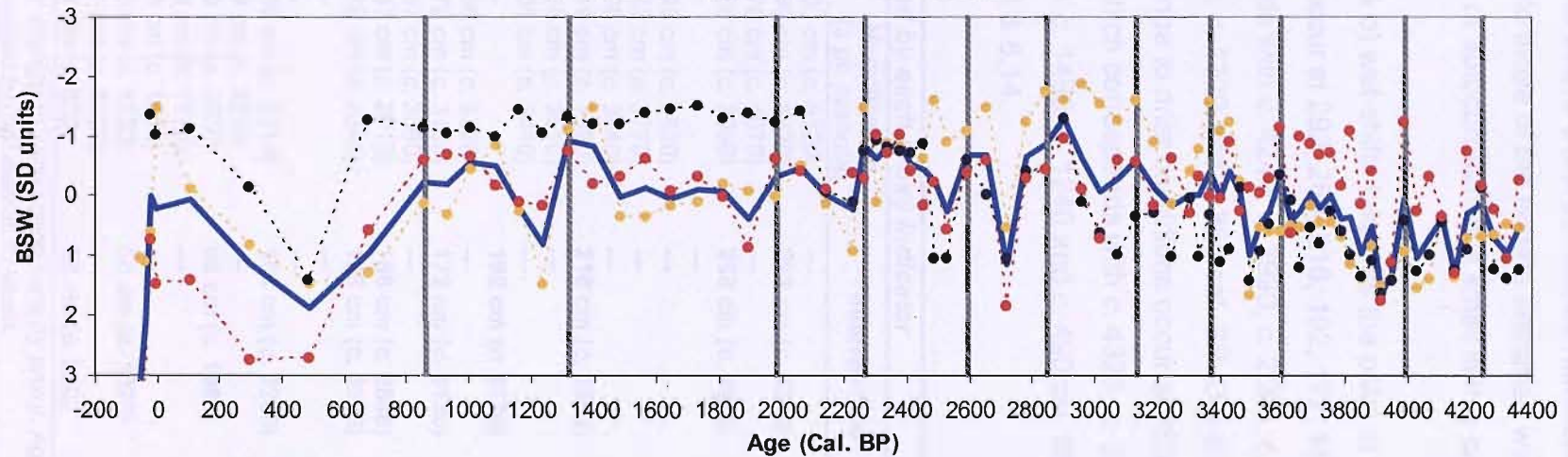


Figure 6.22: MTM Multiproxy comparison and inferred BSW conditions against depth (a) and age (b). Values are normalised for ease of comparison. Black = plant macrofossils, yellow = testate amoebae and red = humification. Bold blue = Inferred BSW conditions based on interpretation of all the data.

It is therefore interesting that in core MTM where UOM dominates humification values continue to show marked trends similar to those of the testate amoebae water table reconstruction, implying that the degree of autocorrelation is small in this case.

Based on the inferred line (Figs. 6.22a & b) wet-shifts taken as the point of onset of a significant change to wetter conditions occur at 292, 268, 216, 192, 172, 156, 136, 104, 88, 56 and 32 cm which corresponds with *c.* 4240, *c.* 3990, *c.* 2590, *c.* 3370, *c.* 3130, *c.* 2840, *c.* 2590, *c.* 2260, *c.* 1980, *c.* 1320 and *c.* 850 cal. BP. Dry-shifts taken as the point of onset of a significant change to drier conditions occur at 300, 260, 208, 180, 144, 132, 100, 64, 52 and 24 cm which corresponds with *c.* 4320, *c.* 3920, *c.* 3500, *c.* 3250, *c.* 2720, *c.* 2530, *c.* 2230, *c.* 1480, *c.* 1240 and *c.* 490 cal. BP. These changes are summarised in Tables 6.13 & 6.14.

Table 6.13: MTM BSW Wet-shifts recorded by each proxy indicator

Testate amoebae	Plant macrofossils	Humification (3 pt. smooth)	Inferred Line
---	---	300 cm (<i>c.</i> 4320)	---
286 cm (<i>c.</i> 4180)	292 cm (<i>c.</i> 4240)	290 cm (<i>c.</i> 4220)	292 cm (<i>c.</i> 4240)
280 cm (<i>c.</i> 4110)	280 cm (<i>c.</i> 4110)	276 cm (<i>c.</i> 4070)	---
268 cm (<i>c.</i> 3990)	268 cm (<i>c.</i> 3990)	268 cm (<i>c.</i> 3990)	268 cm (<i>c.</i> 3990)
256 cm (<i>c.</i> 3880)	---	---	---
---	---	248 cm (<i>c.</i> 3820)	---
---	240 cm (<i>c.</i> 3760)	242 cm (<i>c.</i> 3770)	---
---	---	226 cm (<i>c.</i> 3640)	---
---	220 cm (<i>c.</i> 3590)	219 cm (<i>c.</i> 3590)	216 cm (<i>c.</i> 3590)
212 cm (<i>c.</i> 3530)	---	210 cm (<i>c.</i> 3510)	---
---	204 cm (<i>c.</i> 3460)	201 cm (<i>c.</i> 3440)	---
192 cm (<i>c.</i> 3370)	192 cm (<i>c.</i> 3370)	---	192 cm (<i>c.</i> 3370)
---	184 cm (<i>c.</i> 3300)	186 cm (<i>c.</i> 3320)	---
---	172 cm (<i>c.</i> 3130)	172 cm (<i>c.</i> 3130)	172 cm (<i>c.</i> 3130)
---	---	167 cm (<i>c.</i> 3060)	---
152 cm (<i>c.</i> 2840)	156 cm (<i>c.</i> 2900)	157 cm (<i>c.</i> 2910)	156 cm (<i>c.</i> 2840)
---	136 cm (<i>c.</i> 2590)	139 cm (<i>c.</i> 2640)	136 cm (<i>c.</i> 2590)
128 cm (<i>c.</i> 2490)	---	---	---
112 cm (<i>c.</i> 2340)	---	---	---
104 cm (<i>c.</i> 2260)	108 cm (<i>c.</i> 2300)	109 cm (<i>c.</i> 2310)	104 cm (<i>c.</i> 2260)
---	---	99 cm (<i>c.</i> 2210)	---
92 cm (<i>c.</i> 2060)	---	89 cm (<i>c.</i> 2000)	88 cm (<i>c.</i> 1980)
---	---	78 cm (<i>c.</i> 1770)	---
---	---	68 cm (<i>c.</i> 1560)	---
56 cm (<i>c.</i> 1320)	---	56 cm (<i>c.</i> 1320)	56 cm (<i>c.</i> 1320)
44 cm (<i>c.</i> 1080)	---	41 cm (<i>c.</i> 1030)	---
---	28 cm (<i>c.</i> 680)	31 cm (<i>c.</i> 820)	32 cm (<i>c.</i> 850)

Onset of wet-shifts taken as the onset of a major change to wetter conditions by proxy. Age estimates are based on interpolated data and rounded to the nearest 10 years.

Table 6.14: MTM BSW Dry-shifts recorded by each proxy indicator

Testate amoebae	Plant macrofossils	Humification (3 pt. smooth)	Inferred Line
---	300 cm (c. 4320)	---	300 cm (c. 4320 BP)
---	---	294 cm (c. 4260)	
284 cm (c. 4150)	284 cm (c. 4150)	284 cm (c. 4150)	
272 cm (c. 4030)	272 cm (c. 4030)	272 cm (c. 4030)	
260 cm (c. 3920)	---	259 cm (c. 3910)	260 cm (c. 3920 BP)
252 cm (c. 3850)	252 cm (c. 3850)	---	
---	---	245 cm (c. 3800)	
---	---	237 cm (c. 3730)	
---	228 cm (c. 3660)	224 cm (c. 3630)	
---	---	215 cm (c. 3550)	
208 cm (c. 3500)	208 cm (c. 3500)	205 cm (c. 3470)	208 cm (c. 3500 BP)
---	196 cm (c. 3400)	198 cm (c. 3420)	
---	188 cm (c. 3340)	---	
180 cm (c. 3250)	180 cm (c. 3250)	---	180 cm (c. 3250 BP)
---	---	175 cm (c. 3170)	
---	168 cm (c. 3070)	164 cm (c. 3020)	
144 cm (c. 2720)	144 cm (c. 2720)	145 cm (c. 2730)	144 cm (c. 2720 BP)
---	---	134 cm (c. 2560)	132 cm (c. 2530 BP)
---	128 cm (c. 2490)	---	
108 cm (c. 2300)	---	---	
100 cm (c. 2230)	100 cm (c. 2230)	---	100 cm (c. 2230 BP)
---	---	---	
---	---	85 cm (c. 1920)	
---	---	72 cm (c. 1650)	
64 cm (c. 1480)	---	62 cm (c. 1440)	64 cm (c. 1480 BP)
52 cm (c. 1240)	---	---	52 cm (c. 1240 BP)
---	---	47 cm (c. 1140)	
24 cm (c. 490)	24 cm (c. 490)	21 cm (c. 340)	24 cm (c. 490 BP)

Onset of dry-shifts taken as the onset of a major change to drier conditions by proxy. Age estimates are based on interpolated data and rounded to the nearest 10 years.

6.5 MALHAM TARN

6.5.1 LOSS ON IGNITION

LOI was undertaken at 4 cm resolution throughout the lake cores and used to correlate core sections (Section 3.3.2). Moisture, organic and carbonate content of the sediments were also estimated through LOI analysis and results are displayed in Fig. 6.23. Percentage moisture and LOI₅₅₀ are highly correlated. As with Bigland Tarn the moisture content from the top core was generally lower than the bottom and this is thought to be an artefact of the freezing process which only the top cores were subjected to.

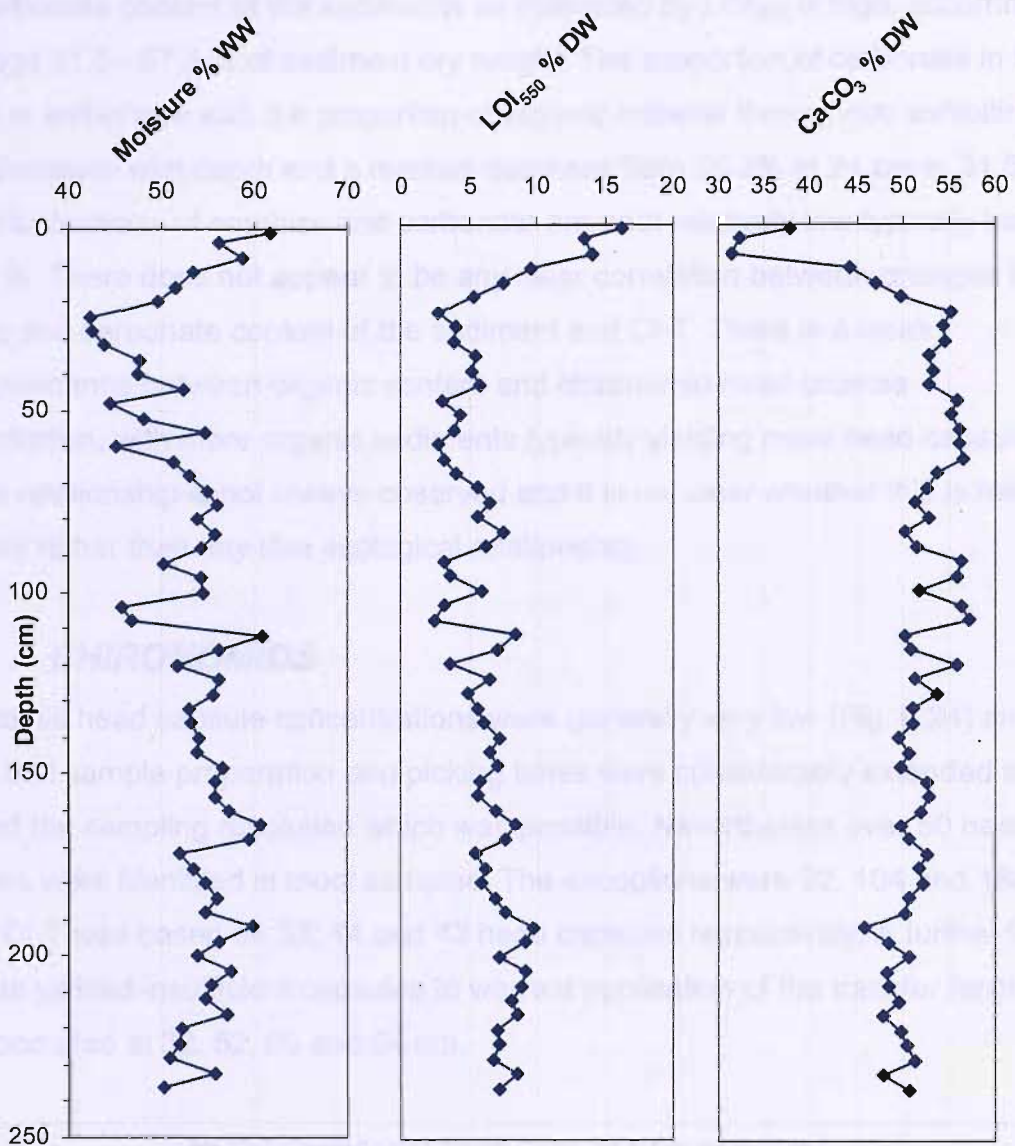


Figure 6.23: Moisture and Loss on Ignition (LOI) data for Bigland Tarn. From the left curves represent moisture content as a percentage of wet weight (WW), organic content as a proportion of dry weight (DW) and carbonate content as a proportion of dry weight

Organic matter estimated by LOI₅₅₀ accounts for between 2.8 and 16.2 % of sediment dry weight. There is a slight increase in organic matter down core but levels are generally below 10 % of dry weight. The most notable change in organic matter occurs from 24 cm upwards where there is a rapid increase in the proportion of organic matter from below 5 % at 24 cm to 16.2 % 2 cm below the sediment water interface.

The carbonate content of the sediments as estimated by LOI_{950} is high, occurring in the range 31.5 - 57.3 % of sediment dry weight. The proportion of carbonate in the core is in anti-phase with the proportion of organic material throughout, exhibiting a slight decrease with depth and a marked decrease from 55.3% at 24 cm to 31.5 % at 8 cm. Fluctuations of organics and carbonate are both relatively low typically less than 5 %. There does not appear to be any clear correlation between changes in organic and carbonate content of the sediment and CI-T. There is a weak correspondence between organic content and chironomid head capsule concentration, with more organic sediments typically yielding more head capsules, but this relationship is not always observed and it is not clear whether this is related to recovery rather than any true ecological relationship.

6.5.2 CHIRONOMIDS

Chironomid head capsule concentrations were generally very low (Fig. 6.24) and this meant that sample preparation and picking times were considerably extended and reduced the sampling resolution which was possible. Nevertheless over 50 head capsules were identified in most samples. The exceptions were 92, 104 and 188 cm where CI-T was based on 33, 44 and 43 head capsules respectively. A further four samples yielded insufficient capsules to warrant application of the transfer function these occurred at 32, 52, 60 and 64 cm.

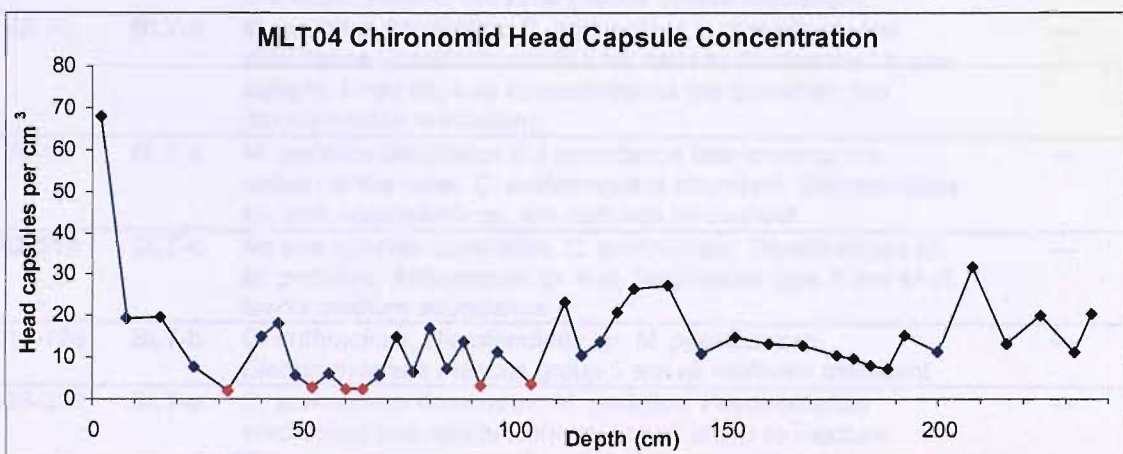


Figure 6.24: Malham Tarn chironomid head capsule concentration. Red diamonds = samples which yielded <50 head capsules. Surface sample concentrations are artificially high due to dewatering of the top of the core as a result of freezing.

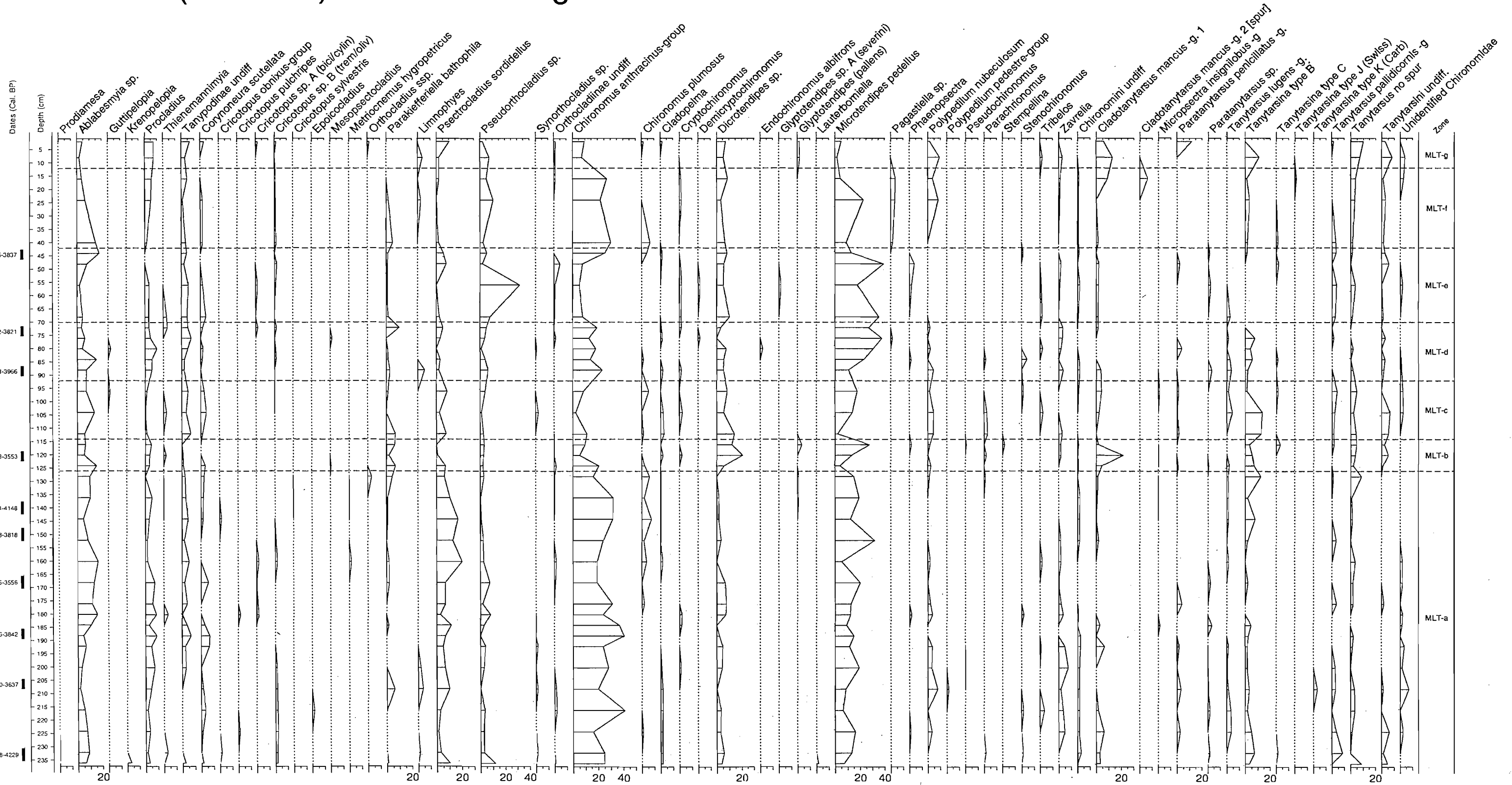
The chironomid biostratigraphy of MLT is displayed in Fig. 6.25. The diagram has been zoned by eye with each zone boundary representing a significant change in assemblage composition. Six zones were identified and these are summarised in Table 6.15. A total of 58 taxa were identified but the majority occur in low abundance. Taxa from the tribe *Chironomini*, particularly *C. anthracinus* and *M. pedellus* dominate much of the core and changes in community structure chiefly involving changes in the relative abundance of the *Chironomini* tribe. The tribes *Tanytarsini*, *Tanypodinae* and *Orthoclaadiinae* are also present but tend to make a relatively small contribution to the assemblage, with the exceptions of *Ablabesmia* sp., *P. sordidellus* and *T. type B* which are common throughout much of the core. Unlike Bigland Tarn the near surface chironomid assemblage at Malham does not appear to have been affected by human activity within the catchment. This may be because carbonate lakes can show a degree of buffering against even quite severe external forcing (Brooks *et al.*, 2005).

Table 6.15: Chironomid zone descriptions for core MLT

Depth (cm)	Zone	Description	Age (cal. BP)
2-16	BLT-g	This topmost zone is characterised by falling <i>C. anthracinus</i> and <i>Microtendipes</i> abundances and an increase in <i>Cladotanytarsus mancus</i> group 1 towards the top.	---
16-42	BLT-f	This zone is dominated by <i>C. anthracinus</i> and <i>M. pedellus</i> . <i>Ablabesmia</i> sp. increases in abundance towards the bottom. Head capsule concentrations are extremely low in the middle and upper parts of the zone (hence coarse resolution).	---
42-70	BLT-e	<i>M. pedellus</i> dominates; <i>C. anthracinus</i> is of relatively low abundance <i>Pseudorthocladus</i> sp. rises to dominance for one sample. Head capsule concentrations are extremely low (hence coarse resolution).	---
70-92	BLT-d	<i>M. pedellus</i> dominates but abundance falls towards the bottom of the zone. <i>C. anthracinus</i> is abundant. <i>Dicrotendipes</i> sp. and <i>Ablabesmia</i> sp. are common throughout.	---
92-114	BLT-c	No one species dominates, <i>C. anthracinus</i> , <i>Dicrotendipes</i> sp. <i>M. pedellus</i> , <i>Ablabesmia</i> sp. and <i>Tanytarsina type B</i> are all of low to medium abundance	---
114-126	BLT-b	<i>C. anthracinus</i> , <i>Dicrotendipes</i> sp. <i>M. pedellus</i> and <i>Cladotanytarsus mancus</i> group 1 are all relatively abundant	---
126-236	BLT-a	<i>C. anthracinus</i> dominates. <i>M. pedellus</i> , <i>Psectrocladius sordidellus</i> and <i>Ablabesmia</i> sp. are all of low to medium abundance throughout. <i>Dicrotendipes</i> sp. is of notably low abundance.	---

No age estimates are possible due to problems with radiocarbon dating

Malham Tarn (core MLT) Chironomid Diagram



While changes in community are evident the degree of variability appears low. DCA confirms the high degree of similarity between samples (Fig. 6.28) with most species plotting in relatively central positions and no clear separation of taxon with different temperature optima along any of the gradients.

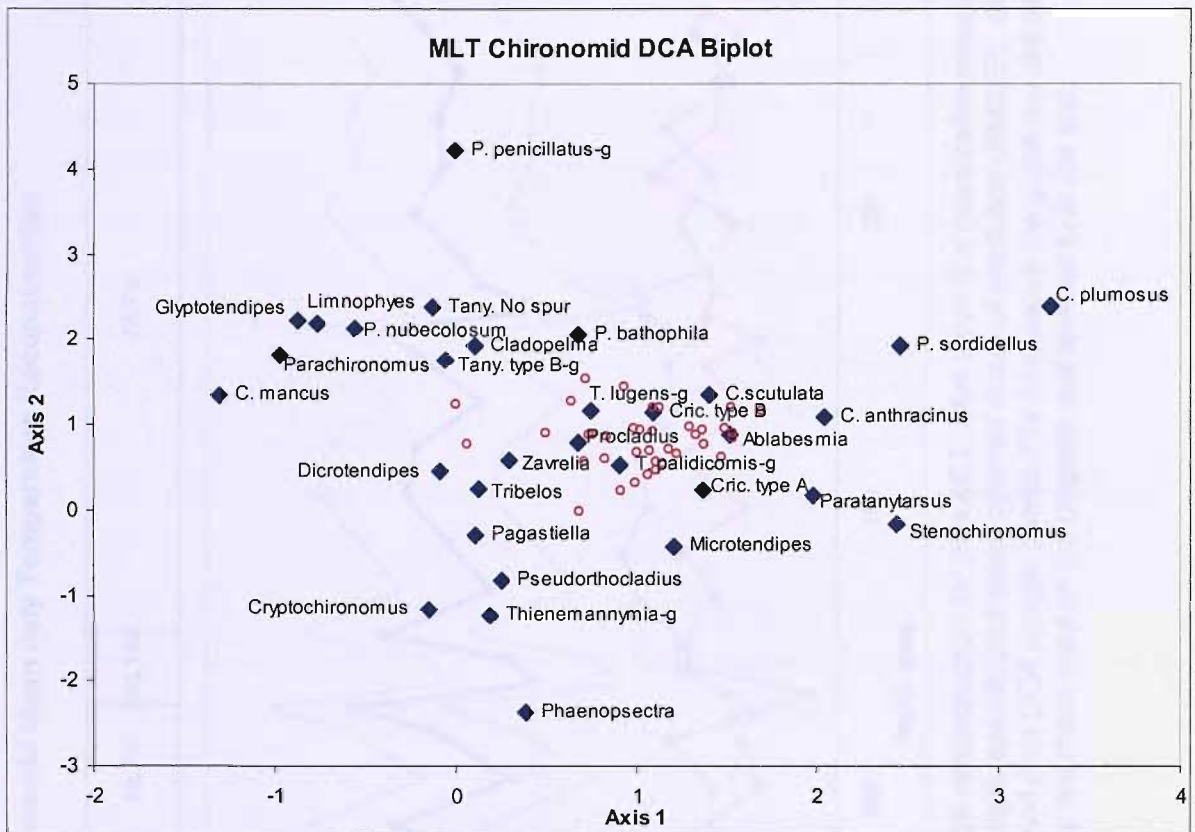


Figure 6.26: Biplot of DCA Axis One and Two scores for chironomid data from core MLT. Diamonds = taxa scores based on their distribution within the samples. Circles = sample scores based on their faunal composition

Quantitative estimates of mean July palaeotemperature were calculated through the application of the Norwegian training set (Brooks & Birks, 2000) and the results are displayed in Fig. 6.27 along with the zones derived from Fig. 6.25. CI-T for the top sample (2 cm) 13 °C is a close match to the 1979-2000 average mean July temperature of 13.4 °C recorded on site at the Malham Field Studies Centre (METOffice, 2005a) and well within the errors of prediction. The accuracy of this reconstruction supports the applicability of the Norwegian training set to this data.

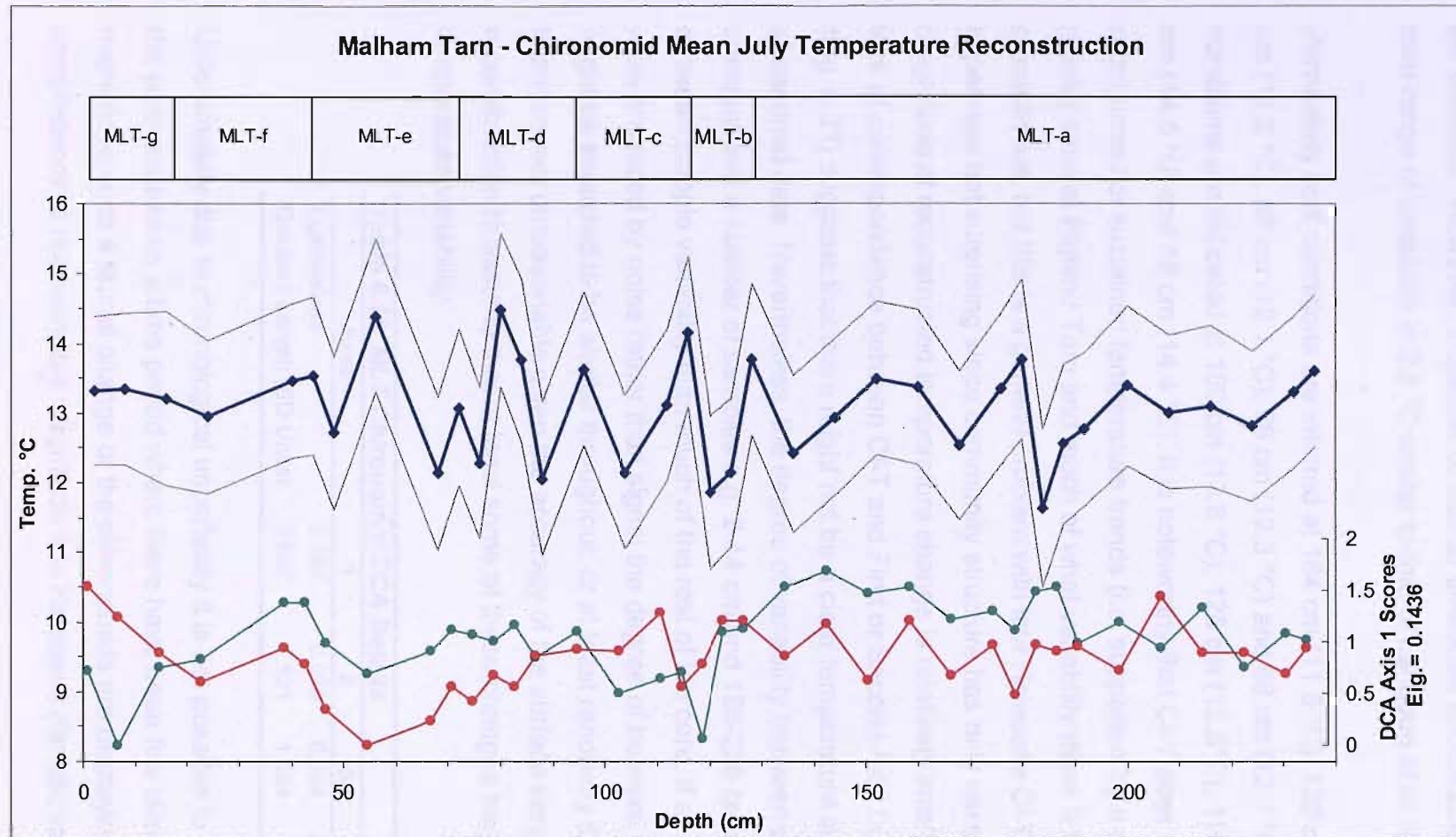


Figure 6.27: Chironomid inferred palaeotemperature reconstruction for core MLT. Blue curve is a quantitative measure of mean July palaeotemperature. Faint curves represent sample specific root mean squared errors of prediction (RMSEP). Green curve = First Axis DCA sample scores. = Red curve = Second Axis DCA sample scores. The bars above the graph are chironomid zones derived from the chironomid diagram and the codes are those used on the diagram and referred to in the text.

The CI-T reconstruction for MLT is quite stable with no clear long term trends in temperature. However, a number of shorter timescale fluctuations are evident. The total range of variability is 2.8 °C similar to that of Langdon *et al.*, (2004).

Particularly cool conditions are inferred at 184 cm (11.6 °C), 120 cm (11.9 °C), 104 cm (12.2 °C), 88 cm (12.1 °C), 76 cm (12.3 °C) and 68 cm (12.1 °C). Whilst warm conditions are indicated at 180 cm (13.8 °C), 128 cm (13.8°C), 116 cm (14.2°C), 80 cm (14.5 °C) and 56 cm (14.4 °C). It is noteworthy that CI-T does not display the pronounced or sustained temperature trends (i.e. supported by a number of data points) seen at Bigland Tarn and much of what variability there is lies within the errors of prediction, but this is a general problem with late Holocene CI-T reconstructions. It is perhaps not surprising since community structure has only varied slightly that the magnitude of reconstructed temperature change is relatively small. Furthermore the lack of correspondence between CI-T and First or Second Axis DCA sample scores (Fig. 6.27) suggests that there might not be a clear temperature signal within the chironomid data. Nevertheless, the degree of variability between samples is not constant and a number of samples e.g. 2-44 cm and 188-236 cm exhibit much lower between sample variability than much of the rest of the core. If all of the CI-T trends were produced by noise rather than signal the degree of between sample variability might be expected to be similar throughout, or at least randomly distributed. It is therefore not unreasonable given the accuracy of the surface temperature reconstruction to assume that at least some of these changes may reflect genuine temperature variability.

Table 6.16: MLT Chironomid DCA Details

Axes	1	2	3	4
Eigenvalues	0.144	0.098	0.054	0.036
Gradient Length (SD Units)	1.692	1.531	1.024	1.015

Unfortunately due to chronological uncertainty it is not possible to determine whether the core represents a time period where there have been few climatic shifts which might drive such a faunal change or the chironomids are displaying a degree of complacency to relatively low magnitude late Holocene climatic variability. In practice

however it is extremely unlikely that the 240 cm of sediment do not span the Little Ice Age and Medieval Warm Period or indeed the 1400 BP or 2600 BP cool events so it is more likely that the chironomid assemblage is displaying some complacency to these relatively low magnitude variations.

7.0 DISCUSSION

7.1 INTRODUCTION

In this chapter the bog surface wetness (BSW) and chironomid inferred temperature (CI-T) results are discussed and their climatic significance explored. Inter-site comparisons are made to provide a means of cross-validating the records as an aid to climatic interpretation and the relationship between CI-T and BSW is then examined in relation to the central project aim. All dates of climatic shifts used for inter-site comparison are rounded to the nearest 50 years.

7.2 BSW INTER-SITE COMPARISONS

The first stage of climatic inference from the bog records can be interpreted with some confidence. Three tried and tested independent palaeoecological techniques were applied to each core and the three records amalgamated into a single inferred line representing changes in BSW conditions at each site (*sensu*. Blundell & Barber, 2005). The similarities between all three proxies and the ability to identify and in most cases explain differences increases the confidence with which these records can be considered to accurately reflect long term changes in BSW at each site. In order to begin to relate BSW conditions to climate it is beneficial to compare between sites so that points of correspondence which might relate to regional climatic change can be picked out. Comparison will therefore be made between the two sites used in this investigation and then with the wider literature.

Fig. 7.1 shows the inferred BSW conditions from both peatland sites (HUL & MTM) normalised for ease of comparison. The weighted average of the radiocarbon distributions along with the 2σ confidence intervals have been plotted as a visual indication of chronological uncertainty for each series. The onset of major wet shifts are marked by blue bars and numbered to aid discussion. Shifts that occur in both cores and which could be contemporary are given the same number. There is some clear correspondence between the two records but also some differences.

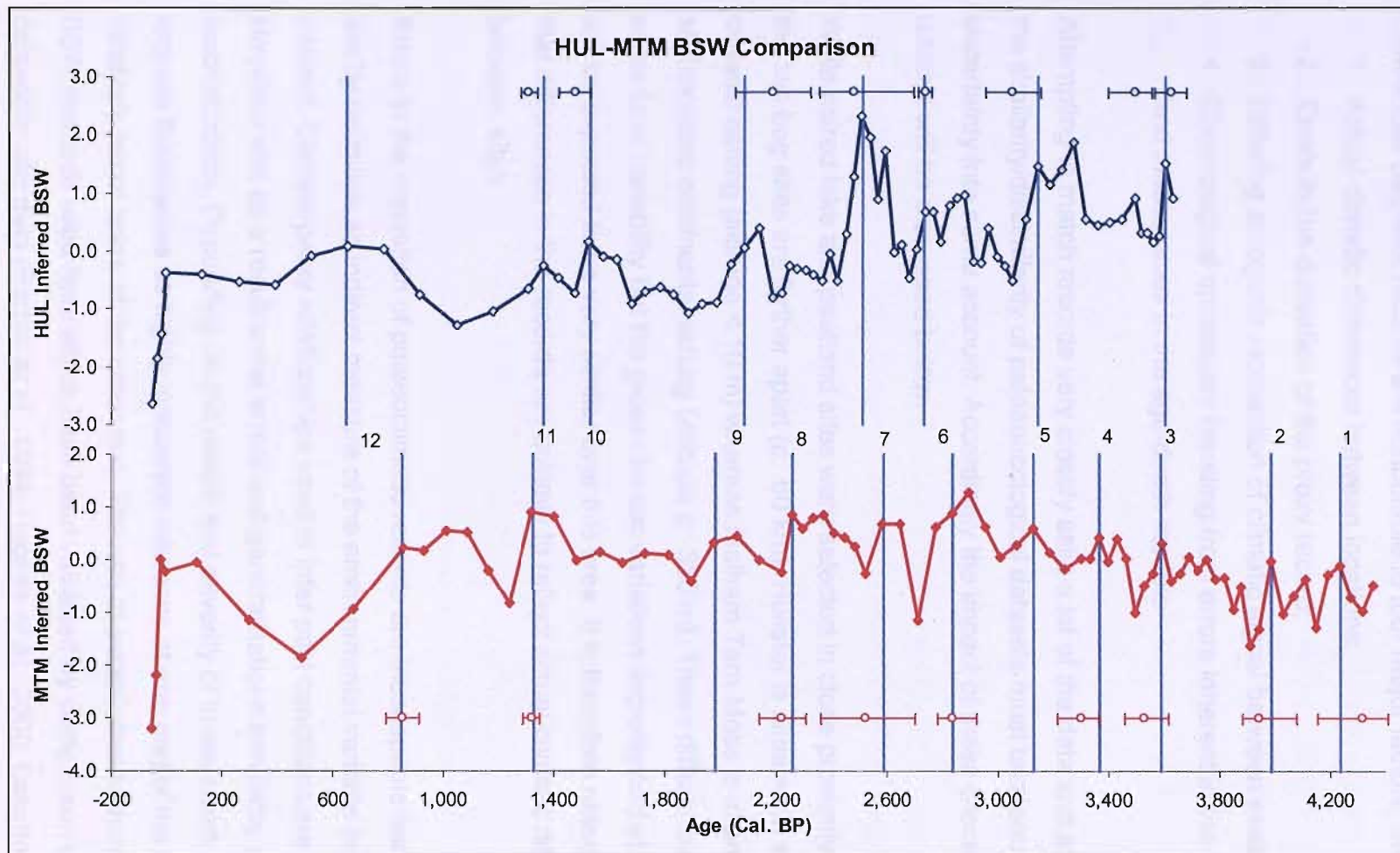


Figure 7.1: Comparison of BSW reconstructions From HUL and MTM. Blue curve = inferred BSW conditions at HUL. Blue circles = WA of radiocarbon distribution and errors represent the 2σ range from HUL. Red curve = inferred BSW conditions at MTM. Red circles = WA of radiocarbon distribution and errors represent the 2σ range from MTM. Blue bars mark the onset of wet shifts and numbers are allocated to aid discussion

Differences between records are attributable to four major factors, these are:

1. Actual climatic differences between locations;
2. Errors in the derivation of the proxy record;
3. Differing autogenic modulation of climatic signal between sites;
4. Chronological uncertainty resulting from errors inherent in the dating technique and inaccuracies in the age-depth models.

Attempting to match records very closely asks a lot of the data and any assessment of the similarity/dissimilarity of palaeoecological datasets must take sources of uncertainty into some account. Accordingly the impact of these processes on the bog records will be discussed below.

While paired lake and peatland sites were selected in close proximity to one another the two bog sites are further apart (*c.* 60 km). Hulleter is situated in a classic lowland oceanic setting (altitude < 10 m) whereas Malham Tarn Moss is in an upland and slightly more continental setting (altitude *c.* 380 m). These differences might lead to some local variability but the gross climatic variations experienced at each site would still be expected to be very similar over this area. It is therefore reasonable to assume that differences in the records are unlikely to reflect actual climatic differences between sites.

Errors in the derivation of palaeoclimatic records are inescapable because proxies are by definition an indirect measure of the environmental variable or variables of interest. Climate-proxy relationships used to infer past conditions are necessarily simplistic and as a result some errors and generalisations inevitably occur within the reconstruction. Depending on the nature and severity of these errors they may express themselves as highly inaccurate inference at one end of the spectrum and relatively minor noise at the other end. The use of established techniques such as the BSW methods used here which have been validated by comparison with other palaeoclimatic data (Barber *et al.*, 1994; Hughes *et al.*, 2000; Langdon *et al.*, 2003),

instrumental data (Charman *et al.*, 2004) and contemporary studies (Bobrov *et al.*, 1999). This reduces the chance that inaccurate results are obtained and the use of multiple independent proxies further strengthens the degree of certainty in the accuracy of palaeoecological inference (Blundell & Barber, 2005). It is therefore possible to be quite confident that the BSW reconstructions from HUL and MTM have only relatively minor errors in their derivation probably expressed as noise superimposed upon the climatic signal.

Site specific or autogenic factors are an extension to the proxy uncertainty problem, but are worthy of consideration separately because the causal relationship differs and there is at least a partial means of reducing or separating out these errors. Autogenic processes have the potential to cause differential sensitivity to environmental forcing (see Section 2.3). Variable sensitivity has been observed within individual sites, typically in relation to microtopographic features which themselves vary through time as a consequence of bog developmental processes (e.g. Barber *et al.*, 1998). These site-specific variations are an inevitable part of the climate-proxy linkage so a degree of dissimilarity between records from different sites attributable to autogenic processes should not be unexpected. In practice the only way to differentiate site specific signal is to compare or better still amalgamate multiple records in order that the regional climatic signal is preserved and the local noise reduced.

Chronological error is inherent in radiocarbon dating, calibration and subsequent age-depth modelling and these errors constitute one of the major limitations of non-annually resolved datasets. While the errors involved in radiocarbon dating and calibration can be estimated with some confidence the problem remains that any chosen point within an age probability distribution is not just possibly but probably incorrect (Telford *et al.*, 2004b). The inability of a single point to adequately represent a probability distribution has consequences for subsequent age depth modelling. Furthermore, disparities between the assumptions of the age-depth model applied and the real world introduce additional, unquantified errors (Telford *et al.*, 2004a). Charman *et al.* (2006) point out that if these sources of error are ignored and age-

depth models are accepted as perfect, the inevitable conclusion is that correlations between records are poor. This proves to be problematic when comparing records and even more so when combining records into a regional index as much significant variability will be lost in the averaging process. In response to the problems of chronological error a simple 'tuning' procedure was developed by Charman *et al.* (2006) which uses the BSW records themselves to select alternative age-depth models from the range of possibilities allowed by the radiocarbon and other age indicators.

The objective of the analysis here is slightly different to that of Charman *et al.* (2006) who were tuning chronologies in order to amalgamate records. Amalgamation of the HUL and MTM records is less valid because two records are insufficient to average out site specific signals. Instead the procedure has been adopted here as a simple means of hypothesis testing. With the hypothesis being that, if it is possible to find a common date for a shift within the radiocarbon dating errors then the shifts could indeed have been synchronous. If however it is not possible to find a common date for a shift within the dating error then the null hypothesis is that the shifts can not have co-occurred, at least not if the radiocarbon dates are to be believed. This procedure therefore offers a means of investigating which of the shifts might have been synchronous between sites. On this basis it is then possible to begin to differentiate between shifts that occur in response to a regional climatic signal and those influenced by local autogenic processes.

The tuning procedure is based primarily on the assumption that significant centennial or longer scale climatic variations are unlikely to be asynchronous between field sites. As already discussed this is a reasonable assumption given the relatively close proximity of the sites (c. 60 km). Major changes in water tables which are primarily forced by prevailing climatic conditions should therefore be synchronous. The procedure applied was a slight modification to that of Charman *et al.* (2006). Key points of change were identified in each record (Fig. 7.1). For each of these matching points an average age was calculated (Table 7.1). The new averaged wet shift ages

were then plotted on the original age-depth models and their position assessed in terms of the radiocarbon error envelope. In most cases wet shifts were dated directly so it was clear if the new intermediate shifts fell within radiocarbon error. Where shifts were not dated directly the errors were interpolated between radiocarbon dates and these used as a tentative indication of whether the new averaged shift dates were in accordance with the radiocarbon chronology. Those match points which were consistent within dating errors were then used as the main age estimates to recalculate the chronologies of each individual record, along with any independent age estimates, in this case SCPs and the surface at the time of coring. For those parts of the curve with no matching points the original radiocarbon ages were used. The use of the original radiocarbon chronologies for sections of the core without matching points differs from the procedure of Charman *et al.* (2006) as this would have been a problem when combining records (Charman pers. comm.) but presents no such difficulty here. The recalculated age-depth models were based on linear interpolation.

Table 7.1: Wet shift match points and age averages

MTM		HUL		Mean Age	Shift No.
Depth	Age	Depth	Age		
292	4240	Pre-dates HUL record		---	1
268	3990			---	2
220	3590	300	3610	3600	3
192	3370	---	---	---	4
172	3130	248	3150	3140	5
152	2840	196	2740	*2790	*6
136	2590	164	2520	2555	7
104	2260	---	---	---	8
88	1980	112	2090	2035	9
---	---	68	1530	---	10
56	1320	56	1360	1340	11
32	850	32	650	*750	*12

Asterisks indicate averages which did not fall within the 2 σ error range.

It would be incorrect to suggest that the new chronologies were any closer to the true age-depth relationship than the original ones and there is a degree of circular reasoning involved in using the palaeoecological data to 'tune' the chronologies.

However Charman *et al.* (2006) point out that the new chronologies are no less consistent with the radiocarbon age estimates than the original model and furthermore suggest that combining and tuning models to each other might result in a greater likelihood that errors in individual chronologies are reduced by the tuning process.

One significant limitation of this particular tuning procedure is that no account is taken of the age probability distribution; instead any point within the two sigma range is considered equally likely. Nevertheless the technique offers a simple and robust method of comparing records and checking for the possibility of synchronous change which might otherwise be obscured by uncertainty in the chronological estimates.

Shift numbers one and two could not correlate between cores because they pre-date the HUL record. Fig. 7.1 and Table 7.1 show that shift numbers 4, 8 and 10 could not be matched to any other shifts. Numbers 3, 5, 6, 7, 9, 10 and 12 were sufficiently similar that they might be contemporary. Fig. 7.2 reveals that the new average timings for shifts 3, 5, 7, 9 and 11 were within the radiocarbon errors but shifts 6 and 12 were not. In the case of shifts 6 and 12 the original radiocarbon dates were used for the recalculated age depth models. However it is noteworthy that shift 12 occurs within a part of the core HUL which is poorly constrained so there is a greater possibility that this shift might have been contemporary between the two cores than that of shift 6 which is relatively well constrained in both cores.

The new tuned chronologies were then used and the data re-plotted (Figure 7.3) in order that their optimal similarity might be seen. Based on these new tuned chronologies shifts 3, 5, 7, 9, and 11 were shown to be potentially synchronous and might therefore represent climatic deteriorations starting at *c.* 3600, *c.* 3150, *c.* 2550, *c.* 2050 and *c.* 1350 Cal. BP respectively. Whereas shifts 1, 2, 4 and 8 which correspond to *c.* 4250, *c.* 4000, *c.* 3350 and *c.* 2250 Cal. BP respectively occurred at MTM but not HUL (although 1 and 2 predate the HUL record). Shift 10 which corresponds to *c.* 1550 Cal. BP occurs at HUL but not MTM. Shifts 6 and 12

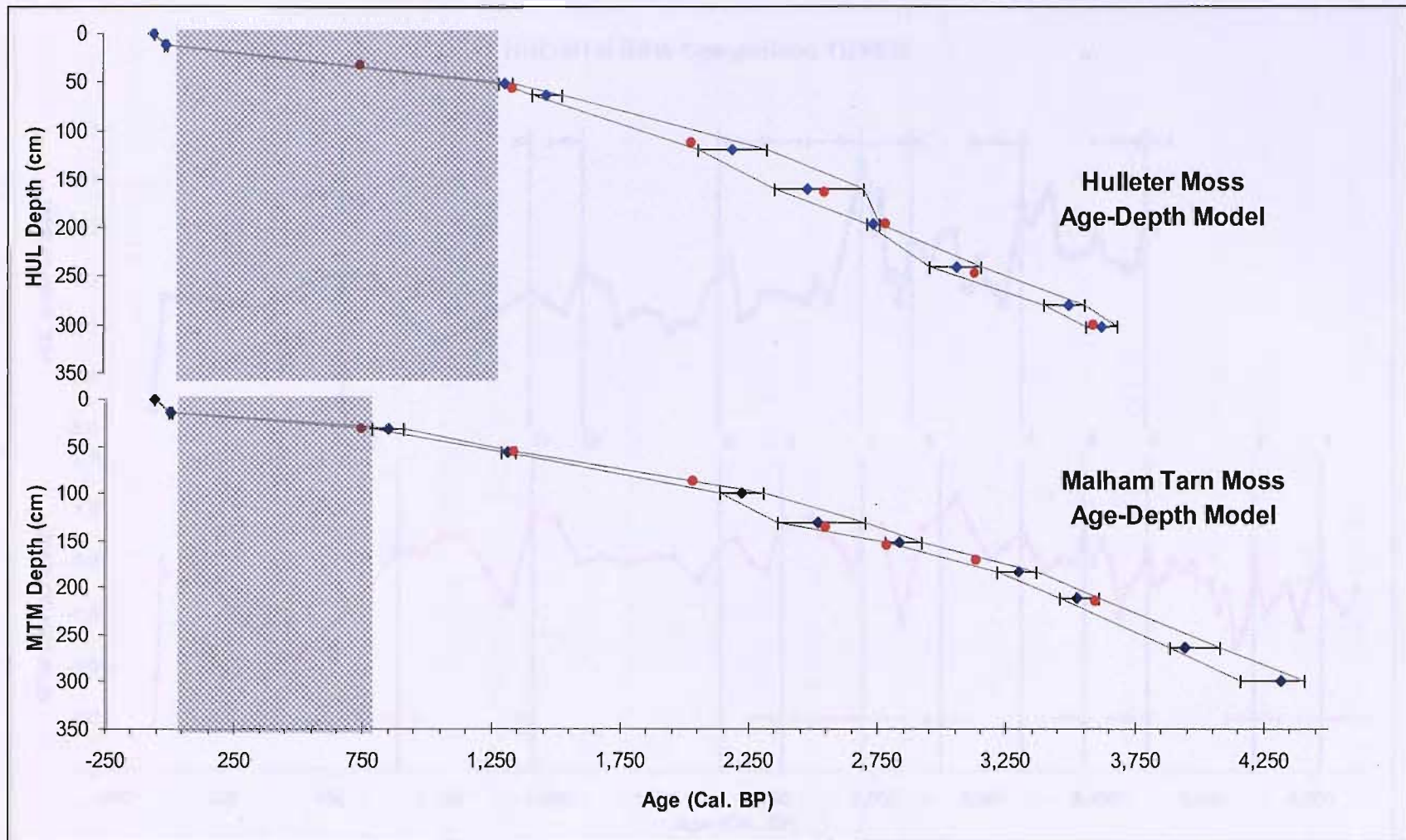


Figure 7.2: Radiocarbon error envelopes for HUL & MTM as an assessment of whether the new averaged shifts conform to the radiocarbon errors. Blue circles = the WA of the age probability distribution. Error bars = the 2 σ error range and red circles the new averaged wet shift timings. Grey shading = sections of poor chronological constraint

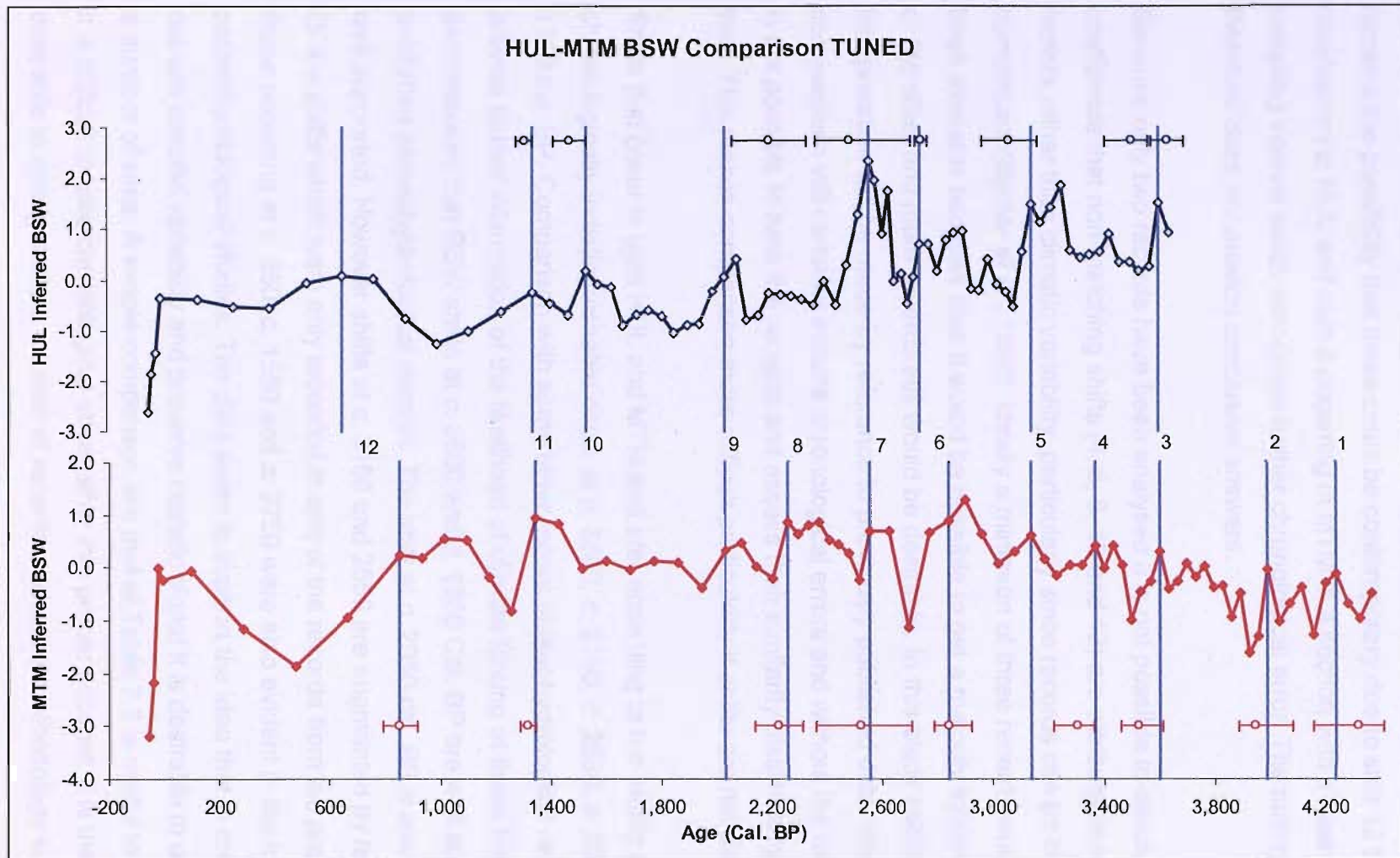


Figure 7.3: Comparison of BSW reconstructions From HUL and MTM based on tuned chronologies. Blue curve = inferred BSW conditions at HUL. Blue circles = WA of radiocarbon distribution and errors represent the 2σ range from HUL. Red curve = inferred BSW conditions at MTM. Red circles = WA of radiocarbon distribution and errors represent the 2σ range from MTM. Blue bars mark the onset of wet shifts and numbers are allocated to aid discussion.

occurred in both cores but could not be matched by the averaging process. There remains the possibility that these could be contemporary due to shift 12 being poorly constrained in HUL and shift 6 occurring in MTM in a section with a lower temporal sampling interval which introduces further chronological error. The tuning procedure therefore does not provide conclusive answers.

Because only two records have been analysed it is not possible to conclude with confidence that non-matching shifts (4, 6, 8, 10 and 12) are attributable to autogenic factors rather than climatic variability, particularly since records can be climatically complacent (Barber *et al.*, 1998). Ideally a minimum of three records would have been available because then it would be possible to get a majority inference one way or the other and more records still would be desirable. In this study additional interpretation will be made by reference to previously published data. However these comparisons will certainly include chronological errors and without the full datasets it is not possible to tune the records and assess their similarity/dissimilarity in the same way. This makes comparison more difficult particularly if shifts are not dated directly.

Shifts that occur in both HUL and MTM and are, according to the tuning procedure, chronologically indistinguishable occur at *c.* 3600, *c.* 3150, *c.* 2550, *c.* 2050 and *c.* 1350 cal. BP. Comparison with some other recent palaeohydrological records may provide further information of the likelihood of climate forcing at these times. Table 7.2 demonstrates that BSW shifts at *c.* 3600 and *c.* 1350 Cal. BP are well supported by published palaeohydrological records. The shift at *c.* 2050 cal. BP is also reasonably well supported. However shifts at *c.* 3150 and 2550 are augmented by fewer studies. Of the shifts which were only recorded in one of the records from the present study those occurring at *c.* 850, *c.* 1550 and *c.* 2750 were also evident in the majority of palaeohydrological studies. The data seem to support the idea that in order to filter out site specific variability and preserve climatic signal it is desirable to use data from a number of sites. A simple comparison like that of Table 7.2 is useful to an extent but it is difficult to take chronological uncertainty into proper account. It is therefore clearly desirable to amalgamate a number of records and use a methodology such as the

tuning procedure of Charman *et al.* (2006) to investigate the influence of the chronological error. The degree of variability between records indicates that individual records should be interpreted with caution, particularly when using them to make assertions about climate-proxy relations which is one of the aims of this investigation. This will be discussed more fully below.

Table 7.2: Comparison of wet shifts with those of select previously published palaeohydrological records.

This Study	Blundell & Barber (2005)	Langdon & Barber (2005)	Charman <i>et al.</i> (2006)	Magny (2004)	Langdon <i>et al.</i> (2003)	Charman <i>et al.</i> (1999)	Hughes <i>et al.</i> (2006)	Fig. 2.1 Section 2.4.6
N England	Scotland	Scotland	N England & Scotland	E France	SE Scotland	N England	Newfoundland	NW European Synthesis
c. 4250	-							c. 4300
c. 4000	-						c. 4000	c. 4000
c. 3600	-		c. 3600	c. 3500	c. 3850	c. 3500		c. 3500
c. 3350	-				c. 3400			
c. 3150	-						c. 3100	
c. 2850	-					c. 2900		c. 2900
c. 2750	-	c. 2700	c. 2750	c. 2750	c. 2650	c. 2700		
c. 2550	c. 2510						c. 2500	
c. 2250								c. 2250
c. 2050	c. 2000		c. 2050			c. 2150	c. 2050	
c. 1550	c. 1520		c. 1600	c. 1800		c. 1550	c. 1700	c. 1700
c. 1350	c. 1400		c. 1250	c. 1300	c. 1400	c. 1350		c. 1350
						c. 1000		c. 1050
c. 850	c. 860		c. 860	c. 750		c. 850		c. 850
c. 650			c. 550			c. 600	c. 600	c. 650
	c. 310		c. 260		c. 200	c. 450		
						c. 100		

All dates are cal. BP and rounded to the nearest 50 years. Shaded rows correspond to those shifts which occur in both MTM and HUL.

7.3 CI-T INTER-SITE COMPARISONS

The chironomid inferred temperature (CI-T) records are somewhat less robust than the BSW reconstructions because they are based on just one proxy. Nevertheless chironomid analysis has been shown to be capable of surprisingly accurate palaeotemperature inference compared to historical data (Larocque & Hall, 2003) and consequently is certainly capable of producing accurate palaeotemperature estimates for relatively low magnitude Holocene temperature variability. Capability does not of course imply infallibility and a number of investigations have experienced problems in reconstructing Holocene temperatures using midge stratigraphies (e.g. Heiri & Lotter, 2003; Velle *et al.*, 2005). Problems are twofold, the first relates to the magnitude of the prediction errors of temperature inference models which are close to the expected magnitude of temperature variation. A second issue relates to catchment driven changes in the lake water and sediment chemistry through processes such as plant succession, soil development and anthropogenic disturbance, which may at times have an overriding influence on midge assemblages compared to temperature (Brooks, 2006). It is obviously desirable to be able to distinguish between climatic and catchment-driven changes in the midge fauna.

There are two basic approaches to reducing the uncertainty associated with proxy data and both of these have been utilised in the bog records. The first is to produce independent multiproxy records from each core and the second is to validate records by comparison with other datasets. In lake ecosystems the multiproxy approach is typically different to that used for peatlands where independent proxies are used in an attempt to reconstruct the same variable (Blundell & Barber, 2005). In palaeolimnological investigations the multiproxy approach is usually aimed at reconstructing multiple variables which represent different aspects of the palaeoenvironmental system, ideally enabling the investigators to build up a picture of gross changes in the whole catchment through time (Battarbee, 2000). Information about catchment change (e.g. through pollen analysis) and water column chemistry (e.g. through diatom analysis) are considerable aids to interpretation of chironomid stratigraphy. Unfortunately these data were not available in the literature or attainable within the

constraints of this project so validation must rest upon comparison with records from different sites.

While there is every reason to believe that the CI-T records from both BLT and MLT are climatically meaningful, at least for most of the records (see Sections 6.3.2 & 6.5.2) the lack of an independent ^{14}C chronology for MLT makes it meaningless to compare between records. The only alternative mid- to late-Holocene chironomid record from northern England is that of Langdon *et al.* (2004) from Talkin Tarn. This record is suitable for comparison with Bigland Tarn since both lakes are in Cumbria and should have experienced similar gross climatic trajectories. Errors in the derivation of the proxy records are quantified at least to some extent and should be comparable between sites since both investigations utilised the same chironomid identification keys (see Section 3.3.3) and used the Norwegian training set of Brooks & Birks (2000; 2001) to calculate the temperature estimates.

The records from BLT and Talkin Tarn are plotted for comparison in Fig. 7.4. The two records are not identical, with BLT showing greater variability overall and in particular displaying very cold mean July temperature estimates at certain times e.g. c. 4800 cal. BP, (9.2°C) c. 1650 cal. BP (10.4°C). The reasons for the relatively high amplitude variability, and low temperature estimates are discussed in Section 6.3.2. The timings of change are not identical either but these differences are easily explicable in terms of the chronological uncertainty, particularly since the Talkin Tarn age-depth model is based on only four radiocarbon dates due to five radiocarbon measurements returning unreliable results (Langdon *et al.*, 2004). Comparison is also inhibited by the differing sample resolutions. The basal part of the BLT core was sampled at low resolution since it is beyond the age of the HUL peatland core with which it was primarily intended for comparison. Nearer the surface the sampling resolution is much higher because this section was intended for comparison with instrumental records and LIA cooling. Unfortunately this was not fruitful because of probable non-climatic influence and poor chronological constraint on the near surface sediments. Perhaps surprisingly despite these complications the two records display

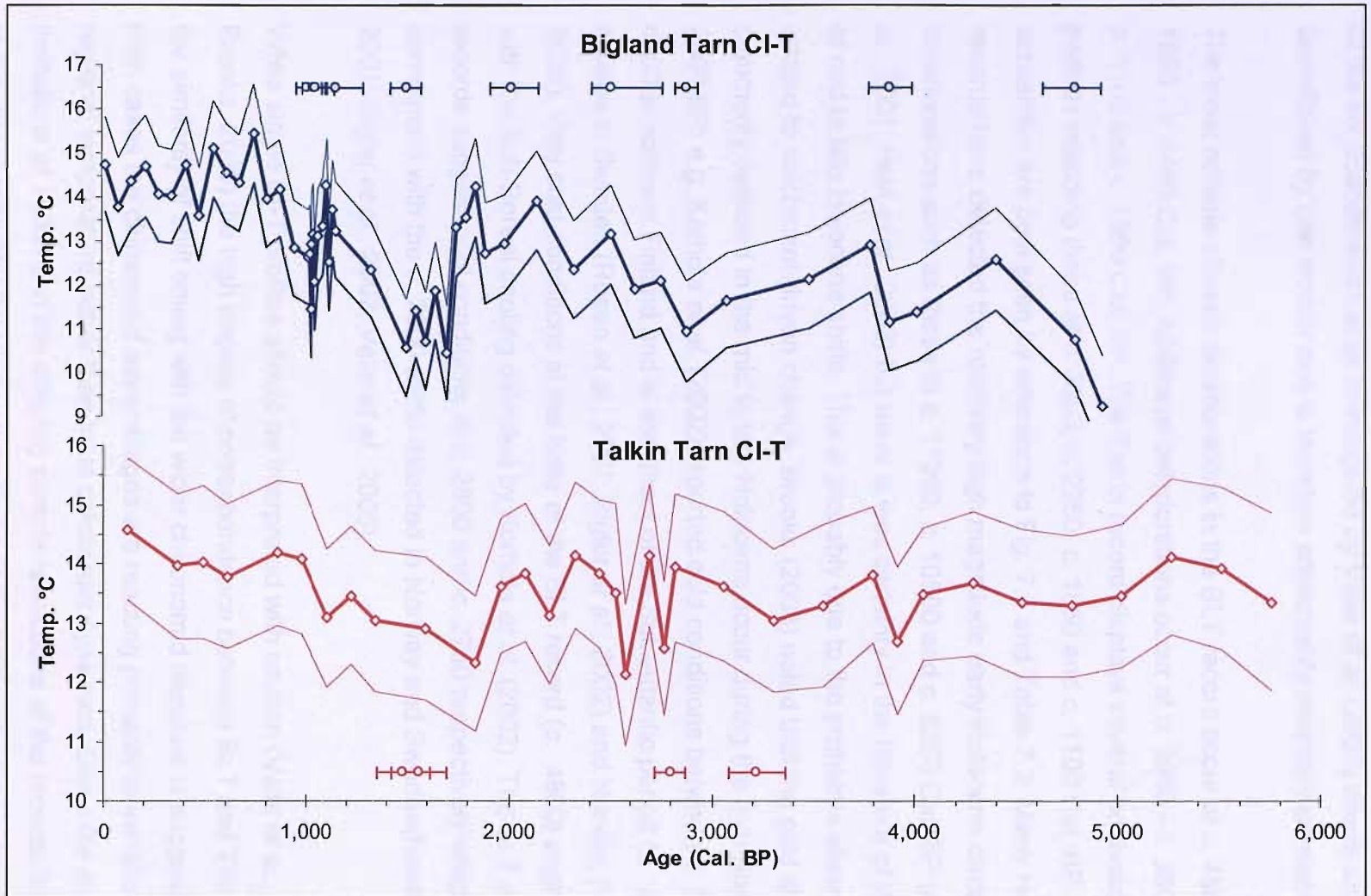


Figure 7.4: Comparison of BLT & Talkin Tarn CI-T Reconstructions. Thick blue = BLT CI-T record, open diamonds = samples analysed. Thick red curve = Talkin Tarn CI-T record, open diamonds = samples analysed. Feint curves = sample specific root mean squared errors of prediction (RMSEP). Blue circles = WA of radiocarbon distribution and errors represent the 2σ range from BLT. Red circles = WA of radiocarbon distribution and errors represent the 2σ range from Talkin Tarn.

a good overall degree of similarity and resemble each other more closely than many of the six Scandinavian sites investigated by Velle *et al.* (2005) where analysis was undertaken by one worker and is therefore presumably internally consistent.

The most notable climatic deteriorations in the BLT record occur at c. 4800 and c. 1650 - c. 1450 Cal. BP. Additional deteriorations occur at c. 3950 - c. 3800, c. 2800, c. 1100 and c. 1000 Cal. BP. The Talkin record displays several equivalent cool periods including those at c. 3900, c. 2750, c. 1850 and c. 1100 Cal. BP. The similarities are best seen by reference to Fig. 7.4 and Table 7.3. Many Holocene CI-T records have detected the relatively high magnitude early Holocene climatic deteriorations such as those at c. 11200, c. 10500 and c. 8200 Cal. BP (e.g. Rosen *et al.*, 2001; Heiri *et al.*, 2003) but there is less certainty in the literature of the detection of mid to late Holocene shifts. This is probably due to the problems already discussed related to catchment-driven change. Brooks (2003) noted that the cold shifts most commonly detected in the mid to late Holocene occur during the Sub-Boreal (5700-2600 BP) e.g. Korhola *et al.* (2002) reported cold conditions between c. 5800 and c. 4200 in northern Finland and at the onset of the Sub-Atlantic period (c. 2600 BP) e.g. studies in Sweden (Rosen *et al.*, 2001; Bigler *et al.*, 2002) and Norway (Velle *et al.*, 2005). Very cold conditions at the base of the BLT record (c. 4800) might correspond with the Sub-Boreal cooling detected by Korhola *et al.* (2002). The BLT and Talkin records suggest cool conditions at c. 2800 and c. 2750 respectively which might correspond with the c. 2600 shifts detected in Norway and Sweden (Rosen *et al.*, 2001; Bigler *et al.*, 2002; Velle *et al.*, 2005).

While single CI-T profiles should be interpreted with caution (Velle *et al.*, 2005; Brooks, 2006) the high degree of correspondence between BLT and Talkin Tarn and the similarity of shift timing with the wider chironomid literature is suggestive that in both cases the chironomid assemblages are reacting primarily to variations in regional temperature rather than local catchment dynamics. Given the chronological limitations of Talkin and the differing sample resolutions of the records it is difficult to make any meaningful detailed comparisons of the timing of change. Nevertheless,

these records seem to provide a promising start for Holocene palaeotemperature estimates in the UK. This satisfies a secondary aim of the research which was to test the ability of chironomid inferred temperature reconstructions to reflect relatively low magnitude Holocene temperature changes.

Table 7.3: CI-T Cool Phases

Bigland Tarn	Talkin Tarn
4800	---
3950-3800	3900
2800	2750
1650-1450	1850
1100	1100
1000	---

Velle *et al.* (2005) produced six quite different CI-T curves from southern Scandinavia; however, after amalgamating the data they found that the resultant curve showed close resemblance to the expected Holocene changes. This suggests that even when catchment dynamics mask climatic influence on chironomid fauna they may not completely overwrite it and the climatic portion of variability may still be drawn out through averaging multiple records. It would therefore seem desirable to produce an amalgamated northern England record. At present there are insufficient datasets and those that do exist would require sample resolution matching and chronological improvement to optimise amalgamation. Further comparison must therefore rest on the BLT record.

7.4 BSW - CI-T COMPARISON

The primary aim of this research was to investigate the nature of the climatic signal recorded in raised bogs and in particular, to test the hypothesis of Barber *et al.* (2000) that temperature, rather than precipitation, is the main climatic signal recorded by changes in bog surface wetness. In order to accomplish this BSW and CI-T records have been produced so that they may be compared and the degree of similarity/dissimilarity used as an empirical assesment of the closeness of the relationship between BSW and temperature. The comparison is particularly appropriate since both chironomid analysis and the various measures of BSW used in

this investigation are indicative primarily of summer conditions. Due to the problems encountered with dating the Malham Tarn profile (Sections 3.4.1 & 5.5.1) the comparison will rest on the HUL bog surface wetness and BLT chironomid inferred temperature data.

When comparing these records the usual sources of error summarised in Section 7.2 might account for differences. However the records are only c. 5 km apart so it is highly unlikely that the climatic parameters differ significantly. Prior to comparison both records have been collated with other datasets produced using the same or similar methods and in both cases much of the variability was found to be reproduced at multiple sites, suggesting that variability in the records is driven primarily by climate. However differences do occur and these are explicable in terms of errors inherent in the proxy techniques and site specific variability overriding the climatic influence, which add noise to the data.

It is not possible to validate the BLT and HUL records against one another in the same way as HUL and MTM or BLT and Talkin Tarn because the comparison is not like with like, so differences between records might reflect genuine differences in the climatic variable-proxy response; indeed this is the intended test. It does, however, make it difficult to differentiate between sources of error and variability related to the climate-proxy linkage. Given the general correspondence between each record with other similar records much of the variability can be attributed to climatic parameters, and consequently differences between records should chiefly reflect differences in the climate-proxy relationships.

Chronological errors also complicate assessment of similarity and although both cores are generally well constrained by the radiocarbon chronology it is not appropriate to attempt to tune the records since there is insufficient certainty that the major changes are driven by the same underlying variable and consequently while both are related to climate the timing and direction of change may not be equivalent. Comparison must therefore make allowance for chronological uncertainty.

The Hulleter Moss BSW and Bigland Tarn CI-T records are plotted together for comparison in fig. 7.5. The original HUL chronology and associated shift dates are used for comparison with BLT since the tuning procedure was only appropriate for comparison between HUL and MTM. The WA of the radiocarbon ages and the 2σ error terms are plotted for each series as a visual indication of chronological uncertainty. A time equivalent sampling interval was not achieved, the reasons for which are explained in Section 7.5, and HUL generally has a higher resolution than BLT. This allows for the possibility that short duration shifts recorded in HUL are simply missed by the analysis at BLT. Despite these limitations comparison of the two records should offer a good insight into the nature of the relationship between temperature and BSW in northern England during the late-Holocene.

The records appear to display little similarity overall but there are a few points of correspondence. The Bigland record displays cool conditions at *c.* 2800 Cal. BP and wet conditions are found at a similar time *c.* 2700 Cal. BP in the HUL record. Both of these are close to the widely reported 2650 BP deterioration (van Geel & Renssen, 1998). While the Bigland phase is based on just one data point this may be due to the relatively coarse sample resolution. The most notable cool phase in the CI-T record from BLT occurs between 1650-1450 cal. BP; the BSW record from HUL displays a wet phase starting at *c.* 1500 and ending at *c.* 1400 Cal. BP. Although the CI-T curve displays a longer and more pronounced shift both of these are close to the previously reported 1400 BP 'Dark Ages deterioration' (e.g. Blackford & Chambers, 1991). Finally the Bigland Tarn CI-T record displays marked variability between *c.* 1100 and *c.* 1000 cal. BP but during this phase particularly cool conditions are indicated at *c.* 1000, which might correspond to wet conditions on HUL at *c.* 1050 cal. BP. However BSW conditions at this time are generally wet and stable and do not fluctuate like the chironomid record. These similarities are the exception rather than the rule and the majority of the records are quite dissimilar. In particular, dry inferred conditions at HUL at *c.* 3250-3150 cal. BP and *c.* 2600-2500 cal. BP have no warm equivalent in the CI-T record.

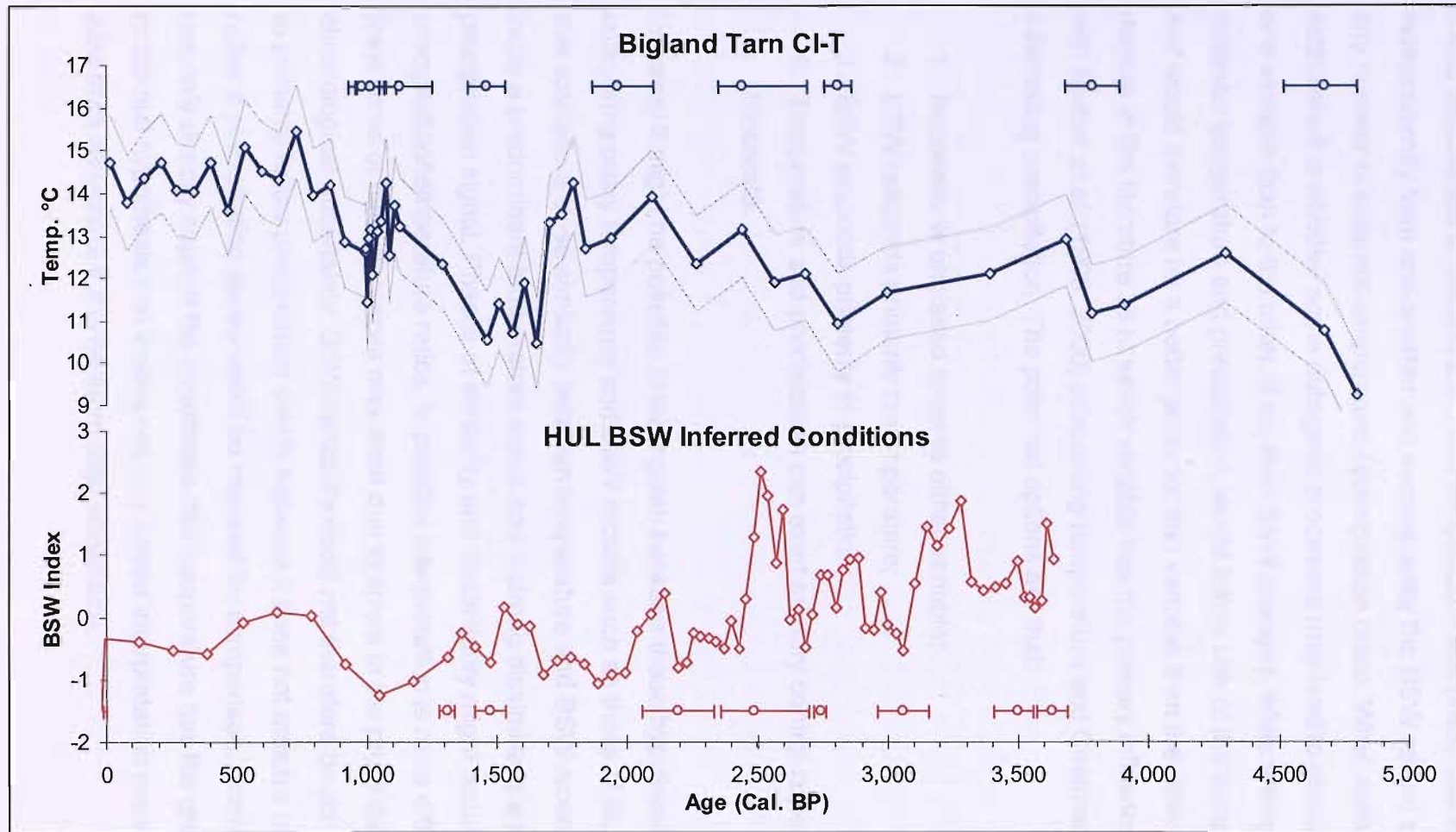


Figure 7.5: Comparison between BLT CI-T and HUL BSW reconstructions. Thick blue curve = BLT CI-T record, open diamonds = samples analysed. Faint grey curves = the BLT sample specific root mean squared errors of prediction (RMSEP). Red curve = HUL BSW reconstruction, red diamonds = samples analysed. Blue circles = WA of radiocarbon distribution and errors represent the 2σ range from BLT. Red circles = WA of radiocarbon distribution and errors represent the 2σ range from HUL.

It was established in Section 2.9.5 that temperature and precipitation can vary independently from one another and consequently the BSW record could result from any number of different temperature / precipitation ratios. What remains to be established is whether some autogenic processes may lead to greater sensitivity to one variable than to the other. If so, then BSW changes, while arising from interplay between temperature and precipitation, would follow one of the variables more closely and would therefore be a better proxy for that variable than the other. There is some dispute in the literature as to which variable has the primary influence on BSW, if any, with Barber *et al.* (1999; 2000) advocating temperature and Charman *et al.* (2004) advocating precipitation. The potential options are that:

1. Response is unbiased towards either variable;
2. BSW responds primarily to temperature;
3. BSW responds primarily to precipitation;
4. Temperature and precipitation can exert primary control depending on the timescale.

In theory it might be possible to distinguish between these hypotheses by simply comparing proxy temperature and BSW records such as those of BLT and HUL. In this scenario a close similarity between temperature and BSW reconstructions would imply a predominant temperature signal and a strong dissimilarity a predominant precipitation signal. Phases of similarity and dissimilarity might result from changing precipitation/temperature ratios. In practice interpretation is more difficult because at least some of the differences may arise due to errors in the proxy data and chronological uncertainty. BSW variability could not therefore be confidently attributed to primarily follow precipitation simply because it does not match a temperature proxy, rather a precipitation series would be required for comparison. Consequently the test can only directly support the hypothesis that temperature has the greatest influence or the null hypothesis that it does not, any further interpretation requires supportive data from elsewhere if it is to be more than conjecture.

It has also been suggested that the role of temperature and precipitation in driving BSW might be timescale dependant with precipitation dominating over decadal timescales and temperature being more important over centennial to millennial timescales (Barber & Langdon, in review). The datasets produced here should be of sufficient length to test the strength of the temperature-BSW relationship over these longer timescales.

The general dissimilarity of the BLT and HUL series supports the null hypothesis that temperature cannot be shown to be an overriding BSW driver over centennial to millennial timescales. The points of correspondence do occur at times when climatic shifts are well known and this demonstrates the expected outcome that temperature has an influence on BSW but there is no evidence that its effects override precipitation since much variability in the BSW reconstruction is not seen in the temperature estimates. A recent paper by Charman (in press) used basic modelling and interpolation of precipitation and primarily temperature-driven evapotranspiration rates to investigate the influence on summer moisture deficit in northern England. The summer moisture deficit drives BSW changes and was found to be much more sensitive to changes in precipitation than to temperature change. This supports the idea put forward in Table 2.1 that BSW variability might be biased towards precipitation variability through some autogenic process and consequently changes will primarily follow precipitation variability. That temperature is not dominant, and precipitation might be, is contrary to conclusions of a palaeoecological investigation similar to this study by Barber & Langdon (in review). It utilises the Talkin record reproduced here (Langdon *et al.*, 2004) and BSW records from Walton Moss in Cumbria including that of Hughes *et al.* (2000). It is interesting that the Bigland Tarn record resembles the Talkin record surprisingly closely and many of the BSW shifts recorded in HUL correspond with those in other investigations including that of Hughes *et al.* (2000) and yet Barber & Langdon (in review) reach the opposing conclusion that temperature does have an overriding influence on BSW over centennial and millennial timescales due to the degree of similarity between CI-T and BSW records.

Barber & Langdon (in review) argue that over short timescales of years to decades the precipitation signal may appear to override temperature in driving BSW (*sensu* Charman *et al.*, 2004) but suggest that wet summers are typically associated with cool conditions related to maritime westerly air masses. This is certainly the case much of the time but the argument is not persuasive in favour of temperature as the primary driver, rather it suggests that temperature and precipitation remain strongly negatively correlated and so exert a consistent relative influence on BSW. If this were so both temperature and precipitation should be easily inferred from BSW reconstructions.

As was discussed in Section 2.9.4 it has been suggested that climatic deteriorations associated with north-south movements of the Polar Front lead to different patterns of hydrological change in Europe with wetter climatic conditions in the mid latitudes (Magny *et al.*, 2003). Furthermore, this middle latitude wet zone is thought to expand and contract latitudinally depending on the extent of cooling. As a consequence sites close to the margin of the middle latitude zone such as those of northern England may have found themselves sometimes experiencing dry and sometimes wet conditions associated with climatic deteriorations. Thus the relationship between temperature and precipitation is unlikely to have remained the same throughout the entire Holocene.

To conclude, the palaeoecological data presented here support the null hypothesis that temperature cannot be shown to drive changes in BSW over and above precipitation. Nevertheless, temperature clearly has an important influence on BSW conditions. The fact that two studies involving similar datasets are able to come to opposing conclusions about the degree of similarity between CI-T and BSW records highlights the issue that accurately reconstructing Holocene environmental variables is challenging and differences may arise due to errors and uncertainties which exist in the data. Sources of error are discussed in the methodological appraisal and methods

of minimisation suggested in the Recommendations for future work Section 7.5 below.

7.5 *METHODOLOGICAL APPRAISAL & RECOMMENDATIONS FOR FURTHER WORK*

The datasets used in this investigation are generally of a high quality. BSW records benefited from a multiproxy approach and both BSW and CI-T records were cross-validated with other similar reconstructions and found to have a good degree of similarity. Nevertheless cross-validation also revealed a degree of dissimilarity and highlights the need to improve chronologies and distinguish between site-specific and regional climatic signal. Key limitations of the datasets have been found to relate to:

1. Chronological constraint;
2. Lack of certainty in the palaeoenvironmental estimates;
3. Different time equivalent sample resolutions;

These limitations will be addressed in order. Firstly, chronological error is one of the primary limitations of non-annually resolved datasets. It provides opportunity for contemporary shifts to appear different and different shifts to appear contemporary and is a serious barrier to record comparison. Comparability would have been significantly improved if pinning points could have been established. Tephra analysis offers the most promising method of correlating between cores and would have been a significant aid to interpretation. The analysis was not carried out due to time constraints but it is felt that this has reduced the strength of inter-site comparability. Tephra analysis would certainly be recommended as an extension to this or as a part of any future project which requires inter-site comparison.

Problems with the MLT chronology were unfortunate but with hindsight a carbonate lake was always going to be challenging to date and the project would probably have been better served by analysis of a record which was more easily dated. The

proximity of Malham Tarn to Malham Tarn Moss and tendency of carbonate lakes to buffer against catchment-driven change were seductive but probably not so important that it was worth risking the chronology. Low chironomid head capsule concentrations further limited the resolution of analysis which was possible both at Malham and at Bigland due to the time consuming nature of sample picking. As an extension to this project Malham might still be dateable through Uranium series dating but in future investigations carbonate lakes might be best avoided unless chironomid head capsule concentrations were significantly higher.

The BSW estimates are close to optimal under current methodologies and little could be added to improve certainty in the reconstructions. The CI-T records by contrast would have benefited from additional analysis of pollen and diatoms to improve understanding of catchment and water column changes and their relationship to the chironomid stratigraphy. This would have certainly aided interpretation and improved confidence in the record. However these analyses are far too time consuming to have been possible within this project. Cross-validation of both the BSW and CI-T records would have been improved if more records had been available for comparison. However, there are still relatively few multiproxy BSW reconstructions and only two CI-T late Holocene reconstructions from Britain (three if Malham is included) so while cross-validation by reference to more records would certainly be recommended in future investigations it could not have been accomplished here.

Perhaps the major shortcoming of the project was the failure to achieve a time equivalent sampling resolution between lake and bog profiles. This would have significantly improved comparability and was recognised as being important at the planning stage. In order to achieve matching time equivalent sampling resolutions an idea of core chronologies is required early in the project so that analysis can be targeted at the relevant areas of the cores, particularly since chironomid analysis is so time consuming that mismatching sampling intervals cannot be quickly rectified. The constraints of the NERC radiocarbon application procedure made this difficult because dates typically will not be awarded until considerable data collection has

been demonstrated. This is understandable given the expense of the dating procedure but makes early planning very difficult because it is typically based on assumptions as to the accumulation rates of the cores in question.

Given that the degree of variability between profiles seemingly allows for the production and comparison of quite similar records and yet interpretation can reach opposite conclusions it is clearly desirable to reduce the degree of uncertainty between profiles. It must of course be realised that some uncertainty is an inevitable part of the reconstructive process but unless site-specific variability can be significantly reduced it will remain very difficult to interpret individual records with any degree of confidence. Consequently, the author would advocate a regional index approach to comparison using, where possible, multiple multiproxy datasets tuned together and amalgamated into regional indexes. These would preserve regional climatic signatures and average out site-specific noise. This kind of comparison, although considerably more time-consuming, would offer a more robust comparison of temperature and BSW variability and hopefully dispel the ambiguity as to the relationship between climate and BSW. This project was designed to produce and compare individual site pairs rather than create regional indexes for comparison. This approach was more achievable within the time constraints of PhD tenure but has resulted in less firm conclusions.

Modelling experiments which take into account bog growth, development and hydrology as suggested by Charman (in press) also offer a promising means of improving understanding of the climate-BSW relationship and might, if successful, offer a method of climatic calibration of BSW records.

While this investigation has focussed on attempts to clarify the nature of BSW in terms of climatic variability Charman & Hendon (2000) make the important point that relative changes in temperature and precipitation control soil moisture and are therefore the most crucial aspects of future climates for agriculture and water supply. Changes in soil moisture related to the ratio of temperature and precipitation is the

variable most easily reconstructed from peatland records and can provide valuable information about soil moisture changes during the Holocene. BSW records are therefore not necessarily devalued simply because they cannot yet be related directly to one climatic variable.

The following text is extremely faint and largely illegible. It appears to be a continuation of the discussion on peatland records and soil moisture changes. The text is too light to transcribe accurately but seems to follow the same logical flow as the first paragraph, discussing the relationship between peatland records and climatic variables.

8.0 CONCLUSIONS

The primary aim of this investigation was to produce and compare BSW and CI-T records in order to test the hypothesis that temperature, rather than precipitation, is the main climatic signal recorded by changes in BSW over centennial to millennial timescales. To accomplish this, sediment from two proximal lake and bog sites have been analysed. As well as providing a means of testing the nature of the palaeoclimatic signal recorded in raised bog stratigraphy the records produced from these four sites represent new palaeoclimatic records with which to augment existing knowledge of Late-Holocene North Atlantic climate variability.

A large number of bog surface wetness records have already been produced from northern England and particularly Cumbria, but there are still surprisingly few detailed multiproxy investigations. This project has produced two new multiproxy records based on plant macrofossil, testate amoebae and peat humification analysis. Both sites show an impressive degree of internal consistency between proxy measures of BSW over the late-Holocene. For each record the three independent datasets were amalgamated into a single inferred BSW index (Blundell & Barber, 2005) by normalising the datasets and carefully scrutinising each for reasons that they may differ. All records were then averaged together unless one could be shown to be unreliable, for example, due to insensitivity or lack of good modern analogues, in these circumstance the samples were omitted. Production of a single index for each site considerably improved the ease with which records could be compared. Comparison between the two peatland sites from this investigation and also with the wider literature revealed a high degree of similarity between the records, further strengthening the theorised climatic control over BSW. However, site-specific variability was identified to be a significant source of error and the amalgamation of multiple datasets from a region is therefore advocated as a means of reducing this uncertainty and improving interpretative confidence.

Very few late-Holocene chironomid-inferred palaeotemperature records are available for Britain. This project has produced two new records although the chronology of one of these (Malham Tarn) remains uncertain. Nevertheless, one well dated CI-T record has been produced and this represents an improvement on earlier studies primarily due to considerably better chronological constraint. High-resolution analysis of near surface sediments was not able to produce suitable data for the intended detection of LIA cooling and comparison with instrumental data because of non-climatic (probably anthropogenic) influence on the chironomid assemblages in recent times.

Nevertheless, comparison of the CI-T record from BLT with the earlier record from Talkin Tarn (Langdon *et al.*, 2004) revealed a high degree of similarity in inferred temperature trends between records. This is encouraging evidence of climatic control over chironomid assemblages and satisfied a secondary project aim by supporting the idea that chironomid analysis is able to reconstruct relatively low magnitude late-Holocene climate variability. Critically this also supports the suitability of a comparison between BSW and CI-T as a measure of the temperature - BSW relationship.

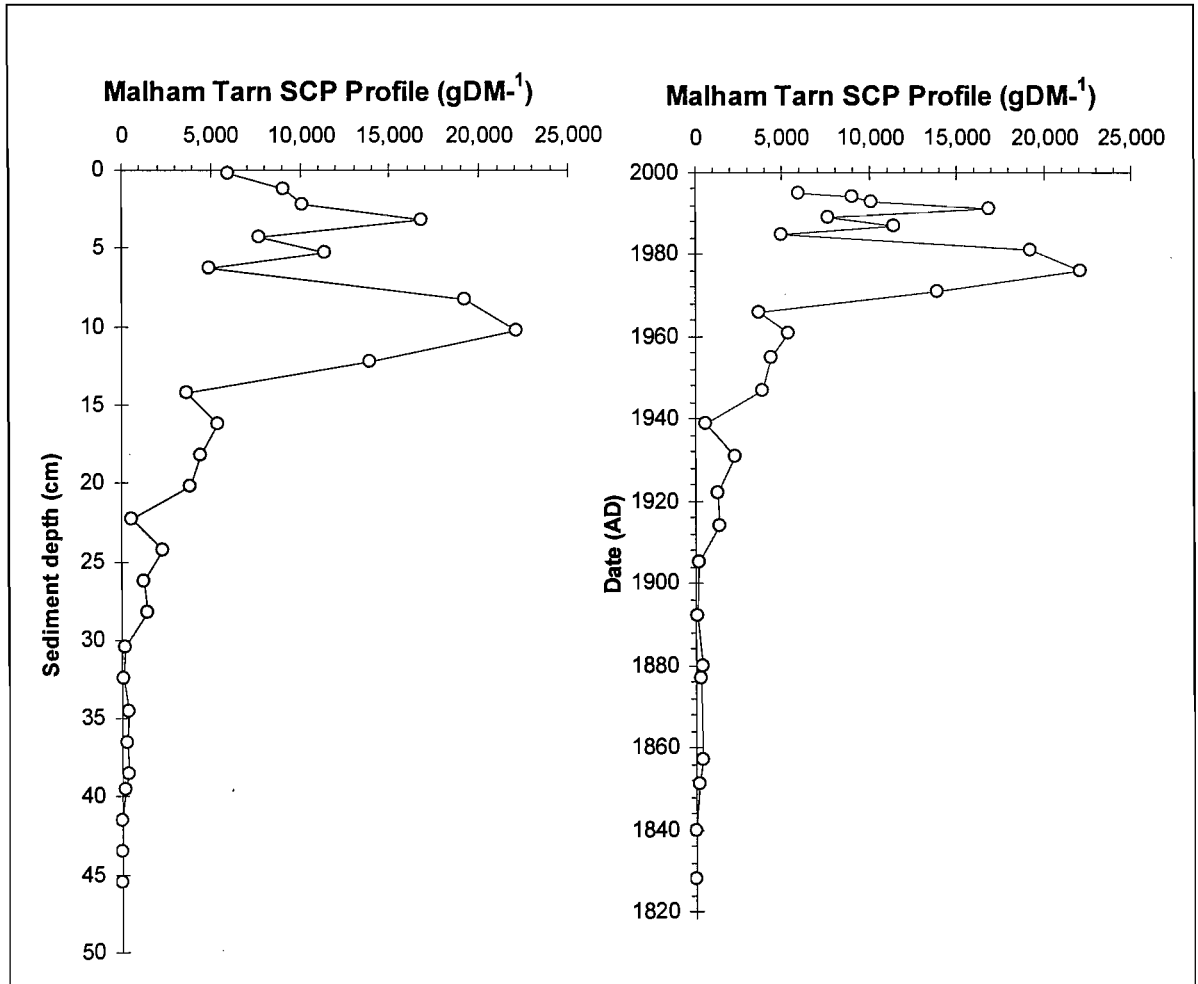
Previous investigations into the nature of the climate-BSW relationship have not come to a consensus and there remains dispute as to whether temperature (Barber *et al.*, 2000; Barber & Langdon, in review), or precipitation (Charman *et al.*, 2004; Charman, in press) has a predominant influence. There also remains the possibility that the nature of the relationship may vary spatially and temporally depending on either the variable nature of the temperature precipitation relationship, or the relative sensitivity of bogs to each of the variables which may vary through several processes.

Comparison of the BSW record from Hulleter Moss and the CI-T record from Bigland Tarn was not able to support the hypothesis that temperature has an overriding control on BSW. There were some points of correspondence between the two records suggesting the expected outcome that temperature does have an influence on BSW but the curves were not sufficiently similar to suggest that this influence is an overriding one. However a number of sources of uncertainty were highlighted when comparing between sites. These originated from proxy uncertainty, in particular

related to site-specific variability and chronological error, related primarily to radiocarbon measurement and calibration. These sources of uncertainty make it difficult to suggest with any confidence that a lack of clear correspondence between temperature and BSW proxies should be interpreted as evidence that BSW responds primarily to precipitation. Chronological uncertainty could have been reduced by establishing pinning points between cores (e.g. Tephra) and ensuring a time equivalent sampling resolution which would require chronological constraint earlier in the analysis. Proxy errors could be reduced by a multiproxy approach to the lake sediment analysis and the amalgamation of a number of records to reduce site-specific signal. Reduction of uncertainty in this way could have improved comparability of the records and enabled more concrete conclusions. Nevertheless, it seems unlikely that it will be possible to apply a universal rule as to which climatic variable primarily drives BSW changes. It is more likely that it will be possible to make state dependent assertions about which variable predominates under certain conditions which may change spatially and temporally.

It is worth reiterating here that a compound measure of temperature and precipitation is not necessarily less useful than for example a temperature proxy. Relative changes in temperature and precipitation control soil moisture and are therefore the most crucial aspect of climate variability for agriculture and water supply. These changes in soil moisture related to the ratio of temperature and precipitation is the first reconstructive step in the peatland palaeoclimate method which can provide valuable information about soil moisture changes in response to climate variability during the Holocene. An understanding of past variability can be used to inform the climate change community about the likely nature and magnitude of soil moisture change in response to future climate change scenarios. Reconstruction of BSW is therefore a useful climate proxy in its own right particularly when used in conjunction with other indicators which are more variable-specific such as stable isotope or chironomid analysis.

Appendix 1- Malham Tarn SCP Profile



Malham Tarn SCP profile against depth and ²¹⁰Pb derived age, kindly provided by Rose, unpublished data

REFERENCE LIST

- Aaby, B. (1976) Cyclic climatic variations in climate over the past 5,500 years reflected in raised bogs. *Nature*, **263**, 281-284.
- Anderson, D.E. (1998) A reconstruction of Holocene climatic changes from peat bogs in north-west Scotland. *Boreas*, **27**, 208-224.
- Andrews, J.T. & Giraudeau, J. (2003) Multi-proxy records showing significant Holocene environmental variability: the inner N. Iceland shelf (Hunafloi). *Quaternary Science Reviews*, **22**, 175-193.
- Andrus, R.E., Wagner, D.J., & Titus, J.E. (1983) Vertical zonation of sphagnum mosses along hummock-hollow gradients. *Canadian Journal of Botany*, **61**, 3128-3139.
- Anon (1895) The North Lonsdale Magazine and Furness Miscellany, Vol. 1.
- Appleby, P.G. (2001). Chronostratigraphic techniques in recent sediments. In *Tracking Environmental Change Using Lake Sediments; Basin Analysis, Coring, and chronological techniques* (eds W.M. Last & J.P. Smol), pp. 171-203. Kluwer Academic.
- Appleby, P.G. & Oldfield, F. (1992). Application of lead-210 to sedimentation rate studies. In *Uranium-series disequilibrium: applications to earth, marine and environmental sciences* (eds M. Ivanovich & R.S. Harman), Vol. 2, pp. 731-778. Clarendon Press, Oxford.
- Armitage, P.D., Cranston, P.S., & Pinder, L.C.V. (1994) *The Chironomidae: Biology and Ecology of Non-biting Midges*.
- Baker, A., Caseldine, C.J., Gilmour, M.A., Charman, D.J., Proctor, C.J., Hawkesworth, C.J., & Phillips, N. (1999) Stalagmite luminescence and peat humification records of palaeomoisture for the last 2500 years. *Earth and Planetary Science Letters*, **165**, 157-162.
- Barber, K.E. (1981) *Peat stratigraphy and climate change. A palaeoecological test of the theory of cyclic peat bog regeneration* Balkema, Rotterdam.

- Barber, K.E. (1994) Deriving Holocene palaeoclimates from peat stratigraphy: Some misconceptions regarding the sensitivity and continuity of the record. *Quaternary Newsletter*, **72**, 1-9.
- Barber, K.E., Battarbee, R.W., Brooks, S.J., Eglinton, G., Haworth, E.Y., Oldfield, F., Stevenson, A.C., Thompson, R., Appleby, P.G., Austin, W.E.N., Cameron, N.G., Ficken, K.J., Golding, P., Harkness, D.D., Holmes, J.A., Hutchinson, R., Lishman, J.P., Maddy, D., Pinder, L.C.V., Rose, N.L., & Stoneman, R.E. (1999) Proxy records of climate change in the UK over the last two millennia: documented change and sedimentary records from lakes and bogs. *Journal of the Geological Society, London*, **156**, 369-380.
- Barber, K.E., Chambers, F.M., & Maddy, D. (2003) Holocene palaeoclimates from peat stratigraphy: macrofossil proxy climate records from three oceanic raised bogs in England and Ireland. *Quaternary Science Reviews*, **22**, 521-539.
- Barber, K.E., Chambers, F.M., Maddy, D., Stoneman, R.E., & Brew, J.S. (1994) A sensitive high-resolution record of late Holocene climate change from a raised bog in northern England. *The Holocene*, **4**, 198-205.
- Barber, K.E. & Charman, D.J. (2003). Holocene palaeoclimate records from peatlands. In *Global Change in the Holocene* (eds A. Mackay, R.W. Battarbee, H.J.B. Birks & F. Oldfield), pp. 210-226. Arnold, London.
- Barber, K.E., Dumayne-Peaty, L., Hughes, P.D.M., Mauquoy, D., & Scaife, R.G. (1998) Replicability and variability of the recent macrofossil and proxy climate record from raised bogs: field stratigraphy and macrofossil data from Bolton Fell Moss and Walton Moss, Cumbria, England. *Journal of Quaternary Science*, **13**, 515-528.
- Barber, K.E., Maddy, D., Rose, N., Stevenson, A.C., Stoneman, R.E., & Thompson, R. (2000) Replicated proxy-climate signals over the last 2000 yr from two distant UK peat bogs: new evidence for regional palaeoclimatic teleconnections. *Quaternary Science Reviews*, **19**, 481-487.
- Battarbee, R.W. (2000) Palaeolimnological approaches to climate change, with special regard to the biological record. *Quaternary Science Reviews*, **19**, 107-124.

- Bedford, A., Jones, R.T., Lang, B., Brooks, S.J., & Marshall, J.D. (2004) A Late-glacial chironomid record from Hawes Water, northwest England. *Journal of Quaternary Science*, **19**, 281-290.
- Bengtsson, L. & Enell, M. (1986). Chemical Analysis. In *Handbook of Holocene palaeoecology and palaeohydrology* (ed B.E. Berglund), pp. 423-451. John Wiley & Sons Ltd, Chichester.
- Bennett, K.D. (1994) Confidence intervals for age estimates and deposition times in late-Quaternary sediment sequences. *The Holocene*, **4**, 337-348.
- Bianchi, G.G. & McCave, I.N. (1999) Holocene periodicity in North Atlantic climate and deep-ocean flow south of Iceland. *Nature*, **397**, 515-517.
- Bigler, C., Grahn, E., Larocque, I., Jeziorski, A., & Hall, R.I. (2003) Holocene environmental change at Lake Njulla (999 m a.s.l.), northern Sweden: a comparison with four small nearby lakes along an altitudinal gradient. *Journal of Paleolimnology*, **29**, 13-29.
- Bigler, C., Larocque, I., Peglar, S.M., Birks, H.J.B., & Hall, R.I. (2002) Quantitative multiproxy assesment of long-term patterns of Holocene environmental change from a small lake near Abisko, northern Sweden. *The Holocene*, **12**, 481-496.
- Birks, H.J.B. (1995). Quantitative palaeoenvironmental reconstructions. In *Statistical modelling of quaternary science data. QRA Technical guide 5* (eds D. Maddy & J.S. Brew), pp. 161-254. Quaternary Research Association, Cambridge.
- Birks, H.J.B. (1998) Numerical tools in palaeolimnology - progress, potentialities, and problems. *Journal of Paleolimnology*, **20**, 307-332.
- Blackford, J.J. & Chambers, F.C. (1991) Proxy records of climate change from blanket mires: Evidence for a Dark Age (1400BP) climatic deterioration in the British Isles. *The Holocene*, **1**, 63-67.
- Blackford, J.J. & Chambers, F.C. (1993) Determining the degree of peat decomposition for peat-based palaeoclimate studies. *International Peat Journal*, **5**, 7-24.
- Blundell, A. & Barber, K.E. (2005) A 2800-year palaeoclimatic record from Tore Hill Moss, Strathspey, Scotland; the need for a multiproxy approach to peat based palaeoclimate reconstructions. *Quaternary Science Reviews*, **24**, 1261-1277.

- Bobrov, A., Charman, D.J., & Warner, B.G. (1999) Ecology of testate amoebae (Protozoa: rhizopoda) on peatlands in western Russia with special attention to niche separation in closely related taxa. *Protist*, **150**, 125-136.
- Boggie, R., Knight, A.H., & Hunter, R.F. (1958) Studies of the root development of plants in the field using radioactive tracers. *Journal of Ecology*, **46**, 621-639.
- Bond, G., Kromer, B., Beer, J., Muscheler, J., Evans, M.N., Showers, W., Hofmann, S., Lotti-Bond, R., Hajdas, I., & Bonani, G. (2001) Persistent solar influence on North Atlantic climate during the Holocene. *Science*, **294**, 2130-2136.
- Bond, G., Showers, W., Cheseby, M., Lotti, R., Almasi, P., deMenocal, P., Priore, P., Cullen, H., Hajdas, I., & Bonani, G. (1997) A pervasive millennial-scale cycle in North Atlantic Holocene and glacial climates. *Science*, **278**, 1257-1266.
- Brodersen, K.F., Odgaard, B.V., Vestergaard, O., & Anderson, N.J. (2001) Chironomid stratigraphy in the shallow and eutrophic Lake Sobygaard, Denmark: chironomid-macrophyte co-occurrence. *Freshwater Biology*, **46**, 253-267.
- Brodersen, K.P. & Anderson, N.J. (2002) Distribution of chironomids (Diptera) in low arctic West Greenland lakes: trophic conditions, temperature and environmental reconstruction. *Freshwater Biology*, **47**, 1137-1157.
- Brodersen, K.P. & Lindegaard, C. (1999) Classification, assessment and trophic reconstruction of Danish lakes using chironomids. *Freshwater Biology*, **42**, 143-157.
- Brodin, Y.W. (1982) Palaeoecological studies of the recent development of the Lake Vaxjosjon. IV. Interpretation of the eutrophication process through the analysis of subfossil chironomids. *Archive fur Hydrobiologie*, **93**, 313-326.
- Brodin, Y.W. (1986) The postglacial history of Lake Flarken, southern Sweden, interpreted from subfossil insect remains. *Int.rev.ges.hydrobiol.*, **71**, 371-432.
- Brodin, Y.W. & Gransberg, M. (1993) Responses of Insects, Especially Chironomidae (Diptera), and Mites to 130 Years of Acidification in a Scottish Lake. *Hydrobiologia*, **250**, 201-212.
- Broecker, W.S. (1998) Paleocean circulation during the last deglaciation: a bipolar seesaw? *Palaeoceanography*, **13**, 119-121.

- Broecker, W.S. (2000) Abrupt climate change: causal constraints provided by the paleoclimate record. *Earth-Science Reviews*, **51**, 137-154.
- Broecker, W.S. & Denton, G.H. (1989) The role of ocean-atmosphere reorganisations in glacial cycles. *Geochemica et Cosmochemica Acta*, **53**, 2495-2501.
- Brooks, S.J. (1996) Three thousand years of environmental history in a Cairngorms lochan revealed by analysis of non-biting midges Insecta: Diptera: Chironomidae. *Botanical Journal of Scotland*, **48**, 89-98.
- Brooks, S.J. (2000) Late-glacial fossil midge stratigraphies (Insecta: Diptera: Chironomidae) from the Swiss Alps. *Palaeogeography, Palaeoclimatology, Palaeoecology*, 261-279.
- Brooks, S.J. (2003). Chironomid analysis to interpret and quantify Holocene climate change. In *Global change in the Holocene* (eds A. Mackay, R.W. Battarbee, J. Birks & F. Oldfield), pp. 328-341. Hodder Arnold.
- Brooks, S.J. (2004) Diagnosis of Tanytarsini. Natural History Museum.
- Brooks, S.J. (2005) Chironomid Ecology Notes. Natural History Museum.
- Brooks, S.J. (2006) Fossil midges (Diptera: Chironomidae) as palaeoclimatic indicators for the Eurasian region. *Quaternary Science Reviews*, **25**, 1894-1910.
- Brooks, S.J., Bennion, H., & Birks, H.J.B. (2001) Tracing lake trophic history with a chironomid-total phosphorus inference model. *Freshwater Biology*, **46**, 513-533.
- Brooks, S.J. & Birks, H.J.B. (2000) Chironomid-inferred late-glacial and early Holocene mean July air temperatures for Krakenes Lake, western Norway. *Journal of Paleolimnology*, **23**, 77-89.
- Brooks, S.J. & Birks, H.J.B. (2001) Chironomid-inferred air temperatures from Lateglacial and Holocene sites in north-west Europe: progress and problems. *Quaternary Science Reviews*, **20**, 1723-1741.
- Brooks, S.J., Langdon, P.G., & Heiri, O. (2006) *The identification and use of Palaeartic chironomid larvae in palaeoecology* Quaternary Research Association, London.

- Brooks, S.J., Mayle, F.E., & Lowe, J.J. (1997) Chironomid-based Lateglacial climatic reconstruction for southeast Scotland. *Journal of Quaternary Science*, **12**, 161-167.
- Brown, A.D., Mathur, S.P., & Kushner, D.J. (1989a) Methane metabolism in raised bogs of northern wetlands. *Geomicrobiology Journal*, **11**, 35-48.
- Brown, T.A., Nelson, D., Mathewes, R.W., Vogel, J.S., & Southon, J.R. (1989b) Radiocarbon dating of pollen by accelerator mass spectrometry. *Quaternary Research*, **32**, 205-212.
- Campbell, I.D., Campbell, C., Apps, M.J., Rutter, N.W., & Bush, A.B.G. (1998) Late Holocene similar to 1500yr climatic periodicities and their implications. *Geology*, **26**, 471-473.
- Caseldine, C.J., Baker, A., Charman, D.J., & Hendon, D. (2000) A comparative study of optical properties of NaOH peat extracts: implications for humification studies. *Holocene*, **10**, 649-658.
- Chambers, F.M., Barber, K.E., Maddy, D., & Brew, J.S. (1997) A 5500-year proxy-climate and vegetation record from blanket mire at Talla Moss, Borders, Scotland. *Holocene*, **7**, 391-399.
- Chambers, F.M., Ogle, M.I., & Blackford, J.J. (1999) Palaeoenvironmental evidence for solar forcing of Holocene climate: linkages to solar science. *Progress in Physical Geography*, **23**, 181-204.
- Chapman, M.R. & Shackleton, N.J. (2000) Evidence of 550-year and 1000-year cyclicities in North Atlantic circulation patterns during the Holocene. *Holocene*, **10**, 287-291.
- Charman, D.J. (2002) *Peatlands and environmental change* Wiley.
- Charman, D.J., Blundell, A., & ACCROTELM (in press) A pan-European testate amoebae transfer function for palaeohydrological reconstruction on ombrotrophic peatlands. *Journal of Quaternary Science*.
- Charman, D.J., Blundell, A., Chiverrell, R.C., Hendon, D., & Langdon, P.G. (2006) Compilation of non-annually resolved Holocene proxy climate records: stacked Holocene peatland palaeo-water table reconstructions from northern Britain. *Quaternary Science Reviews*, **25**, 336-350.

- Charman, D.J., Brown, A.D., Hendon, D., Kimmel, A., & Karofeld, E. (2004) Testing the relationship between Holocene peatland palaeoclimate reconstructions and instrumental data. *Quaternary Science Reviews*, **23**, 137-143.
- Charman, D.J., Caseldine, C.J., Baker, A., Geary, B., Hatton, J., & Proctor, C.J. (2001) Palaeohydrological records from peat profiles and speleothems in Sutherland, northwest Scotland. *Quaternary Research*, **55**, 223-234.
- Charman, D.J. & Hendon, D. (2000) Long-term changes in soil water tables over the past 4,500 years: relationships with climate and north Atlantic atmospheric circulation and sea surface temperature. *Climatic Change*, **47**, 45-59.
- Charman, D.J., Hendon, D., & Packman, S. (1999) Multi-proxy surface wetness records from replicate cores on an ombrotrophic mire: implications for Holocene palaeoclimatic records. *Journal of Quaternary Science*, **14**, 541-464.
- Charman, D.J., Hendon, D., & Woodland, W.A. (2000) *The identification of testate amoebae (Protozoa: Rhizopoda) in peats. QRA technical guide no. 9* Quaternary Research Association, London.
- Charman, D.J. & Warner, B.G. (1992) Relationship between testate amoebae (Protozoa: Rhizopoda) and microenvironmental parameters on a forested peatland in northeastern Ontario. *Canadian Journal of Zoology*, **70**, 2474-2482.
- Charman, D.J. & Warner, B.G. (1997) The ecology of testate amoebae (Protozoa: Rhizopoda) in oceanic peatlands in Newfoundland, Canada: Modelling hydrological relationships for palaeoenvironmental reconstruction. *Ecoscience*, **4**, 562.
- Chiverrell, R.C. (2001) A proxy record of late Holocene climate change from May Moss, northeast England. *Journal of Quaternary Science*, **16**, 9-29.
- Clymo, R.S. (1984) Sphagnum-Dominated Peat Bog - A Naturally Acid Ecosystem. *Philosophical Transactions of the Royal Society of London Series B-Biological Sciences*, **305**, 487-499.
- Coombes, P.M.V. (2003) *The Palaeoecology of Recent Human Impact in the Lake District*, University of Southampton, Southampton.
- Cooper, E.A. & Proctor, C.J. (1998) Malham Tarn national nature reserve: The vegetation of Malham Tarn Moss and fens. *Field Studies*, 277-312.

- Cranston, P.S. (1982) *Orthoclaadiinae Larvae (Chironomidae) A key to the larvae of the British Orthoclaadiinae (Chironomidae)* Freshwater Biological Association.
- Crowley, T.J. & Lowery, T.S. (2000) How warm was the medieval warm period? *Ambio*, **29**, 51-54.
- Daniels, R.E. & Eddy, A. (1990) *Handbook of European Sphagna* Institute of Terrestrial Ecology, Natural Environment Research Council, HMSO.
- Danks, H.V. & Oliver, D.R. (1972) Seasonal emergence of some high arctic chironomidae (Diptera). *Canadian Entomologist*, **104**, 661-686.
- Dansgaard, W., Johnsen, S.J., Clausen, H.B., Dahljensen, D., Gundestrup, N.S., Hammer, C.U., Hvidberg, C.S., Steffensen, J.P., Sveinbjornsdottir, A.E., Jouzel, J., & Bond, G. (1993) Evidence for General Instability of Past Climate from A 250-Kyr Ice-Core Record. *Nature*, **364**, 218-220.
- David, R.G. (1981). Ice Houses of Cumbria. In *Transactions of the Cumberland and Westmoorland Antiquarian and Archaeological Society* (eds J. Charlton & J. Hughes), Vol. LXXXI, pp. 137-155.
- Davies, T., Kelly, M., & Osborn, T.J. (1997). Explaining the climate of the British Isles. In *Climates of the British Isles; present past and future* (eds M. Hulme & E. Barrow), pp. 11-32. Routledge, London.
- Denton, G.H., Alley, R.B., Comer, G.C., & Broecker, W.S. (2005) The role of seasonality in abrupt climate change. *Quaternary Science Reviews*, **24**, 1159-1182.
- Devito, K.J., Waddington, J.M., & Branfireun, B.A. (1997) Flow reversals in peatlands influenced by local groundwater systems. *Hydrological processes*, **11**, 103-110.
- Duller, G. (1995) Troels-Smith plotting program. Kingston: Kingston University.
- Dupont, L.M. (1986) Temperature and rainfall variation in the Holocene based on comparative palaeoecology and isotope geology of a hummock and a hollow (Bourtangerveen, The Netherlands). *Review of Palaeobotany and Palynology*, **48**, 71-159.
- Eggelsmann, R., Heathwaite, A.L., Grosse-Braukmann, G., Kuster, E., Naucke, W., Schuch, M., & Schweickle, V. (1993). Physical processes and properties of

- mires. In *Mires: Process, Exploitation and conservation* (eds A.L. Heathwaite & K.H. Gottlich), pp. 171-262. Wiley, Chichester.
- Eiriksson, J., Knudsen, K.L., Hafliðason, H., & Heinemeier, J. (2000) Chronology of late Holocene climatic events in the northern North Atlantic based on AMS C-14 dates and tephra markers from the volcano Hekla, Iceland. *Journal of Quaternary Science*, **15**, 573-580.
- Ellis, C.J. & Tallis, J.H. (2000) Climatic control of blanket mire development at Kantra Moss, north-west Scotland. *Journal of Ecology*, **88**, 869-889.
- Gams, H. (1927) Die Geschichte der Lunzer Seen, Moore und Wolder. *Int. Revue ges. Hydrobiol. Hydrogr.*, **18**, 305-395.
- Gannon, J.E. (1971) Two counting cells for the enumeration of zooplankton microcrustacea. *Transactions of the American Microscopical Society*, **90**, 486-490.
- Glaser, P.H., Siegel, D.I., Romanowicz, E.A., & Shen, Y.P. (1997) Regional linkages between raised bogs and the climate, groundwater, and landscape of north-western Minnesota. *Journal of Ecology*, **85**, 3-16.
- Grosse-Brauckmann, G. (1986). Analysis of vegetative plant macrofossils. In *Handbook of Holocene palaeoecology and palaeohydrology* (ed B.E. Berglund), pp. 591-618.
- Hall, I.R., Bianchi, G.G., & Evans, J.R. (2004) Centennial to millennial scale Holocene climate-deep water linkage in the North Atlantic. *Quaternary Science Reviews*, **23**, 1529-1536.
- Hann, B.J., Warner, B.G., & Warwick, W.F. (1992) Aquatic invertebrates and climatic change: a comment on Walker et al., (1991). *Canadian Journal of Fisheries and Aquatic Sciences*, **49**, 1274-1276.
- Haslam, C.J. (1987) Late Holocene peat stratigraphy and climate change - a macrofossil investigation from the raised mires of north-western Europe.
- Hays, J.D., Imbrie, J., & Shackleton, N.J. (1976) Variations in the Earth's orbit: pacemaker of the ice ages. *Science*, **194**, 1121-1132.
- Heinrichs, M.L., Walker, I.R., & Mathewes, R.W. (2001) Chironomid-based palaeosalinity records in southern British Columbia, Canada: a comparison of transfer functions. *Journal of Paleolimnology*, **26**, 147-159.

- Heiri, O., Birks, H.J.B., Brooks, S.J., Velle, G., & Willassen, E. (2003a) Effects of within-lake variability of fossil assemblages on quantitative chironomid-inferred temperature reconstruction. *Palaeogeography, Palaeoclimatology, Palaeoecology*, **199**, 95-106.
- Heiri, O. & Lotter, A.F. (2001) Effect of low count sums on quantitative environmental reconstructions: an example using subfossil chironomids. *Journal of Paleolimnology*, **26**, 343-350.
- Heiri, O. & Lotter, A.F. (2003) 9000 years of chironomid assemblage dynamics in an Alpine lake: long-term trends, sensitivity to disturbance and resilience of the fauna. *Journal of Paleolimnology*, **30**, 273-289.
- Heiri, O., Lotter, A.F., Hausmann, S., & Kienast, F. (2003b) A chironomid-based Holocene summer air temperature reconstruction from the Swiss Alps. *The Holocene*, **13**, 477-484.
- Heiri, O., Lotter, A.F., & Lemcke, G. (2001) Loss on ignition as a method for estimating organic and carbonate content in sediments: reproducibility and comparability of results. *Journal of Paleolimnology*, **25**, 101-110.
- Heiri, O., Wick, L., van Leeuwen, J.F.N., van der Knaap, W.O., & Lotter, A.F. (2003c) Holocene tree immigration and the chironomid fauna of a small Swiss subalpine lake (Hinterburgsee, 1515 m asl). *Palaeogeography, Palaeoclimatology, Palaeoecology*, **189**, 35-53.
- Hemond, H.F. (1980) Biogeochemistry of Thoreau's bog, Concord, Massachusetts. *Ecological Monographs*, **50**, 507-526.
- Hendon, D. & Charman, D.J. (1997) The preparation of testate amoebae (Protozoa: rhizopoda) samples from peat. *The Holocene*, **7**, 199-205.
- Hendon, D., Charman, D.J., & Kent, M. (2001) Palaeohydrological records derived from testate amoebae analysis from peatlands in northern England: within-site variability, between-site comparability and palaeoclimatic implications. *The Holocene*, **11**, 127-148.
- Hill, M.O. & Gauch, H.G. (1980) Detrended correspondence analysis, an improved ordination technique *Vegetatio*, **42**, 47-58.

- Hofmann, W. (1971) Zur taxonomie and palokologie subfossiler chironomiden (Dipt.) in sesedimenten. *Archive fur Hydrobiologie*, **6**, 1-50.
- Holmes, P.F. (1965) The natural history of Malham Tarn. *Field Studies*, **2**, 199-223.
- Hughes, P.D.M. (1997) The palaeoecology of the fen/bog transition during the early- to mid-Holocene in Britain, University of Southampton.
- Hughes, P.D.M., Blundell, A., Charman, D.J., Bartlett, S., Daniell, J.R.G., Wojatschke, A., & Chambers, F.M. (2006) An 8500 Cal. year multi-proxy climate record from a bog in eastern Newfoundland: contributions of meltwater discharge and solar forcing. *Quaternary Science Reviews*, **25**, 1208-1227.
- Hughes, P.D.M., Mauquoy, D., Barber, K.E., & Langdon, P.G. (2000) Mire-development pathways and palaeoclimatic records from a full Holocene peat archive at Walton Moss, Cumbria, England. *The Holocene*, **10**, 465-479.
- Hurrell, J.W. (1995) Decadal trends in the North-Atlantic Oscillation - regional temperatures and precipitation. *Science*, **269**, 676-679.
- Hurrell, J.W., Kushnir, Y., Ottersen, G., & Visbeck, M. (2003). An overview of the North Atlantic Oscillation. In *The North Atlantic Oscillation: climatic significance and environmental impact* (eds J.W. Hurrell, Y. Kushnir, G. Ottersen & M. Visbeck). American Geophysical Union, Washington, DC.
- Imbrie, J. & Kipp, N.G. (1971). A new micropalaeontological method for quantitative paleoclimatology: application to late Pleistocene Caribbean core V28-238. In *The late Cenozoic Glacial Ages* (ed K.K. Turekian), pp. 77-181. Yale University Press, New Haven.
- Ingram, H.A.P. (1978) Soil layers in mires: function and terminology. *Journal of Soil Science*, **29**, 224-227.
- Ingram, H.A.P. (1982) Size and shape in raised mire ecosystems: a geophysical model. *Nature*, **297**, 300-303.
- Ingram, H.A.P. (1983). Hydrology. In *Ecosystems of the world. 4A. Mires: swamp, bog, fen, and moor: general studies* (ed A.J.P. Gore), pp. 67-158. Elsevier.
- Ivanov, K.E. (1981) *Water Movement in Mirelands* Academic Press.
- Johansen, S.J., Dahljensen, D., Gundestrup, N.S., Steffensen, J.P., Clausen, H.B., Miller, H., Masson-Delmotte, V., Sveinbjornsdottir, A.E., & White, J. (2001)

- Oxygen isotope and palaeotemperature records from six Greenland ice-core stations: Camp Century, Dye-3, GRIP, GISP2, Renland and NorthGRIP. *Journal of Quaternary Science*, **16**, 299-307.
- Jones, P. & Hulme, M. (1997). The changing temperature of 'Central England'. In *Climates of the British Isles; present past and future* (eds M. Hulme & E. Barrow). Routledge.
- Jones, P.D. & Conway, D. (1997) Precipitation in the British Isles: An analysis of area-average data updated to 1995. *International Journal of Climatology*, **17**, 427-438.
- Juggins, S. (2003) C2 Software for ecological and palaeoecological data analysis and visualisation. University of Newcastle.
- Juggins, S. & Ter Braak, C.J.F. (1995) WAPLS-version 1.0. Unpublished computer program.
- Kapsner, W.R., Alley, R.B., Shuman, C.A., Anandakrishnan, S., & Grootes, P.M. (1995) Dominant Influence of Atmospheric Circulation on Snow Accumulation in Greenland over the Past 18,000 Years. *Nature*, **373**, 52-54.
- Kelly, P.M., Goodess, C.M., & Cherry, B.S.G. (1987) The interpretation of the Icelandic sea-ice record. *Journal of Geophysical Research*, **92**, 10835-10843.
- Kent, M. & Coker, P. (1992) *Vegetation description and analysis, a practical approach* John Wiley & Son.
- Kon, M. (1984) Swarming and mating of *Chironomus yoshimatsui* Diptera: Chironomidae: seasonal change in the timing of swarming and mating. *Journal of Ethology*, **2**, 37-45.
- Korhola, A. (1995) Holocene climatic variations in southern Finland reconstructed from peat-initiation data. *The Holocene*, **5**, 43-58.
- Korhola, A., Vasko, K., Toivonen, H.T.T., & Olander, H. (2002) Holocene temperature changes in northern Fennoscandia reconstructed from chironomids using Bayesian modelling. *Quaternary Science Reviews*, **21**, 1841-1860.
- Kovach, W.L. (1995). Multivariate Data Analysis. In *Statistical modelling of Quaternary science data. QRA technical guide 5* (eds D. Maddy & J.S. Brew), pp. 1-38. Quaternary Research Association.

- Kreutz, K.J., Mayewski, P.A., Meeker, L.D., Twickler, M.S., Whitlow, S.I., & Pittalwala, I.I. (1997) Bipolar changes in atmospheric circulation during the Little Ice Age. *Science*, **277**, 1294-1296.
- Lamb, H.H. (1977) *Climate: Past, Present and Future* Methuen, London.
- Lang, B., Bedford, A.P., Richardson, N., & Brooks, S.J. (2003) The use of ultra-sound in the preparation of carbonate and clay sediments for chironomid analysis. *Journal of Paleolimnology*, **30**, 451-460.
- Langdon, P.G. & Barber, K.E. (2005) The climate of Scotland over the last 5000 years inferred from multiproxy peatland records: inter-site correlations and regional variability. *Journal of Quaternary Science*, **20**, 549-566.
- Langdon, P.G., Barber, K.E., & Hughes, P.D.M. (2003) A 7500 year peat-based palaeoclimatic reconstruction and evidence for an 1100-year cyclicity in bog surface wetness from Temple Hill Moss, Pentland Hills, Southeast Scotland. *Quaternary Science Reviews*, **22**, 273.
- Langdon, P.G., Barber, K.E., & Lomas-Clarke, S.H. (2004) Reconstructing climate and environmental change in northern England through chironomid and pollen analyses: evidence from Talkin Tarn, Cumbria. *Journal of Paleolimnology*, **32**, 197-213.
- Larocque, I. (2001) How many head capsules are enough? A statistical approach to determine sample size for palaeoclimatic reconstructions. *Palaeogeography, Palaeoclimatology, Palaeoecology*, **172**, 133-142.
- Larocque, I. & Hall, R.I. (2003) Chironomids as quantitative indicators of mean July air temperature: validation by comparison with century long meteorological records from Northern Sweden. *Journal of Paleolimnology*, **29**, 475-493.
- Larocque, I., Hall, R.I., & Grahn, E. (2001) Chironomids as indicators of climate change: a 100-lake training set from a subarctic region of northern Sweden (Lapland). *Journal of Paleolimnology*, **26**, 307-322.
- Lindegaard, C., Armitage, P.D., Cranston, P.S., & Pinder, L.C.V. (1995). Classification of water bodies and pollution. In *The Chironomidae: Biology and Ecology of non-biting midges*, pp. 384-404. Chapman & Hall, London.

- Lindsay, R.A. (1995) *Bogs: the ecology, classification and conservation of ombrotrophic mires* Scottish Natural Heritage, Edinburgh.
- Livingstone, D.M. & Lotter, A.F. (1998) The relationship between air and water temperature in lakes of the Swiss plateau: a case study with palaeolimnological implications. *Journal of Paleolimnology*, **19**, 181-198.
- Lotter, A.F., Birks, H.J.B., Hofmann, W., & Marchetto, A. (1997) Modern diatom, cladocera, chironomid, and chrysophyte cyst assemblages as quantitative indicators for the reconstruction of past environmental change in the Alps. 1. Climate. *Journal of Paleolimnology*, **18**, 395-420.
- Lotter, A.F., Walker, I.R., Brooks, S.J., & Hofmann, W. (1999) An intercontinental comparison of chironomid palaeotemperature inference models: Europe vs North America. *Quaternary Science Reviews*, **18**, 717-735.
- Mackay, A.P. (1977) Growth and development of larval chironomidae. *Oikos*, **28**, 270-275.
- Madden, R.A. & Williams, J. (1978) The Correlation between Temperature and Precipitation in the United States and Europe. *Monthly Weather Review*, **106**, 142-147.
- Magny, M. (1993) Solar influences on Holocene climatic changes illustrated by correlations between past lake level fluctuations and the atmospheric 14 C record. *Quaternary Research*, **40**, 1-9.
- Magny, M. (2004) Holocene climate variability as reflected by mid-European lake-level fluctuations and its probable impact on prehistoric human settlements. *Quaternary International*, **113**, 65-79.
- Magny, M. & Begeot, C. (2004) Hydrological changes in the European midlatitudes associated with freshwater outbursts from Lake Agassiz during the Younger Dryas event and the early Holocene. *Quaternary Research*, **61**, 181-192.
- Magny, M., Begeot, C., Guillot, J., & Peyron, O. (2003) Contrasting Patterns of hydrological changes in Europe in response to Holocene climate cooling Phases. *Quaternary Science Reviews*, **22**, 1589-1596.

- Malgorzata, W., Wachnicka, A., Kuijpers, A., Troelstra, S., Prins, M.A., & Witkowski, A. (2005) Holocene North Atlantic surface circulation and climatic variability: evidence from diatom records. *The Holocene*, **15**, 85-96.
- Malmer, N. (1986) Vegetational gradients in relation to environmental conditions in northwestern European mires. *Canadian Journal of Botany*, **64**, 375-383.
- Manley, G. (1974) Central England temperatures: monthly means 1659-1973. *Quarterly Journal of the Royal Meteorological Society*, **100**, 389-405.
- Mann, M.E., Bradley, R.S., & Hughes, M.K. (1999) Northern hemisphere temperatures during the past millennium: Inferences, uncertainties, and limitations. *Geophysical Research Letters*, **26**, 759-762.
- Marchitto, T.M., Curry, W.B., & Oppo, D.W. (1998) Millennial-scale changes in North Atlantic circulation since the last glaciation. *Nature*, **393**, 557-561.
- Maslin, M., Pike, J., Stickley, C., & Ettwein, V. (2003). Evidence of Holocene Climate variability in Marine Sediments. In *Global Change in the Holocene* (eds A. Mackay, R.W. Battarbee, J. Birks & F. Oldfield), pp. 185-209. Arnold, London.
- Mauquoy, D. & Barber, K.E. (1999a) Evidence for climatic deteriorations associated with the decline of sphagnum imbricatum Hornsch. ex Russ. in six ombrotrophic mires from northern England and the Scottish Borders. *The Holocene*, **9**, 423-437.
- Mauquoy, D. & Barber, K.E. (1999b) A replicated 3000 year proxy-record from Coom Rigg Moss and Felecia Moss, The Border Mires, northern England. *Journal of Quaternary Science*, **14**, 263-275.
- Mauquoy, D. & Barber, K.E. (2002) Testing the sensitivity of the palaeoclimatic signal from ombrotrophic peat bogs in northern England and the Scottish Borders. *Review of Palaeobotany and Palynology*, **119**, 219-240.
- Mauquoy, D., van Geel, B., Blaauw, M., & van der Plicht, J. (2002) Evidence from northwest European bogs shows 'Little Ice Age' climatic changes driven by variations in solar activity. *The Holocene*, **12**, 1-6.
- Mayewski, P.A., Rohling, E.E., Stager, J.C., Karlen, W., Maasch, K.A., Meeker, L.D., Meyerson, E.A., Gasse, F., van Kreveld, S., Holmgren, K., Lee-Thorp, J.,

- Rosqvist, G., Rack, F., Staubwasser, M., Schneider, R.R., & Steig, E.J. (2004) Holocene climate variability. *Quaternary Research*, **62**, 243-255.
- McTiernan, K.B., Garnett, M.H., Mauquoy, D., Ineson, P., & Co-teaux, M. (1998) Use of near-infrared reflectance spectroscopy (NIRS) in palaeoecological studies of peat. *The Holocene*, **8**, 729-740.
- Mensing, S.T. & Southon, J.R. (1999) A simple method to separate pollen for AMS radiocarbon dating and its application to lacustrine and marine sediments. *Radiocarbon*, **41**, 1-8.
- METOffice (2005a) Malham Tarn Moss (www.met-office.gov.uk/climate/uk/stationdata/index [accessed 05/01/05]).
- METOffice (2005b) Newton Rigg Meteorological Data (www.met-office.gov.uk/climate/uk/stationdata/index [accessed 05/01/05]).
- Miserere, L., Montacchini, F., & Buffa, G. (2003) Ecology of some mire and bog plant communities in the Western Italian Alps. *Journal of Limnology*, **62**, 88-96.
- Moros, M., Emeis, K.C., Risebrobakken, B., Snowball, I., Kuijpers, A., McManus, J., & Jansen, E. (2004) Sea surface temperatures and ice rafting in the Holocene North Atlantic: climate influences on northern Europe and Greenland. *Quaternary Science Reviews*, **23**, 2113-2126.
- Nesje, A. & Dahl, S.O. (2003) The 'Little Ice Age' - only temperature? *Holocene*, **13**, 139-145.
- Nicholas, D.S. & Brown, J.M. (1980) Evaporation from a Sphagnum moss surface. *Journal of Hydrology*, **48**, 289-302.
- Nilssen, E. & Vorren, K.D. (1991) Peat humification and climate history. *Norsk Geologisk Tidsskrift*, **71**, 215-217.
- Nunez, R., Spiro, B., Pentecost, A., Kim, A., & Coletta, P. (2002) Organo-geochemical and stable isotope indicators of environmental change in a marl lake, Malham Tarn, North Yorkshire, UK. *Journal of Paleolimnology*, **28**, 403-417.
- O'Sullivan, P.E. (1983) Annually laminated lake sediments and the study of Quaternary environmental changes - a review. *Quaternary Science Reviews*, **1**, 245-313.

- Olander, H., Birks, H.J.B., Korhola, A., & Blom, T. (1999) An expanded calibration model for inferring lakewater and air temperatures from fossil chironomid assemblages in northern Fennoscandia. *The Holocene*, **9**, 279-294.
- Oliver, D.R. (1971) Life history of chironomidae. *Annual Review of Entomology*, **16**, 211-230.
- Oliver, D.R. & Roussel, M.E. (1983) *The Insects and Arachnids of Canada, Part 11: The Genera of Larval Midges of Canada, Diptera: Chironomidae* Agriculture Canada.
- Osvald, H. (1923) *Die vegetation des hochmoores Komosse Svenska V.,xtsociologiska S.,llskapets Handlingar.*
- Parker, D.E., Legg, T.P., & Folland, C.K. (1992) A new dailey Central England temperature series, 1772-1991. *International Journal of Climatology*, **12**, 317-342.
- Pentecost, A. (2000) Some obsevation on the errosion of Tarn Moss by the waters of Malham Tarn. *Field Studies*, **9**, 569-581.
- Pigott, M.E. & Pigott, C.D. (1959) Stratigraphy and pollen analysis of Malham Tarn and Malham Tarn Moss. *Field Studies*, **1**, 84-101.
- Pinder, L.C.V., Armitage, P.D., Cranston, P.S., & Pinder, L.C.V. (1995). Biology of the eggs and first-instar larvae. In *The Chironomidae: biology and ecology of non-biting midges*, pp. 87-102. Chapman & Hall.
- Pinder, L.C.V. & Morley, D.J. (1995). Chironomidae as indicators of water quality-with a comparison of the chironomid faunas of a series of contrasting Cumbrian Tarns. In *In Insects in a changing environment* (eds R. Harrington & N.E. Stork), pp. 272–290. Academic Press, London.
- Porinchu, D.F. & MacDonald, G.M. (2003) The use and application of freshwater midges (Chironomidae: Insecta: Diptera) in geographical research. *Progress in Physical Geography*, **27**, 378-422.
- Punning, J.M. & Alliksaar, T. (1997) The trapping of fly ash particles in the surface layers of sphagnum -dominated peat. *Water, Air and Soil Pollution*, **94**, 59-69.

- Quinlan, R. & Smol, J.P. (2002) Chironomid-based inference models for estimating end-of summer hypolimnetic oxygen from south-central Ontario lakes. *Freshwater Biology*, **46**, 1529-1551.
- Quinlan, R., Smol, J.P., & Hall, R.I. (1998) Quantitative inferences of past hypolimnetic anoxia in south-central Ontario lakes using fossil midges (Diptera: Chironomidae). *Canadian Journal of Fisheries and Aquatic Sciences*, **55**, 587-596.
- Rahmstorf, S. (2003) Timing of abrupt climate change: A precise clock. *Geophysical Research Letters*, **30**, 1510-1514.
- Ratcliffe, D.A. & Walker, D. (1958) The Silver Flowe, Galloway, Scotland. *Journal of Ecology*, **46**, 407-445.
- Regnell, J. (1992) Preparing pollen concentrates for AMS dating - a methodological study from a hard-water lake in southern Sweden. *Boreas*, **21**, 373-377.
- Regnell, J. & Everitt, E. (1996) Preparative centrifugation - a new method for preparing pollen concentrates suitable for radiocarbon dating by AMS. *Vegetation History and Archaeobotany*, **5**, 201-205.
- Reimer, P.J., Baillie, M., Bard, E., Bayliss, A., Beck, J.W., Bertrand, C.J.H., Blackwell, P.G., Buck, C.E., Burr, G.S., Cutler, K.B., Damon, P.E., Edwards, R.A., Fairbanks, R.G., Friedrich, M., Guilderson, T.P., Hogg, A.G., Hughen, K.A., Kromer, B., McCormac, G., Manning, S., Ramsey, C.B., Reimer, R.W., Remmele, S., Southon, J.R., Stuiver, M., Talamo, S., Taylor, F.W., van der Plicht, J., & Weyhenmeyer, C.E. (2004) IntCal04 Terrestrial 14C Age Calibration, 0 - 26 Cal kyr BP. *Radiocarbon*, **46**, 1029-1058.
- Rieradevall, M. & Brooks, S.J. (2001) An identification guide to subfossil Tanypodinae larvae (Insecta: Diptera: Chironomidae) based on cephalic setation. *Journal of Paleolimnology*, **25**, 81-99.
- Rohling, E.J. & Palike, H. (2005) Centennial-scale climate cooling with a sudden cold event around 8,200 years ago. *Nature*, **434**, 975-979.
- Rose, N. (2005) Malham Tarn SCP Profile. Department of Geography, University College London.

- Rose, N.L. (1994) A note on further refinements to a procedure for the extraction of carbonaceous fly-ash particles from sediments. *Journal of Paleolimnology*, **11**, 201-204.
- Rose, N.L., Harlock, S., Appleby, P.G., & Battarbee, R.W. (1995) Dating of recent lake sediments in the United Kingdom and Ireland using spheroidal carbonaceous particles concentration profiles. *The Holocene*, **5**, 328-335.
- Rosen, P., Segerstrom, U., Eriksson, L., Renberg, I., & Birks, H.J.B. (2001) Climate change during the Holocene as recorded by diatoms, chironomids, pollen and near-infrared spectroscopy (NIRS) in a sediment core from an alpine lake (Sjuodjijaure) in northern Sweden. *The Holocene*, **11**, 551-562.
- Round, F.E. (1953) An investigation of two benthic algal communities in Malham Tarn, Yorkshire. *Journal of Ecology*, **41**, 174-197.
- Ruddiman, W.F. & McIntyre, A. (1981) The North-Atlantic Ocean during the Last Deglaciation. *Palaeogeography Palaeoclimatology Palaeoecology*, **35**, 145-214.
- Rycroft, D.W., Williams, D.J.A., & Ingram, H.A.P. (1975) The transmission of water through peat. *Journal of Ecology*, **63**, 535-568.
- Schoning, K., Charman, D.J., & Wastegard, S. (2005) Reconstructed water tables from two ombrotrophic mires in eastern central Sweden compared with instrumental meteorological data. *Holocene*, **15**, 111-118.
- Schulz, M. & Paul, A. (2002). Holocene climate variability on centennial-to-millennial time scales: climate records from the North Atlantic realm. In *Climate development and history of the North Atlantic realm* (eds G. Wefer, W.H. Berger, K. Behre & E. Jansen). Springer-Verlag, Berlin.
- Seppa, H., Nyman, M., Korhola, A., & Weckstrom, J. (2002) Changes of treelines and alpine vegetation in relation to post-glacial climate dynamics in northern Fennoscandia based on pollen and chironomid records. *Journal of Quaternary Science*, **17**, 287-301.
- Stace, J. (1991) *New flora of the British Isles* Cambridge University Press, Cambridge

- Stotter, J., Wastl, M., Caseldine, C.J., & Haberle, T. (1999) Holocene palaeoclimatic reconstruction in northern Iceland: approaches and results. *Quaternary Science Reviews*, **18**, 457-474.
- Stuiver, M., Reimer, P.J., & Reimer, R.W. (2005) CALIB 5.0. [WWW program and documentation]. .
- Sutherland, R.A. (1998) Loss-on-ignition estimates of organic matter and relationships to organic carbon in fluvial bed sediments. *Hydrobiologia*, **389**, 153-167.
- Tallis, J.H. (1983). Changes in wetland communities. In *Ecosystems of the world 4A: mires: swamp, bog, fen and moor. General Studies* (ed A.J.P. Gore). Elsevier Science, Amsterdam.
- Telford, R.J., Heegaard, E., & Birks, H.J.B. (2004) All age depth models are wrong: but how badly? *Quaternary Science Reviews*, **23**, 1-5.
- Teller, J.T., Leverington, D.W., & Mann, J.D. (2002) Freshwater outbursts to the oceans from glacial Lake Agassiz and their role in climate change during the last deglaciation. *Quaternary Science Reviews*, **21**, 879-887.
- ter Braak, C.J.F. (1987). Calibration. In *Data analysis in community and landscape ecology* (eds R.H.G. Jongman, C.J.F. Ter Braak & O.F.R. van Tongeren), pp. 78-90. Wageningen.
- ter Braak, C.J.F. (1995). Ordination. In *Data analysis in community and landscape ecology* (eds R.H.G. Jongman, C.J.F. ter Braak & O.F.R. Van Tongeren), pp. 91-173. Cambridge University Press.
- ter Braak, C.J.F. & Juggins, S. (1993) Weighted averaging partial least squares regression (WA-PLS): an improved method for reconstructing environmental variables from species assemblages. *Hydrobiologia*, **269/270**, 485-502.
- Thienemann, A. (1922) Die beiden Chironomusarten der Tiefenfauna der norddeutschen Seen. Ein hydrobiologisches Problem. *Archiv für Hydrobiologie*, **13**, 609-646.
- Tolonen, K. (1986). Rhizopod analysis. In *Handbook of Holocene palaeoecology and palaeohydrology*, pp. 645-666. John Wiley, Chichester.

- Troels-Smith, J. (1955) Karakterisering af løse jordarter (characterisation of unconsolidated sediments). *Danmarks Geologiske Undersøgelse*, **3**, 1-73.
- Valgma, š. (1998a) Impact of precipitation on the water table level of different ombrotrophic raised bog complexes, central Estonia. *Suo*, **49**, 13-21.
- Valgma, š. (1998b) The role of hollows in the regulation of the Bog water balance: Mannikjarve bog, central Estonia. In Proceedings of the British Hydrological Society International Conference, Exeter, July 1998 (eds H. Wheater & C. Kirby), Vol. 1, pp. 465-471. Wiley.
- van der Molen, P.C., Wijmstra, T.A., & Van der, M. (1992). The thermal regime of hummock-hollow complexes on Clara Bog, Co. Offay, Ireland. In *Hummock-hollow complexes on Irish Raised Bogs*, pp. 175-197.
- van der Schaaf, S. (1999) Analysis of the hydrology of raised bogs in the Irish midlands: a case study of Raheenmore and Clara Bog, Wageningen Agricultural University.
- van der Schaaf, S. & Schouten, M.G.C. (2002). Bog hydrology. In *Conservation and restoration of raised bogs: geological, hydrological and ecological studies*, pp. 54-77. Geological Survey of Ireland.
- van Geel, B. (1978) A Palaeoecological study of Holocene peat bog sections in Germany and the Netherlands. *Review of Palaeobotany and Palynology*, **25**, 1-120.
- Vandergoes, M.J. & Prior, C.A. (2003) AMS dating of pollen concentrates - A methodological study of late quaternary sediments from south Westland, New Zealand. *Radiocarbon*, **45**, 479-491.
- Velle, G., Brooks, S.J., Birks, H.J.B., & Willassen, E. (2005) Chironomids as a tool for inferring Holocene climate: an assessment based on six sites in southern Scandinavia. *Quaternary Science Reviews*, **24**, 1429-1462.
- Viau, A.E., Gajewski, K., Fines, P., Atkinson, D.E., & Sawada, M.C. (2002) Widespread evidence of 1500 yr climate variability in North America during the past 14 000 yr. *Geology*, **30**, 455-458.
- von Post, L. (1924) Das genetische system der organogenen bildungen Schwedens. *International de pedologie*, **IV Commission no. 22**.

- Walker, I.R. (2001). Midges: chironomidae and related diptera. In (eds J.P. Smol, H.J.B. Birks & W.M. Last). Kluwer Academic, Dordrecht.
- Walker, I.R., Levesque, A.C., Cwynar, L.C., & Lotter, A.F. (1997) An expanded surface-water palaeotemperature inference model for use with fossil midges from eastern Canada. *Journal of Paleolimnology*, **18**, 165-178.
- Walker, I.R. & Mathewes, R.W. (1989) Chironomidae (Diptera) remains in surficial lake sediments from the Canadian Cordillera: analysis of fauna across an altitudinal gradient. *Journal of Paleolimnology*, **2**, 61-80.
- Walker, I.R., Mott, R.J., & Smol, J.P. (1991a) Allerod-Younger Dryas lake temperatures from midge fossils in Atlantic Canada. *Science*, **253**, 1010-1012.
- Walker, I.R., Smol, J.P., Engstrom, D.R., & Birks, H.J.B. (1991b) An assessment of Chironomidae as quantitative indicators of past climatic change. *Canadian Journal of Fisheries and Aquatic Sciences*, **48**, 975-987.
- Walker, I.R., Smol, J.P., Engstrom, D.R., & Birks, H.J.B. (1992) Aquatic invertebrates, climate, scale, and statistical hypothesis testing: a response to Hann, Warner, and Warwick. *Canadian Journal of Fisheries and Aquatic Sciences*, **48**, 987.
- Warner, B.G. & Charman, D.J. (1994) Holocene changes on a peatland in northwestern Ontario interpreted from testate amoebae (Protozoa) analysis. *Boreas*, **23**, 270-279.
- Weaver, A.J. & Hughes, T.M.C. (1994) Rapid Interglacial Climate Fluctuations Driven by North-Atlantic Ocean Circulation. *Nature*, **367**, 447-450.
- Whittaker, R.H. (1967) Gradient analysis of vegetation. *Biological Review*, **42**, 207-64.
- Wiederholm, T. (1983) *Chironomidae of the Holarctic region. Keys and diagnosis. Part 1. Larvae* Entomol. Scand. Suppl.
- Wiederholm, T., Resh, V.H., & Rosenberg, D.M. (1984). Responses of aquatic insects to environmental pollution. In *The ecology of aquatic insects*, pp. 508-557. Praeger, New York.
- Wigley, T.M.L., Lough, J.M., & Jones, P.D. (1984) Spatial patterns of precipitation in England and Wales and a revised, homogeneous England and Wales precipitation series. *International Journal of Climatology*, **4**, 1-25.

- Wimble, G.T. (1986) The palaeoecology of the lowland coastal raised mires of South Cumbria, University of Wales, Cardiff.
- Woodland, W.A., Charman, D.J., & Smart, P.L. (1998) Quantitative estimates of water tables and soil moisture in Holocene peatlands from testate amoebae. *The Holocene*, **8**, 261-273.
- Yang, H., Rose, N., & Battarbee, R.W. (2001) Dating of recent catchment peats using spheroidal carbonaceous particle (SCP) concentration profiles with particular reference to Lochnagar, Scotland. *The Holocene*, **11**, 593-597.